

**Investigation of the Expression and Localisation of
Caspase-3 in high grade Non-Hodgkin's Lymphoma**

This thesis has been submitted for the degree of
Doctor of Philosophy at the University of Leicester

by

Stephen Donoghue

BSc, MSc

March 2000

Department of Pathology
University of Leicester
Leicester

UMI Number: U138699

All rights reserved

INFORMATION TO ALL USERS

The quality of this reproduction is dependent upon the quality of the copy submitted.

In the unlikely event that the author did not send a complete manuscript and there are missing pages, these will be noted. Also, if material had to be removed, a note will indicate the deletion.



UMI U138699

Published by ProQuest LLC 2013. Copyright in the Dissertation held by the Author.
Microform Edition © ProQuest LLC.

All rights reserved. This work is protected against
unauthorized copying under Title 17, United States Code.



ProQuest LLC
789 East Eisenhower Parkway
P.O. Box 1346
Ann Arbor, MI 48106-1346

ABSTRACT

Although B cell Diffuse Large Cell Lymphoma (DLCL) can respond with chemotherapy and radiotherapy, a large number of patients are still resistant to treatment. The caspase family of enzymes are crucial components of the apoptotic cell death process, and are believed to be important in the pathogenesis and treatment of lymphoid malignancies. It was hoped that the investigation of the expression and localisation of Caspase-3 in high grade Non-Hodgkin's Lymphoma (NHLs) would provide information with respect to the progression and treatment of DLCL.

An ELISA was developed to measure the polyclonal response of mice injected with a peptide mimicking the N-termini of the active p12 fragment of Caspase-3. Screening of 'pre-monoclonal' supernatant from wells was carried out using immunohistochemistry on reactive tonsil tissue. Supernatant from one well appeared to be selectively staining only apoptotic cells within the germinal centre, however, after dilution cloning this antibody was not stabilised.

The pattern of proCaspase-3 expression was then studied using immunohistochemistry with a commercial antibody in 54 cases of DLCL. Quantitative reverse-transcriptase polymerase chain reaction was also carried out with cDNA extracted from the DLCL cases. These data were then correlated with clinical outcome, including stage at presentation, response to therapy, and survival. The patterns of expression of the active p17 fragment of Caspase-3 was also examined using immunohistochemistry in both reactive lymph nodes and DLCL cases. Tumour cells displayed both a diffuse cytosolic and a punctate cytosolic staining for proCaspase-3 and survival curves indicated that tumour cells with a diffuse cytosolic expression of Caspase-3 correlated with a poor prognosis. In addition, a punctate expression was associated with complete response to treatment. Cases with a small percentage of lymphoma cells expressing Caspase-3 also tended to show poor survival. Levels of Caspase-3 mRNA were not significant, although a weak trend was observed similar to the immunohistochemical analysis. Furthermore, a survival curve indicated that a high TUNEL positivity was associated with a poor survival probability. In the reactive lymph node tissue the immunopositivity pattern of the p17 fragment of Caspase-3 mirrored that of the TUNEL staining in that apoptotic cells and the occasional tinged body macrophage were staining. The pattern of staining was very similar to that seen with the 'pre-monoclonal' antibody that appeared to recognise only dying cells.

The coding sequence for the active p17 fragment of Caspase-3 was fused to Green Fluorescent Protein (GFP) in order to determine the *in situ* localisation of the enzyme. A correctly-sized band of 44kDa was detected in Western blots using lysates from transfected cells and when expressed in MCF-7 cells the clone produced a protein that appeared to localise to the mitochondria. Furthermore, the transfected cells appeared to be dying with a necrotic morphological appearance.

These results confirm the dynamic nature of both the proform and the p17 active fragment of Caspase-3 expression in DLCL and suggest that evaluating the patterns and levels of the expression of the enzyme has prognostic significance. The results also suggest that the p17 fragment of Caspase-3 may localise to the mitochondria to amplify a cell death signal.

ACKNOWLEDGEMENTS

Many thanks to Dr. J.H. Pringle for his guidance, enthusiasm and technical support over the years (“I can’t understand why it didn’t work!”). More thanks to Prof. I. Lauder and Dr. J. Shaw for advice and encouragement.

I am also extremely grateful to all the technical staff at the Pathology Department; without their patience many a PhD student would fall overboard and I fully appreciate their contribution.

A big thank you to Dr. S. Sobolewski for his financial assistance and encouragement. In addition, I am much obliged to Dr. H.S. Baden for clinical aid and information.

Finally, I am deeply indebted to Dr. R. James for assistance with antibody screening and Chris D’Lacey for his assistance with confocal microscopy.

Peptide production was carried out by John Kyte

Peptide Immunisation and Monoclonal Antibody Production was carried out by the Monoclonal Antibody Production Team in CSB.

Quantitative PCR ELISA was carried out by Lindsay Primrose.

All other work in this thesis was carried out by Stephen Donoghue

This thesis is dedicated to the goodwill and spirit of Mary Gallagher.

Contents

	Page
Abstract	I-111
Acknowledgements	VI
Contents	V
List of Figures	V-X
List of Tables	XV
Abbreviations	XVI-XVII
<i>Certainties!!</i>	XVIII

Chapter 1	Introduction	1
1.1	Introduction	2
1.2	Apoptosis	3
1.2.3	Morphological and Biochemical Events of Apoptosis	3
1.3	Apoptosis and Disease	4
1.4	Caspases	5
1.5	Classification of Caspases	5
1.6	Specificity and Structure	7
1.6.1	Caspase-1	8
1.6.2	Caspase-2	8
1.6.3	Caspase-3	9
1.6.4	Caspase-4 and -5	11
1.6.5	Caspase-6	11
1.6.6	Caspase-7	11
1.6.7	Caspase-8	11
1.6.8	Caspase-9	15
1.6.9	Caspase-10	15
1.7	Biological Caspase Inhibitors	15
1.7.1	CrmA	14
1.7.2	p35	16
1.7.3	IAPs	16
1.7.4	FLIP	17
1.8	Synthetic Caspase Inhibitors	18

1.9	Substrates	18
1.10	Bcl-2 Family	20
1.10.1	Dimerisation of Bcl-2 family proteins	22
1.10.2	Bcl-2 family interactions with other proteins	23
1.10.3	Subcellular localisation and dynamism of Bcl-2 family members	24
1.10.4	Bcl-2 family and the formation of pores in the mitochondria	26
1.10.5	Bcl-2 family proteins and the mitochondrial permeability transition pore	27
1.11	Receptors in Apoptosis	29
1.12	The 'Apoptosome' – a Model of Cell Death Regulation?	32
1.12.1	CED-4	32
1.12.2	Apaf-1	32
1.12.3	FLASH	34
1.13	Knockout experiments	35
1.13.1	Caspase-1 knockout	35
1.13.2	Caspase-2 knockout	36
1.13.3	Caspase-3 knockout	36
1.13.4	Caspase-6 and -7 knockouts	37
1.13.5	Caspase-8 knockout	37
1.13.6	Caspase-9 knockout	38
1.13.7	Apaf-1 knockout	39
1.13.8	FADD knockout	39
1.14	Receptor-mediated versus Chemical/Damage-induced Apoptotic Cell Death	40
1.14.1	Receptor-mediated Apoptosis	40
1.14.2	Chemical/Damage-induced Apoptosis	41
1.14.3	z-VAD.fmk does not block the commitment to cell death in etoposide treated cells	41
1.14.4	Caspase knockout experiments point to Receptor versus Chemical Apoptosis	42
1.15	Subcellular Localisation of Caspases	42
1.16	- a programmed non-apoptotic cell death?	45
1.17	Non-Hodgkin's Lymphoma	51
1.18	Classification of NHL	51

1.18.1	Diffuse Large Cell Lymphoma	52
1.19	Apoptotic Cell Death in the Pathogenesis of Cancer	54
1.19.1	Fas signalling in B-NHLs	54
1.19.2	Autoimmune lymphoproliferative syndrome (ALPS) and Tumorigenesis	57
1.19.3	Burkitt's Lymphoma and Bax mutations	58
1.19.4	FLIP and Tumorigenesis	59
1.19.5	Caspase Mutations and Tumorigenesis	59
1.19.6	Expression of Caspase-3 in Lymphomas and Leukaemias	60
1.19.7	Tumorigenesis and the Bcl-2 family	60
1.19.8	IAPs and Tumorigenesis	61
1.19.9	CARDs and Translocations	61
1.19.10	Interferon-consensus sequence-binding protein and CML	62
1.19.11	Genes in DLCL Tumorigenesis	62
1.20	Apoptotic Cell Death in Chemotherapy	63
1.20.1	Fas Signalling and Chemotherapy	64
1.20.2	Caspases and Chemotherapy	65
1.20.3	Bcl-2 Homologues and Chemotherapy	66
1.20.5	Death Receptors and Tumour Immunotherapy	67
1.20.6	Caspase Therapy	67
1.21	Aims of project	68

Chapter 2	Developing Immunodiagnostic tools to detect Apoptosis and Apoptotic Pathways	69
2.1	Introduction	70
2.1.1	Production of Anti-Peptide Antibodies	71
2.1.1.1	Peptides	71
2.1.1.2	Continuous and Discontinuous peptides	71
2.1.1.3	Predictions of Antigenicity	72
2.1.1.3.1	Hydrophilicity	72
2.1.1.3.2	Chain Termination	73
2.1.1.3.3	Sequence Variability	73
2.1.2	Single Chain Fragments (ScFvs) and Intracellular Immunisation	73

2.2	Materials and Methods	75
2.2.1	Cloning of Cκ insert into pEGFP-C1 vector	75
2.2.1.1	PCR Amplification of human Cκ Domain	75
2.2.1.2	Purification and Restriction of PCR amplicon	78
2.2.1.3	Ligation/Transformation	79
2.2.1.4	Screening of Clones	79
2.2.2	Expression of pEGFP-C1-Cκ	81
2.2.2.1	Drugs and Chemicals	81
2.2.2.2	Cell Culture Reagents	81
2.2.2.3	Cell Lines	82
2.2.2.4	Transfection of MRC5 cells	82
2.2.2.5	Fluorescent Microscopy	82
2.2.2.6	Western Blotting of Transfected MRC5 cells	83
2.2.3	Production of Anti-Peptide Monoclonal Antibodies	83
2.2.3.1	Peptide Selection and Synthesis	83
2.2.3.2	Peptide Immunisation and Monoclonal Antibody Production Procedure	84
2.2.4	Screening of Antibodies	84
2.2.4.1	ELISA	84
2.2.4.2	Immunocytochemistry	86
2.3	Results	88
2.3.1	Cloning of Cκ insert into pEGFP-C1	88
2.3.2	Transfection and Expression of pEGFP-C1-Cκ	96
2.3.3.	Antibody Screening	102
2.3.3.1	ELISA	102
2.3.3.2	Immunocytochemistry	106
2.4	Analysis of Results	110
Chapter 3	Investigating Caspase-3 Expression and Apoptosis in Diffuse Large Cell Lymphoma	113
3.1	Introduction	114
3.2	Materials and Methods	116
3.2.1	Investigation of Caspase-3 Expression and Apoptosis in DLCL	116

3.2.1.1	Diffuse Large Cell Lymphoma cases	116
3.2.1.2	Immunohistochemistry	116
3.2.1.3	In situ end-labelling (ISEL)	117
3.2.1.4	Solid Phase RT-PCR using magnetic oligo(dT) beads	118
3.2.1.5	Scoring Methods	120
3.2.2	Western Blotting of frozen lymphoma tissue	124
3.2.2.1	Protein extraction from frozen lymphoma tissue	124
3.2.2.2	Protein Transfer using NuPage™ Western Blotting	124
3.2.2.3	Detection of protein on nitrocellulose filters	126
3.2.2.4	Antibodies	126
3.3	Results	127
3.3.1	Investigation of Caspase-3 Expression and Apoptosis in DLCL	127
3.3.1.1	Immunohistochemical analysis of Caspase-3 in lymph node and B-cell DLCL	127
3.3.1.2	Apoptotic Rate in Lymph node and B-cell DLCL	128
3.3.1.3	RT-PCR ELISA	128
3.3.1.4	Correlation between Caspase-3 Immunohistochemical analysis and Clinicopathological Factors	129
3.3.1.5	Survival Analysis	129
3.3.1.6	Immunohistochemical investigation of the p17 fragment of Caspase-3 in lymph node and B-cell DLCL	129
3.3.2	Western Blotting of frozen Lymphoma tissue	142
3.4	Analysis of Results	146
Chapter 4	Investigating the <i>in situ</i> localisation of Caspase-3 and its p17 and p12 fragments using Green Fluorescent Fusion Proteins	148
4.1	Introduction	149
4.2	Materials and Methods	150
4.2.1	Cloning of full-length Caspase-3 and its p17 and p12 fragments into pEGFP-C1 vector	151
4.2.1.1	The pEGFP-C1 Plasmid	152
4.2.1.2	Amplification of the coding sequence for Caspase-3 and its p17 and p12 fragments	153

4.2.1.3	Purification and Restriction of the coding sequence for full-length Caspase-3 and its p17 and p12 fragments	153
4.2.1.4	Ligation/Transformation	154
4.2.1.5	Screening of Clones	159
4.2.2	Expression of putative pEGFP-C1 fusion constructs	160
4.2.2.1	Cell lines	160
4.2.2.2	Transfection of MRC5 and MCF-7	162
4.2.2.3	Confocal Laser Scanning Microscopy	162
4.2.2.4	Staining for Mitochondria using MitoTracker™	163
4.2.2.5	Western Blotting of Transfected Cells	163
4.3	Results	165
4.3.1	Cloning of the coding sequence for full-length Caspase-3 and its p17 and p12 fragments into pEGFP-C1 vector	165
4.3.2	Expression of putative pEGFP-C1 fusion constructs	171
4.3.2.1	Western Blotting of Lysates from Cells Transfected with putative clones	171
4.3.2.2	Confocal Laser Scanning Microscopy of Transfected Cells	173
4.4	Analysis of Results	191
Chapter 5	Discussion	
5.1	Discussion	195
6.1	References	208
7.1	Appendix A	237

List of Figures

Chapter 1

Fig. 1.1	Phylogenetic analysis of caspase family members	6
Fig. 1.2	Processing of Caspase-3	10
Fig. 1.3	Proform organisation of the caspases	13
Fig. 1.4	The commitment to die via different pathways for programmed cell death	49

Chapter 2 **Developing Immunodiagnostic tools to detect Apoptosis and Apoptotic Pathways**

Fig. 2.1	Coding Sequence for immunoglobulin G kappa chain mRNA	76
Fig. 2.2	Cloning strategy for the insertion of C κ coding sequence into the pEGFP-C1 MCS in the correct reading frame	77
Fig. 2.3	Amino Acid sequence for Caspase-3	84
Fig. 2.4	Diagrammatic representation of peptide ELISA used to measure the strength of the polyclonal response	86
Fig. 2.5	Diagnostic PCR amplification of human C κ domain using tonsil cDNA as a template	89
Fig. 2.6	PCR Amplification of human C κ sequence	91
Fig. 2.7	Estimation of excised and restricted human C κ amplicon Concentration	91
Fig. 2.8	Double Restriction of mini-prep DNA of putative pEGFP-C1-C κ with <i>Hind III/Sal I</i>	94
Fig. 2.9	Restriction of mini-prep DNA of putative pEGFP-C1-C κ with <i>Hind III</i> only	94
Fig. 2.10	PCR mini-prep of putative pEGFP-C1-C κ clones	95
Fig. 2.11	Transient transfection of human lung MRC5 cells with both the wild-type pEGFP-C1 vector and the pEGFP-C1-C κ vector	96
Fig. 2.12	Western blot of MRC5 cells transfected with pEGFP-C1 and pEGFP-C1-C κ vector and probed with an anti-GFP polyclonal antibody	101
Fig. 2.15	Anti-peptide p12N ELISA results for animals #1 and #2	104

Fig. 2.16	Anti-peptide p17N ELISA results for animals #1 and #2	105
Fig. 2.17	Photomicrographs of tissue sections of human tonsil stained with a variety of anti-Caspase-3 'pre-monoclonal' antibodies	106
Chapter 3	Investigating Caspase-3 Expression and Apoptosis in Diffuse Large Cell Lymphoma	
Fig. 3.1	Mechanism of solid phase RT-PCR using Dynabead™ extraction	121
Fig. 3.2	Design of primers to measure gene expression of Caspase-3	122
Fig. 3.3	ELISA system to detect and quantify RT-PCR products	3.3
Fig. 3.4	Photomicrographs showing immunohistochemical staining of Caspase-3 in reactive tonsil tissue	131
Fig. 3.5	Photomicrographs showing TUNEL staining in reactive tonsil tissue	132
Fig. 3.6	Photomicrograph showing immunohistochemical staining of Bcl-2 in reactive tonsil tissue	133
Fig. 3.7	Photomicrograph showing immunohistochemical staining of Caspase-3 in DLCL case	133
Fig. 3.8	Photomicrograph showing immunohistochemical staining of Caspase-3 and DNA fragmentation by TUNEL staining in DLCL case 06	134
Fig. 3.9	Photomicrograph showing immunohistochemical staining of Caspase-3 and DNA fragmentation by TUNEL staining in DLCL case 25	135
Fig. 3.10	Photomicrograph showing punctate immunohistochemical staining of Caspase-3 in DLCL cases	136
Fig. 3.11	Photomicrograph showing immunohistochemical staining of the active p17 fragment of Caspase-3 in reactive tonsil tissue and DLCL cases	137
Fig. 3.12	RT-PCR amplification of Caspase-3 and GAPDH gene products	139
Fig. 3.13	Cumulative survival curves of patients with B cell DLCL, according to Caspase-3 immunohistochemical localisation, apoptotic rate, Caspase-3 percentage immunostaining and mRNA expression	140
Fig. 3.14	Western Blot of frozen DLCL tissue probed with anti-p85 subunit of P13K	143

Fig. 3.15	Western blot of frozen DLCL tissue probed with anti-active Caspase-3 antibody	144
Fig. 3.16	Western blot of frozen DLCL tissue probed with anti-Caspase-2 antibody	144
Fig. 3.17	Western blot of frozen DLCL tissue probed with anti-FLIP antibody	145
Fig. 3.18	Western blot of frozen DLCL tissue probed with anti-Caspase-8	145
Chapter 4	Investigating the <i>in situ</i> localisation of Caspase-3 and its p17 and p12 fragments using Green Fluorescent Fusion Proteins	
Fig. 4.1	Restriction map of pEGFP-C1 vector	151
Fig. 4.2	Restriction map and Multiple Cloning Site (MCS) of pEGFP-C1	152
Fig. 4.3	Nucleotide sequence for Caspase-3	155
Fig. 4.4	Cloning strategy for the insertion of the coding sequence for full-length <i>Caspase-3</i> into the pEGFP-C1 MCS in the correct reading frame	156
Fig. 4.5	Cloning strategy for the insertion of the coding sequence for p17 fragment of <i>Caspase-3</i> into the pEGFP-C1 MCS in the correct reading frame	157
Fig. 4.6	Cloning strategy for the insertion of the coding sequence for p12 fragment of <i>Caspase-3</i> into the pEGFP-C1 MCS in the correct reading frame	158
Fig. 4.7	Nucleotide sequence of pEGFP-C1	161
Fig. 4.8	PCR amplification of the coding sequence for Caspase-3 and its p12 and p17 fragments	167
Fig. 4.9	Estimation of excised and restricted DNA sequences for full-length Caspase-3 and its p12 fragment	167
Fig. 4.10	Screening for putative pEGFP-C1-Caspase-3 clones using colony mini-prep PCR	170
Fig. 4.11	Double <i>Hind III/Sal I</i> restriction analysis of putative pEGFP-C1-Caspase-3 and pEGFP-C1-p17 clones	170
Fig. 4.12	Western blot of MRC5 cells transfected with pEGFP-C1 and	

	putative clones and probed with anti-Caspase-3 polyclonal antibody	175
Fig. 4.13	Western blot of MRC5 cells transfected with pEGFP-C1 and putative clones and probed with anti-GFP polyclonal antibody	175
Fig. 4.14	Screening of putative clones using primers flanking the MCS of pEGFP-C1	175
Fig. 4.15	Screening of putative clones using double <i>Hind III/Sal I</i> restriction	
Fig. 4.16	Western blot of MCF-7 cells transfected with pEGFP-C1 and pEGFP-C1-p17 and probed with anti-active Caspase-3 polyclonal antibody	179
Fig. 4.17	Western blot of MCF-7 cells transfected with pEGFP-C1 and pEGFP-C1-p17 and probed with anti-GFP polyclonal antibody	179
Fig. 4.18	Western blot of MCF-7 cells transfected with pEGFP-C1 and pEGFP-C1-p17 and probed with anti-Caspase-8	181
Fig. 4.19	Western blot of MCF-7 cells transfected with pEGFP-C1 and pEGFP-C1-p17 and probed with anti-Caspase-9	181
Fig. 4.20	Confocal Microscopic images of MRC5 cells transfected with pEGFP-C1 after 24 hours	182
Fig. 4.21	Confocal Microscopic images of MCF-7 cells transfected with pEGFP-C1 and pEGFP-C1-p17	185

List of Tables

- | | | |
|-----|---|-----|
| 2.1 | Transformation efficiencies for each cloning regime used in the ligation reaction for the insertion of C κ into the pEGFP-C1 vector and the subsequent transformation into competent DH5 α bacterial cells | 92 |
| 3.1 | Caspase-3 percentage immunostaining and mRNA expression, apoptotic rate and Caspase-3 immunohistochemical localisation of patients with B cell DLCL | |
| 3.2 | Correlation between clinicopathological factors and immunohistochemical localisation, percentage of immunostaining and quantitative RT-PCR analysis for <i>Caspase-3</i> and TUNEL positivity | 140 |
| 4.1 | Transformation efficiencies for each cloning regime used in the ligation reactions for the insertion of the coding sequence of full-length Caspase-3 and its p17 and p12 fragments into pEGFP-C1 vector and the subsequent transformation into competent DH5 α bacterial cells | 168 |

Abbreviations

AIF	apoptosis-inducing factor
ANT	adenine nucleotide translocator
ATP	adenosine triphosphate
BCIP	5' bromo-4' chloro-3' indoyl phosphate
bp	base pair
BSA	bovine serum albumin
CARD	caspase recruitment domain
cDNA	complementary DNA
CHOP	cyclophosphamide, adriamycin, vincristine, prednisone
CoCl ₂	cobalt chloride
CrmA	cowpox response modifier A
DcR	decoy receptor
DD	death domain
DED	death effector domain
DEPC	diethyl pyrocarbonate
dH ₂ O	distilled water
DISC	death induction signalling complex
DLCL	diffuse large cell lymphoma
DNA	deoxyribonucleic acid
DNase	deoxyribonuclease
dNTP	deoxynucleotide triphosphate
DR	death receptor
DTT	dithiothreitol
EBV	epstein-barr virus
EDTA	ethylene diaminetetraacetate
ELISA	enzyme-linked immunosorbent assay
(E)GFP	(enhanced) green fluorescent protein
ER	endoplasmic reticulum
ES	embryonic stem
EF	embryonic fibroblast
FADD	FLICE-activated death domain

ISEL	in-situ end labelling
FLIP	FLICE-inhibitory protein
GAPDH	glyceraldehyde 3-phosphate dehydrogenase
G-CSF	granulocyte-colony stimulating factor
HPV	human papilloma virus
IMS	industrial methylated spirits
Kb	kilobase
KOAc	potassium acetate
LiCl	lithium chloride
MEM	minimal essential media
MgCl ₂	magnesium chloride
NBT	nitroblue tetrazolium
NGF	nerve growth factor
PCR	polymerase chain reaction
PIGs	p53-inducible genes
PT	permeability transition
RNase	ribonuclease
ROS	reactive oxygen species
RPMI	Roswell Park Memorial Institute
RT	reverse transcriptase
SDS	sodium dodecyl sulphate
<i>Taq</i>	<i>Thermus aquaticus</i>
TBE	Tris-borate-EDTA
TBS	Tris buffered Saline
TE	Tris-EDTA
TEMED	N,N,N',N'-tetramethylenediamine
TNF	tumour necrosis factor
TRADD	TNF receptor associated death domain
TRAF	TNF receptor associated factor
TRAIL	TNFR apoptosis-inducing ligand
Tris	tris(hydroxymethyl)amino methane

Certainties!!

**If a man will begin with certainties, he shall end in doubts;
but if he will be content to begin with doubts, he shall end in
certainties.**

Francis Bacon

Chapter 1

INTRODUCTION

1.1 INTRODUCTION

At the heart of the apoptotic process is a large family of enzymes known as caspases (Thornberry and Lazebnik 1998). These are cysteine proteases that become activated after cleavage and act upon a range of substrates to bring about the morphological features of apoptosis. The activity of caspases is positively and negatively regulated by the Bcl-2 family of proteins (Reed *et al.* 1998). Other proteins, such as the inhibitor of apoptosis (IAP) family (LaCasse *et al.* 1998) and Flice-inhibitory protein (FLIP) also function by negatively regulating the cleavage of certain members of the caspase family (Irmeler *et al.* 1997).

A cell can receive a variety of signals to induce the activation of caspases and bring about apoptotic cell death. One of the most important types of signal is transduced by a family of receptors known as the 'death receptors'. The Fas receptor is a crucial member of this family and is especially important in lymphocyte homeostasis. Using adapter proteins some of these 'death receptors' directly engage caspases and bring about their activation. Other types of apoptotic cell death signals can damage DNA or signalling or cytoskeletal proteins. These insults include chemical treatment, UV or gamma irradiation, serum deprivation and heat shock. It is now believed that the majority of these types of signalling engage the mitochondria eventually to link with the caspase machinery to bring about apoptosis. Therefore, two broadly divergent pathways for apoptotic cell death signalling – receptor-mediated versus chemical/damage-induced – are beginning to emerge.

Knockout experiments have confirmed that some caspases act in an extremely tissue-, cell type- and stimulus-dependent manner (Zheng *et al.* 1999). Many other lines of evidence indicate that the concentrations of caspase family members (Donoghue *et al.* 1999), and the various proteins involved in their regulation, such as the Bcl-2 family of proteins, are crucial for the capacity of a cell to die. Important evidence is also beginning to emerge that the subcellular localisation of certain members of the caspase and Bcl-2 family has an impact on the apoptotic threshold of a cell (Lee *et al.* 1999; Zhivotovsky *et al.* 1999). Finally, both the concentration and the subcellular localisation of key caspases, and their regulators, may determine the type of apoptotic pathway –

receptor-mediated versus chemical/damage-induced – that is optimal for cell death (Sun *et al.* 1999).

Apoptotic cell death is known to be extremely important in the maintenance of lymphocyte homeostasis (Nagata 1996). Furthermore, resistance to apoptosis is thought to contribute to the emergence of lymphoid malignancies (Thompson 1995). Moreover, chemoresistant cells are also believed to be resistant to apoptotic cell death (Hannun 1997). Therefore, investigating the expression and localisation of the caspase family of enzymes is crucial for the understanding of the tumorigenesis of lymphoma and the successful treatment of the disease.

1.2 Apoptosis

1.2.3 Morphological and Biochemical Events of Apoptosis

Apoptosis is a morphologically distinct form of cell death that is involved in many physiological and pathological processes. The earliest changes in apoptosis occur in the nucleus where chromatin is compacted and segregated into sharply circumscribed masses that abut on the inner nuclear envelope. Concomitant with these changes, the cell condenses, rounds up, and in tissues, pulls away from its neighbours. Convolution of nuclear and cell outlines then ensues and is followed by the “budding” of the cell with a number of discrete membrane-bounded fragments called apoptotic bodies (Kerr 1971).

During apoptosis the nuclear DNA is degraded. In many cell types, DNA is degraded into fragments the size of oligonucleosomes, whereas in others large DNA fragments are produced (Bortner *et al.* 1995). This is the most commonly recognised biochemical event of apoptosis and if agarose gel electrophoresis is performed a ladder of DNA is observed. This technique has often been used to identify apoptosis, but is not detectable in all cell types (Huang *et al.* 1995). Apoptosis is also characterised by a loss of mitochondrial function (Kerr *et al.* 1972).

When these apoptotic bodies are formed *in vivo* they are rapidly engulfed and phagocytosed by surrounding resident cells or macrophages and degraded within phagolysosomes. Apoptotic bodies formed *in vitro* are seldom phagocytosed and

eventually undergo degenerative changes that have some semblance with necrosis; the term “secondary necrosis” is often applied to this change. The controlled autodigestion of a cell during apoptosis is an extremely important characteristic. It is believed that alterations in the plasma membrane of these cells signal neighboring phagocytic cells to engulf them. Thus, the apoptotic dying cell maintains its plasma membrane integrity and consequently no inflammatory response is initiated (Kerr *et al.* 1972).

1.3 Apoptosis and Disease

Because apoptosis is an integral part of the development programme, and is frequently the consequence of a temporal course of cellular events, it is sometimes referred to as programmed cell death (PCD). Apoptosis has been shown to be involved in cell turnover in many healthy adult tissues and responsible for the elimination of cells during normal embryonic development (Clarke 1990). Furthermore, it has been shown to participate in normal physiological involution (e.g. endometrium) and pathological atrophy of various tissues and organs (e.g. castration - induced involution of rat prostate). It occurs spontaneously in many malignant neoplasms and is enhanced in regressing tumours following some forms of therapy (Ellis *et al.* 1991).

What has propelled apoptosis into the forefront of basic research has been the identification of genes that control cell death (Thornberry 1997) and the appreciation of the role of apoptosis in development and disease. For each cell type, the control of cell number is a delicate balance between cell proliferation and cell death. Regulation of cell death is now recognised as essential for normal development and important defence against viral infection and the emergence of cancer. Too much cell death can lead to impaired development and degenerative diseases, whereas too little cell death can lead to cancer, persistent viral infection and emergence of autoimmune disorders (Thompson 1995). Specific therapies designed to enhance or decrease the susceptibility of individual cell types to undergo apoptosis could form the basis for treatment of a variety of human diseases.

1.4 Caspases

Genetic analyses in the nematode *Caenorhabditis elegans* identified two genes, *ced-4* and *ced-3*, that are necessary for the cell death process (Miura *et al.* 1993). The cloning of *ced-3*, a gene that encodes a protease with homology to mammalian interleukin-1 β -converting enzyme, provided the first indication that cysteine proteases are critical components of the cell death machinery (Yuan *et al.* 1993). This observation led to the discovery and identification of a growing family of cysteine proteases with homology to *ced-3* that have been designated caspases, a family of cysteinyl aspartate-specific proteinases (Alnemri *et al.* 1996).

So far, more than 14 caspases have been cloned and partially characterised in mammals and most, but not all, have been implicated in apoptotic cell death (Ahmad *et al.* 1998). These enzymes are synthesised in the cell as inactive precursors with little, if any, activity that become activated after apoptotic insult. Caspases are composed of three or four distinct domains: an amino-terminal region of variable size – the prodomain -, a large subunit and a small subunit. Some of the enzymes also possess a linker region between the large and small subunits flanked by aspartate (Asp) residues (Thornberry 1997). These enzymes are activated by proteolytic cleavage between domains, resulting in the removal of the prodomain and the linker regions, if present, and the formation of the large and small subunits into an active enzyme complex (Cohen 1997).

1.5 Classification of Caspases

A variety of analyses have been made to classify caspases. A phylogenetic analysis (see Fig.1.1) suggests that the gene family can be classified into two families; those enzymes related to ICE (Caspase-1) or to the mammalian counterparts of CED-3 (Nicholson 1999). Less rigidly, mammalian caspases have been divided into upstream (initiator or activator) and downstream (effector) caspases based on their chronological activation after apoptotic stimuli. Finally, caspases have been divided into three major groups based on their substrate specificities: Group I (LEHD), Group II (DEXD), and Group III (V or L EXD). A comparison of these specificities with sequences found in

known substrates suggests that Group I enzymes are associated with the production of inflammatory cytokines, while Group II and Group III enzymes function primarily as effectors and activators, respectively, of apoptosis (Thornberry 1997). Initiator caspases have long prodomains containing sequences that physically link these proteases to specific activators.

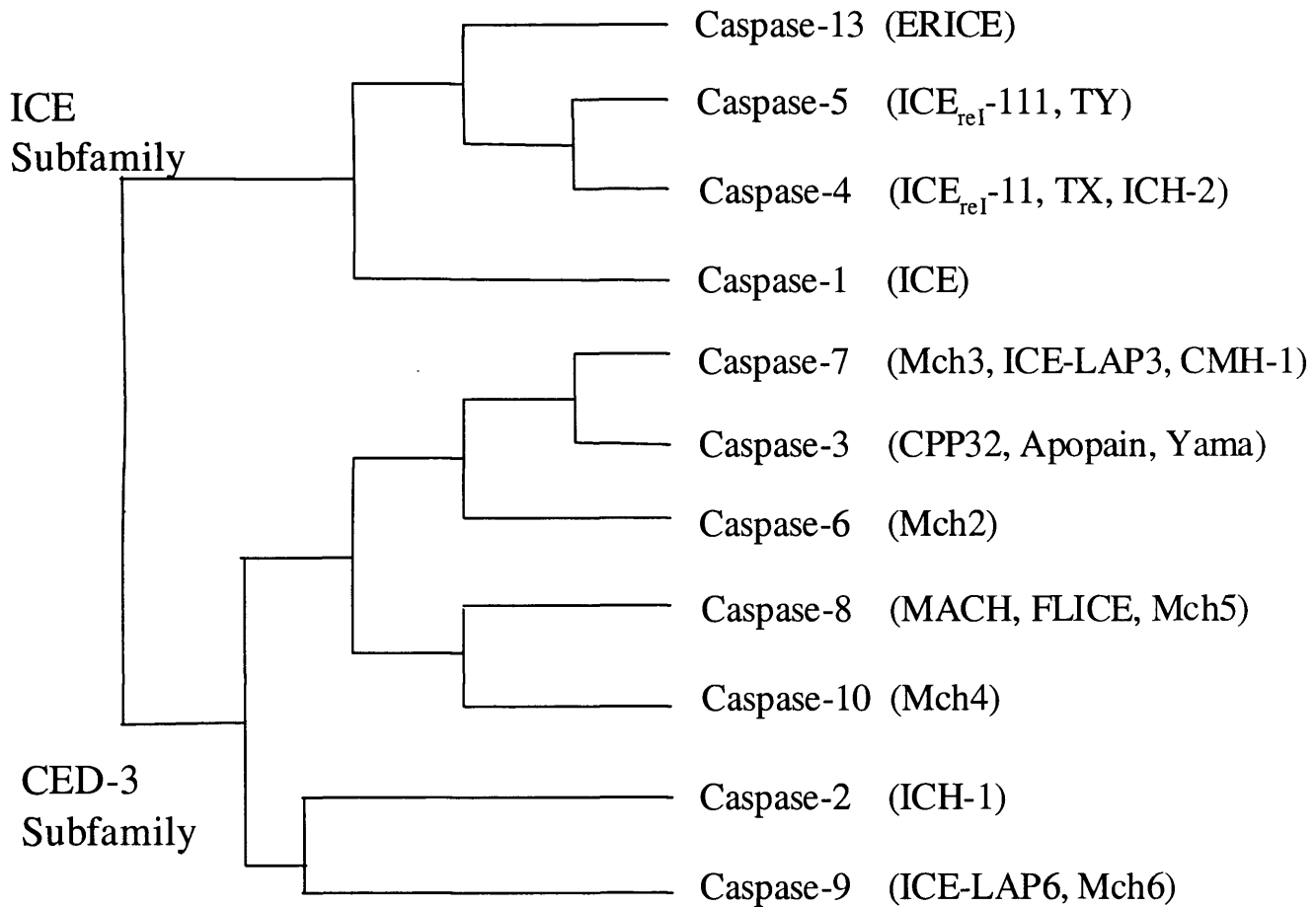


Fig. 1.1 Phylogenetic analysis of caspase family members. The relationships are based on the full-length proenzymes. Caspases can be divided into two major sub-families (ICE and CED-3). Based on their proteolytic specificities, caspases can be further divided into three groups: group I – enzymes involved in cytokine maturation (Caspases -1, -4, -5 and -13); group II – enzymes involved in machinery of cell death (Caspases-3, -6 and -7); group III – enzymes involved in the upstream activation of cell death (Caspases-2, -9, -8 and -10). The original names for the enzymes are illustrated in brackets.

Two types of interaction modules have been detected in the prodomains of initiator caspases: death effector domain (DED) or caspase recruitment domain (CARD). Mammalian caspases-1, -2, -4, -5, -8, -9, -10, -11 -12 and -13 have prodomains with DEDs or CARDS. These domains are believed to physically connect or aggregate initiator caspases with specific regulatory molecules via homophilic interactions. In contrast, caspase-3, -6, -7 and -14 have short prodomains without any observed sequence motifs.

Most importantly, initiator caspases have substrate specificities that are similar to caspase recognition sites present in their own sequence, suggesting that these enzymes are capable of autocatalysis under appropriate conditions (Garcia-Calvo *et al.* 1999). In addition, optimal caspase recognition sites for initiator caspases are present in the sequences of the effector caspases, indicating that these enzymes act downstream in the proteolytic cascade. In short, caspase precursor enzymes are proteolytically cleaved by themselves or by other active caspases.

1.6 Specificity and Structure

Although caspases share an absolute requirement for cleavage after Asp residues at the substrate P1 site, they are very specific in their substrate preferences. This specificity is largely determined by the sequence of four amino acids at the NH₂ – terminal end of the P1 site (Nicholson 1999). In fact, there is an equally stringent requirement for four amino acids to the left of the cleavage site. The P4 residue appears to be the most important amino acid for determining specificity. This P4 binding site (S4) varies markedly between the different caspase family members. A comparison of Caspase-1 versus Caspase-3 illustrates this persuasively, in that the S4 subsites vary radically in both geometry and chemical nature.

The X-ray crystal structure of both Caspase-1 (Walker *et al.* 1994) and Caspase-3 (Wilson *et al.* 1994; Rotonda *et al.* 1996), in complex with specific tetrapeptide inhibitors that bind in the S₁-S₄ sites usually occupied by a peptide substrate, has been determined. In both cases the active protein consists of two small (p10 or p12; Caspase-1 or Caspase-3) subunits surrounded by two large (p20 or p17; Caspase-1 or Caspase-3)

subunits, with most of the area of contact between the dimers occurring between the small subunits. The active site spans both the large and small subunits and explains the necessity for both for activity. For example, the active site pentapeptide, Gln-Ala-Cys-Arg-Gly (QACRG), of Caspase-1 is in the p20 subunit. Nevertheless, residues involved in forming the Asp pocket include Arg-179, Gln-283, Arg-341 and Ser-347, with only the first two present on the p20 subunit.

The most favourable model for activation of the enzyme involves the processing of two precursor proteins after their association, with the small subunit from one caspase protein complexing with the large subunit from another caspase molecule (Rotonda *et al.* 1996, Nicholson *et al.* 1996). The pro-domain from the enzyme is absolutely required for dimerisation and autoproteolysis. The subunits of each heterodimer fold into a compact cylinder that is dominated by a central six-stranded β sheet and five helices which are distributed on opposing sides of the plane formed by the β sheets. In the caspase tetramer, two of these cylinders align in a head to tail configuration, thereby positioning the two active sites at opposing ends of the molecule.

1.6.1 Caspase-1

Initially work on Caspase-1 focused on its ability to cleave the inactive 31kDa cytokine pro-IL-1 β to generate the active 17kDa mature form of IL-1 β , to produce a key inflammatory protein (Howard *et al.* 1991). Cloning of Caspase-1 revealed that it is a 45kDa protein (Miura *et al.* 1993). The active enzyme consists of two subunits of 20 kDa and 10kDa (p20 and p10 respectively) both of which are required for catalytic activity and are produced following cleavage of an 11kDa terminal peptide (pro-domain) and a 2kDa linker peptide (Thornberry *et al.* 1992). After the initial cleavage at Asp-297--Ser-298, autoproteolysis occurs and culminates in an active p20/p10 protease. It is believed that the intermediary cleavage products may have enzymatic activity. In addition, at least four alternatively spliced isoforms of Caspase-1 have been identified (Alnemri *et al.* 1995).

1.6.2 Caspase-2

Caspase-2 (Ich-1) was originally cloned from a human foetal brain cDNA library (Kumar *et al.* 1994). As with the majority of caspases the active site pentapeptide

QACRG was conserved. The *Ich-1* mRNA is alternatively spliced into two forms *Ich1_L* and *Ich1_S*. Overexpression of the longer *Ich-1_L* protein has been shown to suppress apoptosis in certain systems, whereas overexpression of *Ich-1_S* suppresses apoptosis induced by serum withdrawal (Kumar *et al.* 1997). This suggests that *Ich-1* may be the first caspase to be discovered with dual roles; one protein positively regulating cell death and the other protein negatively.

During embryonic development, *Nedd2* is expressed at high levels in various tissues including the liver, kidney and lungs. *Nedd2* is also expressed in several adult tissues, including post-mitotic neurons. Asp-133 is believed to be the cleavage site to produce a p20 fragment and Asp-347 appears to generate a p10 fragment (Kumar *et al.* 1997). These proposed cleavage sites are preserved in *Caspase-2*. As yet, no specific intracellular protein substrates for *Caspase-2* have been discovered.

1.6.3 *Caspase-3*

Caspase-3 (CPP32, Apopain, Yama) was originally cloned from a Jurkat cDNA cell library (Nicholson *et al.* 1995). The enzyme is expressed in many tissues, especially those of lymphocytic origin. This indicates that it may be important in the regulation of the immune system. Using both mass spectroscopy (MS) and N-terminal sequence analysis, the active enzyme was shown to be composed of two subunits of 17kDa and 12kDa derived from the precursor by cleavage at Asp-28 –Ser-29 and Asp-175 –Ser-176 (Fernandes-Alnemri *et al.* 1996). The initial cleavage is probably between the large and small subunit, however it has been suggested that processing within the prodomain occurs initially at Asp-9 and not Asp-28.

In contrast to *Caspase-1*, *Caspase-3* has no linker peptide and the prodomain is much shorter. *Caspase-3* prefers a DXXD-like substrate, whereas *Caspase-1* prefers a YVAD-like substrate. Both enzymes appear to have an absolute requirement for an Asp in the P1 position and both can tolerate a fair degree of substitution in the P2 and P3 positions, but in the P4 position *Caspase-1* prefers a hydrophobic amino acid such as Tyr, whereas *Caspase-3* prefers Asp.

Caspase-3 is frequently activated in apoptotic cell death and is believed to be responsible for the cleavage of the majority of substrates and is classified as a Group II

enzyme. It is therefore a crucial enzyme with respect to the morphological appearance of apoptosis. The sequence of events to bring about the cleavage and activation of Caspase-3 are amongst the most studied within the caspase family and are shown in Fig. 1.2. For a putative effector protease Caspase-3 is also capable of cleaving a variety of caspases very efficiently *in vitro*.

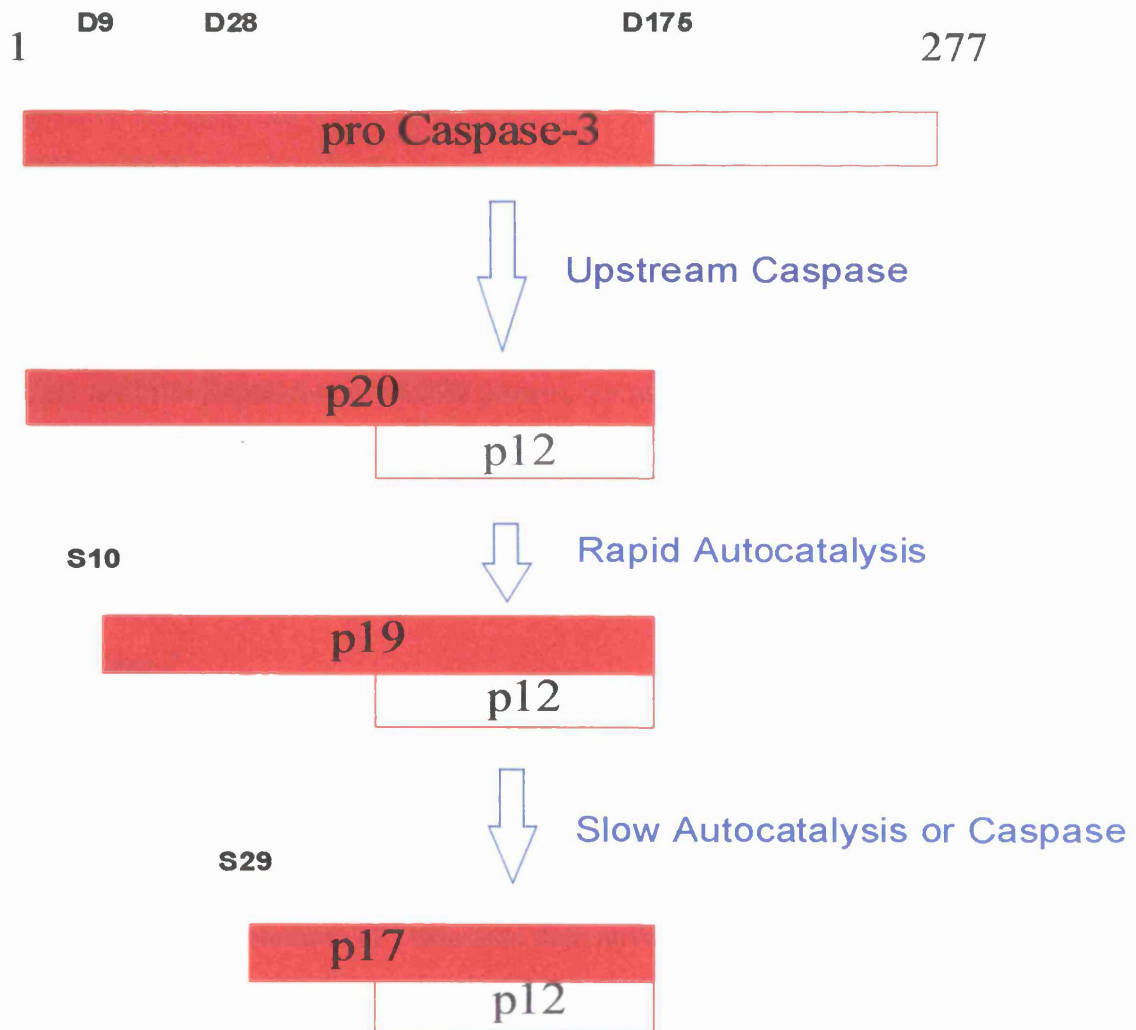


Fig. 1.1 Processing of Caspase-3. The initial cleavage occurs after aspartate 175 and this generates a p12 fragment that is believed to dimerise with a larger p20 fragment. Rapid autocatalysis is then believed to generate a p19 fragment with cleavage aspartate 9. Finally, the p19 fragment is cleaved to a p17 fragment. This may occur due to a caspase or autocatalysis. This is believed to be the final product of Caspase-3 processing. **Source: Fernandes-Alnemri *et al.* 1996**

1.6.4 Caspase-4 and -5

Both Caspase-4 and -5 are members of the Caspase-1 subfamily (Group I) and are more closely related to each other than any other homologues (Faucheu *et al.* 1996). The tissue distribution of Caspase-4 is similar to Caspase-1, with notable exceptions. Caspase-4 is found in both ovary and placenta, where Caspase-1 is barely detectable. In general, Caspase-5 is expressed at much lower levels than Caspase-4. The exact cleavage sites at which Caspase-4 and -5 are processed is still controversial.

1.6.5 Caspase-6

Caspase-6 (Mch2) was originally cloned from a human Jurkat T lymphocyte cDNA library (Fernandes-Alnemri *et al.* 1995). Two transcripts, *Mch2 α* and *Mch2 β* , were detected. The former encodes for the full length enzyme, and the latter encodes for a shorter isoform. Expression of Mch2 α protein, but not Mch2 β , results in apoptotic cell death in insect cells. Caspase-6 is a member of the CED-3 subfamily and is closely related to Caspase-3. The enzyme is believed to be primarily responsible for the cleavage of lamin.

1.6.6 Caspase-7

Caspase-7 is also a member of the CED-3 subfamily and is closely related to Caspase-3 (Pai *et al.* 1996). In addition, an alternatively spliced isoform of the enzyme, which may act as a negative regulator of apoptosis, has been described. Overexpression of full length Caspase-7 protein in MCF-7 breast carcinoma cell lines does not induce apoptosis, whereas expression of a truncated derivative, lacking the residues corresponding to the putative prodomain, induces apoptotic cell death.

1.6.7 Caspase-8

Caspase-8 (FLICE/MACH) contains both a subunit with homology with caspases and an N-terminal prodomain with homology with the N-terminal DED of an adapter protein named FADD (Irmeler *et al.* 1997). This protein is a member of the CED-3 subfamily, contains a long prodomain and is also regarded as an activator (Group III). Caspase-8 is a very important enzyme as it is believed to be crucial for cell death induction by members of the Fas and Tumour Necrosis Factor (TNF) receptor family through its involvement in the death induction signalling complex (DISC). The enzyme

occurs in multiple isoforms and Northern blot analysis revealed a heterogeneity of transcripts which varied in amount and size in different human tissues. A high level of expression is observed in tissues of lymphocytic origin, again indicating a role in lymphocyte homeostasis.

Overexpression of Caspase-8 results in apoptosis, however, expression of the enzyme in the presence of isoforms markedly reduces cell death induction. This suggests the isoforms may exert a dominant-negative effect and may be important in the regulation of apoptosis *in vivo*. It has been suggested that the heterogeneity of isoforms of Caspase-8, compared with other caspases, points to the importance of the enzyme in regulating cell death after Fas and TNF ligation. Most importantly, *in vitro* experiments indicate that recombinant Caspase-8 is remarkably efficient at activating all human caspases, however its most preferred substrate appears to be Caspase-3.

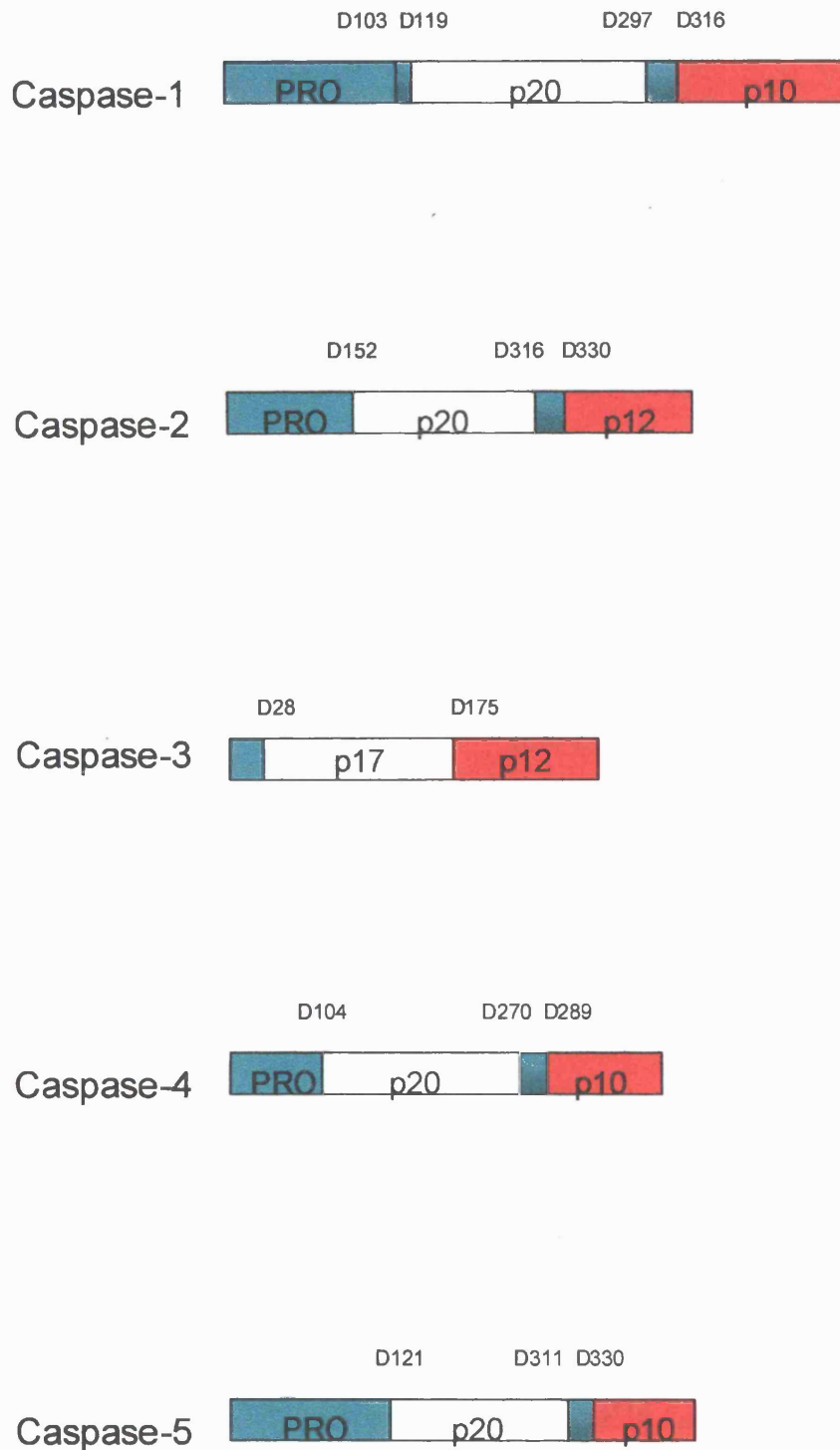
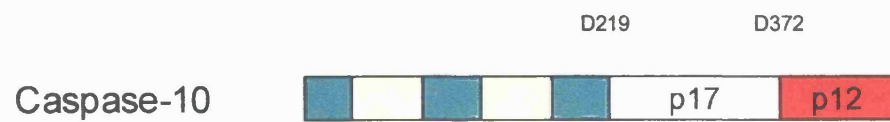
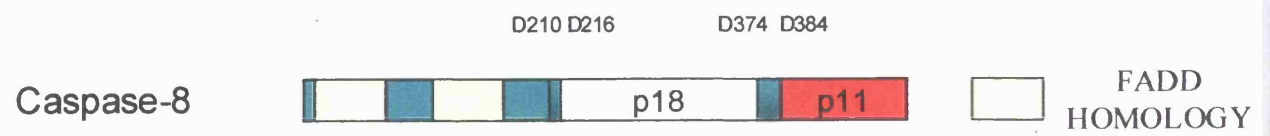
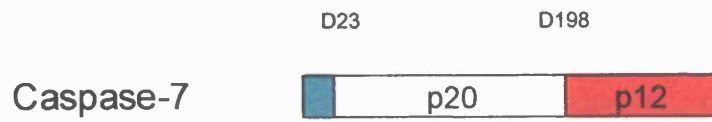
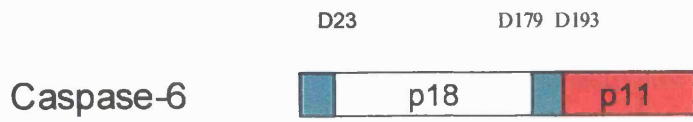


Fig. 1.2 Proform organisation of the caspases. All enzymes (Caspases 1-10) are synthesised as proenzymes that encode an N-terminal domain, and a large and small subunit that constitute the mature, heterodimeric enzyme. In some cases there is a linker peptide between the two subunits of the heterodimer. The proenzymes are cleaved at specific Asp (D) residues.



1.6.8 Caspase-9

Caspase-9 (ICE-LAP6/Mch6) is a member of the CED-3 subfamily, with a large prodomain, and is therefore regarded as an activator (Group III) of the proteolytic cascade (Duan *et al.* 1996). Its prodomain also has a high degree of homology with the prodomain of Caspase-2. Northern blot analysis revealed the presence of multiple RNA species, suggesting alternatively spliced isoforms.

Caspase-9 has been shown to be extremely important in its interaction with Apaf-1, an adapter protein containing a CARD. The Bcl-x_L/Apaf-1/Caspase-9 complex is believed to be the human counterpart of the CED-9/CED-4/CED-3 ternary complex observed in *C. elegans* (Pan *et al.* 1998). The formation of the apoptosome, with Apaf-1, Caspase-9, cytochrome c and dATP results in the activation and recruitment of Caspase-3 and the concomitant apoptotic cell death (Li *et al.* 1997). Interestingly, active Caspase-3 is also very efficient at activating Caspase-9.

1.6.9 Caspase-10

Caspase-10 (Mch4) was also cloned from a Jurkat cell cDNA library (Fernandes-Alnemri *et al.* 1996). Caspase-10 is another member of the CED-3 subfamily, and is very closely related to Caspase-8. Like Caspase-8, Caspase-10 has an active site QACQG pentapeptide and also contains two FADD-like DEDs in its N-terminal domain.

1.7 Biological Caspase Inhibitors

1.7.1 CrmA

The first caspase inhibitor to be identified was the Cowpox virus product Cytokine Response Modifier A (CrmA) and this was found to bind to active Caspase-1 to reduce the defensive inflammatory response triggered after activation of IL-1 β by the enzyme (Ray *et al.* 1992). CrmA can also bind to and inhibit Caspase-8 and this prevents apoptosis triggered by activation of Fas receptor. Structurally CrmA belongs to the serine protease inhibitor (serpin) group, but unlike other serpins, it inhibits caspases.

A mammalian homologue of CrmA, the cytotoxic lymphocyte serpin proteinase inhibitor 9 (PI-9 – also known as Granzyme B inhibitor (GBI)), can protect against Granzyme B-mediated apoptosis, but not against TNF receptor-mediated apoptosis (Bird *et al.* 1998).

1.7.2 p35

Baculoviruses produce a protein p35 that can block the defensive apoptotic response of insect cells to viral infection (Clem *et al.* 1991). p35 can inhibit CED-3 and mammalian caspases -1, -3, -6, -7, -8 and -10 with relative efficiency (Zhou *et al.* 1998). After cleavage by a caspase p35 forms a complex with the active enzyme and blocks its ability to bind other proteins. The p35 protein is highly efficient at inhibiting apoptosis in different species. In *Drosophila*, transgenic expression of p35 can prevent apoptotic death of cells in the embryo and eye (White *et al.* 1996).

1.7.3 IAPs

Crook *et al.* (Crook *et al.* 1993) identified a family of proteins in baculoviruses they designated inhibitor of apoptosis proteins (IAPs) because these proteins could inhibit the apoptotic response of insect cells to viral infection. Baculoviral IAP proteins typically have two N-terminal repeats designated baculovirus IAP repeats (BIRs) and a C-terminal RING finger domain. At least five mammalian homologues of these proteins have now been identified; XIAP (MIHA), HIAP-1 (MIHC), HIAP-2, NAIP and Survivin (LaCasse *et al.* 1998). All members of this family bear from one to three baculoviral IAP repeats (BIRs) which are responsible for the interactions between IAPs and other proteins. NAIP is unique in that it has no C-terminal RING finger domain. Most importantly, Survivin and XIAP, in particular, have been reported to bind to and inhibit Caspase-3 and Caspase-7 very efficiently (Deveraux *et al.* 1997; Tamm *et al.* 1998).

The mRNA transcription distribution for each of these IAPs can vary significantly. *Xiap-1* mRNA was observed in all adult and foetal tissues examined except peripheral blood leukocytes (Deveraux *et al.* 1997). *Hiap-1* mRNA displayed a unique foetal distribution, in which lung and kidney, but not brain or liver, expressed high levels of the transcript. In the adult *Hiap-1* mRNA was highly expressed in lymphoid tissues. *Hiap-2* mRNA was present in many foetal and adult tissues, but was

most highly expressed in adult skeletal muscle and pancreas (Roy *et al.* 1997). Survivin is expressed in cells that are rapidly dividing, including embryonal tissues and tumour lines, but not in adult tissues (Ambrosini *et al.* 1997).

Controversially, emerging evidence suggests these IAPs may function in cytokinesis as well as, or perhaps rather than, the regulation of apoptosis. Survivin, which is expressed in highly proliferative cells, can associate with tubulin (Li *et al.* 1998). In common with many transformed cell lines, Jurkat T cells express abundant Survivin but remain sensitive to killing after Fas and dexamethasone treatment and Bax overexpression. Therefore, Survivin's function may not be to regulate apoptosis but to direct events during cell division. This proposal has been strengthened by the observation that a role for yeast IAPs in cell division has been determined recently (Uren *et al.* 1999). Also, when apoptosis is inhibited by XIAP, HIAP-1 or HIAP-2, the cells do not accumulate cleaved caspases complexed with the IAPs, but instead are found to have increased numbers of pro-caspases. This also implies a role in cell division. Most interestingly, HIAP-1 and -2 can bind to TNF receptor associated factors TRAF1 and TRAF2 in yeast two-hybrid assays, and HIAP-1 and -2 have been found in protein complexes with the TNF-R2 cytoplasmic domain in mammalian cells (Roy *et al.* 1997).

1.7.4 FLIP

FLIP (FLICE-inhibitory protein) contains DED motifs at its amino-terminus and through them it can bind to other DED-containing proteins. The FLIP mRNA contains two splice variants. FLIP_L contains a region that closely resembles the carboxy-terminal-protease-precursor regions in Caspase-8 and Caspase-10. However, in FLIP_L this region lacks several of the sequence features required for protease activity. It is believed that FLIP blocks death induction via the TNF receptor family by interfering with the binding of DED-containing caspases to FADD. Furthermore, binding of the carboxy-terminal region in FLIP to Caspase-8 and -10 may constitute a further inhibitory mechanism, preventing the proteolytic self-processing of the caspases (Tschopp *et al.* 1998). Interestingly, another group (Rasper *et al.* 1998) have cloned the gene encoding the same protein and named it Usurpin. They propose that at least three isoforms of the enzyme (α , β , χ) exist arising from alternative mRNA splicing

1.8 Synthetic caspase inhibitors

The substrate cleavage sites of the caspases have formed the basis for the development of a number of caspase inhibitors with a range of specificities. Generally these peptides act as pseudosubstrates for active caspases and therefore as competitive inhibitors. Most peptide inhibitors used are trimers (e.g. Benzyloxycarbonyl-val-ala-asp (OMe) fluoromethylketone: z-VAD.fmk) Peptides linked to fluoro-methyl ketone groups produce irreversible, competitive inhibitors, whereas peptides linked to aldehyde groups (CHO) act as reversible inhibitors (Thornberry *et al.* 1994; Thornberry *et al.* 1997).

The activity of these peptide caspase inhibitors is partially determined by their membrane permeability. The fmk adducts are much more permeable than their aldehyde counterparts and hence more effective at inhibiting caspases. In general, the shorter peptides are more permeable than the tetramers. Most importantly, the range of specificity of these caspase inhibitors varies enormously. Z-VAD.fmk, z-DEVD.fmk and Ac-YVAD.cmk are all capable of binding and inhibiting some serine proteases, such as Cathepsin B, at concentrations known to be physiologically relevant *in vivo* (Schotte *et al.* 1999). Probably the only enzyme-specific inhibitor is YVAD-CHO, which binds to Caspase-1 with extreme efficiency. However, the other caspase inhibitors do not target individual caspases. For example, while it is not usually regarded as a broad range caspase inhibitor and potently inhibits Caspase-3, DEVD-CHO also strongly inhibits Caspase-7 and -8. Z-VAD-CHO can strongly inhibit Caspase-1, -3, -5, -7, -8 and -9, but is not a good inhibitor of Caspase-2.

1.9 Substrates

So far, more than 70 proteins have been found to be cleaved by caspases (Stroh and Schulze-Osthoff 1998), and new substrates are continuously being discovered. The known substrates can be loosely categorised into a few functional groups including proteins involved in scaffolding of the cytoplasm and nucleus, signal transduction and transcription-regulating proteins, cell-cycle controlling components and proteins involved in DNA replication and repair. Furthermore, activation of members of the first

subfamily of caspases, Caspase-1 and presumably Caspase-4 and -5, results in the processing of cytokine precursors (Zeuner *et al.* 1999). The exact role of these proteins in cell death remains obscure.

Most substrates are functionally inactivated upon caspase cleavage, mostly by cleavage of an inhibitory or regulatory domain within the substrate. A number of structural proteins in the cell nucleus and cytoplasm are known to be caspase substrates such as fodrin (Cryns *et al.* 1996), catenins (Brancolini *et al.* 1997), Gas2 and lamins (Rao *et al.* 1996). Degradation of lamin b leads to disassembly of the nuclear envelope and is carried out solely by Caspase-6. Cleavage of gelsolin (Kothakota *et al.* 1997), a cytoplasmic actin-severing protein, contributes to membrane blebbing and other morphological features of the apoptotic phenotype. Caspase-3 cleaves gelsolin to generate a constitutionally active fragment that can de-polymerise F-actin. Interestingly, it has been reported that actin can be directly cleaved by caspases in ovarian carcinoma cells whereas in many other cell types no cleavage could be detected (Kayalar *et al.* 1996). Therefore, it is likely that certain protein cleavages may be cell type-specific that may also be due to variations in the expression of individual caspases in different cell types.

Activation of caspases may also be required for the detachment and clearance of an apoptotic cell from the embedding tissues as illustrated by the cleavage of substrates β -catenin (Brancolini *et al.* 1997) and focal adhesion kinase (Crouch *et al.* 1996). A large number of caspase targets are involved in cell cycle and DNA repair mechanisms. One of the earliest substrates to be discovered was poly(ADP-ribose) polymerase (PARP) which catalyses the transfer of ADP-ribose polymerase to nuclear proteins (Kaufmann *et al.* 1991). Due to its role in DNA repair, cleavage of PARP may compromise its activity, and hasten the demise of the cell. Other examples of substrates involved in repair mechanisms include the retinoblastoma protein (Janicke *et al.* 1996) and the mouse double mutant-2 protein (MDM2) (Erhardt *et al.* 1997). MDM2 normally retains p53 in the cytoplasm and cleavage may allow p53 entry into the nucleus to induce apoptosis or arrest.

Caspases also cleave substrates involved in cell cycle regulation such as p21 and p27 (Levkau *et al.* 1998). A large number of recently identified substrates are protein kinases or other proteins involved in signal transduction. Proteolytic activation of the p21-activated kinase (PAK2) has been reported during Fas and TNF-mediated apoptosis (Rudel *et al.* 1998). PAK2 triggers stress-activated kinases of the JNK/SAPK pathway and may provide a link between caspases and JNK/SAPK activation during apoptotic cell death.

Furthermore, certain anti-apoptotic proteins of the Bcl-2 member family, including Bcl-2 itself and Bcl-x_L, are believed to be cleaved by caspases (Cheng *et al.* 1997; Clem *et al.* 1998). This has been proposed to result in the formation of pro-apoptotic proteins that may act similarly to Bax and amplify the cell death signal. Also, Caspase-8 can cleave the Bcl-2 protein Bid into an active fragment that induces cytochrome c release from mitochondria (Luo *et al.* 1998).

1.10 BCL-2 Family

One of the most important families of apoptosis regulators is represented by Bcl-2 and its homologues. The product of the proto-oncogene was first described as being overexpressed in follicular lymphomas and was originally identified during analysis of the t(14;18) breakpoint common in this disease (Tsujiimoto *et al.* 1985). Bcl-2 is homologous to the *Ced-9* gene product in *C. elegans* (Hengartner and Horvitz 1994) and initial transfection studies indicated that overexpression of the protein significantly prolonged cell survival after a variety of insults, including factor deprivation, glucocorticoid treatment of thymocytes and λ -irradiation (Reed 1994). Thus Bcl-2 emerged as an intracellular apoptosis-suppressor and the first identified proto-oncogene that contributed to tumour development through effects on cell survival rather than cell division.

The Bcl-2 gene family comprises death-inducing and death-inhibitory members, which differ in their tissue- and activation-dependent expression patterns, as well as in structural features (Reed *et al.* 1998). The majority of members of the Bcl-2 family

possess a carboxy-terminal transmembrane TM region that targets them predominantly to the outer mitochondrial membrane, the endoplasmic reticulum and the outer nuclear envelope (Krajewski *et al.* 1993; Nguyen *et al.* 1993). In the mitochondrion Bcl-2 is distributed to the contact sites between the outer and inner mitochondrial membranes. Some pro-apoptotic proteins, such as Bad and Bid, (Wang *et al.* 1996) lack a hydrophobic signal-anchor sequence at the C-terminus and exhibit a diffuse cytoplasmic distribution in the absence of a death signal.

At least 16 different Bcl-2 family members have been identified in mammalian cells and many others in viruses (Reed *et al.* 1998). A common motif is shared by all members of the family known as a Bcl-2 homology domain (BH1 to BH4). The variable BH regions determine the capacity of the family members to interact with each other or with other unrelated proteins. The majority of pro-survival members of the family contain at least BH1 and BH2 and those with greatest homology with Bcl-2 share all four BH domains. The pro-cell death members of the Bcl-2 family have been divided into two subfamilies. Bax, Bak, and Bok, which contain BH1, BH2, and BH3 have close homology with Bcl-2. In contrast, the other members of the pro-apoptotic family possess only the central short domain BH3 domain. Members of this 'BH3-only' group include the proteins Bid and Bad, and within this subfamily only Bik and Blk are similar (Reed *et al.* 1998).

Some members of the Bcl-2 gene family can produce splice variants. Bcl-x transcripts are alternatively spliced into long (L) and short (S) forms (Boise *et al.* 1993). Bcl-x_L is functionally similar to Bcl-2 in that it is a potent inhibitor of cell death. The shorter form, Bcl-x_S, antagonises cell death inhibition by the Bcl-2/Bcl-x_L gene products. The Bcl-2 gene itself can encode for splice variants; one isoform of Bcl-2 encodes a protein that lacks a TM domain (Borner *et al.* 1994). A variety of splice variants of the pro-apoptotic protein Bax have recently been reported (Thomas *et al.* 1999).

1.10.1 Dimerisation of Bcl-2 family proteins

A key discovery was made when it was shown that Bcl-2 was capable of heterodimerising with its pro-apoptotic relative Bax (Oltvai *et al.* 1993). The hypothesis then emerged that the Bcl-2:Bax ratio was key to determining the sensitivity or resistance of cells to apoptotic cell death. However, recently it has been shown conclusively with knockout mice that Bcl-2 and Bax have intrinsic independent functions as effectors of cell survival and death respectively (Miller *et al.* 1997). Therefore, Bcl-2 can prolong cell survival, even in the absence of Bax: conversely, Bax is capable of promoting cell death, even without Bcl-2 expression (St. Clair *et al.* 1997).

Most of the so-called 'BH3-only' branch of the Bcl-2 subfamily, including Blk and Bad, operate as trans-dominant inhibitors of anti-apoptotic proteins, such as Bcl-2 and Bcl-x_L, relying exclusively on dimerisation for their bioactivities (Kelekar and Thompson 1998). In general these proteins do not dimerise with other pro-apoptotic proteins and cannot homodimerise. Deletion of the BH3 domains in these proteins prevents their death-induction capabilities. The dimerisation properties of the 'BH3-only' subfamily can be contrasted with pro-apoptotic properties such as Bax and Bak, which share greater amino acid sequence identity with Bcl-2. Unlike 'BH3-only' proteins Bax and Bak can homodimerise with themselves, in addition to heterodimerising with Bcl-2 and Bcl-x_L (Schendel *et al.* 1998).

Heterodimerisation is not necessarily required to antagonise cell death. For pro-apoptotic activity, heterodimerisation is essential in the 'BH3-only group', but less so for those of the Bax group, which appears to have an independent cytotoxic activity. It also appears that certain members of the Bcl-2 family preferentially bind others. For example, Bok interacts with Mcl-1 and the Epstein-Barr viral protein BHRF-1, but not with Bcl-2, Bcl-x_L or Bcl-w (Hsu *et al.* 1997). Within the 'BH3-only' group, Bid is promiscuous and binds to Bax and Bak as well as to pro-survival proteins (Wang *et al.* 1996), but many of the other proteins within the BH3 group only bind certain proteins. Very recent evidence suggests that Bcl-w will bind Bax, Bak, Bad and Blk, but A1 will bind only Bak and Bik. In addition, heterodimerisation was not necessarily an indicator of function: Bcl-w and A1 protect cells against apoptosis induced by overexpression of Bax and Bad but not that induced by Bak or Bik (Holmgren *et al.* 1999). These results

may reflect critical threshold affinities but also suggest that certain pro-apoptotic proteins may also contribute to apoptosis by a mechanism independent of binding pro-survival proteins.

1.10.2 *Bcl-2 family interactions with other proteins*

Other evidence suggests that the Bcl-2 family proteins interact with a vast range of seemingly unrelated proteins. Bcl-2 or Bcl-x_L have been reported to bind many proteins, including the caspase-activating CED-4 homologue Apaf-1 (Hu *et al.* 1998), the protein kinase Raf-1 (Wang *et al.* 1996), the p53-binding protein p53-BP2 (Naumovski and Cleary 1996), and the Hsp70 molecular chaperone Bag-1 (Takayama *et al.* 1995). In most cases, when investigated, dimerisation of Bcl-2 or Bcl-x_L with pro-apoptotic proteins such as Bax or Bad, disrupts interactions with other non-Bcl-2 family proteins. This implies either that the same hydrophobic pocket implicated in dimerisation of Bcl-2 family proteins is involved, or that dimerisation induces conformational changes in Bcl-2/Bcl-x_L that trigger release of these heterologous proteins.

Arguably, of all the proteins with which Bcl-2/Bcl-x_L can interact, those directly linked to caspase activation seem likely to be the most important. Strong genetic evidence from *C. elegans* implies a critical role for CED-9 interactions with CED-4 in the activation of CED-3, which is a homologue of the mammalian caspase family (Chinnaiyan *et al.* 1997). Indeed, Bcl-2 family members are believed to be crucial in the regulation of the apoptosomes and consequently the activation of various caspases (Kluck *et al.* 1997).

Recently, it has been shown that Bcl-2 can be cleaved during apoptosis by Caspase-3 at Asp-34 (Cheng *et al.* 1997). This has been confirmed by both *in vitro* and *in vivo* studies (Grandgirard *et al.* 1998). Interestingly, the cleaved protein was pro-apoptotic and capable of releasing cytochrome c into the cytosol. Bcl-2 may also be inactivated by other proteases. The variable region of Bcl-2 (residues 37 to 85 between BH4 and BH1) which has little homology with Bcl-x_L, is highly susceptible to digestion by proteases such as trypsin and chymotrypsin. Another mechanism to degrade Bcl-2 is to target the protein to the ubiquitin-dependent degradation pathway. One group showed that this occurred during TNF- α -induced apoptosis (Borner *et al.* 1999).

It now appears that posttranslational modification of Bcl-2-regulated proteins also has a major impact cell death signalling. Serine phosphorylation of Bcl-2 family members may also modulate their ability to regulate cell death (Haldar *et al.* 1995).

Chemotherapeutic agents which act on microtubules (for example taxol and vincristine) have been shown to induce phosphorylation of Bcl-2 and this has been proposed as a mechanism to abrogate the anti-cell death properties of the protein (Basu and Haldar 1998).

Remarkably the Bcl-2 family appears capable of regulating the cell cycle also. Under suboptimal growth conditions Bcl-2 can promote entry into the quiescent state and block re-entry into the cycle (Linette *et al.* 1996). Most importantly, this activity is genetically separable from its survival function as mutation studies indicate cell cycle inhibition but not anti-apoptotic cell death function is ablated with a deletion in the nonconserved loop (Huang *et al.* 1997). It has been proposed that the mechanism behind the observation of reduced level of T cell IL-2 production is due to the expression of Bcl-2 (Linette *et al.* 1996). During S phase the transcription factor NFAT is translocated into the nucleus. NFAT translocation requires comigrating calcineurin and Bcl-2 may sequester calcineurin on cytoplasmic membranes.

1.10.3 Subcellular localisation and dynamism of Bcl-2 family members

The localisation of the Bcl-2 family members appears to be crucial to their function. As mentioned earlier, the majority of Bcl-2 family members contain a C-terminal stretch of amino acids that anchors them to membranes. Deletion of the TM domain either reduces or eliminates the death-inhibitory effects of Bcl-2 (Reed *et al.* 1998). It has been proposed that Bcl-2 and its homologues may act as docking or adaptor proteins, pulling other proteins from the cytosol and targeting them for interaction with membrane associated proteins. Furthermore, removal of TM from Bax prevents targeting to mitochondria and completely abolished its cytotoxic function in yeast cells, suggesting that membrane targeting is crucial for Bax-mediated death. However at least two pro-apoptotic 'BH3-only' proteins, Bad and Bid, lack these TM sequences. The locations of these proteins in cells is controlled by other Bcl-2 family proteins or caspases.

Engagement of the Fas receptor has been shown to lead to an extremely rapid activation of Caspase-8. This enzyme can directly activate Caspase-3, -6 and -7, (Slee *et al.* 1999) however it can also activate these downstream caspases indirectly by causing cytochrome c release via Apaf-1 and apoptosome formation (Luo *et al.* 1998). The exact mechanism of communication between Caspase-8 activation and the mitochondria may have been isolated recently (Li *et al.* 1998). This group isolated a protein from the cytosol of mammalian cells which is capable of releasing cytochrome c from isolated mitochondria after Caspase-8 activation. After cleavage the COOH fragment of Bid translocates onto mitochondria where it is believed to interact with Bax. However, the activated Bid by itself is able to induce complete release of cytochrome c. Interestingly, Bid is a much more potent cytochrome c releasing factor than Bax, needing up to a 500-fold lower concentration to cause complete cytochrome c release (Luo *et al.* 1998). Overexpression of the protein also potentiates apoptosis induced by serum withdrawal and it will be interesting to see if other death signals such as DNA damage and growth factor deprivation exert their effects on mitochondria through Bid.

Moreover, caspase-independent mechanisms for Bid translocation to membranes and dimerisation with Bcl-2 family members may also exist. Interestingly, mutagenesis studies of the BH3 domain of Bid suggests that its binding to Bax rather than pro-survival members is critical for its pro-apoptotic function (Wang *et al.* 1996). If true, this raises the possibility that 'BH3-only' proteins may function either as activators of Bax or inhibitors of Bcl-2/Bcl-x_L. This would also suggest a co-translocation of Bax from the cytosol to the mitochondria, as outlined earlier, is necessary for Bid to act on Bax at the mitochondria.

Although many members reside on the mitochondria, some such as Bcl-2/Bcl-x_L also reside on the endoplasmic reticulum (ER)/nuclear membrane (Krajewski *et al.* 1993). Adenoviral E1B-19K, a potent anti-apoptotic protein, has recently been shown to attract CED-4 to the ER membrane. Recently the importance of the ER in regulating cell death signalling has grown. Evidence suggests the pro-apoptotic Bak binds to the cytoplasmic face of the ER-resident chaperone protein calnexin and needs this protein for its lethal effect in yeast (Torgler *et al.* 1997). Bak may interfere with the ability of calnexin to correctly retain folded ER proteins. Most importantly, it has recently been shown that Bcl-2 targeted to the ER can inhibit Myc-, but not etoposide-induced

apoptosis in the Rat-1 fibroblast cell line (Lee *et al.* 1999). In contrast, wild type Bcl-2 can inhibit apoptosis triggered by either death agonist. Interestingly, Bcl-2 targeted to the ER inhibited mitochondrial membrane potential ($\Delta\psi_M$), demonstrating that Bcl-2 does not have to reside at the mitochondria to control mitochondrial PT and abrogate apoptosis.

1.10.4 Bcl-2 family and the formation of pores in the mitochondria

Although Bcl-2 family proteins lack significant amino acid sequence homology with other proteins, the three dimensional structure of Bcl-x_L reveals a striking familiarity to the pore-forming domains of certain bacterial toxins that act as channels for either proteins or ions (Muchmore *et al.* 1996). Both the pore-forming colicins and the diphtheria toxin are close in structure to Bcl-x_L. Molecular modelling studies also suggest that anti-apoptotic proteins such as Bcl-2 and some types of pro-apoptotic proteins such as Bax, share the same structure as Bcl-x_L (Schendel *et al.* 1998). Details about the structures of Bcl-2 and Bcl-x_L channels are only beginning to be resolved and a variety of sizes for these channels have been reported.

The relative conductances, ion-selectivities and dynamic characterisation of the channels formed by these proteins appear to differ. It has been reported that Bcl-2 and Bcl-x_L form discrete channels *in vitro* which mostly assume a closed conformation, open only sporadically and yield conductances ranging from 20 to 300 picoSiemens (pS). Bax, however, tends to form larger channels, which assume a mostly open conformation. However evidence has been found for the creation of larger pores by Bcl-2 and Bcl-x_L under some conditions, which assume a mostly open conformation and produce channels with conductances >1nS (Schendel *et al.* 1998). Related to this is the issue of the stoichiometry of these channels. How many molecules of Bcl-2 or Bcl-x_L assemble in membranes to create channels is not known, but the existence of multiple Bcl-2/Bcl-x_L conductance states suggests a range of possibilities, at least *in vitro*. A concerted effort is now being made to demonstrate that Bcl-2/Bcl-x_L channels exist *in vivo* and to determine their structures.

The mechanism of cytochrome c release in response to apoptotic stimuli and its regulation by the Bcl-2 family is unclear. It has been hypothesised that Bcl-x_L may

function as an ion channel that regulates the permeability of mitochondria. Such an ion channel could minimise osmotic stress and in doing so could prevent cytochrome c release due to mitochondrial matrix swelling and outer membrane disruption (Vander Heiden *et al.* 1997).

1.10.5 *Bcl-2 family proteins and the mitochondrial permeability transition pore*

Several years ago, reactive oxygen species, which are produced as a by-product of mitochondrial respiratory electron transport, were implicated in certain models of apoptotic cell death (Zamzami *et al.* 1995). Focus shifted away from the mitochondria with the discovery of caspases and the observation that cells lacking a functional mitochondrial electron transport chain still undergo apoptosis (Zamzami *et al.* 1995). However, recently this interest in the role of the mitochondrion in apoptotic cell death has been revived. This followed experiments which showed that in many cases cells undergoing apoptosis show a large reduction in mitochondrial membrane potential ($\Delta\psi_M$) before they show signs of fragmentation of nuclear DNA (Kroemer 1998).

This reduction in electrochemical gradient is believed to result from a phenomenon extensively studied using isolated mitochondria *in vitro*, referred to as the permeability transition (PT). Mitochondrial PT involves the opening of a large (1.3nS) channel in the inner membrane of the mitochondrion. Evidence suggests that the opening of these 'pores' occurs at points of junction between the inner and outer membranes of mitochondria. The pores are thought to consist of multi-proteins assembled together, incorporating the adenine nucleotide translocator (ANT) in the inner mitochondrial membrane and possibly other proteins in the outer mitochondrial membrane, including the benzodiazepine receptor and the Voltage-Dependent Anion Channel (VDAC) (Kroemer 1998).

The function of PT in normal cell physiology still remains uncertain. It is thought that a reversible PT pore opening may allow for the release of Ca^{2+} from the mitochondrial matrix, thus allowing calcium homeostasis. Permeation studies suggest that PT pores allow unrestricted passage of molecules less than 1500 daltons in either direction across the mitochondrial membranes. Interestingly, it has also been reported that PT can trigger the release of proteins from mitochondria (Marzo *et al.* 1998; Susin

et al. 1999). PT has therefore been suggested as a mechanism for the generation of oxygen free radicals, the dumping of stored Ca^{2+} into the cytosol, and the release of mitochondrial proteins such as cytochrome c and apoptosis-inducing factor (AIF) in order to activate caspases (Susin *et al.* 1999). The volume dysregulation that occurs upon PT pore opening results in the entry of water into the mitochondrial matrix and its expansion. This matrix volume expansion causes the outer membrane to rupture, releasing proteins within the inner mitochondrial space (IMS) into the cytosol.

The exact mechanism of how cytochrome c escapes from mitochondria during apoptosis is still unclear. As indicated earlier, certain members of the Bcl-2 family may be able to induce pores in membranes and hence facilitate the release of proteins. Interestingly, immuno-electron microscopic studies have shown that Bcl-2 is located at contact sites between the inner and outer mitochondrial membranes (de Jong *et al.* 1994). Most importantly, Bcl-2 family proteins have been shown to associate with PT-pore constituents and regulate its function in both isolated mitochondria and whole cells (Susin *et al.* 1996). Overexpression of Bcl-2 or Bcl-x_L has been reported to make it difficult for many stimuli to induce PT pore opening. Conversely overexpression of the pro-apoptotic protein Bax in cells has been demonstrated to induce loss of $\Delta\psi_M$ through a caspase-independent mechanism. The anti-survival protein also reportedly co-purifies with the multi-protein PT pore complex from mitochondria and regulates its activity when reconstituted *in vitro*. Indeed, direct interactions between Bax and ANT have been reported (Marzo *et al.* 1998). The importance of this interaction was confirmed when the ANT agonist atracyloside was shown to be incapable of inducing ANT channel opening in the absence of Bax *in vitro* when reconstituted into liposomes and in isolated mitochondria derived from Bax null mice (Marzo *et al.* 1998).

However it is unsure how the fall in membrane potential and the release of cytochrome c are linked. It has been shown that the loss of $\Delta\psi_M$ after UV light insult occurred downstream of caspase activation and many hours after cytochrome c activation (Borner *et al.* 1999). Another group also showed that cytochrome c release in response to the chemotherapeutic agent didemnin B is an early event independent and before the loss of $\Delta\psi_M$ (Borner *et al.* 1999). These data are consistent with those reported from Apaf-1 and Caspase-9 knock-out mice, where cytochrome c was still

released in response to apoptotic stimuli, but no further changes in $\Delta\psi_M$ occurred (Kuida *et al.* 1998; Yoshida *et al.* 1998).

Therefore, caspase activation may be required for the loss of $\Delta\psi_M$ but not for the release of cytochrome c and PT pore opening may be a consequence of the formation of the apoptosome and Apaf-1-mediated caspase activation. In the Apaf-1 and Caspase-9 knockout experiments cytochrome c was still released after treatment with a variety of apoptotic insults however no changes in $\Delta\psi_M$ occurred. In addition, apoptosis and cytochrome c release can occur in the absence of any evidence of swelling which is supposed to be a consequence of PT pore opening. It has also been shown that Bax-induced cytochrome c release is independent of PT (Martinou *et al.* 1999). However, it is also clear that Bcl-2 can protect against oxidants and other stimuli that can directly affect the constituents of the PT-pore, thus preventing swelling of the mitochondrion (Susin *et al.* 1996).

1.11 Receptors in Apoptosis

Interleukins and other cytokines are believed to control the haematopoietic system and ultimately determine whether an uncommitted pluripotent stem cell proliferates and eventually differentiates along the myeloid, lymphoid or erythroid lineages (Boise and Thompson 1996). Obviously this process is under tight control and mammals have developed a mechanism that enables the organism actively to direct individual cells to self-destruct at different stages of development. This is illustrated in the case of the immune system, where it is necessary to eliminate the presence of T and B cell populations following their expansion in response to activation. This direct mechanism involves the activation of 'death receptors' by 'death ligands' (Ashkenazi and Dixit 1998).

The best characterised death receptors are Fas (also named CD95) (Nagata and Golstein 1995), Tumour Necrosis Factor receptor (TNFR – also called p55) (Smith *et al.* 1994). Other receptors include CD40, Death Receptor 3 (DR3), DR4 and DR5 (Ashkenazi and Dixit 1998). The ligands that activate these receptors include FasL (CD95L) (Nagata and Golstein 1995), TNF, lymphotoxin- α , CD40L, Apo3 Ligand

(Apo3L) and TRAIL (Ashkenazi and Dixit 1998). Fas and FasL play an extremely important role in the regulation of the immune response (Nagata 1994). Signalling through Fas is important in the peripheral deletion of activated mature T cells at the end of an immune response, in the killing of tumour cells or infected cell by CTLs and NKs, and in the killing of inflammatory cells at so called 'immune-privileged' sites like the testis and the eye (Hahne *et al.* 1996). TNF is also important in the immune system as it is produced mainly by activated macrophages and T cells in response to infection (Smith *et al.* 1994).

Fas and TNFR1 can self-associate (Smith *et al.* 1994), and this association is via a sequence known as the death domain. Fas ligation leads to aggregation of the receptor's death domains. An adaptor protein Fas-associated death domain (FADD) then binds through its own death domain to the aggregated receptor death domains. FADD also contains a death effector domain (DED) that binds to a similar domain within the pro-active form of Caspase-8 (Chinnaiyan *et al.* 1995). The DED within FADD is a specific example of a homophilic interaction domain termed CARD (Caspase recruitment domain), which is present in many of the caspases with large prodomains. After FADD recruits Caspase-8 oligomerisation the enzyme is autocatalysed and an activation of downstream effector caspases eventually commits the cell to apoptotic cell death (Muzio 1998).

One family of proteins, the TRAF (TNF receptor associated factor) family are recruited to the TNF receptor after ligation. All TRAF proteins share several structural motifs and distinct domains (Rothe *et al.* 1995). The N-terminus of these proteins contains a RING finger motif which is believed to mediate both DNA-protein and protein-protein interactions. While the resulting phenotype associated with the overexpression of these proteins is rather pleiotropic, they appear to modulate the expression of genes which often lead to the induction of an immune response and NF- κ B activation (Rothe *et al.* 1995).

DR3, which shares the most homology with TNFR, can induce apoptosis as well as NF- κ B activation in response to Apo3L binding (Chinnaiyan *et al.* 1996). A TNF family member with homology to FasL was recently identified and named TRAIL

(Wiley *et al.* 1995). Similar to FasL, TRAIL induces apoptosis in many tumour cell lines (Mariani *et al.* 1997). However, unlike expression of FasL, which is restricted mainly to activated T cells and NK cells, and to immune-privileged sites, TRAIL mRNA expression is constitutive in many tissues (Wiley *et al.* 1995). Nevertheless, similar to FasL, TRAIL transcription is elevated upon stimulation in peripheral blood T cells. Furthermore, a distinct subset of mature T cells acquires sensitivity to TRAIL-induced apoptosis after stimulation by IL-2, suggesting that TRAIL may play some role in peripheral T cell deletion (Marsters *et al.* 1996). Overexpression of a negative inhibitor of FADD was sufficient to block Fas-induced cell death but did not block death induction by TRAIL, implying that a FADD-independent pathway links TRAIL to the caspase mechanism of apoptosis (Marsters *et al.* 1996).

TRAIL binds to DR4 and DR5 and overexpression of these receptors induces apoptosis. However, there are conflicting reports with regard to the necessity of FADD for the death signalling via these receptors. Nevertheless, cells from FADD^{-/-} mice, which are resistant to apoptosis induction by Fas, TNFR and DR3, show full responsiveness to DR4, confirming the existence of a FADD-independent pathway that couples TRAIL to caspases (Yeh *et al.* 1998).

Like TRAIL mRNA, DR4 and DR5 transcripts are ubiquitous, suggesting that there may be mechanisms that protect cells from apoptosis induction by TRAIL. A unique set of receptors that compete with DR4 and DR5 for ligand binding have been discovered, identified as DcR1 (Pan *et al.* 1997) and DcR2 (Marsters *et al.* 1997). DcR1 is a glycosyl phosphatidylinositol (GPI)-anchored cell surface protein that resembles DR4 and DR5, but lacks a cytoplasmic tail. DcR1 appears to function as a decoy that prevents TRAIL from binding to receptors containing death domains. DcR2 is another receptor that resembles DR4 and DR5, however it has a substantially truncated death domain. Transfection with the receptor inhibits apoptosis induction by TRAIL indicating that it also acts as a decoy receptor.

1.12 The 'Apoptosome' – a Model of Cell Death Regulation

1.12.1 CED-4

The mechanism of activation of the caspase homologue CED-3 in *C. elegans* has been the focus of an intense area of research. Recently, it was shown that CED-3 is activated through a physical interaction between proCED-3 and CED-4 (Yang *et al.* 1998). Interaction with CED-4 seems to be the only mechanism available for CED-3 activation, because there is no apoptotic cell death in *ced-4* mutant organisms. Negative regulation of the activation of CED-3 is provided by CED-9, a Bcl-2 homologue, which binds to CED-4 and holds it in an inactive conformation (Chinnaiyan *et al.* 1997). This prevents CED-4-mediated activation of proCED-3. This ability of CED-9, CED-4 and CED-3 to exist in a multiprotein complex has led to the 'apoptosome' model of cell death regulation (Hengartner 1997)

1.12.2 Apaf-1

The human homologue of CED-4 was recently identified using an *in vitro* reconstitution approach (Zou *et al.* 1997). This finding was extremely important and has allowed a whole new area of apoptosis to branch out. The CED-4 homologue was termed Apaf-1 (apoptotic protease activating factor) and it is now believed to play a key role in the auto-proteolytic activation of Caspase-9. Unlike CED-4, Apaf-1 needs a co-factor, cytochrome c, which is normally present on the outer surface of the inner mitochondrial membrane, and the presence of dATP to bring about the activation of Caspase-9 (Li *et al.* 1997).

The amino-terminal domain of Apaf-1 contains a CED-3 –like domain, including a caspase recruitment domain (CARD), and a CED-4-like domain which contains a conserved P loop. There is also an elongated domain at the carboxy-terminal rich in WD-40 repeats, involved in protein-protein interactions. A number of proteins have been shown to interact with these domains; the most crucial may turn out to be the formation of the Bcl-x_L/Apaf-1/Caspase-9 complex (Pan *et al.* 1998), which, of course, represents the structural counterpart of CED-9/CED-4/CED-3 complex. *In vitro* binding of Apaf-1, pro-Caspase-9 and cytochrome c, in the presence of dATP, results in Caspase-9 activation followed by Caspase-3 activation.

In *C. elegans* the interaction between CED-3 and CED-4 is relatively complex with an alternatively spliced isoform of CED-4 which can block apoptosis (Shaham and Horvitz 1996). The interaction between Caspase-9 and Apaf-1 appears to be under the regulation of a variety of factors. Already an alternatively spliced isoform of Caspase-9 has been identified which inhibits binding of the caspase and formation of the apoptosome (Srinivasula *et al.* 1999). Also, a new human CED-4/Apaf-1 family member called CARD4 has been identified and at least three cDNAs encoding for novel forms of Apaf-1 have been cloned from lymphoma cell lines (Bertin *et al.* 1999). Furthermore, one group (Cardone *et al.* 1998) showed that two survival factors, Akt and p21-Ras, induce phosphorylation of proCaspase-9, inhibiting its processing and activation. Occupation of binding sites on Apaf-1 by endogenously phosphorylated Caspase-9 proteins have been proposed to play a dominant negative effect in the apoptotic cascade.

As described before, Bcl-x_L has also been shown to co-immunoprecipitate with Caspase-9 and Apaf-1 (Pan *et al.* 1998). Bcl-x_L binds the CED-4-like domain of Apaf-1 and hence does not compete with Caspase-9 for the CARD interaction. Obviously the anti-apoptotic function of Bcl-x_L has been proposed to be antagonised by pro-apoptotic members of the Bcl-2 family, such as Bax and Bak. Another anti-apoptotic protein member of the Bcl-2 family, termed Boo (Song *et al.* 1999) has recently been identified. Boo has a very limited expression, being detected only in the ovary and the epididymis in the adult tissue, but extensively in several embryonic tissues. However, Boo has the ability to bind at least three distinct regions of Apaf-1. It has been proposed that these interactions induce conformational change in Apaf-1 and block the processing of Caspase-9 (Song *et al.* 1999). Although the expression of Boo in adult tissues is restricted, the presence of other 'Apaf-1-only' anti-apoptotic proteins cannot be excluded.

The conformation of Apaf-1 appears to be a complex regulation. A series of experiments indicate that the protein adopts a 'closed' structure when the WD-40 domain interacts with its own amino-terminus, thus inhibiting Caspase-9 activation. It has been suggested that anti-apoptotic Bcl-2 family members could be involved in maintaining this 'closed' conformation and, conversely, cytochrome c and dATP could

allow the protein to take on a more open structure. This would result in Apaf-1 self-association and the dimerisation of Caspase-9, which in turn leads to Caspase-9 autoactivation (Cecconi 1999).

1.12.3 FLASH

The mechanism of signal transduction of Fas-mediated apoptosis has been extensively investigated as a model of mammalian apoptotic cell death. Several proteins have now been identified that bind the intracellular domain of the Fas receptor, designated the death domain (DD), which is essential for the transduction of the cell death signal (Muzio *et al.* 1998).

Of the Fas-binding proteins, the adaptor protein FADD, which also has a death domain in its carboxy-terminal region, has been shown to be recruited to the receptor after ligation (Chinnaiyan *et al.* 1996). FADD then binds Caspase-8 through homophilic interaction between the amino terminal domains of FADD and Caspase-8, which are known as the death-effector domains (DED). The complex of Fas, FADD and Caspase-8 has been termed the death-inducing signalling complex (DISC) (Kischkel *et al.* 1995). After DISC formation Caspase-8 becomes proteolytically activated by oligomerisation, whereupon it induces a death signal, either by cleavage of Bid (Li *et al.* 1998) or the direct cleavage of Caspase-3 (Muzio *et al.* 1998).

However, this scheme has now been shown to be grossly oversimplified. Recently, a group has identified a protein called FLASH, which interacts with the DED of Caspase-8 (Imai *et al.* 1999). The carboxy-terminal region of FLASH contains a DED-like domain, which is responsible for the interaction with Caspase-8. FLASH also has a region of homology to CED-4/Apaf-1, through which FLASH proteins appear to associate with each other. A number of factors indicate that FLASH is important in Fas-mediated apoptosis. FLASH is associated with Caspase-8 in non-apoptotic cells, however after Fas engagement it is recruited to the receptor and is part of the DISC. Also, Fas-induced apoptosis is facilitated by overexpression of FLASH and mutants of the protein inhibit apoptosis in a dominant-negative fashion.

The similarities between FLASH and CED-4/Apaf-1 are remarkable. Each of them can self-associate through the 'CED-4-like' domain; each of them can bind ATP

and interact with a caspase. Furthermore, FLASH has also been shown to interact with a member of the Bcl-2 family, the adenoviral protein E1B19K, which is known to inhibit Fas-induced apoptosis (Imai *et al.* 1999). Obviously it is tempting to speculate that FLASH represents a crucial protein in another 'apoptosome' Bcl-2 family member/FLASH/Caspase-8 complex.

1.13 Knockout experiments

Although ectopic overexpression of all caspases individually can induce apoptosis *in vitro* in many cell types, the exact importance of the contribution of each caspase to apoptotic cell death after insult remains uncertain. The issue of functional redundancy, especially, is crucial. Are caspases redundant, as suggested by the overlapping expression of multiple caspases in any given cell type, or is each caspase essential for its own distinct function? Recently several groups have generated various caspase deficient mice through gene targeting and this has allowed the exact physiological function of each enzyme to be examined definitively.

1.13.1 Caspase-1 knockout

Deficiency in the *Caspase-1* gene did not have any discernible effect on mouse development (Kuida *et al.* 1995). Moreover, studies from *Caspase-1*^{-/-} mice confirmed the essential role of the enzyme in mediating the processing and export of mature interleukin-1 β . *Caspase-1*-deficient mice were resistant to endotoxic shock induced by lipopolysaccharide (LPS) challenge and *Caspase-1*^{-/-} monocytes failed to produce mature IL-1 β following LPS treatment (Li *et al.* 1995). Surprisingly, the secretion, but not processing, of IL-1 α was also defective in these mice, revealing a previously unknown function of Caspase-1 in bringing about the release of both IL-1 α and - β . Subsequently, other experiments demonstrated that processing of another cytokine, IL-18, also required Caspase-1. It appears that this caspase plays an important role in the production of cytokines that lack conventional signal peptide sequences. Controversially, cells from mice deficient in Caspase-1 were also reported to be less susceptible to Fas-mediated apoptosis (Kuida *et al.* 1995).

1.13.2 Caspase-2 knockout

Caspase-2 mutant mice reached adulthood without gross abnormality and there was no difference in survival between Caspase-2-deficient mice versus wild type or heterozygous (Bergeron *et al.* 1998). However, interesting results were obtained with specific cell types from Caspase-2^{-/-} mice. The number of motor neurons in the facial nuclei of late embryonic and newborn Caspase-2 mutant mice amounted to only 73% of that in the wild type animals, suggesting that this gene can partially protect against facial motor neuron death. In the adult brain the levels of the long and the short form of the protein appear to be roughly equivalent. Both isoforms were disrupted and this may have offset the balance between these positive and negative regulators. Also, Caspase-2 was not required for the death of sympathetic neurons induced by trophic factor withdrawal. Indeed, Caspase-2-deficient sympathetic neurons died slightly faster after Nerve Growth Factor (NGF) withdrawal. Because Caspase-2 has two spliced isoforms, Caspase-2_L and Caspase-2_S, that can induce and inhibit apoptosis respectively, it is perhaps not surprising that deletion of the gene has both a negative and a positive effect on apoptosis in a tissue-specific fashion.

Most importantly, Caspase-2-deficient B lymphoblasts were more resistant to apoptosis induced by Granzyme B and perforin than their wild type counterparts suggesting that Caspase-2 is a downstream target of this enzyme in B cells. Interestingly, Caspase-2 appears to be an important mediator of the death of germ cells that occurs in the foetal ovary to establish the germ cell pool of the female. Wild type oocytes are very sensitive to the chemotherapeutic drug doxorubicin, however oocytes collected from Caspase-2-deficient females were almost completely resistant to the effects of the drug. In conclusion, the results from Caspase-2^{-/-} mice indicated that the enzyme is a highly specific positive and negative effector of apoptosis.

1.13.3 Caspase-3 knockout

Deletion of the *Caspase-3* gene in mice produces gross natural abnormalities and the mice die after only a few weeks (Kuida *et al.* 1996; Woo *et al.* 1998). These mice have a striking phenotype in which there are skull defects with masses of supernumerary cells that represent the failure of programmed cell death during development in the brain, but not, surprisingly on other organs or tissues. Thus, Caspase-3 acts in a tissue-selective manner during development and at least two possible explanations have been

proposed for this. There may be a shortage of other effector caspases that can substitute for Caspase-3 at some critical stage in neural development; alternatively, Caspase-3 may act as an apical, regulatory caspase at the heart of a particular pathway in these neural cells.

Consistent with this lack of any obvious morphological defects in tissues or organs other than the brain, immature T and B cells from these mice undergo apoptosis normally. Interestingly however, Caspase-3^{-/-} peripheral T cells are less susceptible to Fas receptor-induced cell death than wild type cells. This indicates that Caspase-3 contributes to apoptosis in peripheral T cells, but is dispensable during T and B cell differentiation. Furthermore, Caspase-3-deficient embryonic stem (ES) cells are highly resistant to apoptosis induced by UV-irradiation, but are sensitive to γ -irradiation. MEFs transformed with the adenovirus *E1A* gene and the activated *p21^{ras}* oncogene show reduced and delayed death. Finally, almost all cell types examined from Caspase-3^{-/-} mice failed to display extensive chromatin condensation and DNA fragmentation after apoptotic insult. In conclusion, Caspase-3 makes a contribution to cell death in a remarkable tissue-, cell type- and stimulus-specific manner.

1.13.4 Caspase-6 and -7 knockouts

While Caspase-6^{-/-} mice seemed to develop normally, Caspase-7^{-/-} mice died early during embryogenesis. However, both of these reports are unpublished and as of yet the apoptotic phenotype of the cells of these mice are not determined (Zheng *et al.* 1999).

1.13.5 Caspase-8 knockout

Mutation of the *Caspase-8* gene in mice results in embryonic lethality (Varfolomeev *et al.* 1998). Surprisingly, Caspase-8 was found to be important for regulation of erythropoiesis and proper development of heart muscles during embryogenesis. Caspase-8-deficient embryos died with impaired formation of cardiac muscles and haemorrhage in the abdominal area, in particular the liver. Hyperemia was also detected in major blood vessels and in other organs, including the lung and the retina. The underlying reason for these developmental abnormalities are unknown, however it is likely to be a result of signalling of death receptors in the absence of

Caspase-8, as the almost identical phenotypes were observed in embryos that lacked FADD (see below).

MEFs derived from Caspase-8^{-/-} mice were resistant to apoptosis mediated through p55 TNF receptor, Fas and DR3 – unlike the wild type cells that were sensitive to these insults. However Caspase-8^{-/-} MEFs were not resistant to death induction after treatment with dexamethasone, etoposide, UV-irradiation, staurosporine and serum deprivation. These data also indicate that Caspase-8 functions in apoptotic cell death signalling in a highly tissue-, cell type- and stimulus-dependent manner.

1.13.6 Caspase-9 knockout

Mutation of the Caspase-9 *gene* results in embryonic lethality and defective brain development associated with decreased apoptosis (Hakem *et al.* 1998; Kuida, Haydar *et al.* 1998). The requirement for Caspase-9 in apoptosis is also remarkably cell type- and stimulus-specific, indicating the existence of multiple complex apoptotic pathways. Mutation of *Caspase-9* protects thymocytes from dexamethasone- and γ -irradiation-induced cell death. *In vitro* and *in vivo* studies have indicated a direct link between Caspase-9 and Caspase-3 activation. However, as mentioned earlier, Caspase-3^{-/-} thymocytes were shown to be sensitive to all apoptotic stimuli tested, including dexamethasone- and γ -irradiation-induced cell death (Kuida *et al.* 1996). This therefore implies the existence of a pathway in thymocytes that is Caspase-3 independent but Caspase-9 dependent. In fact Caspase-9 deficiency protected splenocytes, MEFs and ES cells from γ -irradiation-induced cell death. Although Caspase-9^{-/-} ES cells were resistant to a broad range of apoptotic stimuli, Caspase-9 deficiency did not protect other cell types from death induced by the same insults. For example, unlike ES cells, Caspase-9^{-/-} thymocytes and splenocytes underwent apoptotic cell death in response to UV irradiation.

Conversely, the existence of an apoptotic pathway independent of Caspase-9 but dependent on Caspase-3 is implied from the response of activated T cells to Fas and CD3 ϵ . Caspase-3 deficiency has, as mentioned before, been shown to protect activated splenocytes from Fas- and CD3 ϵ -induced apoptotic cell death (Kuida, Zheng *et al.* 1996). However, Caspase-9 deficiency did not protect T cells from apoptosis induced by

these insults *in vivo* (Kuida *et al.* 1998). These data strongly support the existence of a Caspase-9-independent, Caspase-3-dependent apoptotic pathway.

The gross morphological features observed in Caspase-9^{-/-} mice were remarkably similar to those observed in mice lacking Caspase-3 (Kuida *et al.* 1996; Kuida *et al.* 1998). Although gene disruption of either caspase causes severe brain malformations, the abnormality was far more severe in mice lacking Caspase-9. For example, Caspase-3-deficient fetuses rarely exhibited an overt exencephaly abnormality whereas Caspase-9^{-/-} fetuses regularly showed prominent brain malformations. One possible reason suggested for the severity of malformation is the involvement in Caspase-9 in other effector caspases, such as Caspase-7, in the nervous system.

1.13.7 Apaf-1 knockout

Mutation of the *Ced-4* homologue, the *Apaf-1* gene, also produced gross abnormalities, including severe craniofacial malformations, brain overgrowth, persistence of the interdigital webs, and dramatic alterations of the lens and retina (Cecconi *et al.* 1998; Yoshida *et al.* 1998). All Apaf-1^{-/-} mice were found to die perinatally. Apaf-1-deficient embryonic fibroblasts were also less susceptible to apoptotic stimuli, although in very different patterns. After 8 hours no difference was observed in homozygous and wild type Apaf-1 MEFs responses to an agonistic Fas antibody. However, after treatment for 20 hours almost all wild type cells were dead, while almost half the mutant MEFs were still alive. After 8 hours of treatment with C6-ceramide, the second messenger in the sphingomyelin pathway, cell death was absent in the Apaf-1 mutant MEFs, while only half the wild type cells were alive. Similarly, staurosporine treatment of mutant MEFs only produced 30% cell death, while almost all the wild type cells were alive. Most interestingly, in these studies it was reported that *in situ* immunodetection of active Caspase-3 could not be observed in Apaf-1 mutant neural cells.

1.13.8 FADD knockout

A mutation in the *FADD* gene was also found to be lethal and the mice showed signs of cardiac failure and abdominal haemorrhage (Yeh *et al.* 1998). FADD was specifically required for the development of the ventricular myocardium, and it is

intriguing that the heart was the primary site affected, despite widespread embryonic expression. FADD-deficient embryos were also retarded developmentally. FADD^{-/-} MEFs were deficient in Fas, TNFR-1- and DR3-induced apoptosis. In addition, overexpression of TRADD did not cause cell death, whereas overexpression of either FADD or Caspase-8 did. No observable difference in apoptotic cell death was found between wild type and FADD^{-/-} MEFs after expression of *c-myc* oncogene. Also, FADD-deficient cells transformed by Ras were as sensitive to various concentrations of adriamycin as their wild type counterparts. Finally, no difference was found in cell death induced by DR4 between the FADD^{-/-} and wild type MEFs.

1.14 Receptor-mediated versus Chemical/Damage-induced Apoptotic Cell Death

1.14.1 Receptor-mediated Apoptosis

The death receptors are a subset of the TNF receptor family of cell surface molecules that possess a common motif within their cytoplasmic tails, called the death domain. These domains recruit adapter molecules that, in turn, recruit caspases to the receptor complex. It is believed that the proximity of certain caspases with each other brings about autoproteolysis and hence the apoptotic cascade is initiated. As indicated earlier, the Fas signalling pathway via the death-induction signalling complex (DISC) and the activation of Caspase-8 is the most studied receptor-mediated apoptotic death.

The exact processes after Fas ligation and Caspase-8 activation are becoming clear. Using peptide inhibitors and affinity labelling techniques it is known that in some cells Caspase-3 and -7 are directly and simultaneously activated by Caspase-8 (Slee *et al.* 1999). Once processed, Caspase-3 can then activate Caspase-6 and bring about the morphological features of apoptosis. In many models this seems to fit as the anti-apoptotic proteins Bcl-2/Bcl-x_L are unable to protect these cells from apoptosis. Bcl-2/Bcl-x_L proteins reside on the mitochondria and their inability to intervene in Fas-mediated apoptotic death in certain cell types confirms the direct nature of the process.

However, in certain cell types Bcl-2/Bcl-x_L are capable of reducing the apoptotic effects of Fas ligation. This has led to the proposal that at least two distinct routes to

apoptotic cell death can be initiated with Fas ligation. In type I cells, the direct pathway is engaged and Bcl-2 fails to protect from apoptosis; in type II cells Bcl-2 can confer protection as the death signal is routed via the mitochondria. A link between Caspase-8 and the mitochondria has been proven. Caspase-8 catalyses the cleavage of cytosolic Bid (Li *et al.* 1998), a pro-apoptotic member of the Bcl-2 family, that is then translocated to the mitochondria. Bid then brings about the release of cytochrome c, perhaps through interaction with Bax, and the formation of the Apaf-1 apoptosome results in the activation of Caspase-9 and other caspases. Therefore, in certain cell types, even receptor-mediated apoptotic cell death involves signalling via the mitochondria.

1.14.2 Chemical/Damage-induced Apoptosis

All apoptotic stimuli, aside from the TNF death ligands, have been grouped into this category, primarily because how these insults engage the caspase death machinery is still largely unknown. This group includes diverse stimuli such as cytotoxic drugs, radiation, survival factor deprivation, heat shock and other cellular stresses. Most importantly, all these insults appear to act on mitochondria and are believed to involve the formation of the Apaf-1 apoptosome. In addition, many members of the Bcl-2 family, both anti- and pro-apoptotic, seem to be capable of intervening in these pathways – again implicating the mitochondrial pathway. Thus although the exact nature of the link between chemical/damage insult to the cell and the engagement of the caspase death machinery is still unknown, all these pathways appear to converge on the mitochondrion (Kroemer *et al.* 1998)

1.14.3 z-VAD.fmk does not block the commitment to cell death in etoposide-treated cells

One group (Sun *et al.* 1999) has highlighted the differences in cytochrome c release between receptor-mediated and chemical-induced apoptosis. They demonstrated that in Fas-mediated cell death in Jurkat T cells z-VAD.fmk inhibited apoptosis prior to commitment by inhibiting the activation of the upstream enzyme Caspase-8. Consequently no release of cytochrome c or cleavage of Bid was detected. In addition, there was no reduction in mitochondrial membrane potential. In contrast z-VAD.fmk treatment did not inhibit the release of mitochondrial cytochrome c in etoposide-induced apoptosis in Jurkat T cells. Interestingly, this treatment did not completely inhibit the processing of Caspase-3, -7 and -9. Thus in chemical-induced apoptosis, z-VAD.fmk

did not inhibit the commitment to cell death, but rather inhibited the biochemical changes associated with the release of mitochondrial cytochrome c and consequent apoptosis. Most importantly, and in contrast with cells induced with Fas ligation, z-VAD.fmk treatment of etoposide-treated cells did not reduce their mitochondrial membrane potential.

1.14.4 Caspase knockout experiments point to Receptor versus Chemical Apoptosis

The caspase knockout experiments have also confirmed broadly divergent signalling pathways between receptor-mediated and chemical/damage-induced apoptotic cell death. For example, Caspase-9 *-/-* thymocytes exhibited resistance to diverse apoptotic stimuli including dexamethasone, etoposide and γ -irradiation, while they remain sensitive to apoptosis induced by death receptors such as Fas and TNF (Kuida *et al.* 1998). Conversely, MEFs derived from Caspase-8 *-/-* mice were resistant to apoptosis induced by Fas, TNF and DR3, but died rapidly after treatment with dexamethasone, etoposide, UV-irradiation, staurosporine and serum starvation (Varfolomeev *et al.* 1998).

It should be noted that the knockout experiments point to a degree of complexity in the death signalling pathways induced by chemical/damage – the broad group referred to earlier. For example, Caspase-9 *-/-* thymocytes were resistant to etoposide and γ -irradiation, but remained sensitive to apoptosis induced by UV-irradiation, heat and osmotic shock (Kuida *et al.* 1998). In addition, Caspase-3-deficient ES cells were highly resistant to apoptosis induced by UV-irradiation, but sensitive to γ -irradiation (Kuida *et al.* 1996).

1.15 Subcellular Localisation of Caspases

The morphological appearances of apoptosis are brought about by the effects of caspases. These proteins cleave several proteins localised to cytosol, cytoskeleton, intracellular membranes and nuclei, although the significance of any one particular of these cleavages in the cell death process is still unclear. The cellular localisation of

caspases could be an important determinant of their activations, substrate specificity and the ultimate cellular response.

Most caspases were considered to be cytosolic because of demonstrations that in a cell-free system based on cytosol from normally growing cells, three protease activating factors (Apaf-1-3) were required to activate proCaspase-3. Of course, the identity of protease activating factors are now known to be the constituents of the apoptosome (Li *et al.* 1997). The fact that the release of cytochrome c, and AIF, from mitochondria leads to activation of Caspase-3 in cytosol, and that Bcl-2 can block the release of cytochrome c, brought mitochondria back into the focus of apoptosis research.

Mancini *et al* first demonstrated beyond doubt that proCaspase-3 was present not only in the cytosol of some cell types, but also in the intermembrane space of the mitochondria of the same cells (Mancini *et al.* 1998). This was shown using with immuno-electron microscopy using a highly specific antibody for the proform of the enzyme. The researchers also indicated that the localisation of the proCaspase-3 determined the efficacy of Bcl-2 in blocking apoptotic stimuli.

One group then showed that proCaspase-3 was localised to cytosol and mitochondria of various rat tissues (brain, heart, kidney, liver, spleen and thymus) using differential centrifugation (Samali *et al.* 1998). The ratio of cytosolic and mitochondrial pools of proCaspase-3 appeared to vary between different tissues, with the higher amount of mitochondrial enzyme found in the thymus and spleen. Furthermore, of the tissues analysed, it appeared that a higher pool of mitochondrial proCaspase-3 was conversely proportional to the levels of cytochrome c. That is, the heart, kidney and brain all had high levels of mitochondrial cytochrome c. The authors proposed that the high levels of mitochondrial proCaspase-3 in lymphoid tissues was related to the high susceptibility of cells in these tissues to undergo spontaneous as well as induced apoptosis.

Another group then reported the different subcellular distribution of Caspase-3 and Caspase-7 following Fas-induced apoptosis in mouse liver (Chandler *et al.* 1998). After massive hepatocytic apoptosis, active Caspase-3 was confined primarily to the cytosol, whereas active Caspase-7 was associated almost exclusively with the

mitochondrial and microsomal fractions. Translocation and activation of Caspase-7 to the ER correlated with the proteolytic cleavage of the ER-specific substrate, sterol regulatory element-binding protein. Interestingly, proCaspase-3 was also only detected in the cytosol in this study.

The very first study investigating the subcellular localisation of a caspase found that Caspase-1 (ICE) was found predominantly in the cytosol, although some active enzyme localised to the external surface membrane (Singer *et al.* 1995). This seemed to concur with developing role of Caspase-1 in the activation and secretion of pro-inflammatory cytokines. However, another group showed that after treatment of HeLa cells with TNF- α proCaspase-1 was translocated to the nucleus where it was proteolytically activated, releasing the intact prodomain (Mao *et al.* 1998). A nuclear localisation signal was identified in the prodomain and, surprisingly, transfected MCF-7 cells overexpressing the prodomain also underwent apoptosis without any external insult. This apoptotic cell death was dependent on the nuclear targeting of the prodomain.

Similarly, another group showed using green fluorescent protein fusion (GFP) constructs that both precursor and processed Caspase-2 localise to the cytoplasmic and nuclear compartments and that the nuclear localisation of Caspase-2 was strictly dependent on the prodomain of the enzyme (Colussi *et al.* 1998). Confirming this, it was shown that when the prodomain of Caspase-2 was fused to proCaspase-3 it can mediate the nuclear transport of the enzyme. Furthermore, in this study both proCaspase-3 and -9 were also fused with GFP and for both proteins the majority of fluorescent signal was diffuse cytosolic. It is important to note that these constructs were transfected into NIH3T3 fibroblast cells.

In a comprehensive study, using differential centrifugation, the intracellular localisation and translocation of Caspases-2, -3, -7, -8 and -9 were examined in Jurkat T lymphocytes pre- and post-apoptosis (Zhivotovsky *et al.* 1999). This recent report mostly confirmed the previous experiments, with some interesting exceptions, and shed some light on the localisation of other enzymes. It was found that proCaspases-2, -3 and -9 were present in both the mitochondrial and cytosolic fractions of untreated

lymphocytes. Only proCaspase-2 was found in the nuclear fraction. The precursor enzymes proCaspase-7 and -8 were found only in the cytosolic fraction. In apoptotic cells, active Caspases -3, -8 and -9 were present in the cytosolic fraction, whereas active Caspases-3 and -9 were also found in the mitochondrial fraction and active Caspase-7 in the microsomal fraction. Interestingly, in apoptotic cells Caspase-2 and -3 were present in the nuclear fraction. Also, proCaspase-1 was not found in any of the fractions of Jurkat cells.

At a workshop meeting it was recently reported that in MCF-7 cells Caspase-8 is located primarily at the mitochondria (Medema *et al.* 1999). Upon Fas triggering, it is processed and the active subunits are assembled. These subunits translocate to the structural protein plectrin which was subsequently shown to be a substrate for Caspase-8. This is one of the first examples where for a particular cell type a caspase can be shown to translocate directly to one of its targets. The contradictory nature of some of these reports imply that the localisation of caspases may vary according to cell type.

1.16 – a programmed non-apoptotic cell death?

Many researchers have divided the apoptotic process into three phases; the induction phase, depending on the nature of death signal; the effector phase, during which the cells are committed to die; and the degradation phase, during which the cells acquire the morphological features of apoptosis and are phagocytosed by their neighbours. The determination of what constitutes the commitment point – the point of no return – for a cell during apoptosis is an extremely important scientific goal. Unravelling this information would impact on our understanding of apoptotic cell death in development, homeostasis and disease, especially with respect to the application of chemo- and radiotherapy.

If caspases are the only tool to effect the apoptotic process, specific protease inhibitors should prevent apoptotic morphology and death and allow cells to survive. This concept has been widely tested with the broad range caspase inhibitor z-VAD.fmk. This compound is effective in blocking apoptosis in different animal disease models such as stroke, myocardial ischaemia/reperfusion injury (Hara *et al.* 1997), liver disease

(Rodriguez *et al.* 1996) and traumatic brain injury (Loddick *et al.* 1996). In both liver and ischaemic brain models, the cells were shown to be functional after rescue.

However, an increasing number of reports published recently have questioned the ability of broad range caspase inhibitors to effectively block cell death (Kitanaka and Kuchino 1999). A concept of programmed cell death with 'necrotic'-like morphology is beginning to emerge. This type of death, termed autophagic degeneration, is characterised by the early appearance of large inclusions in the cytoplasm derived from autophagic vacuoles or autolysosomes. In addition, there is a lack of DNA fragmentation and other nuclear events associated with apoptosis,

The first clear demonstration of caspase-independent programmed cell death was illustrated with the overexpression of Bax in the presence of z-VAD.fmk (Xiang *et al.* 1996). Other studies confirmed that caspase inhibitors could not rescue different cell types from etoposide (Benson *et al.* 1998), staurosporine (Deas *et al.* 1998) and class I MHC antibody induced cell death (Woodle *et al.* 1997). This death was accompanied by cytoplasmic vacuolation and partial chromatin condensation and hence looked necrotic. With the exception of the models of ischaemia and liver damage described earlier, no rescue and/or clonogenic growth is possible at any time after removal of the inhibitor with a variety of cell types (Borner and Monney 1999). Furthermore, with respect to these models, it has recently been suggested that the rescue may not be as complete as thought (Harada and Sugimoto 1998).

It has also been well documented that TNF induces not only apoptotic cell death but also cell death with necrotic morphology depending on the cell type. This necrotic death was shown to be independent of caspase activation (Vercammen *et al.* 1998). The overexpression of the promyelocytic (PML) gene product has also been reported to induce cell death with apoptotic or non-apoptotic morphology depending on the cell type (Quignon *et al.* 1998). Although there is now strong evidence for the existence of such a necrotic programmed cell death *in vitro*, it is not yet clear whether such mechanisms occur *in vivo*. However, one group recently demonstrated that the activation of Ras signalling pathway leads to necrotic-like programmed cell death without the activation of caspases (Chi *et al.* 1999).

In the majority of apoptotic systems z-VAD.fmk does not block mitochondrial changes, such as $\Delta\psi_M$, the production of ROS or the release of cytochrome c and AIF. Therefore, despite caspase inhibition, the mitochondria of cells receiving death stimuli display apoptotic features. A key protein responsible for this may be Bax, a pro-apoptotic homologue of the Bcl-2 family. As described earlier, Bax is translocated to the outer mitochondrial membrane after apoptotic insult where it brings about the release of cytochrome c (Hsu *et al.* 1997). It may also bring about the release of AIF and other apoptogenic factors. Alternatively Bax may promote the opening of the mitochondrial PT through its association with the ANT, a key component of the pore (Marzo *et al.* 1998).

How AIF and other released proteins could trigger cell death in the absence of caspase function is unknown. An attractive proposal is the possibility that AIF activates other enzymes, such as serine proteases calpains and cathepsins. These could replace the caspases, but in a far less efficient manner. AIF has been cloned and shown to migrate to the nucleus after release from the mitochondria and induce chromatin condensation and $\Delta\psi_M$ in a z-VAD.fmk-insensitive manner (Susin *et al.* 1999). In support of this, there is a quantity of literature implicating non-caspase proteases in apoptosis (Berridge *et al.* 1998; Hughes *et al.* 1998).

The calpains, in particular, would appear to be a strong candidate for involvement in caspase-independent apoptosis (Squier *et al.* 1994; Squier and Cohen 1997). As they are calcium-dependent enzymes they may be activated in response to increased cytoplasmic calcium levels. As outlined earlier, calcium cycling is increased during mitochondrial damage. Furthermore, calpains are known to cleave some similar substrates as caspases.

This caspase-independent death is not simply a result of the treatment irreparably damaging the cells so they cannot function since, in some cases, anti-apoptotic oncogenes are able to rescue cell survival. For example, Bcl-2 allows cells to survive after over-expression of c-Myc, (Brunet *et al.* 1998) Bax (Xiang *et al.* 1996) or Bak. (McCarthy *et al.* 1997). This is an extremely important observation; the commitment event that determines whether or not a cell dies is under regulation by Bcl-

2 even when it is independent of caspase activation. As described earlier, the ability of Bcl-2 to block cell death is known to occur at many levels. Bcl-2 can interfere with the induction of apoptosis by microinjected cytochrome c (Brustugun *et al.* 1998). Another study suggests it can act to prolong cell survival following the release of cytochrome c induced by overexpression of Bax (Rosse *et al.* 1998). These observations suggest that Bcl-2 might act not only to prevent cytochrome c release but also to prevent the cyclic amplification of the effects of this release. The role of mitochondria in this process raises the possibility that changes in mitochondrial function could be the point of no return – the commitment to death.

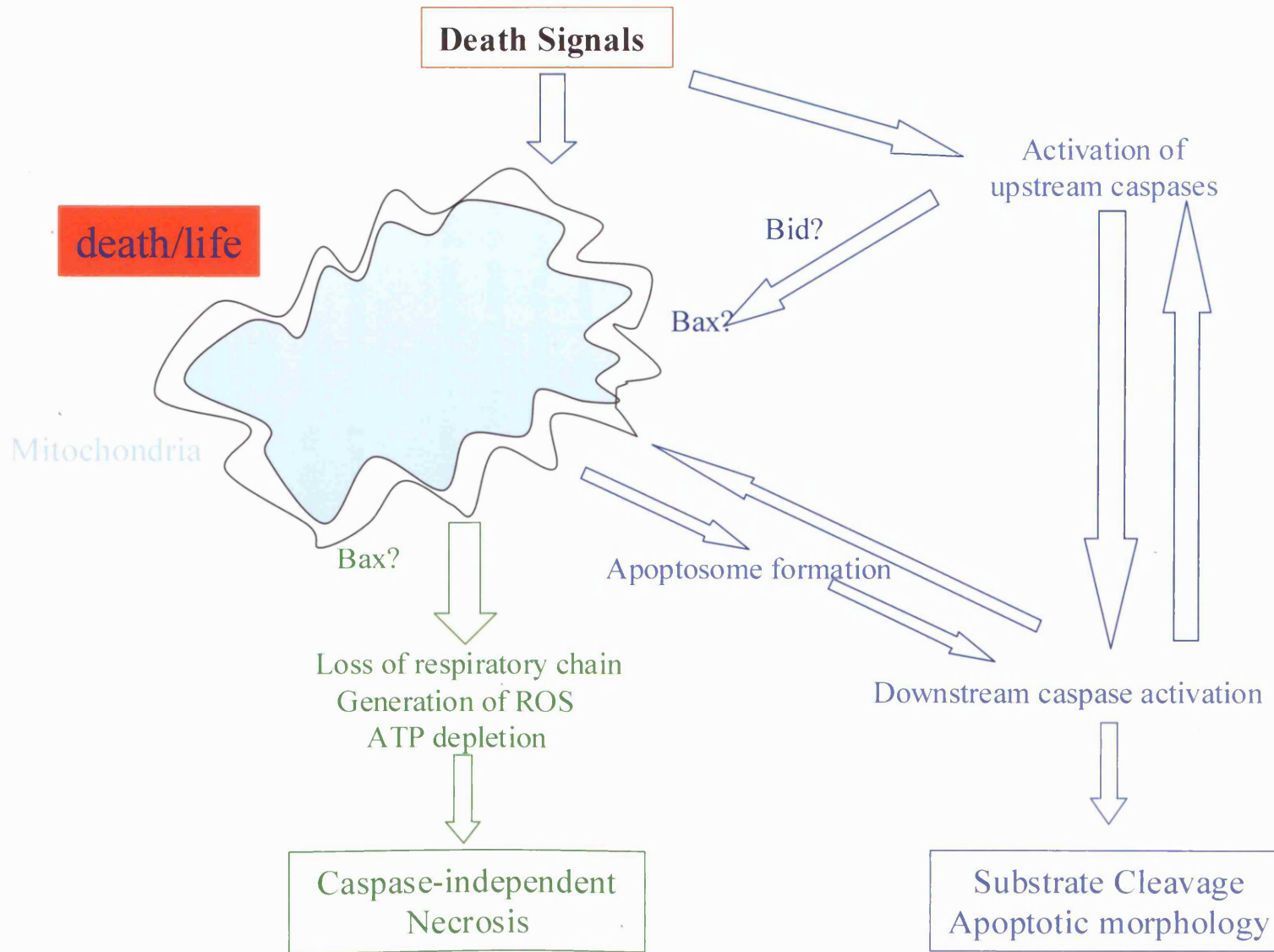
The mitochondrial PT pore might constitute a point of integration of multiple apoptotic pathways because several messengers, including Ca^{2+} ions (Kroemer 1998), reactive oxygen species (ROS) (Polyak *et al.* 1998), ceramide-derived ganglioside GD3 (De Maria *et al.* 1997), overexpression of caspases (Susin *et al.* 1997) and Bax (Marzo *et al.* 1998), facilitate its opening. Opening of the PT pore can cause disruption of the $\Delta\psi_M$ and the release of cytochrome c and AIF. Bcl-2 and Bcl-x_L can prevent the opening of the PT pore in isolated mitochondria (Marzo *et al.* 1998). In those pathways in which the second messenger responsible for mitochondrial PT pore opening is not a caspase, inhibition of caspases will not prevent cell death driven by a mitochondrial dysfunction. However, inhibition of caspases might retard (but not prevent) cell death, because it slows down a caspase-dependent self-amplification loop resulting in accelerated mitochondrial dysfunction.

The evidence suggests the cell makes two fundamentally distinct choices; a choice between death and life, and a choice between the mode of death – apoptotic programmed cell death or ‘necrotic’ programmed cell death. Again data supports the observation that a death/life decision is linked to the status of mitochondrial membranes. In this model the opening of the PT pore and the resulting dissipation of $\Delta\psi_M$ represents the ‘point of no return’.

Fig. 1.4 The commitment to die via different pathways for programmed cell death.

The decision of a cell to live or die following a death signal involves interaction with the mitochondrion. A 'death receptor' signal activates upstream Caspase-8 which can either cleave Caspase-3 directly, or the pro-apoptotic protein Bid. Bid then brings about the release of cytochrome c, perhaps via an interaction with Bax. This results in the formation of the Apaf-1 apoptosome and the cleavage of Caspase-3. The release of proCaspase-2, -3 and -9 may also occur at this stage. If Caspase-8 directly cleaves Caspase-3, then there is evidence to suggest activated Caspase-3 can interact with the PT pore and also bring about cytochrome c release and the concomitant formation of the apoptosome. Alternatively, a cell can receive a Chemical/Damage signal that eventually is routed via the mitochondria. Again, this results in cytochrome c release and the formation of the apoptosome. Therefore, a circular feedback mechanism that involves the activation of Caspase-3 seems to be crucial for both the 'commitment' and the 'amplification' of apoptotic cell death.

Most importantly, if a cell is committed to die, a nonapoptotic death with necrotic morphology can still proceed even if caspase activity is still blocked. One of the crucial determinants of whether the morphology of death is apoptotic or necrotic is the cellular levels of ATP. If mitochondrial cytochrome c release occurs in a cell with high enough ATP levels, Caspase-9 activation results and apoptotic death is initiated. However, if ATP levels are depleted, continued cytochrome release leads to a permanent reduction in mitochondrial membrane potential and the morphological appearance of necrosis



1.17 Non-Hodgkin's Lymphoma

Non-Hodgkin's lymphomas (NHLs) are a heterogeneous group of lymphoproliferative malignancies with differing patterns of behaviour and response to treatment (Harris *et al.* 1994). Similar to Hodgkin's disease (HD), NHL originates in lymphoid tissue and can spread to other organs. However, NHL is far less predictable than HD and is more likely to disseminate to extranodal sites (Lennert *et al.* 1990). The overall prognosis for a NHL patient depends on a variety of factors, including histologic type, stage and treatment. Most importantly, the incidence of NHL has increased over the past decade and is expected to continue to rise in developed countries.

Generally, the NHLs can be divided into two prognostic groups: the indolent lymphomas and the aggressive lymphomas. Indolent NHL types tend to have a reasonably good short term prognosis, with median survival as long as 10 years, but they usually are not curable in advanced clinical stages (Lennert *et al.* 1990). Early stage (I and II) indolent NHL can be effectively treated with radiation therapy alone. The aggressive type of NHL has a shorter natural history, and a large number of these patients can be cured with intensive combination chemotherapy regimes. Overall survival at 5 years of patients with aggressive NHL is approximately 50% to 60%; indeed 30% to 60% of patients with aggressive NHL can be cured.

1.18 Classification of NHL

From the mid-50s Rappaport in the United States began the process that led to the classification of NHL (Rappaport *et al.* 1956). The Rappaport classification, which is based purely on morphological classification, was used as a tool for predicting the clinical outcome of patients with lymphoma and to some extent is still useful for this purpose. A proposal of a radically new type of classification of NHL by Lennert in Germany and Lukes and Collins in the United States came about in the late 60s (Lukes and Collins 1975). The basic concept was that lymphomas were populations of defective lymphocytes that were arrested at one of the intermediate stages of differentiation. Luke and Collins suggested that this process was in some way analogous to the cellular

defects seen in congenital immunodeficiency disorders, where a block in normal maturation led to impaired immune function.

In 1982, results of a consensus study were published in the Working Formulation (National Cancer Institute 1982). This system combined results from 6 major classification systems into one classification. Recently, this formulation has been replaced by a new classification, the Revised European American Lymphoma (REAL) Classification (Harris *et al.* 1994). This system is believed to encompass all the lymphoproliferative neoplasms .

1.18.1 Diffuse Large Cell Lymphoma

Diffuse Large Cell lymphoma (DLCL) is the most common of the NHLs, comprising 30% of newly-diagnosed cases. It is an aggressive high-grade lymphoma. Patients with DLCL present with rapidly expanding nodal masses. In most cases there will be a short history of lymphadenopathy, which may be at any site, although the neck is the most common. A proportion of patients may present with localised disease although in many cases imaging will show evidence of disseminated disease. About one third of DLCL cases are of extranodal origin and the distinction of nodal and extranodal DLCL is of great importance from the point of view of clinical presentation, staging, therapy and efficacy of therapy.

An international index for aggressive NHL identifies 5 significant risk factors prognostic of overall survival: age (<60 years of age), serum lactate dehydrogenase (normal versus elevated), performance status (0 or 1 versus 2-4), stage (I or II versus III or IV), and extranodal site involvement (0 or 1 versus 2-4). Patients with 2 or more negative factors have less than a 50% chance of relapse-free and overall survival at 5 years.

A variety of regimes have been reported for the treatment of aggressive NHL. Six to eight cycles of full dose CHOP (cyclophosphamide, doxorubicin, vincristine, prednisone) has been a conventional therapy, although some groups report better success with cyclophosphamide, mitoxantrone, vincristine, etoposide, bleomycin and prednisone (VNCOP-B) for elderly patients (Zinzani *et al.* 1999). Treatment with chemotherapy and granulocyte-colony stimulating factor (G-CSF) has been shown to

reduce neutropenia-induced morbidity in elderly patients with aggressive NHL. Indeed, a subset of patients over the age of 65 with aggressive NHL can tolerate full dose CHOP chemotherapy without G-CSF support (Campbell *et al.* 1999). Another study has shown that 3 cycles of CHOP followed by involved-field radiotherapy are superior to eight cycles of CHOP alone for the treatment of localised intermediate- and high-grade NHL (Miller *et al.* 1998).

Patients with DLCL achieve a complete response in the majority of cases, but some data suggests at least one third of them eventually relapse, with those patients with a late relapse achieving a second CR more frequently and having better survival than early relapsed patients. The most important variables at diagnosis for predicting relapse are advanced stage and bone marrow infiltration. Low-grade relapse is not uncommon in patients who initially present with DLCL. As the management of low-grade lymphoma is different, knowledge of the nature of the relapse after CR is of value. Some evidence suggests a role for dose intensification and autologous stem cell transplantation as front-line therapy in aggressive NHL patients at high risk of resistance or relapse according to the international prognostic index (IPI), although the data is still controversial.

The complete range of remission rates reported with a variety of chemotherapy regimes varies from 45-85% with early death rates from 1-15%. The implication of this is that there is a high percentage of patients with primary refractory disease. Of the patients who relapse the majority do so in the first year, fewer in the second year and by the third the curves are approaching a plateau. DLCLs are very heterogeneous and morphological and phenotypical methods of subclassification are often difficult and not reproducible. This heterogeneity is also believed to be the primary factor in the variable prognosis and response to treatment (Harris *et al.* 1994). However, one recent study has shown that both immunoblastic (IB) and centroblastic (CB) groups do not differ with respect to major clinical features and laboratory parameters (Salar *et al.* 1998). Therefore, the morphologic subdivision of DLCL cases with CB and IB may have little clinical or prognostic significance. The basis of a genetic classification of DLCL is starting to emerge and may be of importance in designing future treatment strategies.

1.19 Apoptotic Cell Death in the Pathogenesis of Cancer

Many cancers are now believed to be the consequence of failed apoptotic cell death instead of enhanced cell growth, as was originally thought (Thompson 1995). In most tissues, cell survival appears to be dependent on the constant supply of survival signals provided by neighbouring cells and the extracellular matrix. It appears that most cells are programmed to commit suicide if survival signals are not received from the environment. Therefore, apoptotic cell death can be used as a default pathway. Cells from a wide variety of human malignancies have a decreased ability to undergo apoptosis in response to at least some physiological stimuli. Aberrant cell survival resulting from inhibition of apoptosis is believed to contribute to tumour progression and oncogenesis as cancer cells gain a selective advantage by blocking apoptosis. In a tumour proliferation may be slow or fast, but in all cases exceeds the rate of cell death.

Most importantly, certain types of cancer cells appear to have developed strategies to either evade or counterattack the immune system. In certain cases tumour cells express Fas ligand on their surface and are thought to thereby kill infiltrating CTLs, NK cells and possibly also neutrophils and macrophages, which also express Fas receptor (Krammer *et al.* 1998). However, technical problems with respect to the correct detection of Fas ligand has provoked controversy in this area and how essential immune evasion is for tumour initiation and progression is still unclear. Nevertheless, immunocompromised humans have an abnormally high incidence of cancers in which viral oncogenes contribute to cell transformation (such as EBV-linked lymphomas and Kaposi's sarcoma). However, increased risk in such cases may be a consequence of a failure to clear infections rather than defective immune surveillance of developing tumours.

1.19.1 *Fas signalling in B-NHLs*

B cells from malignant NHLs are derived from a clonal expansion of B cells arrested at different stages of differentiation (Harris *et al.* 1994). Therefore, lymphoma cells can be seen as the neoplastic counterparts of naïve, activated and memory normal B cells that each express a particular BCR. Both Follicular Lymphoma (FL) and B-cell Diffuse Large Cell Lymphoma (DLCL) are probably derived from germinal centre B cells. The nature of the antigen BCR recognises is uncertain, although the association

between NHL and autoimmune diseases suggest it may be an autoantigen occasionally. Interestingly, malignant B lymphocytes from NHL maintain their antigen presenting function and are capable of eliciting an anti-tumour lymphocyte reaction. Furthermore, CD40 is functional in tumour B cells because its engagement induces resistance to spontaneous apoptosis in an *in vitro* system.

Some reports on the sensitivity of B cells from NHLs to Fas-mediated apoptosis have recently been published (Plumas *et al.* 1998). Firstly, they indicate that the expression of Fas is highly variable, with DLCL cells especially expressing a high level of the receptor. However, regardless of the intensity of expression, Fas triggering with an anti-Fas antibody did not induce apoptosis of lymphoma B cells, while these cells underwent apoptosis after irradiation or staurosporine treatment. Using cytotoxic T cells, FasL was also ineffective in inducing apoptosis in lymphoma B cells, whereas these cells were killed by the perforin pathway. Furthermore, CD40 ligation in the presence of IL-4 strongly increased Fas expression, but did not markedly increase Fas-mediated apoptosis.

The results presented in this study strongly suggest that the Fas death pathway is totally or partially blocked in human B lymphoma cells. The mechanism behind this is still unknown. Overexpression of anti-apoptotic Bcl-2 has been demonstrated in follicular and other lymphomas (Tsujiimoto and Croce 1988). Interestingly, Bcl-x_L, another anti-apoptotic protein, has been shown to be upregulated in response to CD40 receptor engagement in murine B cells and human tonsillar B cells centroblasts (Tuscano *et al.* 1996). Indeed, this protein is believed to be the primary mechanism for the survival of B cells which react with antigen within the germinal centre.

However, as indicated earlier, the role of Fas in B cell homeostasis is very complex. One of the earliest reports of treatment of human malignant B cells from chronic lymphocytic leukaemias (BCLL) by engagement of Fas receptor produced some surprising results. All BCLL cells upregulated Fas following activation with *S. aureus* Cowan I (SAC) and/or IL-2. The vast majority of the cells died after engagement of the receptor with a concomitant increase in Bcl-2. However, one BCLL case actively proliferated after Fas upregulation, with no increase in Bcl-2 production (Mapara *et al.* 1993). Finally, *in vitro* studies where primary cultures of fresh tumour cells from a

variety of haematological malignancies were treated with FasL and TRAIL also produced surprising results (Snell *et al.* 1997). Although both ligands induced cell death in several types of B and T lymphoid and myeloid malignancies, they also produced proliferation in other cases.

The expression and sensitivity of the Fas/FasL pathway in a variety of B-NHLs and their surrounding reactive cells has been analysed (Xerri *et al.* 1997). The study shows that FasL is expressed by neoplastic and reactive cell components in the majority of human lymphoma tissues, and that FasL can be co-expressed with Fas on malignant cells. Interestingly, Fas positive malignant B cells were less sensitive to Fas-mediated apoptosis than reactive T cells. These results implied that the lymphoma cells were capable of inducing death in the reactive cells, but were more resistant to CTL killing via the Fas pathway.

One group has very recently examined the entire coding region and all splice sites of the Fas gene in 150 cases of NHL (Gronbaek *et al.* 1998). Mutations were identified in 16 of the tumours (11%). Missense mutations within the death domain of the receptor were associated with retention of the wild type allele, indicating a dominant negative mechanism. Conversely, missense mutations outside the death domain were associated with allelic loss, indicating that classical two-hit mode of gene inactivation may be necessary to disrupt gene function in these cases. The highest frequency of Fas mutation (60% of cases) was seen in low grade MALT-lymphomas. Most of the remaining mutations were seen in B-cell DLCL cases. Most interestingly, all but one of the patients with Fas mutations showed extranodal disease at presentation. Also, the majority of these patients with mutations displayed autoreactive phenomena.

Another group examined the expression of the Fas receptor in bone marrow specimens from myeloma patients (Landowski *et al.* 1997). Of those cases which expressed Fas, 10% displayed point mutations in the cytoplasmic death domain of the receptor. This was the only area where any mutations could be detected. Two individuals demonstrated an identical mutation known to be important in autoimmune lymphoproliferative syndrome (ALPS I). These data strongly suggest that Fas receptor mutations may contribute to the pathogenesis of myeloma in some patients.

1.19.2 Autoimmune lymphoproliferative syndrome (ALPS) and Tumorigenesis

More evidence does exist for the importance of immune surveillance in tumorigenesis. Data for immune-mediated regression of some cancers has been reported (see administration of TRAIL) and tumour immunotherapy has met with some success. Consequently, focus has shifted onto the role of the known death receptors in haematopoietic cell homeostasis. Naturally occurring mutants of the Fas/FasL pathway, described in both mice and in humans, have shed light on the importance of these molecules in peripheral T- and B-lymphocyte cell death. Both Fas ligand-deficient *gld* mice and Fas-deficient *lpr* mice develop a T- and B-lymphoproliferative syndrome that is variably associated with autoimmune manifestations depending on the genetic background (Nagata and Suda 1995).

Many human patients have been reported to develop similar lymphoproliferative symptoms, known as autoimmune lymphoproliferative syndrome (ALPS I) or Canale-Smith syndrome (Rieux-Laucat *et al.* 1995). In these patients heterozygous Fas mutations, often in the death domain, result in defective Fas-mediated lymphocyte apoptosis (Bettinardi *et al.* 1997). As a consequence, there is an accumulation of lymphocytes, including the expansion of a rare CD4-/CD8- T-lymphocyte subset, and other autoimmune disorders. In the majority of cases, the disease follows a dominant inheritance pattern. However, the pathology appears to be complex, as there is a variable penetrance and additional genetic factors may modulate disease progression. Most importantly, number of different clinical observations suggest an association exists between lymphoid malignancies and autoimmune disease. T-cell-rich-B-cell lymphoma and Hodgkins disease have been reported in ALPS. Indeed, one patient with ALPS developed multiple tumours (Drappa *et al.* 1996). Furthermore, mice bearing a *Fas* gene mutation have recently been shown to develop plasmacytoid tumours (Davidson *et al.* 1998).

A similar disease, referred to as ALPS II, has also been reported in some patients. This syndrome is also characterised by defective lymphocyte Fas-mediated apoptosis, however these patients do not have Fas/FasL mutations (Dianzani *et al.* 1997). A very recent report indicated that two out of 68 patients with ALPS II had inherited mutations in Caspase-10, but not in other death receptor genes such as Fas, FasL, p55 and p75, Caspase-8 or FADD (Wang *et al.* 1999). The study illustrated that

each kindred of ALPS II patients had a distinct missense mutation in the p17 protease domain of Caspase-10, which includes the catalytic site. Cells transfected with the mutant Caspase-10 were resistant to a variety of death receptor pathways. The study also illustrated that the mutated Caspase-10 was recruited to a DISC, along with Caspase-8. This implies that the mutant form of the enzyme may have a dominant effect on blocking caspase activation.

The pathological consequences of the Caspase-10 mutation varied between the cases. One patient, who was heterozygous for the mutation had a massive accumulation of T and B cells, as well as multiple and severe autoimmune manifestations including haemolytic anaemia and a severe clotting disorder (Wang *et al.* 1999). The variable clinical features of the ALPS II patients with Caspase-10 mutations mirrors the variable penetrance seen in ALPS I patients. Furthermore, the majority of ALPS II cases do not appear to have mutations in Caspase-10.

1.19.3 Burkitt's Lymphoma and Bax Mutations

In a crucial study the Fas-mediated cell death pathway was analysed in a panel of 11 EBV-negative and 10 EBV-positive Burkitt's lymphoma (BL) cell lines (Gutierrez *et al.* 1999). In EBV-positive cell lines the increased expression of Fas is dependent on the expression of the LMP-1 gene. However, an increased expression of the receptor did not correlate to susceptibility to Fas-mediated apoptosis; of the 17 cell lines resistant to Fas-mediated death 10 could be sensitised by upregulating Fas either by ectopic expression of LMP-1 or treatment with CD-40L. However, 7 BL cells lines still could not be sensitised to Fas-mediated cell death. Further analyses showed that 5 out of the 7 cell lines were also compromised in the integrity or expression of the pro-apoptotic gene *Bax*. These data showed a correlation between *Bax* mutation and irreversible Fas resistance. Loss of expression of Bax has also recently been shown to exist in BL biopsies and may result from null mutations in the Bax gene. Indeed, in general Bax frameshift mutations in cell lines derived from human haematopoietic malignancies are associated with resistance to apoptosis and microsatellite instability.

1.19.4 FLIP and Tumorigenesis

Recently a group has proposed that FLIPs may be a new class of tumour progression factors (Djerbi *et al.* 1999). They have shown that Kaposi sarcoma-associated herpesvirus protein (KSHV)-FLIP_L, which is expressed by human herpesvirus 8 (HHV-8), which in turn is associated with malignancies such as Kaposi's sarcoma and certain lymphomas, can act as a tumour progression factor by promoting tumour growth in vivo. Murine B lymphoma cells (A20) transfected with KSHV-FLIP_L rapidly develop into aggressive tumours when injected into immunocompetent mouse strains. It has also been shown (Tepper and Seldin 1999) that the sensitivity to Fas-mediated apoptosis in Epstein-Barr virus (EBV)-positive Burkitts lymphoma (BL) cell lines may be due to the relative levels of Caspase-8 and FLIP_L. Obviously, a higher transcript level of FLIP_L to Caspase-8 was associated with resistance to receptor-induced apoptosis.

1.19.5 Caspase Mutations and Tumorigenesis

It is likely that certain members of the caspase family may function as tumour suppressors. A very important report identified an antigen recognised by autologous cytolytic T lymphocytes on a human squamous cell carcinoma of the oral cavity. The antigen was encoded by a mutated form of the *Caspase-8* gene (Mandrizzato *et al.* 1997). This mutation was not found in the normal cells of the patient and its presence was shown to modify the stop codon and lengthen the protein by 88 amino acids. The tumour cells of the patient expressed both a normal and a mutated allele of the gene. Conclusive evidence for the impairment of the function of the altered Caspase-8 was obtained when the mutated *Caspase-8* gene was transiently transfected in 293-EBNA cells: its ability to trigger apoptosis was reduced relative to the normal Caspase-8 but not abolished.

One group has reported the detection of frameshift mutations in Caspase-5, a member of the caspase family of proteases that has an (A)₁₀ repeat within its coding region (Schwartz *et al.* 1999). This mutation was detected in microsatellite mutator phenotype (MMP) of the endometrium, colon and stomach. The authors were uncertain whether the selective advantage of cells with Caspase-5 mutations in MMP tumours is due to inhibition of apoptosis or to inhibition of the inflammatory response.

Recent experiments with Apaf-1 and Caspase-9-deficient mice (Soengas *et al.* 1999) have shed some light on the importance of these genes in tumour development. MEFs from the mutant mice were examined for their response to c-Myc expression, which is known to activate p53 to promote apoptosis. As expected, Myc sensitised wild type cells to apoptosis after growth factor depletion or hypoxia. However, p53^{-/-}, Caspase-9^{-/-} and Apaf-1^{-/-} cells expressing Myc were resistant to apoptotic cell death. Furthermore, inactivation of Apaf-1 and Caspase-9 was as effective as the inactivation of p53 at producing colonies in soft agar and at forming tumours in immunocompromised mice. This enhanced tumorigenicity was due to inefficient apoptosis.

1.19.6 Expression of Caspase-3 in Lymphomas and Leukaemias

One group published a comprehensive review of the expression of Caspase-3 in a variety of NHLs and B-CLLs (Krajewski *et al.* 1997). A moderate to strong intensity was found in 75% of B-cell DLCLs and 57% of FLCL. All 12 peripheral blood B-CLL samples were strongly positive, whereas all 3 of the SLL cases were immunonegative. In general the researchers found a highly variable expression of Caspase-3 in NHLs and B-CLLs. Another study by the same group investigated the expression of Caspase-3 in Hodgkin's disease (HD) and nodular lymphocyte predominant HD (NLPHD) (Chhanabhai *et al.* 1997). 96% of HD cases expressed Caspase-3 in the Reed-Sternberg cells, whereas the lymphohistiocytic cells in all cases of NLHPD lacked expression of the enzyme. The authors claimed that this gave more evidence to the argument that NLHPD is a phenotypically different disease distinct from classical forms of HD.

1.19.7 Tumorigenesis and the Bcl-2 family

As indicated earlier, several genes that are critical in the regulation of apoptosis have been defined and consequently experiments are beginning to shed some light on the molecular bases for the increased resistance of tumour cells to undergo apoptosis. For example, the introduction of genes that inhibit Bcl-2 can induce apoptosis in a wide variety of tumour types, which suggest that many tumours continually rely on *Bcl-2* or related homologues to prevent cell death. Consistent with this observation, *Bcl-2* expression has been associated with poor prognosis in lymphoma (Sarris and Ford 1999), squamous cell carcinoma (Xie *et al.* 1999) and colorectal carcinoma (Giatromanolaki *et al.* 1999). Furthermore, reduced expression of Bax, a pro-apoptotic

homologue of Bcl-2, was found to be associated with poor response to combination chemotherapy and worse survival in patients with metastatic breast carcinoma (Krajewski *et al.* 1995).

1.19.8 IAPs and Tumorigenesis

The foetal IAP member, survivin, is not usually expressed in normal adult tissue, however it is expressed in most cancers tested (lung, colon, breast, prostate, pancreas, neuroblastomas, gastric, high grade lymphomas) with the exception of low grade lymphoma (Ambrosini *et al.* 1997). The protein has been shown to protect against apoptosis induced by IL-3 withdrawal in IL-3-dependent pre-B cells, against Taxol-induced apoptosis in NIH3T3 cells and against Bax overexpression, Fas engagement and etoposide treatment in 293 cells (Tamm *et al.* 1998). Immunohistochemical analysis has revealed that 60% of stage III-IV neuroblastomas are positive, while 53% of colon cancers and 35% of gastric cancers are positive. Expression of survivin correlates with decreased apoptotic index in gastric and colon cancer. Bcl-2 expression was also associated with survivin expression in colon cancer and, moreover, patient 5-year disease survival rates were significantly lower in patients with a low apoptotic index (Ambrosini *et al.* 1997).

1.19.9 CARDs and Translocations

The t (11;18) (q21;q21) appears to be the major genetic lesion in MALT lymphomas and is found in approximately 50% of the disease. It has been shown that the *HIAP1* gene and a novel gene on 18q21 characterised by several Ig-like C2-type domains, named *MLT*, are rearranged in the t (11;18). The breakpoint in *HIAP1* occurred in the intron separating the exons coding respectively for the BIR domains and the CARD. The breakpoints within *MLT* differed but the open reading frame was conserved in both cases (Dierlamm *et al.* 1999).

Another translocation in MALT B-cell lymphomas, the t (1;14) (p22;q32), shows a recurrent breakpoint upstream of the promoter of a novel gene, *Bcl-10*. The latter is a cellular homologue of the equine herpesvirus-2 *E10* gene and both also contain a CARD. Wild-type Bcl-10 and E10 activate NF- κ B but also induce apoptosis in MCF-7 and 293 cells. However, *Bcl-10* cDNA from t (1;14)-positive MALT

lymphomas contained a variety of mutations, most resulting in truncations either in or carboxy terminal to the CARD (Willis *et al.* 1999). CARD-truncated mutants were unable to either induce apoptosis or activate NF- κ B, whereas mutants with C-terminal truncation retained NF- κ B activation but did not induce apoptosis. Therefore, mutant Bcl-10 might have a two-fold tumorigenic potential: it may provide a survival advantage to MALT B cells, and it may also provide a proliferative signal.

1.19.10 Interferon-consensus sequence-binding protein and CML

Interferon consensus sequence-binding protein (ICSBP) null mice develop a disease remarkably similar to chronic myelogenous leukaemia (CML) (Gabriele *et al.* 1999). In general, CML cells display a decreased response to chemotherapy. Similarly, myeloid cells from ICSBP *-/-* mice exhibited reduced spontaneous apoptosis and a decrease in sensitivity to apoptosis induced by DNA damage. Interestingly, apoptosis in thymocytes from the ICSBP *-/-* mice is unaffected. However, overexpression of ICSBP protein in the human U937 monocytic cell line enhances the rate of spontaneous apoptosis and increases sensitivity to etoposide-induced apoptosis. Studies showed that cells overexpressing ICSBP have enhanced expression of Bcl- x_L . Therefore, the ICSBP gene modulates survival of myeloid cells by regulating expression of apoptosis-related genes.

1.19.11 Genes in DLCL Tumorigenesis

In a landmark study patients with *de novo* DLCL were studied for rearrangements of *bcl-2*, *bcl-6* and *myc* oncogenes by Southern blot analysis (Monni *et al.* 1999). The protein expression of Bcl-2 was also analysed. Approximately 35% of cases had rearrangements of *bcl-6* and 16% of cases had rearrangements of *bcl-2*. Less than 10% of cases had rearrangements in the *myc* gene. *bcl-2* rearrangement was found more often in extensive and primary nodal lymphomas than in extranodal cases. It was also present in none of the patients with stage 1 disease but in 22% of patients with stage II to IV. However the presence of these Bcl-2 rearrangements did not significantly affect overall survival or disease-free survival. In contrast high Bcl-2 protein expression adversely affected both OS and DFS. Interestingly *bcl-2* rearrangement did not correlate with protein expression.

Chromosomal translocations leading to deregulation of specific oncogenes have been shown to characterise approximately 50% of cases of DLCL (Rao *et al.* 1998). In addition gene amplification has been shown to occur in *rel* (2p12-16), *myc* (8q24), *bcl-2*(18q21), and *mdm2* (12q13-14). Each of these genes was amplified with incidence ranging from 11% to 23%; *rel* amplification was previously associated with extranodal presentation. Rearrangement of *bcl-6* did not correlate with DFS and OS and stage. Of the low percentage of cases with *myc* rearrangements, 16% were found in primary extranodal lymphomas versus 2% of primary nodal cases. Gastrointestinal lymphomas in particular were affected by *myc* rearrangements (28%). The distinct biological nature of these extranodal cases was reflected by a higher complete remission rate. Other studies have confirmed the molecular differences of extranodal DLCL, such as testicular lymphoma (Hyland *et al.* 1998).

1.20 Apoptotic Cell Death in Chemotherapy

The mechanisms causing resistance to chemotherapeutic drugs in cancer patients are complex and poorly understood. It is now certain that a major mode of resistance to antitumour treatment may be insensitivity to apoptosis induction. Furthermore, emerging evidence suggests that thresholds for drug-induced cell death differ among different types of tumours. The thresholds appear to be determined by genes that modulate apoptosis and, as each new gene is discovered, corresponding defects in its expression or activity are uncovered in human tumours. Very convincing evidence supporting the role of apoptosis in chemotherapy is emerging from studies involving the interaction of chemotherapeutic insults with proteins known to modulate apoptosis.

With the developing understanding of mechanisms regulating apoptosis, it is becoming increasingly clear that the majority of chemo- and radiotherapeutic agents operate through broadly similar mechanisms. Effective chemo- and radiotherapy has been proposed to act through three distinct phases. (1) Phase I: the insult. In this phase the chemo- or radiotherapeutic agent interacts with a specific target such as DNA, RNA or proteins involved in the cytoskeletal structure, such as microtubules. This interaction results in injury or dysfunction. (2) Phase II: signal transduction. In this phase the cell recognises the injury and transduces a signal within the cell for apoptotic death. This

mechanism is very poorly understood. For example, after a DNA-damaging insult p53, or some of its homologues, may be activated. However, the exact consequences of this and how an injurious signal is translated to the effectors of apoptosis is still uncertain.

(3) Phase III: induction of apoptosis. In this phase a decision is made such that susceptible cells react to the signals generated in response to chemotherapy-induced injury. In this phase the susceptible cells are committed to die and the orderly breakdown of macromolecules through the operation of a variety of proteases.

1.20.1 Fas Signalling and Chemotherapy

As described earlier, the Fas/FasL pathway is widely involved in apoptotic cell death in lymphoid and non-lymphoid cells. It has recently been postulated, primarily by the Krammer and Debatin group, that many chemotherapeutic agents also induce cell death by activating the Fas/FasL pathway (Krammer *et al.* 1998). One of the earliest reports by this group illustrated that doxorubicin and methotrexate induced apoptosis via the Fas/FasL system in a variety of human leukaemia T cell lines (Friesen *et al.* 1997). Drug-induced apoptosis was completely blocked by inhibition of gene expression and protein synthesis, and by blocking the binding of Fas receptor. Furthermore, doxorubicin and methotrexate increased FasL gene and protein expression in the cells. Another report by this group indicated that similar results could be obtained in the treatment of neuroblastoma cells with a range of chemotherapeutic drugs. In addition, an increase in both Fas and FasL was displayed by these cells. Finally the same group illustrated that apoptosis induced by a variety of anti-cancer drugs in hepatoma cells was mediated by p53-dependent stimulation of the Fas/FasL system (Muller *et al.* 1997).

The basic scenario being proposed was this; drug treatment causes damage of the DNA in the treated cells, sensed by p53 (or a p53 homologue) which is activated as a consequence. Upregulated p53 then activated directly the Fas receptor promoter and directly or indirectly the promoter of the FasL. Alternatively, p53 might activate transcription factors which regulate the Fas receptor gene. Binding of the expressed death ligand to the death receptor will result in autocrine apoptotic suicide or in fratricide of neighbouring cells.

Numerous reports by a variety of groups have contradicted this data. Perhaps the most important observations have been described in a report which examined whether

the Fas system is required for p53-dependent apoptosis and whether stimuli that induce activation of Caspase-3 induce apoptosis in p53-deficient cells (Fuchs *et al.* 1997). Thymocytes or activated T cells from Fas-deficient mice were resistant to apoptosis induced by ligation of Fas, but remained normally susceptible to irradiation-induced cell death. Thymocytes from p53-deficient mice, although resistant to DNA damage, remained sensitive to Caspase-3-mediated apoptosis induced after ligation of Fas. Therefore, these results demonstrated that, at least in thymocytes and T cells, DNA damage-induced apoptosis requires p53-mediated activation of Caspase-3 by a mechanism independent of Fas/FasL interactions.

Most groups have confirmed that chemotherapy-induced apoptosis is not dependent on Fas/FasL interactions. One study confirmed that the application of doxorubicin, fludarabine, or cisplatin enhanced FasL expression in the T-acute lymphatic leukaemia model CEM. However, overexpression of CrmA, an inhibitor of Caspase-8 and therefore of the Fas pathway, had no effect on drug-induced apoptosis. Neither did incubation with inhibitory monoclonal antibodies against Fas that completely block this pathway. Obviously the precise role of Fas/FasL interactions for sensitivity or resistance to chemotherapy of human cancer is still a matter of controversy. Indeed, the group which originally proposed the importance of the Fas/FasL pathway in chemotherapy-induced apoptosis, have recently published results confirming that the drug-induced changes in Fas and FasL expression in human malignant glioma cells are epiphenomenal, and do not play any role in their death (Glaser *et al.* 1999).

1.20.2 Caspases and Chemotherapy

Since the discovery of the caspase family numerous researchers have treated various neoplastic cell lines with chemotherapeutic agents and measured the effects on the levels of transcription and activation of select caspases. For example, one group (Shibata *et al.* 1996) showed that the levels of Caspase-1mRNA increased in the human myeloid leukaemic cell line K562 after insult with CPT-11, a water soluble derivative of camptothecin. In addition, another group indicated that the appearance of DNA fragmentation in leukaemic HL60 cells after treatment with etoposide could be blocked with z-VAD.fmk – a general caspase inhibitor as outlined earlier (Yoshida *et al.* 1996).

It was also found that the treatment of human myeloid leukaemia U937 cells with 1- β -arabinofuranosylcytosine (ara-C) activated Caspase-3 and induced apoptosis in these cells (Datta *et al.* 1996). Chen *et al.* have shown that human ovarian carcinoma cells undergo apoptotic cell death when treated with chemotherapeutic agents cisplatin and etoposide (Chen *et al.* 1996). The authors concluded that Caspase-3 “ could be a common mediator involved in the process of chemotherapy-induced apoptosis of cancer cells”.

Furthermore, researchers have implicated low levels of Caspase-3 in resistance to chemotherapy- and radiotherapy-induced apoptosis in cell lines (Eichholtz-Wirth *et al.* 1997). Another group (Donoghue *et al.* 1999) found that both the localisation and the levels of Caspase-3 were related to clinical outcome in DLCL.

1.20.3 Bcl-2 Homologues and Chemotherapy

The Bcl-2 protein and its homologues are extremely important regulators of apoptosis. Cells from transgenic mice overexpressing Bcl-2 have been shown to be highly resistant to a number of apoptotic stimuli (Offen *et al.* 1998). One group showed that glucocorticoid-induced apoptosis of human pre-B-leukaemias was dependent on the expression of Bcl-2 protein (Alnemri *et al.* 1992). Overexpression of another anti-apoptotic homologue Bcl-x_L has been shown to protect human neuroblastoma cells from apoptosis induced by the chemotherapeutic agents, 4 hydroperoxycyclophosphamide and cisplatin (Dole *et al.* 1995). In contrast, overexpression of Bcl-x_S, an alternatively spliced short form of Bcl-x, sensitised MCF-7 human breast cancer cells to apoptosis induced by the chemotherapeutic agents etoposide and Taxol (Sumantran *et al.* 1995).

It has been demonstrated that Bcl-x_L expression is up-regulated in myeloma cells at the same time of relapse and correlates with a decreased response rate to subsequent chemotherapy, suggesting that high levels of the protein may be a marker of chemoresistance (Tu *et al.* 1998). Interestingly, the short form of the protein, Bcl-x_S, could not be detected in either malignant human plasma cells or malignant cell lines. Furthermore, although Bcl-x_L and Bcl-2 expression appear to be regulated in reciprocal fashion during normal T- cell and B-cell differentiation, at relapse in myeloma most patients samples expressed both proteins.

1.20.4 Death Receptors and Tumour Immunotherapy

The concept of targeting specific death receptors to induce apoptosis in tumour cells is attractive for a number of reasons. Obviously, the specificity of the therapy would allow a window of opportunity to selectively kill cancer cells without killing the host tissues. In addition, death receptors initiated apoptosis independently of the *p53* tumour suppressor gene, which is inactivated by mutation in more than half of human cancers.

Despite the advantages, the clinical efficacy of both TNF and Fas is limited due to toxic side effects. Injection of agonistic antibody to Fas in tumour-bearing mice can be lethal, due to massive induction of apoptosis in hepatocytes (Galle *et al.* 1995). Systemic administration of TNF can cause a severe inflammatory response syndrome that resembles toxic shock (Havell *et al.* 1988). This is believed to be due to the induction of pro-inflammatory genes in macrophages and endothelial cells through NF- κ B activation. A relatively high proportion (approximately two-thirds) of tumour cell lines tested so far are sensitive to the cytotoxic effects TRAIL *in vitro*, indicating that TRAIL may prove to be a powerful cancer therapeutic (Snell *et al.* 1997). It has been reported that systematically administered TRAIL is not only tumoricidal in mice but is also non-toxic (French and Tschopp 1999).

1.21.6 Caspase Therapy

A new therapeutic strategy has been developed utilising the gene transfer of caspases into adult brain tumours. Malignant gliomas are very resistant to current therapeutic approaches, including irradiation, chemotherapy and immunotherapy. Retroviral transfer of Caspase-3 and -6 was very effective at inducing apoptosis in malignant glioma cells *in vitro* (Kondo *et al.* 1998). Furthermore, treatment of tumours grown in mice with a vector expressing Caspase-3 significantly inhibited the growth of the tumour through inhibition of apoptosis. This may, therefore, represent a novel and promising approach for the treatment of malignant glioma.

AIMS OF THE PROJECT

Early experiments with Caspase-3 indicated that it was an enzyme crucial to the apoptotic process, and that it was highly expressed in lymphoid tissue. Furthermore, an early report indicated that cleavage of Caspase-3 could be a common event in malignant cells successfully treated with chemotherapy. This was followed by a report indicating that the levels and localisation of the enzyme were significant in childhood neuroblastomas. The aim of the study was, therefore, to examine the expression and subcellular localisation of Caspase-3 in B- cell Diffuse Large Cell Lymphoma (DLCL). This lymphoma was chosen because there appears to a subgroup of patients with this disease that respond very well to chemo- and radiotherapy. It was hoped that analysis of an enzyme at the core of the apoptotic process would illustrate why treatment of these patients was successful.

In general, a number of questions were being addressed;

- (a) How does the expression of Caspase-3 relate to the apoptotic rate in patients with B-cell DLCL?
- (b) Do these factors influence the clinical outcome of patients with DLCL?
- (c) Where are the proCaspase-3 enzyme and its active fragments localised at the subcellular level?
- (d) How does this subcellular localisation relate to the propensity of the cell to undergo apoptosis, and is the cell death signal important with respect to the localisation of Caspase-3?

In order to answer these questions 'in-house' monoclonal antibodies were developed using synthetic peptides mimicking the newly-created N-terminii of the cleaved p12 and p17 fragments of Caspase-3. In addition, a retrospective study was carried out with a cohort of DLCL cases using immunohistochemistry, quantitative RT-PCR and Western blotting. Finally, experiments were undertaken to fuse full-length Caspase-3 and its active p17 and p12 fragments to Green Fluorescent Protein in order to determine the *in situ* localisation of the enzyme and its active fragments.

Chapter 2

DEVELOPING IMMUNODIAGNOSTIC TOOLS TO INVESTIGATE APOPTOSIS AND APOPTOTIC PATHWAYS

2.1 INTRODUCTION

The activation of caspases and their substrates by cleavage adjacent to aspartic acid residues makes them ideal candidates for the development of monoclonal antibodies using synthetic peptides. Cleavage of these proteins usually produces a unique N-terminus or C-terminus; these sequences may then be used as an antigen to mount an immune response.

The aim of this part of the study was to elicit a specific immune response from mice using peptides representing the newly created N-termini of the p17 and the p12 fragment of Caspase-3. This enzyme was selected partially due to its ubiquitous nature, and early evidence suggesting its importance in lymphocyte homeostasis (Krajewska *et al.* 1997). In addition, early studies had suggested that measuring its activation may be an ideal indicator of the efficacy of chemotherapy (Chen *et al.* 1996). From the polyclonal response a number of monoclonal antibodies could be produced. These antibodies would then be utilised in immunocytochemistry studies on paraffin-embedded lymphoma tissue. Theoretically, they may also be used for Western blotting in primary culture and cell line studies. It was hoped this would provide information with respect to the tissue specificity of caspase-3 and determine whether levels of active or inactive caspase-3 are disrupted in lymphoid malignancies.

Phage display technology would then be utilised (Hoogenboom *et al.* 1991) to produce single-chain fragments (ScFvs) from the mRNA from the spleens of the immunised mice, and from the hybridoma cell lines producing the specific monoclonal antibodies, that bind to the respective antigens. These ScFvs would then be cloned into vectors that allow intracellular expression (Beerli *et al.* 1996). Blocking a protein in this manner will allow the elucidation of the signalling pathways initiated by various drugs in diverse tumour cell-types.

In this section of the study, a dual approach was utilised. In one part Caspase-3 was selected as an enzyme for which antibodies recognising its inactive forms, and perhaps its active form would be developed. With the other part of the study, a vector was constructed that would allow future intracellular immunisation studies. A particular

problem with the intracellular expression of proteins is their rapid degradation, thus reducing their effect. The C-terminus end of the human kappa sequence (C κ) has been reported to be able to stabilise a protein when fused to it (Mhashilkar *et al.* 1995). Therefore, the aim of the other part of the study was to fuse the coding sequence of C κ to the C-terminus of a vector encoding for Green Fluorescent Protein (GFP) and determine whether this enhances the stabilisation of the protein. If successful, the C κ sequence would then be fused with any specific ScFvs directed against active Caspase-3 to increase the blocking of a cell death signal.

2.1.1 Production of Anti-Peptide Antibodies

2.1.1.1 Peptides

Proteins used to immunise animals for the production of antibodies, either for vaccination or for harvesting, have to be of an extremely high level of purity. The task is often made more difficult when antibodies against natural fragments obtained by cleavage of a protein are required. It can often be an extremely difficult task to separate the required fragment from the others and purify it to a high enough level for immunological studies. The development by Merrifield (1963) of the solid - phase method of peptide synthesis made it easier to obtain short fragments of a protein by synthesis rather than by enzymatic or chemical cleavage of the protein. Subsequently, many studies have established that synthetic peptides are able to mimic the antigenic sites of proteins, i.e. peptides are able to elicit antibodies that cross - react with the corresponding complete protein.

2.1.1.2 Continuous and Discontinuous Epitopes

Peptides have been classified as continuous and discontinuous (also called contiguous and discontiguous). Continuous epitopes are defined as a stretch of contiguous residues in direct peptide linkage endowed with distinctive conformational features, while discontinuous epitopes consist of a group of residues that are not contiguous in the sequence but are brought together by the folding of the polypeptide chain or by the juxtaposition of two separate peptide chains. It is important to recognize that both types of epitopes may be sensitive to conformational changes occurring in the protein. For instance, the reactivity of a continuous epitope may depend on the ability

of a stretch of contiguous residues to assume the correct conformation. In general, continuous epitopes represent any linear peptide fragment of a protein that is found to react with antibodies raised against the intact molecule.

2.1.1.3 Predictions of antigenicity

The accumulated knowledge of the antigenic structure of a few well characterised proteins has led to a concerted effort to find empirical rules for predicting the position of continuous epitopes in proteins from certain features of their primary structure

2.1.1.3.1 Hydrophilicity

It has been known for many years that hydrophobic amino acids tend to be buried within the native structure of globular proteins, while hydrophilic side - chains are on the exterior where they can interact with water. This approach was used (Hopp and Woods 1981) to show that the most hydrophilic segments of a protein tend to correspond to continuous epitopes. However, further experiments showed that the correlation between antigenicity and hydrophilicity was only strong for the most hydrophilic sequences.

Several methods for predicting antigenicity were compared by (Hopp 1986) on the basis of known epitopes in 12 proteins. The distinguishing features of the Hopp and Woods scale (Hopp and Woods 1981) is that the four charged residues (K,R, D and E) were given the maximum value of 3.0 because this seemed to improve epitope selection within the set of 12 proteins studied. On the other hand, the scale of Kyte and Doolittle (Kyte and Doolittle 1982) somewhat arbitrarily emphasised the hydrophilic nature of R and K, which results in predictions which tend to overlook negatively charged epitopes. The scale of Parker *et al* (Parker *et al.* 1986) is the only one that takes into account the increased hydrophilicity brought about by the presence of charged groups at the N- and C- termini. Amphipathicity, which is related to hydrophilicity, may also be used to determine antigenicity.

2.1.1.3.2 Chain termination

In a majority of proteins, the N- and C- termini are located on the surface of the molecule, and in close proximity to each other. Being at the end of the chain, they are

less constrained than internal segments of the peptide and have a high relative flexibility. These features are probably responsible for the finding that the termini of many proteins correspond to continuous epitopes. Synthetic peptides corresponding to the 10 - 15 terminal residues of any protein are thus likely to be suitable immunogens for raising antibodies that cross - react with intact protein.

Another reason advanced for the exceptionally high rate of antigenic cross - reactivity between terminal peptides and the whole molecule is the presence of free NH₂ and COOH terminal groups in both the peptides and the end regions of the protein. In contrast, in the case of peptides corresponding to inner regions of the protein, these free end groups in the peptide are not found as such in the protein, since they are involved in the formation of a peptide bond.

2.1.1.3.3 Sequence Variability

In families of homologous proteins, it is commonly observed that the regions that present high sequence variability tend to correspond to the location of epitopes. Regions of the protein in which changes in local conformation arising from point mutation can be tolerated are most likely to be on the surface, where they are not involved in the long range interactions that stabilize the internal folding of the molecule.

2.1.2 Single Chain Fragments (ScFvs) and Intracellular Immunisation

Single-chain fragments (ScFvs) represent the variable light chain (V_L) and the variable heavy chain (V_H) chains of specific monoclonal antibodies, bound together by a flexible linker peptide into a single protein molecule (Winter and Milstein 1991). The source of genetic material for ScFvs can be the mRNA from either an antibody-producing mouse hybridoma or from an immunised spleen. V_H and V_L chain genes are separately amplified, assembled into a ScFv and cloned into an expression vector. ScFvs can be produced using the Recombinant Phage Antibody System (RPAS) which relies upon the ability of M13 phage to display functional antibody fragments as fusion proteins on their tips. The antigen-positive phage can then be selected using affinity chromatography.

There are many advantages of ScFvs compared to monoclonal antibodies: (a) it is possible to use human genes and thus avoid an immunogenic reaction if used in humans; (b) they are produced from a much more stable genetic source; (c) they are easily cloned and screened; (d) they are easily genetically manipulated and can be used for intracellular immunisation.

The intracellular expression of ScFvs ('intracellular intrabodies) directed to various subcellular compartments is emerging as a powerful technology and these constructs have been demonstrated to alter various normal and cellular physiological processes. Anti-Tat and anti-Rev ScFvs have been extremely successful in inhibiting HIV replication in lymphocytes (Mhashilkar *et al.* 1995). Furthermore, anti-ErbB2 ScFvs dramatically reduce the tumorigenicity of ErbB2-transformed fibroblasts (Beerli *et al.* 1996) and caused a marked cytotoxic effect in ErbB2-overexpressing human ovarian tumour cells (Deshane *et al.* 1996).

2.2 MATERIALS AND METHODS

2.2.1 Cloning of C κ insert into pEGFPC-1 vector

pEGFP-C1 (Clontech, Palo Alto, U.S.A.) is a mammalian expression vector which contains a multiple cloning site (MCS) at the C-terminus. When transfected into mammalian cells transformed with the simian virus (SV) 40 T antigen these vectors express a protein (GFP) which yields a green fluorescence when excited at 488 nm. The MCS at the C-terminus allows for the expression of GFP fusion proteins. The use of GFP in this capacity provides a “fluorescent tag” on the protein, which allows for *in situ* localisation of the fusion protein and permits kinetic studies of protein localisation and trafficking. For more details of the vector see Figs. 4.1 and 4.2.

2.2.1.1 PCR Amplification of human C κ Domain

PCR reaction mixtures were carried out in 50 μ l containing 1 x PCR buffer [45mM Tris, pH8.8; 11mM (NH₄)₂SO₄; 4.5mM MgCl₂; 200 μ M dNTPs; 110 μ g/ml of BSA (Advanced Protein Products Ltd., Brierly Hill, U.K.); 6.7mM β -mercaptoethanol; 4.4 μ M EDTA, pH 8.0], 1U of *Taq* polymerase (Life Technologies, Paisley, UK) and 10pmoles of each primer. To amplify the human C κ domain reactions were subjected to 5 cycles consisting of 95°C for 1min., 52°C for 30s and 72°C for 30s; and then 30 cycles of 95°C for 30s, 62°C for 30s and 72°C for 30s. In addition, all the PCR reactions were subjected to denaturation at 98°C for 5 min. and 72°C for 1min. (hot start) before the first cycle and a final extension at 72°C for 10min. For the hot-start the reaction mix was held at 59°C pending the addition of *Taq* polymerase. The predicted size of the human C κ amplicon was 327 bp.

Once the appropriately-sized band was detected the PCR reaction was repeated in order to obtain more amplicon for cloning. In this reaction 3 μ l (1 μ g) of tonsil cDNA was used as template. Reactions were subjected to 5 cycles consisting of 95°C for 30s, 55°C for 30s and 72°C for 30s; and then 30 cycles of 95°C for 30s, 65°C for 30s and 72°C for 30s. Again, the experiment was repeated with annealing temperatures

increased to 60°C for 5 cycles and 65°C for 30 cycles respectively. Again, all the PCR reactions were subjected to denaturation at 98°C for 5 min. and 72°C for 1min. (hot start) before the first cycle and a final extension at 72°C for 10min. The sequence of the primers used were:

C κ (forward) 5' GCTCAAGCTTCGACTGTGGCTGCAC 3'

C κ (reverse) 5' ACCGTCGACACACTCTCCCCTGTTG 3'.

The *Hind III* restriction site in the forward primer and the *Sal I* restriction site in the reverse primer are underlined. The restriction sites were engineered into the primers such that the amplicon would be inserted into the vector in the correct reading frame (see Figs. 2.1 and 2.2). For all PCR reactions the amplification of actin was used as a positive control. The primers used to amplify actin were:

Actin (F) 5' GGAGACAAGCTTGCTCATCACCATTGGCAATGAGCG 3

Actin (R) 5' GCGAATTCGAGCTCTAGAAGCATTGCGGTGGACG 3'.

The predicted size of the actin amplicon was 416 bp. Sterile H₂O was used as a negative control template.

```

1 gagctcgtga tgaccagtc tccagacacc ctgtctttgt ctccagggga aacagccacc
61 ctctcctgca ggaccagtca gagtattagc agcaactact acttagcctg gttccagcag
121 aaacctggcc aggctcccag gctcctcatg ttgtctacat cctacatgac ctogactttc
181 ccagacaggt tcagtggcag tgggtctggg acagacttca ctctcaccat cagcagacgt
241 cagtccgaag atggtgcagt gtattatggt cagcagtatg gttactcacc gtggtcgttc
301 ggccaagggga ccaaggtgga aatcaaacga acgactgtgg ctgcaccate tgtcttcate
361 ttcccgccat ctgatgagca gttgaaatct ggaactgcct ctggttggtg cctgctgaat
421 aacttctatc ccagagagge caaagtacag tggaaaggtg ataacgcctt ccaatcgggt
481 aactcccagg agagtgtcac agagcaggac agcaaggaca gcacctacagcctcagcagc
541 accatgacgc tgagcaaagc agactacgag aaacacaaag tctacgcctg cgaagtcacc
601 catcagggcc tgagctcgcc cgtcacaaag agcttcaaca ggggagagtg t

```

 Primers used for amplification of coding sequence of human C κ domain

Fig. 2.1 Coding sequence for immunoglobulin G kappa chain mRNA. Primers for amplification of the amplicon range from 333-691bp and are colour-coded.

2.2.1.2 Purification and Restriction of PCR amplicon

The Nucleon™ easiClene (Lanarkshire, UK) kit was used for the excision of the correctly sized PCR amplicon. The procedure was followed as according to the manufacturer's instructions. Briefly, the correctly sized band was excised from a ethidium bromide-stained agarose gel with a razor band. The agarose was weighed, chopped into approx. 2mm cubes and transferred into a 1.5 ml centrifuge tube. Three volumes of NaI stock solution was added to the tube (approx. 3 times the weight of the excised gel) and the mixture placed in a 55°C waterbath incubator. The solution was left in the waterbath until it had completely dissolved. Following this, 1/10 volume of the solution of TBE inhibitor was added. 5µl of well mixed easiClene silica suspension was then added to the solution, mixed and left at room temperature for 5 min. to allow binding of the DNA to the silica matrix. To ensure thorough mixing, the solution was vortexed every minute. The suspension was then spun for approx. 5 seconds in a microcentrifuge. The supernatant was removed and the pellet washed three times with 500µl of ice-cold wash solution. After resuspension the solution was spun for approx. 5 seconds. The washed pellet was then resuspended in 5µl of TE and incubated at 55°C for 2 mins. The tube was then centrifuged again for about 30 seconds and the supernatant containing the eluted DNA carefully removed and placed in a new eppendorf. Several purifications were carried out and the solutions pooled.

The restriction reaction for the excised DNA was carried out in 20µl. 8µl of excised DNA was used in the reaction with 10U of *Hind III* and 10U of *Sal I* (Life Technologies, Paisley, UK). A small volume of the restricted, excised DNA solution was run on a 2.5% electrophoretic gel beside a known quantity of restricted φX 174 DNA in order to estimate the concentration of the DNA recovered. Restriction of the pEGFP-C1 vector was carried out in 50µl. 4µg of the vector were used in the reaction with 10U of *Hind III* and 10U of *Sal I*. Both reactions were carried out at 37°C for 2 hours. As a restriction control, vector DNA that was only digested with *Hind III* was used. This reaction was also carried out in 50µl. 4µg of the vector were used in the reaction with 20U of *Hind III*.

2.2.1.3 .Ligation / Transformation

Ligation reactions were carried out in 20 μ l. The concentration of the excised, restricted C κ amplicon was estimated to be \approx 4ng/ μ l (see Fig. 2.7). The double digest of the pEGFP-C1 vector was assumed to be 100% effective and hence the concentration of restricted vector was estimated at 0.5 μ g/ μ l. Three ligation reactions containing the restricted vectors and inserts were carried out at ratios of 1:50, 1:10 and 1:5 vector : insert. 1U of T4 DNA ligase was used and the reactions were incubated overnight at 15°C. Various ligation controls were also carried out. A reaction containing the double digest of the vector without the insert was ligated; a reaction containing vector restricted with *Hind III* with and without insert was also ligated. Again, all ligation reactions were carried out in 20 μ l overnight at 16°C.

Vectors were transformed into DH5 α TM E. coli cells as according to the procedure outlined by the suppliers (Life Technologies, Paisley UK). 50 μ l of cells were aliquoted into chilled microcentrifuge tubes. 3 μ l of the DNA ligation reaction were added to the tube. The pipette was gently moved through the cells while they were dispersed. The mix was incubated on ice for at least 30 minutes; the cells were then heat-shocked for 20s at 37°C. Following this, the cells were then placed on ice for 2 min. 0.95 ml of SOC medium was then added and the mixture shaken at 225rpm for up to 2 hours at 37°C. After expression, the reaction was diluted 1:10 with medium and 100 μ l of the undiluted and the diluted reaction was spread onto LB plates containing 30 μ g/ml kanamycin (Sigma-Aldrich, Poole, UK). To determine the transformation efficiency of the DH5 α cells, 5 μ l (0.5ng) of control pUC19 was gently added to a tube containing 50 μ l of competent cells and mixed as before. The above procedure was carried out except the reaction was plated onto LB plates containing 50 μ g/ml ampicillin. (Sigma-Aldrich, UK). After all transformations colonies were counted and the efficiencies calculated.

2.2.1.4 Screening of Clones

At least twenty colonies from each plate were picked and grown overnight in 10ml LB broth containing 30 μ g/ml kanamycin. Plasmid DNA from these cultures was

then isolated using the Wizard™ miniprep DNA purification system as recommended by the supplier (Promega, Madison, WI, USA). This procedure is based on a modification of the alkaline lysis method of DNA extraction (Birnboim and Doly, 1979).

Briefly, 1ml of each overnight bacterial culture was spun in a microcentrifuge at 13000 rpm for 2 mins. and the pellet redissolved with 200µl of a buffer containing 50 mM Tris -Hcl pH 7.5, 10mM EDTA and 100mg/ml RNaseA. The cells were then lysed with 200µl of a buffer containing 0.2M NaOH and 1% sodium dodecyl sulphate (SDS). The lysate was then precipitated with 1.32M potassium acetate, pH 4.8. 1ml of Wizard™ resin was then added to each supernatant and the solution applied to a Wizard™ column. After washing with a 95% ethanol solution, the DNA was eluted from the column with 50µl dH₂O. DNA was quantified by O.D. at 260nm. Calculation of the A_{260/280} value was used to estimate the purity of the DNA.

Positive clones were then identified using restriction analysis with both *Hind III* and *Sal I* and with just *Hind III*, as outlined earlier. In order to further confirm the existence of positive clones, a PCR mini -prep was carried out on other putative positive clones. Clones from a vector : insert plate containing the most colonies were resuspended in 0.95 ml of UP H₂O and boiled for 5 minutes. After spinning in a microcentrifuge, 5µl of the supernatant was used as a template for a PCR reaction. As before, PCR reaction mixtures were carried out in 50µl containing 45mM Tris, pH8.8; 11mM (NH₄)₂SO₄; 4.5mM MgCl₂; 200µM dNTPs; 110µg/ml of BSA; 6.7mM β-mercaptoethanol; 4.4µM EDTA, pH 8.0 and 10pmoles of each primer. However, with this experiment, 2.5U of *Taq* polymerase were used. All reactions were subjected to 5 cycles consisting of 95°C for 1min., 60°C for 30s and 72°C for 30s; and then 30 cycles of 95°C for 30s, 64°C for 30s and 72°C for 30s. In addition all the PCR reactions were subjected to denaturation at 98°C for 5 min. and 72°C for 1min. (hot start) before the first cycle and a final extension at 72°C for 10min. Sterile UP H₂O was used as a negative control template for the reaction and the putative positive clone from the restriction analysis was used as a positive control.

Once a positive clone was identified large-scale maxi - prep plasmid purification was carried out as according to the procedure supplied by the manufacturers (Qiagen, Valencia, CA, USA). As with the Wizard™ mini -prep system, the Qiagen maxi-prep protocol is based on a modified procedure of the alkaline lysis method (Birnboim and Daly, 1979). Briefly, the pellet from a 50ml bacterial culture was resuspended in a buffer containing 100µg/ml Rnase, 50mM Tris/HCl, 10mM EDTA pH 8.0. The cells were then lysed in a NaOH/SDS solution as before. Cellular debris and proteins were then precipitated with addition of 3.0M KAc, pH 5.5. The precipitated debris was removed by centrifugation and the clear supernatant loaded onto the anion-exchange Qiagen-tip columns.

The columns were equilibrated with a buffer containing 750mM NaCl. After loading, they were washed with a buffer containing 1.25M NaCl at pH 8.5. The eluted plasmid DNA was then desalted and concentrated by isopropanol. After centrifugation, the pellet is washed in 70% ethanol, re-centrifuged and allowed to air -dry before resuspension on 100µl of Tris-EDTA pH 8.0. As before, DNA was quantified by O.D. at 260nm. Calculation of the A_{260}/A_{280} value was used to estimate the purity of the DNA.

2.2.2 Expression of pEGFP-C1-Cκ

2.2.2.1 Drugs and Chemicals

Unless stated otherwise all chemicals were obtained from Sigma-Aldrich (Poole, U.K.)

2.2.2.2 Cell Culture Reagents

The original MRC-5 SV1 TG1, HL60 and U937 cultures were obtained from the European Collection of Animal Cell Cultures (ECACC; Porton Down, U.K.). RPMI 1640, penicillin-streptomycin (10, 000U/ml penicillin and 10,000µg/ml streptomycin), alpha medium minimal essential medium (EMEM), L-glutamine (2mM), foetal calf serum (FCS), Non-Essential Amino Acids (NEAA), Hank's Balanced Salt Solution (HBSS) and Lipofectamine were all obtained from Life Technologies (Paisley, U.K.).

2.2.2.3 Cell Lines

Each cell line was passaged every 48 -72 hrs, assuming they had reached confluence. The MRC5 cell line was maintained in DMEM, 2mM glutamine, 1% non-essential amino acids (NEAA) and 10% FCS. Approximately 1×10^6 cells were seeded per 25cm² flask every passage. Spent media was removed by aspiration and the cells rinsed with 5ml HBSS. The HBSS was removed before addition of 1 ml trypsin -EDTA to each flask and incubation for several minutes at 37°C, until the cells could be dislodged by knocking the side of the flask. They were then resuspended in 10ml of media and pelleted by spinning in a centrifuge at 1000 rpm for 5 min. The supernatant was then removed by aspiration and the pellet resuspended by pipetting up and down in fresh media. The cells were usually split between two 25cm² flasks with media to a total volume of 10 ml per flask and replaced in the incubator at 37°C in a humidified atmosphere of 5% CO₂. The HL60 cell line was diluted 1:5 every 72 hours in RPMI 1640 medium containing 10% FCS and 1% penicillin-streptomycin and maintained at 37°C in a humidified atmosphere of 5% CO₂.

2.2.2.4 Transfection of MRC5 cells

For the transient transfection of MRC5 adherent cells, the procedure was as follows. In a six-well tissue culture plate, seed $\approx 1-3 \times 10^5$ cells per well in 2 ml of the appropriate growth medium with serum. The cells were incubated at 37°C in a CO₂ incubator until the cells are 50 - 80% confluent. Two solutions were then prepared; in solution (A) 2µg of plasmid DNA was added to 100µl of Opti-Mem® I Reduced Serum Medium; in solution (B) 8µl of Lipofectamine Reagent was added to 100µl of Opti-Mem® I Reduced Serum Medium. The two solutions were then combined, mixed gently, and incubated at room temperature for 30min. to allow the DNA - liposome complexes to form. While the complexes formed, the cells were rinsed once with 2ml of Opti-Mem® I Reduced Serum Medium. For each transfection, 0.8 ml of Opti-Mem® I Reduced Serum Medium was added to the tube containing the complexes. The solution was mixed gently and overlaid onto the rinsed cells. The cells were incubated with the complexes for 5 hours at 37°C in a CO₂ incubator. Incubation was carried out for at least 5 hours. Following incubation, 1 ml of growth medium containing twice the normal concentration of serum was added without removing the transfection mixture.

The medium was replaced with fresh, complete medium 24 hours following the start of transfection.

2.2.2.5 *Fluorescent Microscopy*

48 and 72 hours after transfection the cells were trypsinised and washed, as described earlier, to give an approx. concentration of 1×10^6 cells/ml. Cytospin slides were then prepared using Cytospin 3 (Shandon, Pittsburgh, PA, USA) at 3000 rpm for 3 minutes. The slides were immediately immersed in 95% ethanol for 2 minutes, then washed in PBS and then mounted in 1,4-diazobicyclo[2,2,2,] octane (Dabco). A Zeiss fluorescent microscope was then used to analyse the slides.

2.2.2.6 *Western blotting of Transfected MRC5 Cells*

The protein extraction of the MRC5 cells transfected with pEGFP-C1 and pEGFP-C1-C κ was carried out as described in 3.2.2.1. The amount of extracted protein was measured using the Bradford assay and Western blotting was carried out as according to the NuPage™ method described in 3.2.2.2. An anti-GFP polyclonal antibody (Clontech, Palo Alto, CA, USA) that recognises the 27kDa protein was used to detect the expression of the fluorescent protein. The blots were developed using enhanced chemiluminescence (ECL; Amersham) according to the manufacturer's instructions. The filters were then exposed to photographic film (Kodak Hyperfilm ECL).

2.2.3 Production of Anti-Peptide Monoclonal Antibodies

2.2.3.1 *Peptide Selection and Synthesis*

Two peptides were selected for synthesis; p12N (SGVDDDMAC) and p17N (SGISLDNSYKC). p12N is the sequence of the newly-created N-terminus of the p12 fragment of caspase-3 after the initial cleavage. p17N is the sequence of the newly created N-terminus of the p17 fragment after sequential proteolysis (see Fig. 2.3). According to both the Hopp and Woods (1981), and the Parker *et al.*(1986) hydrophilicity scale, p12N should be highly immunogenic as it scores 5 and 12.4 respectively. p17N should also be immunogenic but not to the same degree as it scores 2.5 and 10.21 according to the same scales.

MENTENSVDSKSIKNLEPKIIHGSESMDSGISLDNSYKMDYPEMGLCIIINNKNFH
KSTGMTSRSGTDVDAANLRETFRNLYEVRNKNNDL TREEIVELMRDVSKEDHS
KRSSFVCVLLSHGEEGIIFGTNGPVDLKKITNFFRGDRCSRSLTGKPKLFIIQACRG
TELDGCIETD SGVDDDMAC HKIPVDADFLYAYSTAPGYYSWRNSKDGSWFIQS
LCAMLKQYADKLEFMHILTRVNRKVATEFESFSFDATFHAKKQIPCIVSMLTKE
LYFYH'

Fig. 2.3 Amino acid sequence for Caspase-3. The newly created N-terminus of the p17 fragment is represented by **SGISLDNSYK**. The newly created N-terminus of the p12 fragment is represented by **SGVDDDMAC**.

Peptides were synthesised by the solid-phase method (Merrifield, 1963) with an Applied Biosystems model 430A peptide synthesiser and purified by reverse-phase high performance chromatography on a C18 column. With the p17N peptide a cysteine residue was added at the carboxy terminus for conjugation with carrier protein. A cysteine residue at the end of p12N was used to conjugate to the carrier protein. KLH conjugates for immunisation and peptide-bovine serum albumin (BSA) conjugates for assay of antibodies were prepared as described by Liu *et al.* (1977).

2.2.3.2 Peptide Immunisation and Monoclonal Antibody Production Procedure

See Appendix A.

2.2.4. Screening of Antibodies

2.2.4.1 ELISA

The Covalink (Nunc, Rochester, NY, USA) plates were pre-coated by incubation at 4°C overnight with 0.2µg peptide conjugated to BSA. 0.2µg of unconjugated p12N peptide was also pre-coated overnight, however p17N peptide would not dissolve in the appropriate buffer. 0.1M carbonate buffer at pH 8 was used as a diluent. After washing x 3 times with PBS / 0.01% Tween 20 the plates were blocked

with PBS / 3% BSA for at least 1 hour at room temperature. After washing as before mouse serum at dilutions of 1/100, 1/1000, 1/10,000 and 1/100,000 were added to the plate. Blocking buffer was used as a diluent. Approximately 10µl of blood from tail was provided and this was made up to 1ml with PBS / 3% BSA. This constitutes a 1/100 dilution. 50µl per reaction was used. The plates were then left at room temperature for at least 1 hour. After washing as before, 100µl of rabbit anti - mouse immunoglobulin conjugated to alkaline phosphatase (AP) was added to each well at a concentration of 1/500. Again, blocking solution was used as diluent. The plates were then left at room temperature for at least 1 hour again. Meanwhile the substrate for AP was prepared. The diluent 1M diethanolamine (DEA) was heated at 37°C for approx 15 mins. For every 10ml of 1M DEA 2 tablets of phosphatase substrate (p-nitrophenyl phosphate) was dissolved. After washing x 3 times with PBS/ 0.01% Tween 20, 100µl of substrate was added to each well and left to react at 37°C for over 1 hour. The plates were read at 405nm.

Given the lack of availability of a definite positive control, it was important to include an extensive range of controls. The procedure as above was repeated with serum from a mouse that had not been injected. In addition, the procedure was repeated with serum from both injected and non-injected mice without antigen (i.e., using plates which had not been pre - incubated overnight with peptide or peptide conjugate). The procedure was also repeated without any serum whatsoever; in this experiment one was testing for the ability of the secondary antibody to bind to peptide and peptide - conjugates. The ability of the secondary antibody to bind to a blank well was also tested. Finally, the procedure was repeated with and without serum, using 0.2µg of BSA as the pre - coated antigen; this test was designed to evaluate whether the secondary antibody would bind to BSA. Furthermore, a monoclonal antibody which theoretically detects both the pro-form 32 KDa (Transduction Laboratories, Lexington, KY, USA) on a Western blot was also used as a positive control.

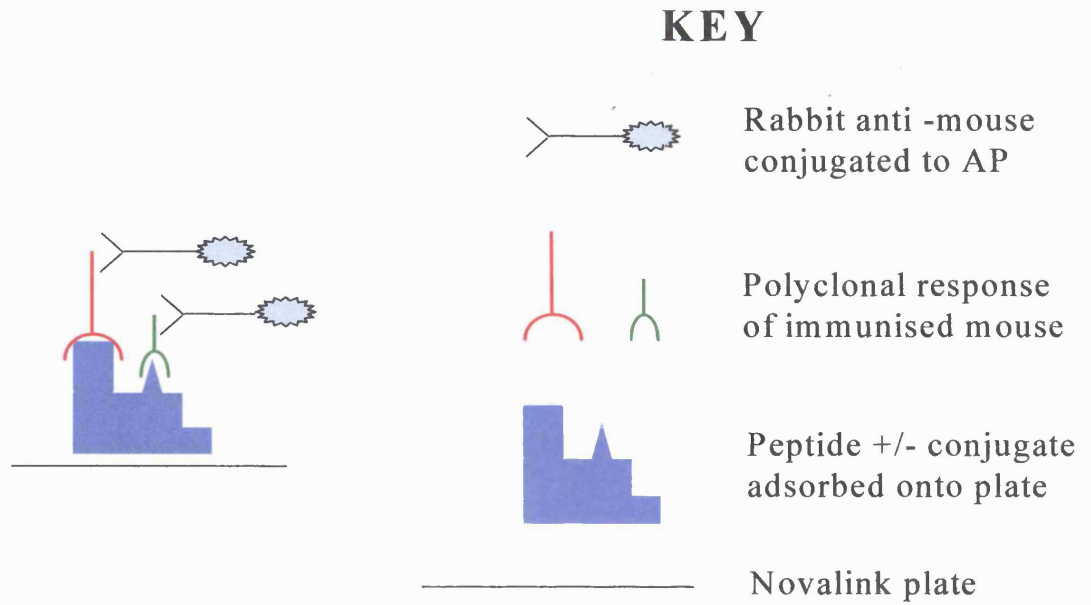


Fig. 2.4 Diagrammatic representation of peptide ELISA used to measure the strength of the polyclonal response of the mouse.

2.2.4.2 Immunocytochemistry

The sections were dewaxed and rehydrated. The slides were then placed in a plastic box and immersed in 10mM citrate buffer pH 6.0. The sections were then treated at full power in a 750W microwave oven for 20 mins. After microwaving, the sections were left to stand in the hot buffer for 30 mins. and allowed to cool to room temperature. They were then rinsed in TBS pH 7.6, drained and covered with 20% normal rabbit serum diluted in blocking solution (3% BSA / 0.1% Triton in TBS). The slides were then incubated for 10 minutes in a covered chamber. Without rinsing, the slides were drained and the excess serum removed. For the initial screening of the supernatant from the wells, a 1:20 dilution in blocking solution was applied overnight at 4°C. For the screening of the supernatant from stabilised monoclonal antibodies a dilution of 1:10 was used.

After washing x 2 times in TBS for 5 min., the slides were drained, the excess buffer removed from around the sections, and covered with rabbit anti -mouse immunoglobulin link antibody diluted 1:50 in blocking solution. The sections were then

incubated in a covered chamber for 30 mins. Again, the slides were washed x 2 times in TBS for 5 mins., drained and covered with mouse APAAP (Dako, Denmark) diluted 1:100 in blocking solution. Following incubation for 30 min. in a covered chamber the slides were washed in TBS. Meanwhile the appropriate volume of alkaline phosphatase substrate buffer consisting of 0.1M Tris pH 9.2, 0.1M NaCl and 0.05M MgCl₂ was made up and filtered through a 150mm Whatman paper. The slides were washed in UP H₂O for another 5 min. and then visualised using the substrate 5-bromo-4-chloro-3-indolyl phosphate (BCIP) and the chromogen nitroblue tetrazolium (NBT). For exact details of the procedure see section 3.2.1.2

2.3 RESULTS

2.3.1 Cloning of Cκ insert into pEGFP-C1

Diagnostic amplification of the human Cκ domain appeared to be successful in that it amplified a product of the correct approximate size of 327 bp (see Fig. 2.5). In addition, at least four other bands were also amplified, including one product of approximately 700 bp. The reaction containing the actin primers also appeared successful as it amplified a product of the correct approximate size of 416 bp.

The PCR reaction to obtain more DNA for cloning was also successful (Fig.2.6). In this reaction, the lower molecular weight bands present in the diagnostic amplification did not appear to be produced. Furthermore, the increased annealing temperatures seemed to produce more of the specific amplicon. Nevertheless, the high molecular weight band of approx. 700 bp that was present in the diagnostic amplification was also present in this PCR reaction.

The efficiency of the excision reaction is unknown, however a sample of the DNA solution did not appear to contain any contaminating bands when run on an electrophoretic gel. From this experiment the concentration of the solution containing the excised DNA was estimated to be approx. 0.4ng/μl (Fig. 2.7). With regard to transformation efficiencies, both the 1:50 and the 1:10 ligation reactions were significantly more efficient than the 1:5 ratio (Table 2). From the transformation with the positive control pUC19 plasmid, the data also indicate that the competent cells were sub-optimal as the suppliers document a transformation efficiency of $> 1 \times 10^6$ transformants/μg DNA.

From the Optical Density $_{260/280}$ data (not shown) and the restriction analyses (Figs. 2.8 and 2.9) the quality of the DNA purified by the Wizard™ mini-prep procedure was high. Initial screenings using restriction analysis with *Hind III* and a double digest with *Hind III* and *Sal I* indicated that only one of the colonies picked was a clone. The double digest reaction released a fragment corresponding to the size of the fragment

originally amplified using PCR (Fig. 2.8). Restriction with *Hind III* alone also confirmed that the same clone contained an insert as the restricted vector ran at a molecular size of approx. 5Kb (Fig. 2.9).

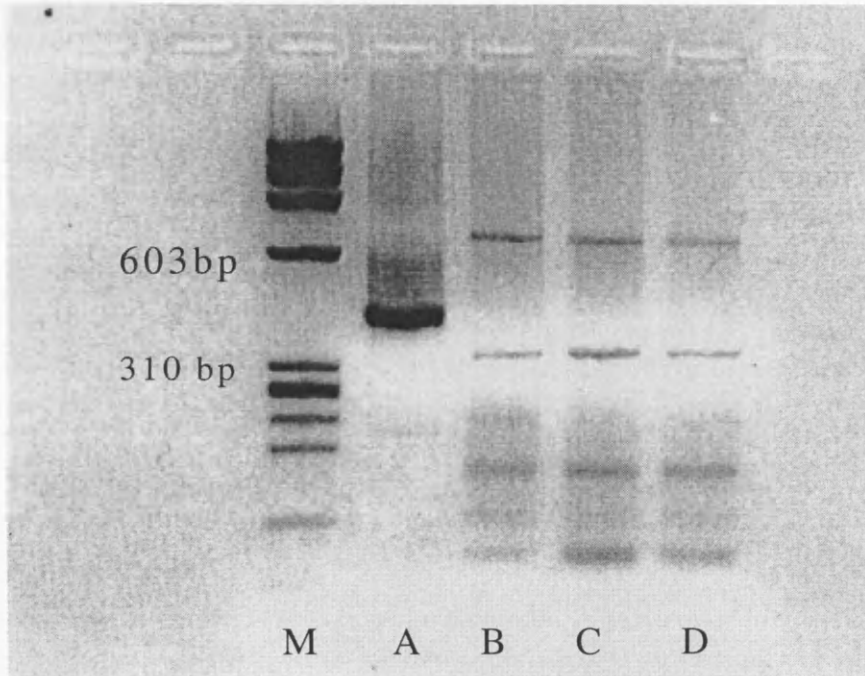


Fig. 2.5 Diagnostic PCR amplification of human C κ domain using tonsil cDNA as a template. The PCR reaction was carried out using primers that amplify a 327 bp product. (M) ϕ x174 DNA restricted with *Hae III* was used as a marker. (A) Actin positive control; (B) - (D) PCR amplification of human C κ sequence with annealing temperatures of 52°C for 5 cycles and 62°C for 30 cycles. 20 μ l aliquots of the reaction were run on a 2.5% agarose gel at 100V for 3 hours and then stained with ethidium bromide (0.5 μ g/ml). The gels were then visualised by exposure to UV light on a transilluminator.

Fig. 2.6 PCR amplification of human C κ sequence using tonsil cDNA as template. (B) - (G) PCR amplification of human C κ sequence with annealing temperatures of 55°C for 5 cycles and 65°C for 30 cycles; (H) - (K) PCR amplification of human C κ sequence with annealing temperatures of 60°C for 5 cycles and 65°C for 30 cycles. (M) ϕ x174 DNA restricted with *Hae III* was used as a marker. 20 μ l aliquots of the reaction were run on a 2.5% agarose gel at 100V for 3 hours and then stained with ethidium bromide (0.5 μ g/ml). The gels were then visualised by exposure to UV light on a transilluminator.

Fig. 2.7 Estimation of excised and restricted human C κ amplicon concentration. (A) The PCR product was excised using the Nucleon™ easiClene kit and then restricted with 10U of *Sal I* and 10U of *Hind III*. 5 μ l from a 20 μ l reaction were run on a 2.5% agarose gel at 100V for 3 hours and then stained with ethidium bromide (0.5 μ g/ml). The gel was then visualised by exposure to UV light on a transilluminator. 20 μ l of a solution containing ϕ x174 DNA restricted with *Hae III* was used as a marker. The 310 bp marker contains approx. 58 ng; therefore it was estimated that the amplicon contained \approx 20ng. The solution containing the restricted PCR product was taken to be 4ng/ μ l.

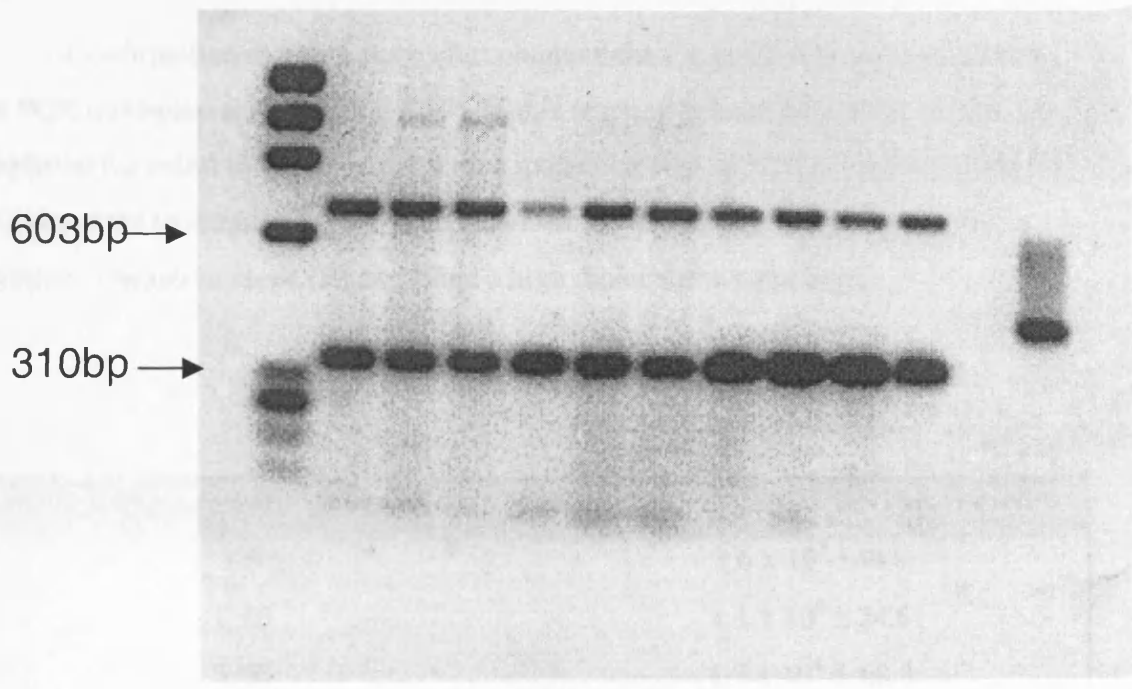


Fig. 2.6 PCR amplification of human Cκ sequence

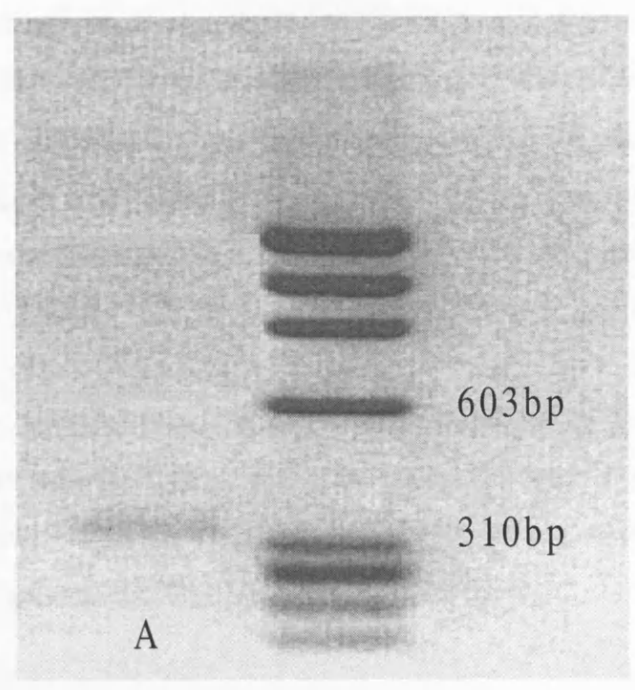


Fig. 2.7 Estimation of excised and restricted human Cκ amplicon concentration

Confirmation that this clone (B) contained the C κ insert was also provided by the PCR mini-prep analysis (Fig. 2.10). In this reaction at least three other clones amplified the insert in that they ran with a molecular size of 327 bp. Another clone (J) also appeared to amplify the C κ band, however the signal was much weaker. In addition, a negative clone (E) amplified a high molecular weight band.

Ligation Regime ; vector : insert	Transformation Efficiency ($\mu\text{g} / \text{DNA}$)
1:5	$3.6 \times 10^3 \pm 44.8$
1:10	$1.1 \times 10^4 \pm 24.6$
1:50	$1.3 \times 10^4 \pm 68.8$

Table 2.1 Transformation efficiencies for each cloning regime used in the ligation reaction for the insertion of C κ into the pEGFPC1 vector and the subsequent transformation into competent DH5 α bacterial cells. Results are expressed as Average \pm S.E.M. 0.5 microlitre aliquots of the 1:25 dilution of the restricted vectors (0.5 $\mu\text{g}/\mu\text{l}$) were used for ligation and the corresponding volume of the excised, restricted amplicon to give a vector:insert ratio of 1:5, (12.5 μl) 1:10 (6.25 μl) and 1:50 (1.25 μl). Ligation reactions were carried out in 20 μl . 3 μl of the ligation reaction was used for transformation. The number of colonies generated from transformation with a negative control ligation reaction (using a vector restricted with *Sal I* and *Hind III* without any insert) was used as background and subtracted from the colony count. The positive control pUC 19 transformation reaction gave an efficiency of $5.6 \times 10^5 \pm 35.8$.

Fig. 2.8 Restriction of mini-prep DNA of putative pEGFP-C1-C κ clones with *Hind III* and *Sal I*. Reactions were carried out in 20 μ l with 10U of each enzyme at 37°C for 2 hours. Restriction reactions were run on a 2.5% agarose gel at 100V for 3 hours and then stained with ethidium bromide (0.5 μ g/ml). The gel was then visualised by exposure to UV light on a transilluminator. (M1) 20 μ l of a solution containing ϕ x174 DNA restricted with *Hae III* was used as a marker alongside (M2) λ bacteriophage DNA restricted with *Hind III*. The only clone which appears to release an insert the same size as C κ is (B).

Fig. 2.9 Restriction of mini-prep DNA of putative pEGFPC1-C κ clones with *Hind III* only. Reactions were carried out in 20 μ l with 20U of *Hind III* at 37°C for 2 hours. Restriction reactions were run on a 1% agarose gel at 100V for 2 hours and then stained with ethidium bromide (0.5 μ g/ml). The gel was then visualised by exposure to UV light on a transilluminator. (M) λ bacteriophage DNA restricted with *Hind III* was used as a marker. As in Fig. 10, the only clone which appears to contain an insert and thus generate a band \approx 5Kb is (B).

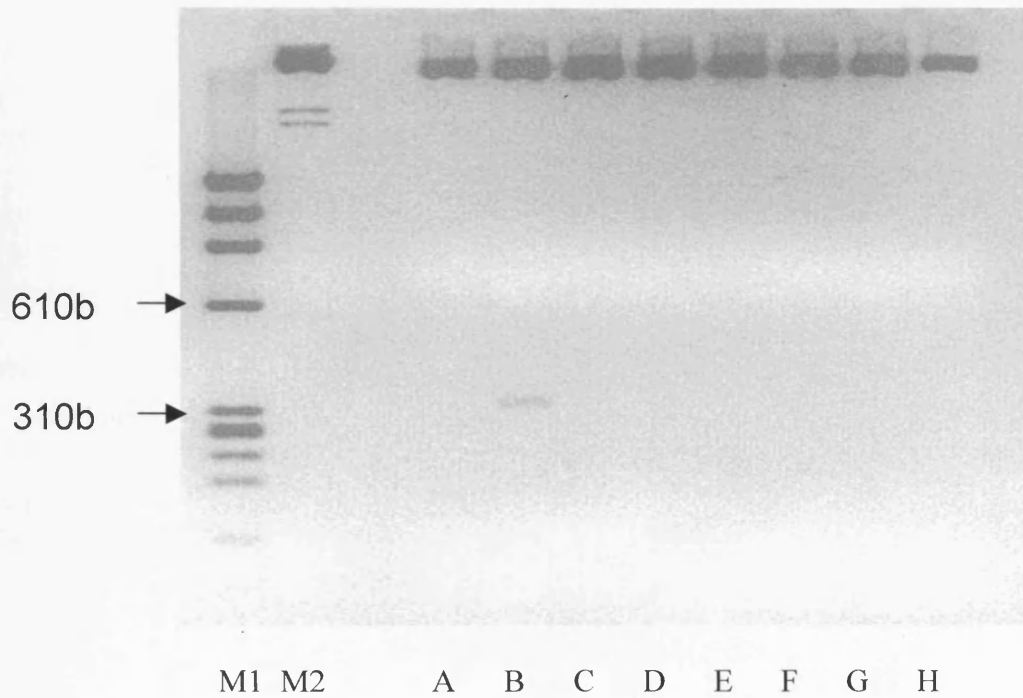


Fig. 2.8 Double Restriction of mini-prep DNA of putative pEGFP-C1-C κ with *Hind III/Sal I*

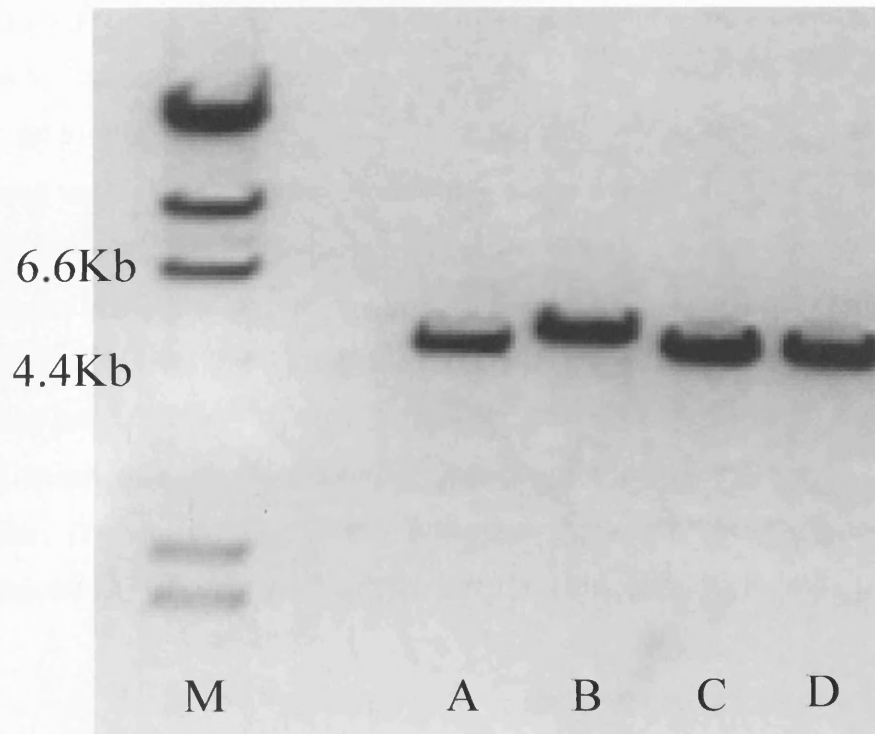


Fig. 2.9 Restriction of mini-prep DNA of putative pEGFP-C1-C κ with *Hind III* only

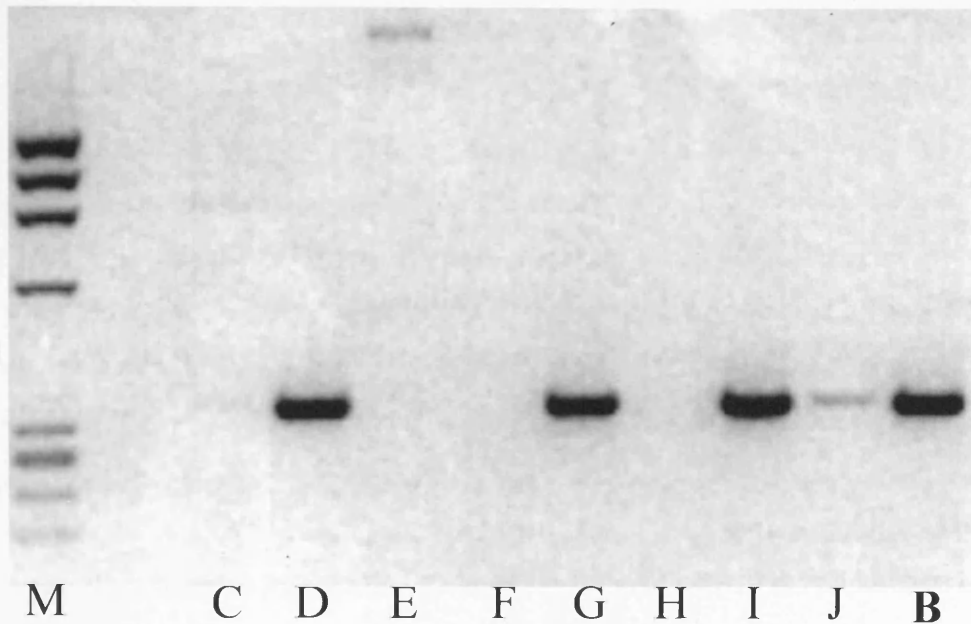


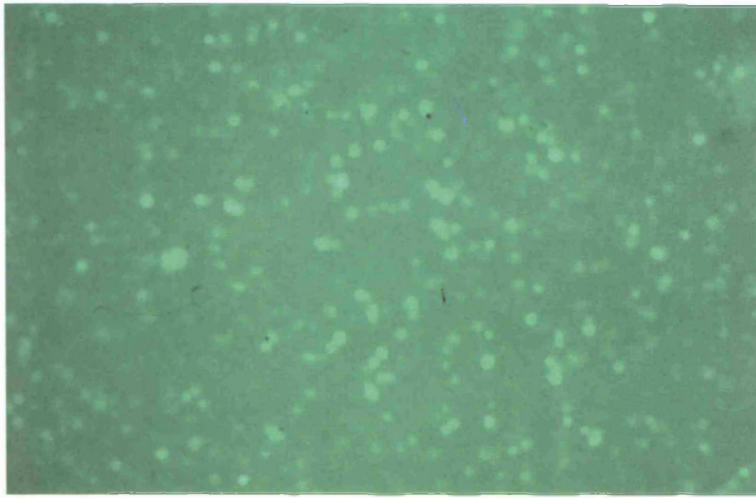
Fig. 2.10 PCR mini-prep of putative positive clones. Clones from the vector:insert containing the most colonies (1:50) were resuspended in 0.95ml of UP H₂O and boiled for 5 min. After spinning in a microcentrifuge, 5 μ l of the supernatant was used as a template for a PCR reaction. Amplification mixtures were carried out in 50 μ l containing 1 x PCR buffer as outlined before. 2.5U of Taq polymerase were used. Annealing temperatures of 60°C for 30s and 5 cycles and 65°C for 30s and 35 cycles were used. Sterile UP H₂O was used as a negative control template for the reaction and the positive clone **(B)** confirmed by restriction analysis was used as a positive control. All reactions were run on a 2.5% agarose gel at 100V for 2 hours and then stained with ethidium bromide (0.5 μ g/ml). The gel was then visualised by exposure to UV light on a transilluminator. Clones (D), (G), (I) and possibly (J) amplified the C κ insert of the correct size of 327 bp. (B) also confirmed it's status as a positive clone.

2.3.2 Transfection and Expression of pEGFP-C1-C κ clone

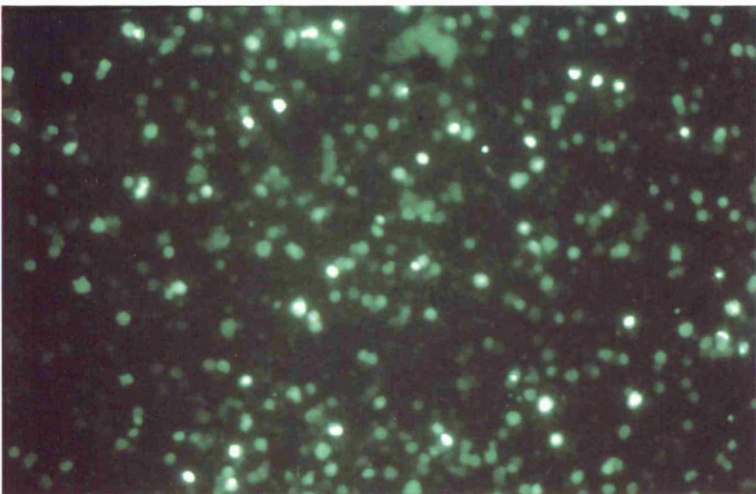
The microscopy images confirm that the vector emits a green fluorescent light when excited at 488nm (Fig. 2.11). More importantly, they clearly show that the pEGFPC1-C κ clone emits a significantly more intense fluorescence than the wild-type (wt) vector. In addition, these images also indicate that after 48hrs. the wt protein producing the fluorescence begins to degrade. There is a marked difference between the sharpness of the wt vector's fluorescence at 48 hrs. and its fluorescence at 72hrs., especially at higher magnification. Interestingly, the images from the clones at 48hrs. and at 72hrs. appear to be as sharp as each other at higher magnification. However, at low magnification, it could be argued that after 72hrs. the population transfected with clone does begin to lose some intensely fluorescent cells. This population appears to indicate both cytoplasmic and nuclear fluorescence.

Fig. 2.11 Transient transfection of human lung MRC5 cells with both the wild type (wt) pEGFPC1 vector **(A)**, **(C)**, **(E)** and **(G)** and the pEGFP-C1-C κ vector **(B)**, **(D)**, **(F)** and **(H)**. The cells were transfected using 2 μ g of plasmid DNA and 8 μ l of lipofectamine reagent. They were then incubated with the DNA-lipofectamine complex for 5 hours at 37°C in a CO₂ incubator. Following incubation, 1ml of growth medium containing twice the normal concentration of serum was added to the transfection mixture. The medium was then replaced with fresh, complete medium 24 hours following the start of transfection. After 48 and 72 hours of transfection, the cells were trypsinised and washed, as described earlier, to give an approx. concentration of 1 x 10⁶ cells /ml. Cytospin slides were then prepared and immediately fixed in 95% ethanol after centrifugation. They were then washed in PBS and mounted in Dabco. A Zeiss fluorescent microscope was then used to analyse the slides.

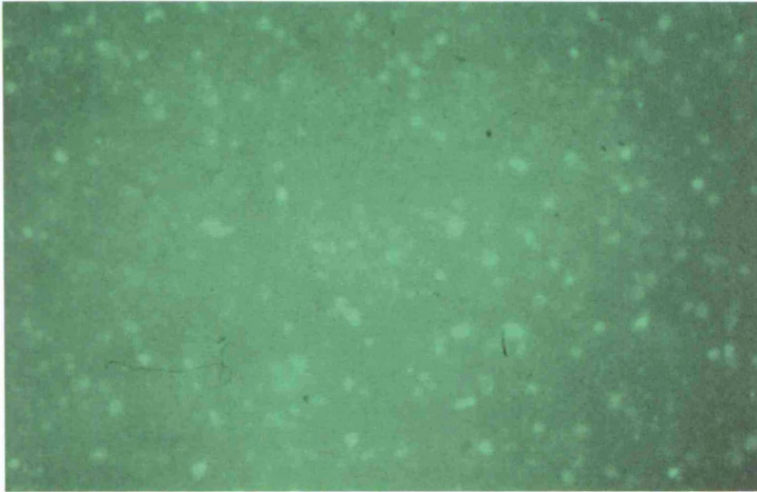
(A), **(B)**, **(E)** and **(F)** were analysed for fluorescence 48 hours after transfection.
(C), **(D)**, **(G)** and **(H)** were analysed for fluorescence 72 hours after transfection.



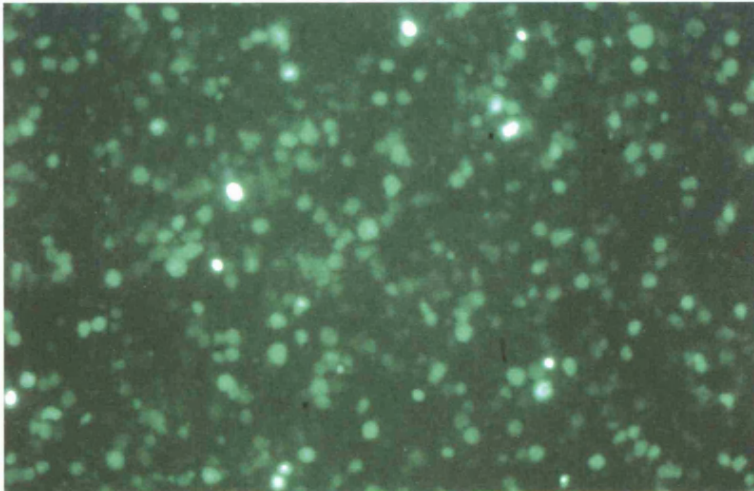
(A) x 10 magnification; cells transfected after 48 hrs. with wt vector



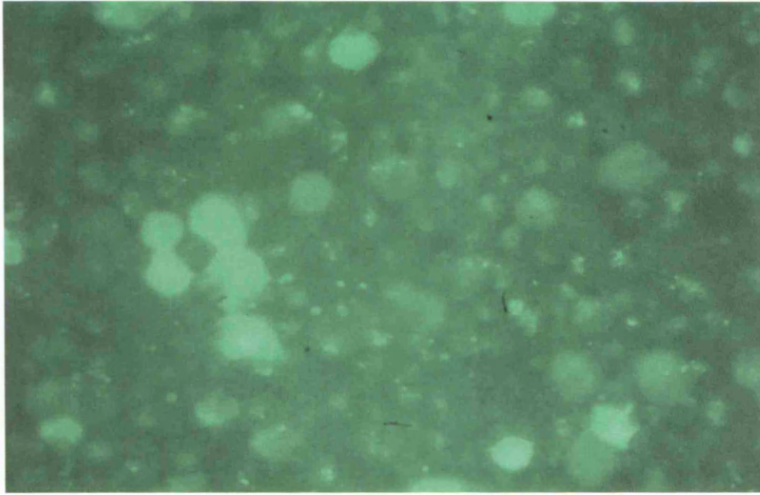
(B) x 10 magnification; cells transfected after 48 hrs. with pEGFPC1-C κ



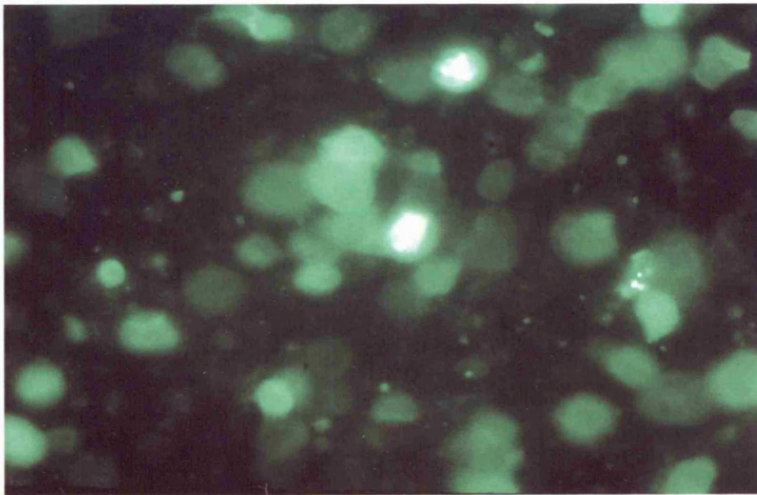
(C) x 10 magnification; cells transfected after 72 hrs. with wt vector



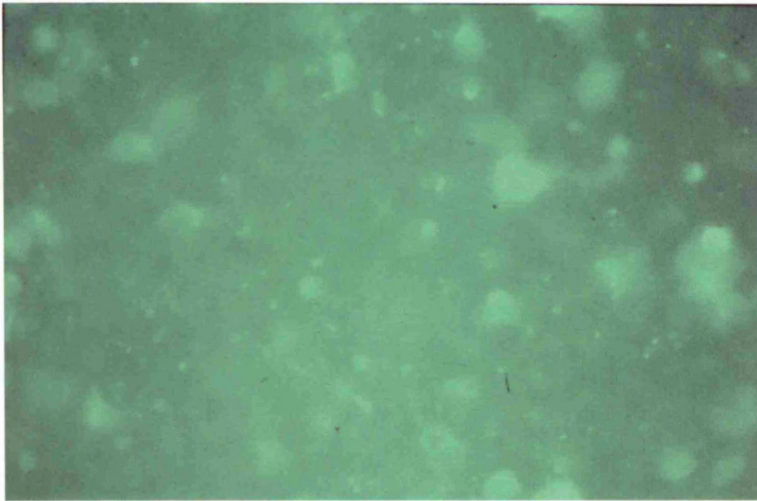
(D) x 10 magnification; cells transfected after 72 hrs. with pEGFPC1-C κ



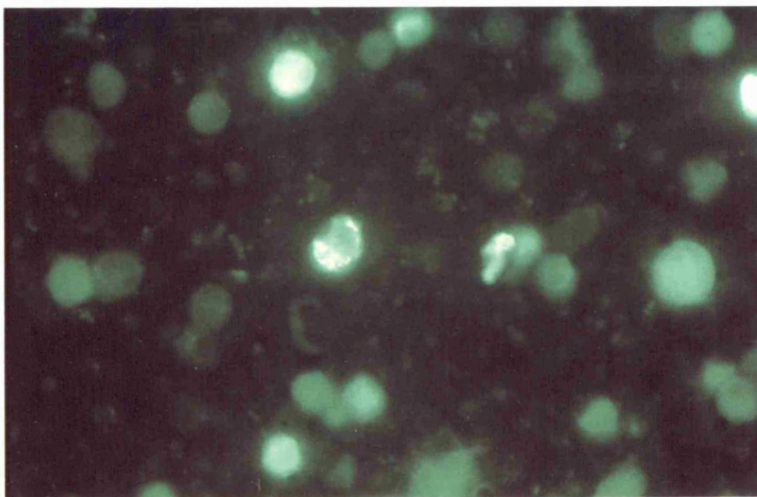
(E) x 40 magnification; cells transfected after 48 hrs. with wt vector



(F) x 40 magnification; cells transfected after 48 hrs. with pEGFPC1-C κ



(G) x 40 magnification; cells transfected after 72 hrs. with wt vector



(H) x 40 magnification; cells transfected after 72 hrs. with pEGFPC1-C κ

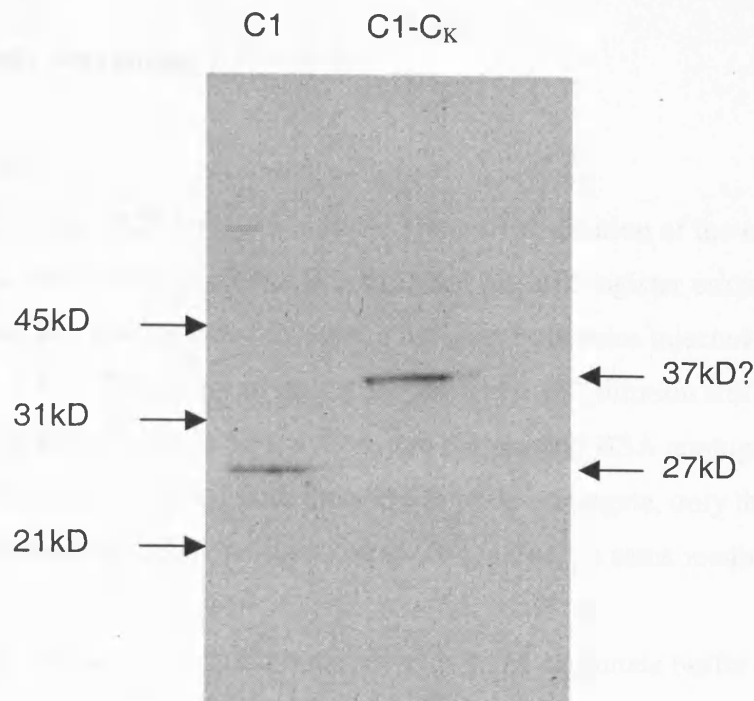


Fig. 2.12 Western blot of MRC5 cells transfected with pEGFP-C1 and pEGFP-C1-C κ and probed with an anti-GFP polyclonal antibody. MRC5 cells were transfected in a 6 well plate using Lipofectamine and 2 μ g of vector DNA as described. After 24 hours the cells were lysed and the amount of protein extracted using the Bradford assay. 8 μ g of extracted protein from each well was run on a NuPage™ MES 4-12% polyacrylamide gel as described. The membrane was then probed with an anti-GFP polyclonal antibody that detects the 27kDa protein. Binding of the antibody was then detected using the ECL chemiluminescence system.

Fig. 2.12 illustrates the results obtained after MRC5 cells were transfected with pEGFP-C1 and pEGFP-C1-C κ for 24 hrs and the lysates probed with a polyclonal anti-GFP antibody. In the lysate from cells transfected with pEGFP-C1 a band of the correct approximate size of 27 kDa protein was detected. Furthermore, in the lysates from cells transfected with the pEGFP-C1-C κ clone a band of an approximate size of 37kDa protein was detected. This appears to confirm that a fusion protein was being expressed.

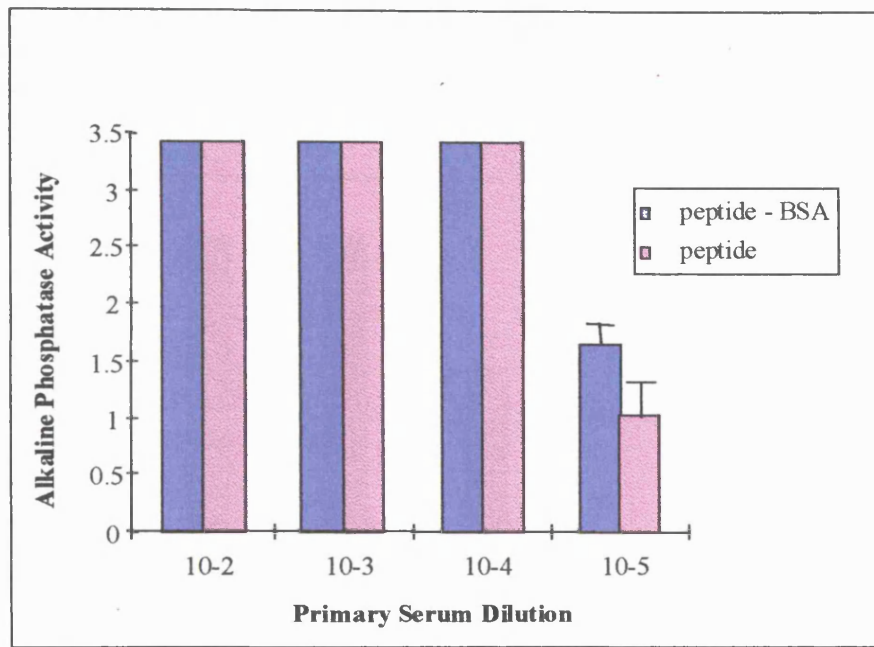
2.3.3 Antibody Screening

2.3.3.1 ELISA

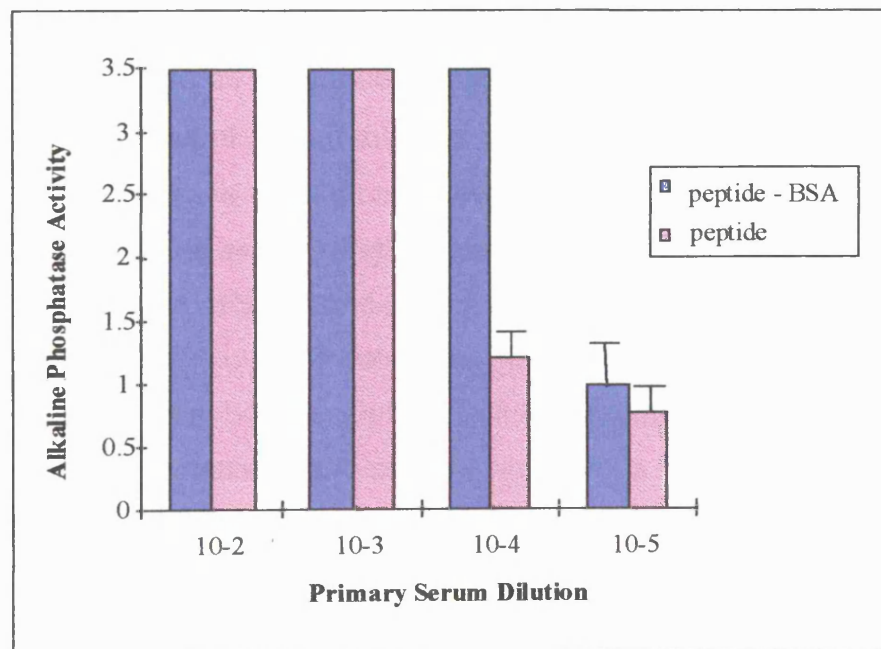
The peptide ELISA results indicated that a 10^{-5} dilution of the serum from both mice injected with both peptide-KLH conjugates can still register enzymatic activity. In addition, there was a significant difference between both mice injected with same peptide (Fig. 2.15). The serum of one of the mice at a 10^{-4} dilution still gave an off-scale reading with both the peptide on it's own, and the peptide-BSA conjugate (Fig. 2.15A). With the other mouse injected with the same peptide-conjugate, only the wells containing the peptide-BSA conjugate went off-scale at the same reading (Fig. 2.15B).

The p17N peptide would not dissolve in 0.1M carbonate buffer and hence only the peptide-BSA conjugate was used for screening the anti-serum. Again, the immunogenic response of both mice to the peptide-KLH varied considerably. At a 10^{-3} dilution, the serum from one of the mice bound to the conjugate to give an enzymatic activity reading which was off-scale; the binding of the serum of the other mouse at the same dilution was barely detectable (Fig. 2.16). In all cases, the peptide-BSA conjugate bound more serum than the peptide alone. In addition, the anti-caspase-3 antibody did not bind to either the peptide or the peptide-BSA conjugate.

Fig. 2.15 Anti-peptide p12N ELISA results for animals #1 (A) and #2 (B). Mice were immunised with peptides as described in Materials and Methods. Approx. 10µl of blood from tail was supplied and this was diluted in blocking buffer. 0.2µg of conjugated and unconjugated peptide were pre-coated onto Covalink plates by incubation at 4°C overnight. Dilutions of the serum ranging from 10^{-2} - 10^{-5} were used to detect the peptide or it's BSA conjugate. Rabbit anti-mouse immunoglobulin conjugated to alkaline phosphatase was used to detect the polyclonal titre. p-nitrophenyl phosphate was used as substrate. Optical Density readings were carried out at 405nm. Results are expressed as Average \pm Mean. As a negative control the same diluted serum was applied to Covalink plates without any coated peptide or peptide conjugate. For animal #1 values were obtained ranging from 0.5 for the 10^{-2} dilution to 0.07 for the 10^{-5} dilution; for animal #2 values were obtained ranging from 0.3 for the 10^{-2} dilution to 0.08 for the 10^{-5} dilution.



(A)



(B)

Fig. 2.15 Anti-peptide p12N ELISA results for animal #1 (A) and animal #2 (B).

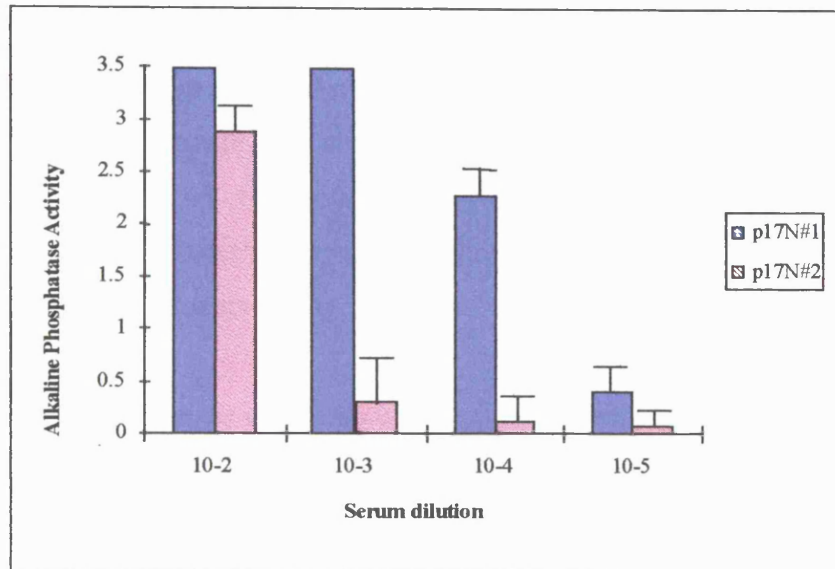


Fig. 2.16 Anti-peptide p17N ELISA results for animals #1 and #2. Mice were immunised with peptides as described in Materials and Methods. Approx. 10 μ l of blood from tail was supplied and this was diluted in blocking buffer. 0.2 μ g of conjugated peptide was pre-coated onto Covalink plates by incubation at 4 $^{\circ}$ C overnight. Dilutions of the serum ranging from 10⁻² - 10⁻⁵ were used to detect the peptide - BSA conjugate. Rabbit anti-mouse immunoglobulin conjugated to alkaline phosphatase was used to detect the polyclonal titre. p-nitrophenyl phosphate was used as substrate. Optical Density readings were carried out at 405nm. Results are expressed as Average \pm Mean. As a negative control the same diluted serum was applied to Covalink plates without any coated peptide conjugate. Values were obtained ranging from 0.3 for the 10⁻² dilution to 0.07 for the 10⁻⁵ dilution.

2.3.3.2 Immunocytochemistry

In certain cases the supernatant from antibody producing wells gave a similar immunopositivity pattern to a commercial monoclonal antibody that recognises the 32kDa proform of the enzyme (see Fig. 3.14; Fig. 2.17 A). The germinal centre was intensely stained, although in many cases the outer ring of the centre was the most intense. The surrounding mantle zone area was mostly immunonegative. In addition, the plasma cells and the epithelial cells were intensely stained. In general, 'pre-monoclonals' that had this pattern of immunopositivity were the only monoclonal antibodies produced from the screening.

However, other patterns were also observed. Supernatant from one well stained select crypt epithelial cells (Fig. 2.17B). Most importantly, supernatant from another well stained select cells within the germinal centre, and also the occasional epithelial and plasma cell (Fig. 2.17C, D, E, F, G). Higher magnification of the pattern of staining from this well seemed to indicate that the antibody (or antibodies) was recognising apoptotic cells and apoptotic bodies (Fig. 2.17H). In addition, the occasional tingebale body macrophage was staining positively. Unfortunately, after stabilisation and dilution cloning the monoclonal antibody produced from this well and the well recognising the select crypt epithelial cells was not stabilised.

Fig. 2.17 (A - H) Photomicrographs of tissue sections of human tonsil stained with a variety of anti-caspase-3 'pre-monoclonal' antibodies. After microwaving for 20 min. in 10 mM citrate buffer, the sections were allowed to cool to room temperature for 30 min. They were then washed in PBS and blocked with 20% normal rabbit serum in blocking solution. The slides were then incubated with a 1:10 or a 1:20 dilution of the supernatant overnight at 4°C. The slides were then washed and incubated with secondary rabbit anti-mouse antibody. After washing, they were incubated with mouse APAAP. They were then detected with an alkaline phosphatase detection system and mounted using Aquamount.

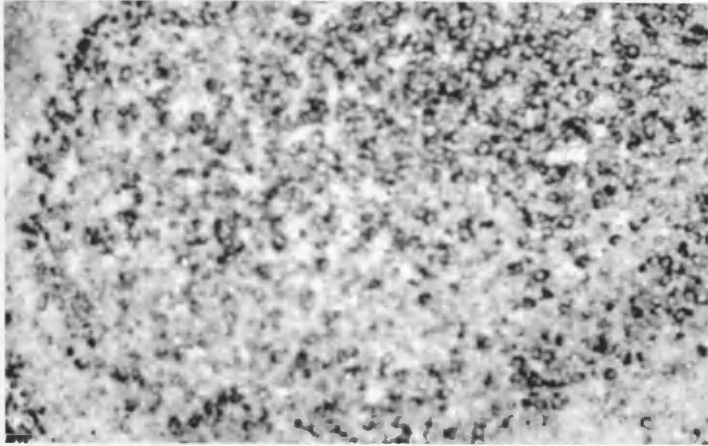


Fig. 2.17A Supernatant from pre-monoclonal well #37 x 16

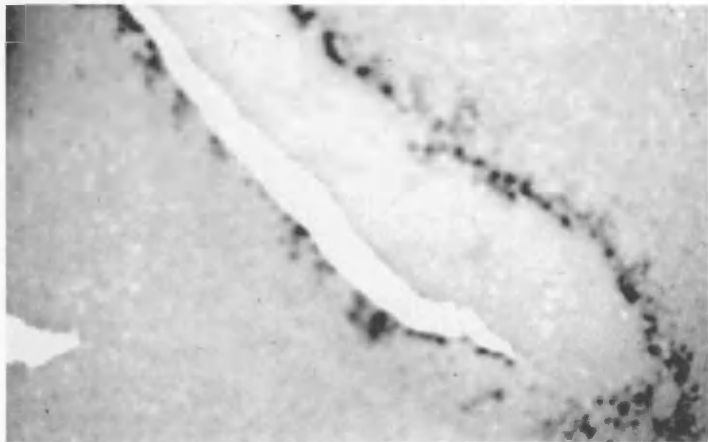


Fig. 2.17B Supernatant from pre-monoclonal well #3 x 6

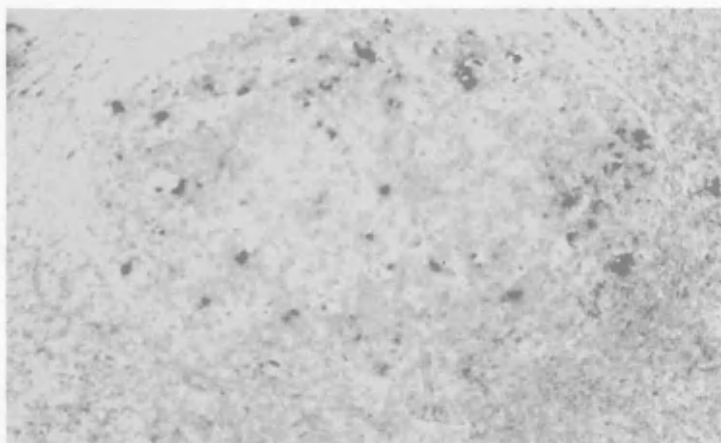


Fig.2.17C Supernatant from pre-monoclonal well #11 x 16

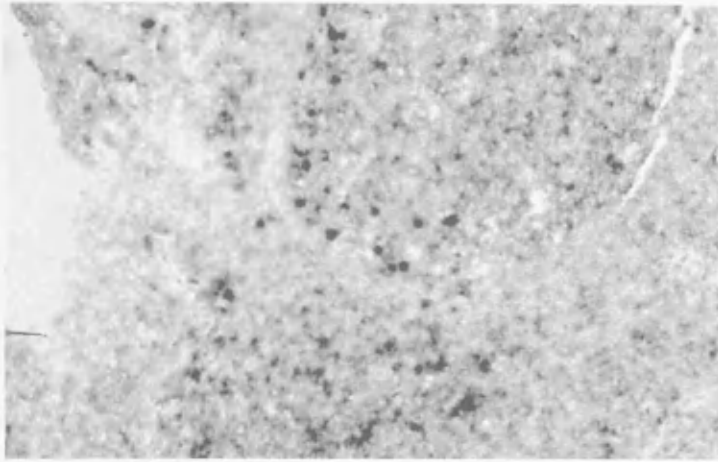


Fig. 2.17D Supernatant from pre-monoclonal well #11 x 16

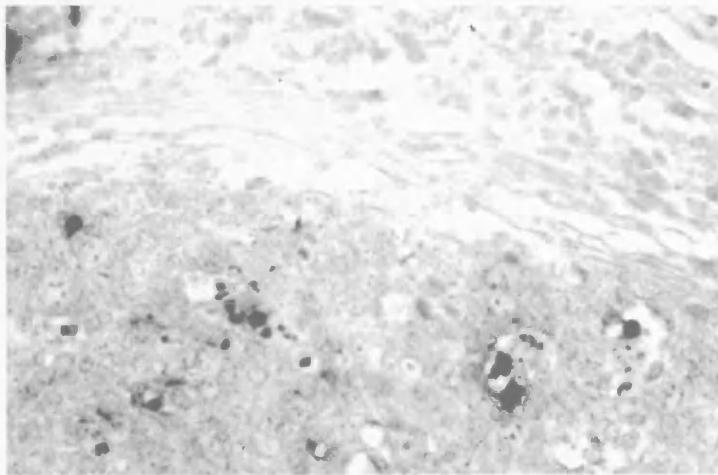


Fig. 2.17E Supernatant from pre-monoclonal well #11 x 40

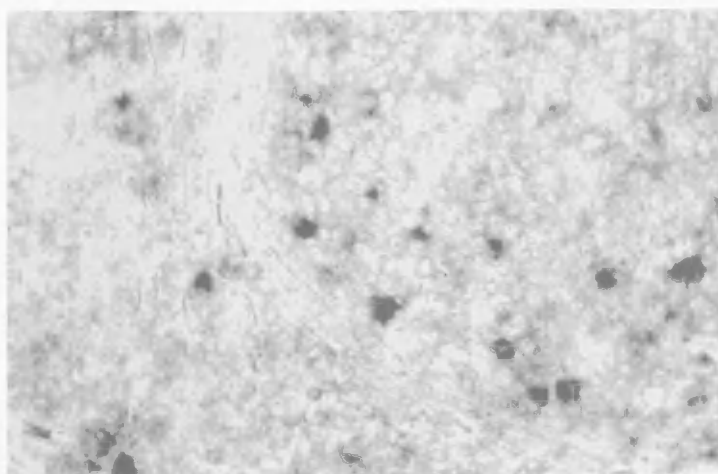


Fig. 2.17F Supernatant from pre-monoclonal well #11 x 40

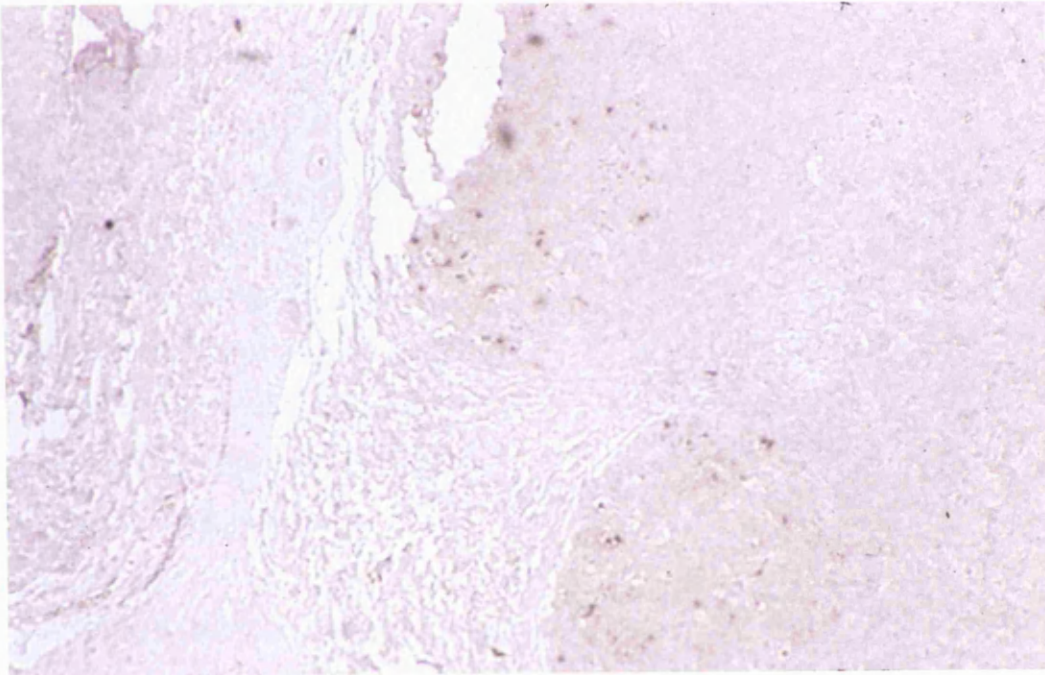


Fig. 2.17G Supernatant from pre-monoclonal well #11 x 6

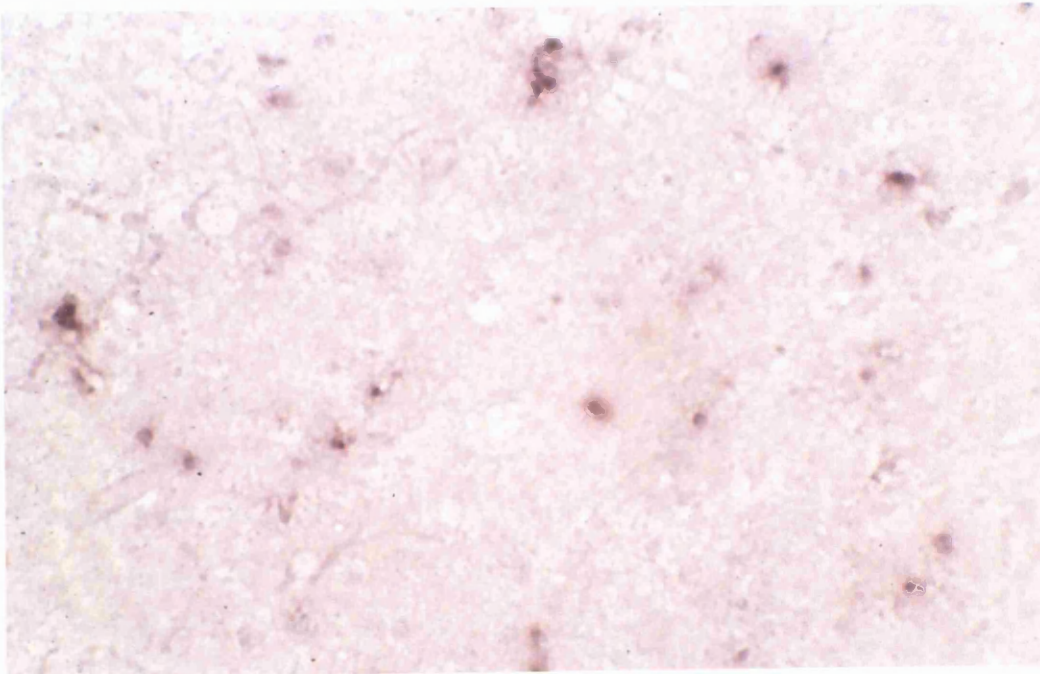


Fig. 2.17H Supernatant from pre-monoclonal well #11 x 100

2.4 ANALYSIS OF RESULTS

With the exception of the high molecular weight band, the extra bands produced in the diagnostic amplification of the Cκ insert appeared to disappear when the annealing temperature and the amount of template DNA was increased. These lower molecular weight bands may have just have been products of an incomplete extension reaction with the correct Cκ sequence. However, the 30 seconds used for extension in the PCR reaction should be sufficient time and therefore it is more likely that they were non-specific products. The high molecular weight band may be a section of DNA which is spliced and recombined to produce the Cκ sequence, or it may be the result of genomic DNA contamination.

Before ligation, no ethanol precipitation on either the restricted vector or the restricted amplicon was carried out due to concerns about loss of DNA. The transformation reaction with the positive pUC control indicated that the DH5α bacterial cells were sub-optimal. Nevertheless, restriction analysis identified a clone; of the twenty colonies analysed by restriction, only one appeared to contain the insert. Further confirmation that this clone contained the insert was provided by PCR mini-prep analysis. However, according to these reactions, many more of the fresh colonies picked for amplification contained an insert. It may be that the levels of enzyme used in the restriction analyses were not enough, although this seems unlikely as two different regimes isolated the same clone.

The transfection procedure into mammalian cells appeared to be very successful and approximately 20-30% of cells produced a green fluorescence using fluorescent microscopy. Without doubt, the images produced by the cells containing the cloned vector were sharper and much more fluorescent. This shows that it is very likely that the amplicon excised and cloned into the pEGFPC1 vector was the Cκ domain. The more intense and sharper images produced by these transfected cells were probably due to the greater stability of the green fluorescent protein fused to the Cκ insert at the C-terminus.

A Western blot of lysates from MRC5 cells transfected with pEGFP-C1 and probed with an anti-GFP polyclonal antibody produced a band of the correct approximate size of 27kDa. Lysates from the same cells transfected with pEGFP-C1-Ck produced a higher band of approximately 35kDa indicating that a fusion protein with GFP was being produced.

The peptide ELISA only provided information with respect to the strength of the polyclonal response of the mouse. It gives us no information with regards to whether the antibodies elicited from a peptide would recognise a native antigen. It confirmed the massive variability within species immunised with the same antigen. Another result was that the peptide-BSA conjugates consistently gave higher enzymatic values than the peptide alone, thus indicating that more polyclonal serum was binding. This was probably due to the presentation of the antigen to the serum in the well. Smaller-size peptides may be harder for antibodies to recognise unless they are conjugated to a bulky protein. These results may have been different with the peptide mimicking the N-terminus of the p17 fragment, as it was larger and may not have had this difficulty. However, because this peptide would not dissolve on its own and only the BSA conjugate was used to measure the response, this cannot be evaluated. The ELISA results did appear to confirm that p12N was substantially more immunogenic, as estimated using the different antigenic values given to amino acids. In addition, the commercial murine monoclonal anti-caspase-3, which should recognise the inactive 32KDa proform, did not bind any peptide ELISA. This is not surprising, considering that a protein may have many epitopes.

With respect to the screening of the pre-monoclonals using immunocytochemistry, at least three patterns emerged. One pattern mirrored many times produced intense immunoreactivity within the germinal centre. The mantle zone, which consists of long-lived lymphocytes, was predominantly negative. With this pattern the epithelial cells were moderately positive also. Most importantly, this pattern of staining was also obtained with the commercial murine monoclonal antibody that recognises the proform of the Caspase-3 (see Fig. 3.14). The stabilised clone from this well gave a similar immunopositivity pattern when screened using immunohistochemistry, however,

initial Western blot results indicated that this enzyme may not have been specific for Caspase-3 (data not shown).

Epithelial cells are known to express Caspase-3 and hence the staining of the select crypt epithelial staining cells may represent cells with an active p12 fragment, however, the antibodies from this well did not produce a stable clone. It may be that the antibody (or antibodies) which bound to the antigen present in the crypt epithelial lining recognised an active form of caspase-3, whose epitope was unique to the particular cell type. The immunostaining of the select cells within the germinal centre was exactly what the peptide was designed for, in that it appeared to be binding only the active fragment of caspase-3. Higher magnification also indicated a very intense, non-cytosolic immunostaining pattern; furthermore, some of the cells staining appear very similar to apoptotic bodies. In addition, the occasional tingeable body macrophages appear to be staining with supernatant from this 'pre-monoclonal' well.

Of course, without any blotting evidence, the possibility exists that the anti-peptide 'pre-monoclonal' antibodies may be cross-reacting with an entirely different antigen. However, the very specific affinity of the supernatant from one of the wells for select cells within the germinal centre that are dying or being phagocytosed suggests an apoptotic-body binding antibody. Unfortunately, dilution cloning of the cells from this well did not produce a stable clone.

Chapter 3

INVESTIGATING CASPASE-3 EXPRESSION AND APOPTOSIS IN DIFFUSE LARGE CELL LYMPHOMA

3.1 INTRODUCTION

The heterogeneous nature of B cell Diffuse Large Cell Lymphoma (DLCL) has often made the basis of classification very difficult and is believed to be the major reason for the variation in clinical outcome which has been reported (Harris *et al.* 1994). Although these tumours can be successfully treated with chemotherapy or radiotherapy, primary chemoresistance and relapse often occurs and is the major cause of death in these patients. Most importantly, tumours that relapse are frequently resistant not just to the initial agent used for treatment but also to other unrelated compounds.

Many haematopoietic malignancies display a multidrug-resistance phenotype and this is thought in part to be due to the overexpression of proteins such as P-glycoprotein (P-gp), glutathione S-transferase (GST) and members of the multidrug resistance - associated protein family (MRP) (Cole *et al.* 1992; Tew 1994; Shustik *et al.* 1995). However, differences in primary and secondary chemoresistance do not appear to be solely attributable to the expression of these proteins. Emerging evidence suggests that many tumour cells, including DLCL cells, are intrinsically unable to activate the apoptotic machinery and may therefore be fundamentally resistant to chemotherapy (and possibly radiotherapy) (Hannun 1997).

Evidence has shown for some time that most chemotherapy agents used to treat tumours induce apoptosis in their target cells (Thompson 1995). The expression of Caspase-3, a crucial enzyme in the apoptotic process, in a variety of non-Hodgkin's Lymphomas (NHL) and Hodgkin's Disease has already been reported and found to be highly variable (Krajewska *et al.* 1997; Krajewski *et al.* 1997; Xerri *et al.* 1997). Recent data, however, suggests that the level of expression and the localisation of this enzyme may have significance with respect to the progression of tumorigenesis (Nakagawara *et al.* 1997).

The aim of this study, therefore, was to investigate the expression of Caspase-3 using immunohistochemistry and a quantitative reverse transcriptase-polymerase chain reaction technique (RT-PCR) in DLCL patients prior to treatment. In addition, the rates

of apoptosis as measured by DNA fragmentation were estimated and examined with respect to the expression of Caspase-3. Also, the pattern of expression of the p17 fragment of Caspase-3 was evaluated in reactive lymphoid and DLCL tissue. Various data was then correlated with clinical outcome, including stage at presentation, response to therapy, and survival. Finally, Western blotting of select cases of frozen DLCL tissue was carried out with anti-Caspase-8, anti-FLIP and anti-Caspase-3 and -2 to investigate the variation of levels of these proteins.

3.2 MATERIALS AND METHODS

3.2.1 Investigation of Caspase-3 Expression and Apoptosis in DLCL

3.2.1.1 Diffuse Large Cell Lymphoma cases

Fifty-four consecutive cases of high grade DLCL tissue biopsies taken for routine diagnosis with patient consent and ethical permission were used in this study. The cases were diagnosed as high-grade-B-cell lymphomas by an experienced histopathologist and confirmed by a standard panel of lymphoma antibodies. The ages of the patients ranged from 18 to 85 years, with a median of 69 years and a mean of 65 years. All cases used were diagnosed between 1991 and 1996, and analysis was carried out in April 1998. Treatment for the vast majority of patients consisted of a variety of cycles of regime of CHOP (cyclophosphamide, adriamycin, vincristine and prednisone), and in some cases this was combined with radiotherapy. Staging of the tumours was carried out as according to Ann Arbour. No primary extra-nodal cases of DLCL were included in the study. Complete remission was defined as absence of clinically detectable disease for 6 months after completion of treatment, and partial remission was defined as a reduction in disease bulk short of 50% as measured by computed topography scanning. All patients presented without prior treatment.

3.2.1.2 Immunohistochemistry

Formalin-fixed paraffin-embedded tissue sections were dewaxed in xylene and rehydrated through graded alcohol to distilled water. The sections were subjected to antigen retrieval by boiling in a microwave for 20 min. 0.01M sodium citrate buffer (pH 6.0). The primary monoclonal antibody to the pro-form of Caspase-3 (Transduction Laboratories, Lexington, KY) was applied at a dilution of 1:1000. The primary polyclonal antibody to the p17 fragment of Caspase-3 (Pharmingen, San Diego, USA) was applied at a dilution of 1:1500. The primary monoclonal antibody to Bcl-2 was applied at a dilution of 1:1000. All antibodies were incubated overnight at 4°C. After incubation, the slides treated with monoclonals were treated with biotinylated rabbit antimouse immunoglobulin (1:600 for 30 min.; Dako Ltd., Ely UK); the slides treated

with the polyclonal primary antibody were treated with biotinylated goat antirabbit immunoglobulin (1:1500 for 30 min.; Dako Ltd., Ely UK). After secondary antibody treatment all slides were washed in TBS thrice for 5 min. The signal was then visualised using the substrate 5-bromo-4-chloro-3-indolyl phosphate (BCIP) and the chromogen nitroblue tetrazolium (NBT). The substrate and chromogen solution was made up in substrate buffer containing 0.1M Tris pH 9.5, 0.1M NaCl and 0.05M MgCl₂. A 0.1M solution of NBT was made up in 70% dimethylformamide (DMF) and a 0.1M BCIP solution was made up in UP H₂O. A detection solution was then made up consisting of 10mM NBT, 10nM BCIP and 10mM Levamisole. The slides were treated with the detection solution for 10 min. to 1 hour. After substrate development, the sections were washed in tap water and mounted in an aqueous solution. A negative control with no primary antibody was always carried out alongside the reaction containing sample.

3.2.1.3 *In situ end-labelling (ISEL)*

The tissue sections were treated with Proteinase K at 5µg/ml in 0.05M Tris pH 7.65 for 1 hour and then rinsed twice in UP H₂O at 4°C for 5 min. After washing the sections were incubated at 4°C in 0.4% paraformaldehyde in PBS for 20 min. They were then rinsed twice in UP H₂O at room temperature. After this washing the sections were incubated in terminal deoxynucleotidyl transferase (Tdt) buffer [140mM sodium cacodylate (C₂H₆AsO₂Na) and 1mM cobalt chloride (CoCl₂) brought to pH 7 with HCl] for 5 min. before labelling. The sections were then incubated in 50µl labelling solution at 37°C for 2 hours. Labelling solution consisted of 100pmoles digoxigenin-11-dUTP (DIG-11-dUTP) and 10 units of Tdt enzyme per 50µl Tdt buffer. A negative control of labelling solution without Tdt enzyme was always included in the reactions. After incubation in the labelling solution the sections were rinsed twice in UP H₂O at room temperature and incubated in blocking solution [3% BSA; 0.1% Triton X100 in TBS] at room temperature for 10 min. They were then incubated with polyclonal sheep anti-digoxigenin alkaline phosphatase conjugate diluted 1:600 in blocking solution for 30 min. The sections were then rinsed twice in TBS for 5 min. and then twice in UP H₂O. Finally the sections were incubated in substrate buffer for 5 min. and then the signal was visualised using the substrate 5-bromo-4-chloro-3-indolyl phosphate and the chromogen nitroblue tetrazolium (see 3.2.1.2). After substrate development, the sections were washed in tap water and mounted in an aqueous solution.

3.2.1.4 Solid Phase RT-PCR using magnetic oligo(dT) beads

Dynabeads™ (Dyna, Oslo, Norway) are magnetic beads coated with oligo(dT) sequences and can be used to capture poly(A) mRNA from total RNA preparations or directly from cell/tissue lysates. Once the mRNA is captured the oligo(dT) can be used as a primer for reverse transcriptase and produce cDNA that remains covalently bound to the beads. The reaction is therefore a solid phase RT-PCR (see Fig. 3.1).

A 10µm slice of each frozen tumour section was cut on a cryostat and immediately resuspended in 100µl of lysis/binding buffer (100mM Tris-HCl, pH 8.0, 1% w/v sodium dodecyl sulphate (SDS), 5mM dithiothreitol (DTT) at 4°C. The tissue suspension was then incubated with 50µg/ml proteinase K for 1 hour at 37°C. The lysate was centrifuged for 30s at 10,000 g, and the supernatant mixed with oligo(dT)-linked Dynabeads. The mRNA was allowed to anneal to the Dynabeads for 10 min. at room temperature. mRNA-linked Dynabeads were washed twice in a buffer containing LiDS (10mM Tris-HCl, pH 8.0, 0.15M LiCl, 1mM EDTA, 0.1% LiDS: Dynal) and three times in the same buffer without LiDS. After washing, the Dynabeads were finally resuspended in diethyl pyrocarbonate (DEPC)-treated water.

Dynabead-linked mRNA was then resuspended in reverse transcriptase buffer (Promega, Southampton, UK) containing 10mM DEPC-treated dNTPs (Pharmacia Biotech, Uppsala, Sweden), 25U RNasin™ and 5U AMV Reverse Transcriptase (both from Promega). Priming was by the oligo(dT) Dynabeads and incubation was for 1 hour at 42°C. A similar reaction, set up without the reverse transcriptase, was used as a control for genomic contamination.

The cDNA-linked beads were then resuspended in PCR buffer [45mM Tris, pH 8.8, 11mM (NH)₄SO₄, 4.5mM MgCl₂, 200 µM dNTPs, 110µg/ml ultrapure BSA (Advanced Protein Products Ltd., Brierly Hill, UK), 6.7mM β-mercaptoethanol, 4.4µM EDTA, pH 8.0], containing 10pmol of forward and 10pmole reverse primer. The following primers were used for amplification of the Caspase-3 and GAPDH genes:

Forward Caspase-3 primer: 5'-CAAACCTTTTTTCAGAGGGGATCC-3'

Reverse Caspase-3 primer: 5'-GCATACTGTTTCAGCATGGCAC-3'

Forward GAPDH primer: 5'-AGAACATCATCCCTGCCTC-3'

Reverse GAPDH primer: 5'-GCCAAATTCGTTGTCATACC-3'

A "hot-start" PCR was then carried out as follows: one cycle of denaturation at 98°C for 3 min. holding at 60°C during addition of 1U of *Taq* DNA polymerase (Life Technologies Ltd., Paisley, Scotland): primer extension at 72°C for 30s; 4 cycles of denaturation at 94°C for 1 min. annealing at 60°C for 30s, and primer extension at 72°C for 30s; 23 cycles and 30 cycles for GAPDH and Caspase-3, respectively, of denaturation at 94°C for 30s, annealing at 60°C for 30s, and primer extension at 72°C for 30s. Preliminary experiments were carried out to confirm that the respective number of cycles maintains the amplification reaction in exponential phase. All PCR products were then visualised using agarose gel electrophoresis. The predicted sizes of the amplified products of Caspase-3 and GAPDH were 272 and 354 bp, respectively.

An ELISA system (see Fig. 3.3) was used to detect and quantify the RT-PCR products. Covalink™ plates (Nunc, Rochester, NY, USA) were biotinylated by incubation overnight with n-hydroxy-succinyl biotin (20µg/ml in PBS) at room temperature. Plates were then washed three times with Buffer 1 (2M NaCl, 40mM MgSO₄, 0.05% vol/vol Tween 20 in PBS) and treated with avidin (50µg/ml in Buffer 1) for 30 min. at room temperature, with agitation. Following three washes in Buffer 2 (0.02% Tween 20 in PBS), the plates were treated 3% PBS/BSA for 15 min. at room temperature, with agitation. The PCR products were dissolved 1:100 in PBS/BSA and allowed to bind to the avidin-coated plates for 1h at room temperature, with agitation. The non-biotinylated (in this case the reverse strand) PCR products were denatured from the biotinylated (the forward strand) by addition of 0.25M NaOH for 10 min. at room temperature. The plates were then incubated for 1.5h at 42°C with oligonucleotide probes previously labelled with a 1:5 ratio digoxigenin-11-dUTP:dATP by terminal deoxytransferase (Promega) in the supplied buffer and diluted to 0.2pmol/100µl in rapid hybridisation buffer (Amersham International, Bucks, UK). The probe used for Caspase-

3 hybridisation was 5'-CAATGCCACAGTCCAGTTCT (see Fig 3.2) and the probe used for GAPDH hybridisation was 5'-GTTGAAGTCAGAGGAGACC-3'. The plates were then washed three times in Buffer 2, before incubation with alkaline phosphatase-conjugated, anti-digoxigenin diluted 1:500 in PBS /BSA, for 30 min. at room temperature. The plates were then washed three times in Buffer 2 again, followed by incubation in 1mg/ml para-nitrophenyl phosphate in 1M diethanolamine, pH 9.8, for up to 2.5h at 37°C. The samples were then read at 405nm with a differential of 630nm on a WellScan Multiwell Plate Reader (Denley Instruments Ltd., Billingham, UK). All ELISA measurements were performed in duplicate with controls for nonspecific probe binding and plate quality.

3.2.1.5 Scoring Methods

Scoring was carried out blind to the outcome status of the patient. The immunohistochemical results with anti-proCaspase-3 and the TUNEL results were reviewed by two observers (S. Donoghue and H.S. Baden). The percentage of tumour cells with immunostaining was graded as follows: 1 (0-25%), 2 (26-50%), 3 (51-75%), or 4 (76-100%). The number of positive nuclei detected by the TUNEL assay was graded as 0 (0-1), + (2-5), ++ (6-10), or +++ (>10). The expression of proCaspase-3 was graded as diffuse cytosolic or punctate cytosolic if >50% of tumour cells showed one of these patterns of immunohistochemical localisation. All scoring methods were measured in four random fields using a X40 objective. Due to the extensively scattered nature of the immunostaining with the anti-p17 fragment of Caspase-3, no scoring was carried out.

3.2.1.6 Statistics

Variables associated with Caspase-3 immunostaining and immunohistochemical localisation, RT-PCR data and TUNEL positivity were analysed by χ^2 test. The survival curves were plotted according to Kaplan-Meier procedure and confirmed by a log-rank test using the statistical package SPSS™. A value of $P < 0.05$ was considered statistically significant.

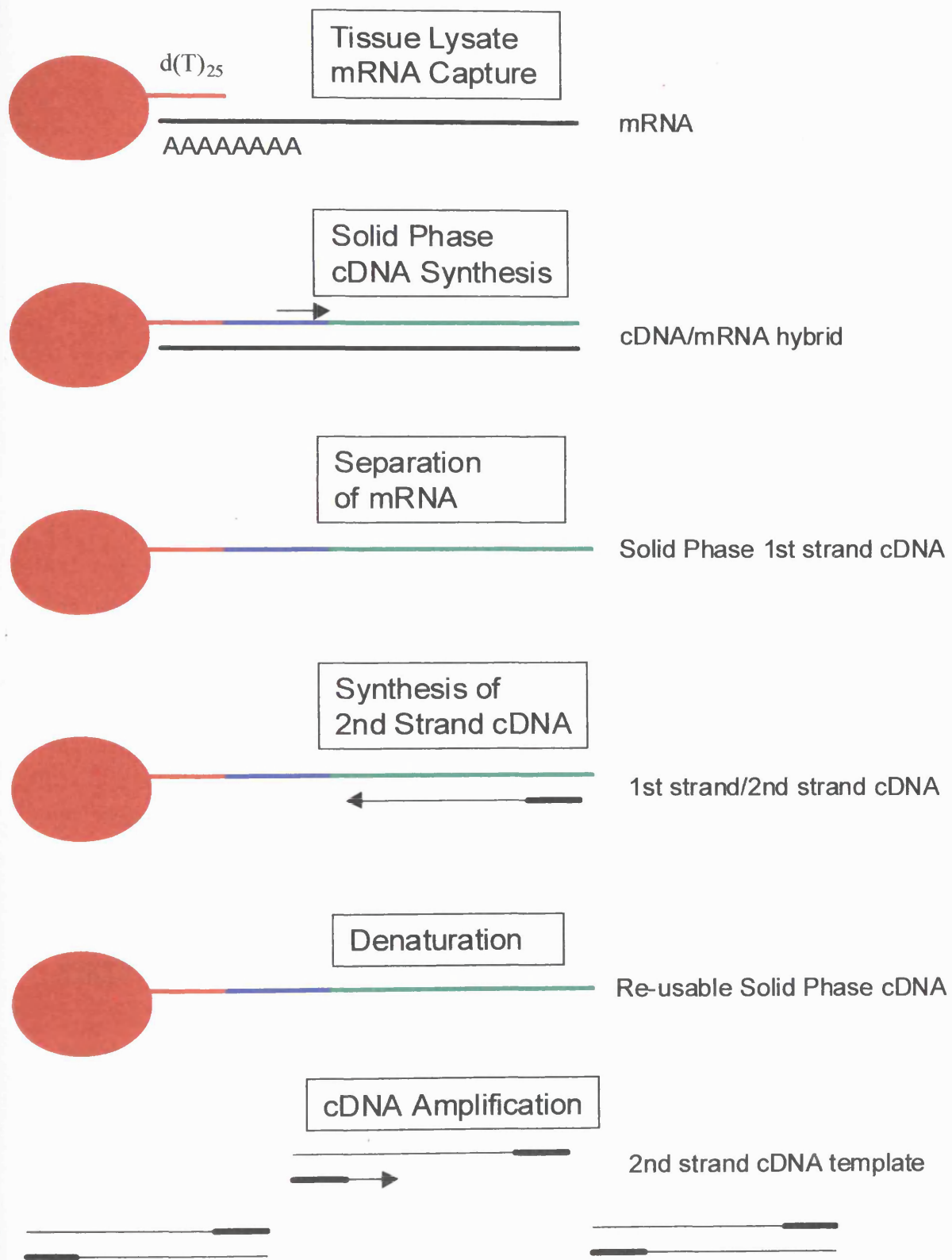


Fig. 3.1 Mechanism of solid phase RT-PCR using Dynabead™ extraction. The magnetic beads are coated with oligo(dT) sequences that capture mRNA from cell/tissue lysates. The captured mRNA can then be used as a primer for the RT reaction.

```

1  gaattcggca cgaggggtgc tattgtgagg cggttgtaga agagtttcgt gagtgctcgc
61  agtcataacc tgtggctgtg tatccgtggc cacagctggg tggcgtcgcc ttgaaatccc
121 aggccgtgag gagttagcga gccctgctca cactcggcgc tctggtttcc ggtgggtgtg
181 cctgcacct gcctcttccc ccattctcat taataaaggt atccatcgag aacactgaaa
241 actcagtgga ttcaaaatcc attaaaaatt tggaaaccaa gatcatacat ggaagcgaat
301 caatggactc tggaaatacc ctggacaaca gttataaaat ggattatcct gagatgggtt
361 tatgtataat aattaataat aagaattttc ataaaagcac tggaatgaca tctcggctcg
421 gtacagatgt cgatgcagca aacctcaggg aacattcag aaacttgaaa tatgaagtca
481 ggaataaaaa tgatcttaca cgtgaagaaa ttgtggaatt gatgcgtgat gtttctaaag
541 aagatcacag caaaaggagc agttttgttt gtgtgcttct gagccatggt gaagaaggaa
601 taatTTTTGG aacaaatgga cctgttgacc tgaaaaaat aaCAAacttt ttcagagggg
661 atcgtttag aagtctaact ggaaaacca aacttttcat tattcaggcc tgccgtggta
721 cagaactgga ctgtggcatt gagacagaca gtggtgttga tgatgacatg gcgtgtcata
781 aataccagt ggatgccgac ttcttgtatg catactccac agcacctggt tattattott
841 ggcgaaatc aaaggatggc tcttggttca tccagtcgct ttgtgccatg ctgaaacagt
901 atgdcgacaa gcttgaattt atgcacattc ttaccgggt taaccgaaag gtggcaacag
961 aatttgagtc ctttctcttt gagctactt ttcatgcaa gaaacagatt ccatgtattg
1021 tttccatgct cacaaaagaa ctctatTTTT atcacaaag aaatggttgg ttggtgggtt

```

-  Forward biotinylated primer
-  Reverse non-biotinylated primer
-  Probe to detect amplified product.

Fig. 3.2 Design of primers to measure gene expression of Caspase-3. A forward biotinylated primer and a probe were used to detect Caspase-3 for quantitative reverse-transcription PCR. The START and STOP sites are indicated.

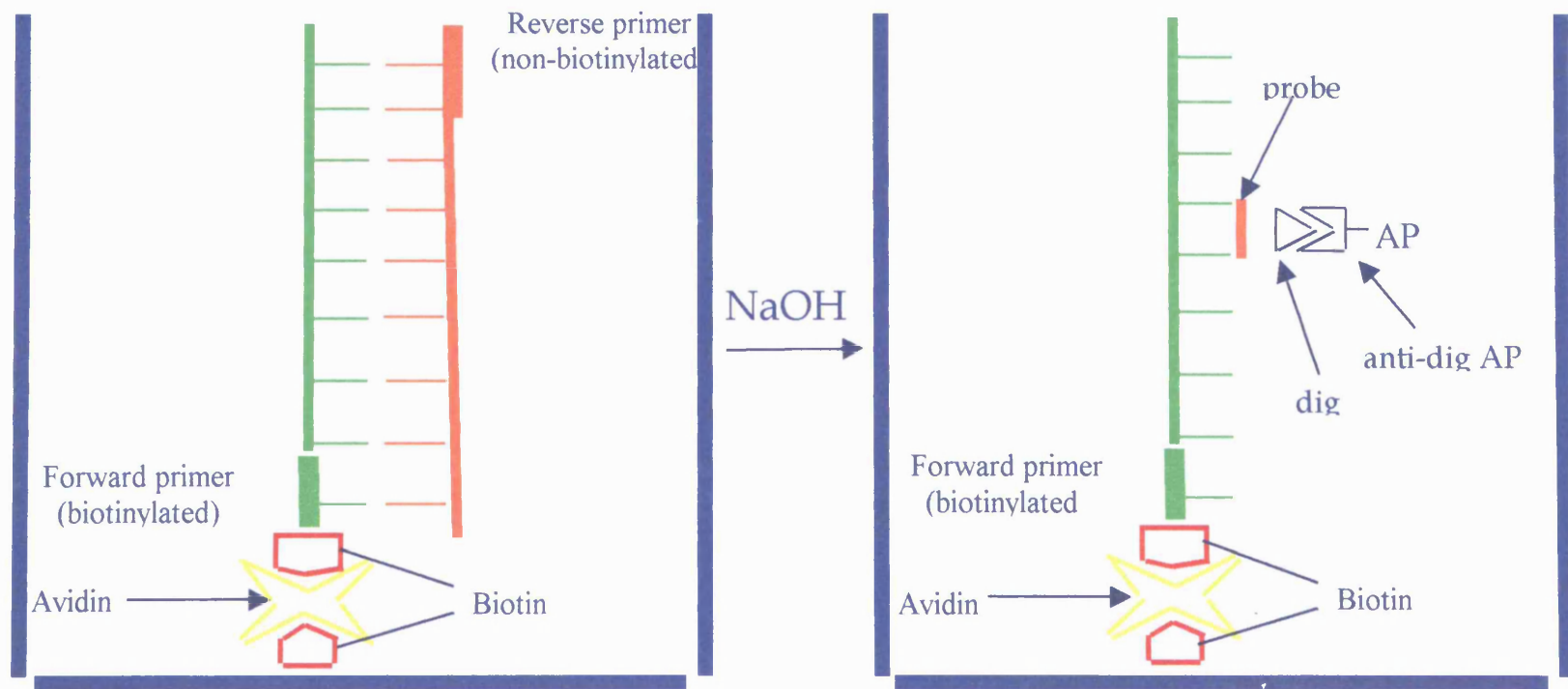


Fig. 3.3 ELISA system to detect and quantify RT-PCR products. Covalink™ plates were biotinylated overnight and, after washing, treated with avidin. After blocking, the PCR products were allowed to bind to the avidin-coated plates. The non-biotinylated PCR product was denatured using NaOH treatment. The biotinylated forward strand was then hybridised with a probe previously labelled with digoxigenin. This was then detected using an anti-digoxigenin antibody conjugated to alkaline phosphatase and the enzyme activity measured using p-nitrophenyl phosphate.

3.2.2 Western Blotting of frozen Lymphoma tissue

3.2.2.1 Protein extraction from frozen lymphoma tissue

Approximately 10-15 slices of tissue were cut on a cryostat (6 μ width) and placed immediately into 100 μ l of lysis buffer on ice. Lysis buffer consisted of 2M NH₂CONH₂ (urea); 50mM Tris-HCl; 17mM NaCl; 2.7mM EDTA; 0.1mM phenylmethanesulphonylfluoride (PMSF) and 1ml/L Brij 35 adjusted to a pH of 7.6 with NaOH. The solution containing the tissue was then put through a 25 x g needle using a 2ml syringe on ice. This was repeated vigorously with each case until no more tissue fragments could be seen. The mixture was then spun at 6500 rpm at 4°C for 10 min. The supernatant (90 μ l) was then removed. Care was taken not to disturb the pellet. The amount of extracted protein was then measured using the Bradford assay.

For each batch of protein extractions a standard curve ranging from 5 μ g/100 μ l to 60 μ g/100 μ l BSA was prepared in lysis buffer. Bradford reagent was also freshly prepared as according to manufacturers instructions. The concentrate was diluted 1:5 with H₂O and filtered using a Whatman paper. 10 μ l of sample and standards were then added to the wells of a microplate. All samples were measured in triplicate. 200 μ l of Bradford reagent were then added to the wells and the O.D₆₃₀ measured after 5 minutes and before 30 minutes. The protein concentration was then measured from a standard curve. The lowest amount extracted was used as the equivalent amount to load onto a polyacrylamide gel for Western blotting. This was typically in the range 7-10 μ g

3.2.2.2 Protein Transfer using NuPAGE™ Western Blotting

The NuPAGE electrophoretic system is based upon the running of a Bis-Tris-HCl buffered (pH6.4) polyacrylamide gel. In general, 4-12% 2-(N-morpholino) ethane sulphonic acid (MES) NuPAGE gels were run on the electrophoretic system. Running buffer was made up as according to manufacturers instructions. A 20X MES buffer contained 1M MES, 1M Tris Base, 69.3mM SDS and 3g EDTA.

The supplied gel pouch was cut open and the NuPAGE gel removed and rinsed with UP H₂O. The tape was peeled from the bottom of the gel. In one smooth motion the comb was pulled out of the cassette. The sample wells were rinsed with running buffer a few times. One or two gels were orientated in the Mini-Cell such that the notched “well” side of the cassette faced inwards towards the buffer core. The Mini-Cell was then assembled as according to the manufacturers’ instructions.

All samples were run under reducing conditions. The volume of sample loaded onto the gel varied according to efficiency of extraction but was usually 13-17µl. 5µl of NuPAGE sample buffer and 2.5µl of β-mercaptoethanol was added to the sample and the mix heated for 99°C for 5 min. The heated prepared sample was then loaded onto the prepared gel electrophoretic system as quickly as possible.

The inner buffer chamber was filled with 200ml of running buffer and 500µl of the antioxidant supplied by the manufacturers. The lower chamber was filled with 600ml of running buffer. 4-12% MES gels were run at a constant voltage of 200V for approximately 35 minutes. After the run was completed the gels were removed from the Mini-Cell. The three bonded sides of the cassette were separated by inserting a knife between two plates. This was repeated on each side of the cassette until the plates were completely separated. The top plate was removed, allowing the gel to remain on the bottom plate. The “grooves” left over from the removal of the comb were cut off the gel, and the foot of the gel was sliced to ensure easy transfer to a filter paper.

A piece of pre-soaked filter paper was placed on top of the gel. The filter paper was saturated with transfer buffer. Very slowly and carefully, the filter paper was peeled with the attached gel away from the cassette plate. The gel/membrane sandwich for Western blotting was then assembled. Two transfer buffer-soaked blotting pads were placed onto the cathode core of the blot module. The gel membrane assembly was then placed on the pads such that the gel was closest to the cathode plate.

3.2.2.3 *Detection of protein on nitrocellulose filters*

The filters were incubated for 1 hour or overnight in blocking buffer [TBS / 0.1% Tween 20 / 5% Marvel]. After blocking the membranes were washed in rinsing buffer [TBS / 0.1% Tween 20] x 3 times for 15 minutes. After incubation with the primary antibody for at least 1 hour the membranes were washed as before. The membranes were then blocked again for another hour to reduce non-specific binding from the secondary antibody. After washing as before the membranes were incubated with a secondary antibody for at least 1 hour. All membranes treated with a primary monoclonal antibody were incubated with rabbit anti-mouse immunoglobulins conjugated to horseradish peroxidase. All membranes treated with a primary rabbit polyclonal were incubated with a goat anti-rabbit immunoglobulins conjugated to horseradish peroxidase. The secondary antibodies were diluted between 1:1500 and 1:3000 in rinsing buffer depending on background. After a final wash with the rinsing buffer the membranes were detected using the ECL chemiluminescence kit. The filters were then exposed to photographic film (Kodak Hyperfilm ECL).

3.2.2.4 *Antibodies*

In order to ensure that the levels of expression of the various proteins could be compared between different samples, blots were also probed with a polyclonal antibody directed against the p85 subunit of phosphatidylinositol-3-OH kinase (PI3K), which displays a uniform level of expression among lymphoid tissues (Ghiotto-Rageuneau et al. 1996). Cases with little reactive infiltrate, as determined by histology, were used to analyse the expression of a number of proteins using Western blotting. Rabbit polyclonal antibodies directed to the p17 large subunit of Caspase-3 which recognises the proform and the p21 and p17 subunits of the enzyme. The anti-Caspase-2 polyclonal antibody recognises the proCaspase-2 enzyme and the p12 subunit. The anti-Caspase-8 polyclonal antibody recognises the 55 and 53kDa proforms and the p43 and p18 activated subunits. The anti-FLIP antibody recognises the 55, 53 and 33 kDa forms of the protein. The anti-Caspase-3 and anti-FLIP antibodies were kind gifts of Dr. D. Nicholson (Merck Frosst Centre for Therapeutic Research, Quebec, Canada). The anti-Caspase-2 and anti-Caspase-8 antibodies were kindly provided by Prof. G. Cohen (MRC Toxicology Unit, University of Leicester, Leicester, UK).

3.3 RESULTS

3.3.1 Investigation of Caspase-3 Expression and Apoptosis in DLCL

3.3.1.1 Immunohistochemical analysis of Caspase-3 in lymph node and B cell DLCL

The results of the Caspase-3 immunostaining for lymph node tissue are shown in Fig. 3.4. The majority of the cells within the germinal centre are positive and appear to have a homogenous diffuse cytosolic staining. Fewer cells outside the germinal centre are positive for staining, however, most of these appear to be plasma cells and immunoblasts. In addition, there is a population of immunopositive cells within the germinal centre that have a more intense staining. The majority of the staining cells in the interfollicular region also appear to be more intensely stained. Furthermore, most of the cells within the germinal centre have a homogenous, diffuse cytosolic staining.

A marked difference in the pattern of expression of Caspase-3 was observed in the lymph nodes of DLCL patients. Half of cases appeared to have the diffuse cytosolic staining for caspase-3 (53.7%) similar to that observed within the germinal centre of lymph nodes (see Figs. 3.7, 3.8 and Table 3.1). However, the remainder of the cases tended to display a punctate pattern of expression of Caspase-3 (see Figs. 3.9, 3.10 and Table 3.1). Out of the 54 cases only 5 appeared to have a highly mixed pattern of staining. There was also a large variation in the number of tumour cells with positive immunostaining for Caspase-3 with the majority of cells >50% positive (70.3%). At least two of the cases appeared to have no tumour cells positive for Caspase-3 whatsoever (data not shown). There did appear to be variation in intensity of staining between cases however this could not be quantified using this technique.

Interestingly, the immunopositivity of Caspase-3 expression in the lymph node appeared to be almost directly converse to that of Bcl-2. With Bcl-2 staining of reactive nodes, there is very little staining within the germinal centre and almost all of the interfollicular cells stain positive for the protein (Fig. 3.7). Furthermore, many of the cells appear to have a punctate pattern of staining. This converse relationship between Caspase-3 and Bcl-2 was not observed in the cases of DLCL (data not shown).

3.3.1.2 Apoptotic Rate in Lymph node and B-cell DLCL

Fig. 3.5 and Table 3.1 illustrates the results obtained with TUNEL staining in the reactive lymph nodes. Most of the staining is due to the activity of the tingible body macrophages within the germinal centre, with little if any staining elsewhere. The majority of DLCL cases had a high apoptotic count (++, +++) as assessed by TUNEL staining (59.3%; see Table 3.1). As shown in Fig. 3.8B both apoptotic bodies and tingible body macrophages could be observed throughout the tissue. In addition, a significant number of the cases had very little evidence of TUNEL staining (29.6%; see Fig. 3.9B and Table 3.1), including the two cases observed earlier with no tumour cells immunopositive for Caspase-3. A general trend was observed in that DLCL cases with a diffuse cytosolic staining for Caspase-3 tended to have a high apoptotic rate (see Figs. 3.8 and 3.9) as measured by TUNEL staining ($p=0.03$; Kruskal-Wallis; data not shown). It would also appear that the tingible-body macrophages containing apoptotic bodies within the germinal centre were not Caspase-3 immunopositive, as illustrated by the areas without staining in Fig. 3.4. It was difficult to assess, however whether isolated apoptotic bodies were positive.

3.3.1.3 RT-PCR ELISA

Only 42 cases of the 54 in the archive were analysed by quantitative RT-PCR for Caspase-3 expression as the quality of the mRNA extracted in the other specimens was poorly preserved. Fig. 3.12 shows an agarose gel illustrating the range of expression ratios calculated for Caspase-3 mRNA versus GAPDH mRNA in the DLCL cases analysed. The median ratio value within the group was found to be 1 and hence the cases were subdivided into <1 and ≥ 1 . The gel shows minimal variation in GAPDH levels between the two groups 1-5 (≥ 1) and 6-10 (<1), however the variation in the levels of Caspase-3 mRNA is striking. A weak trend was observed when the gene expression of Caspase-3 as measured by this assay was correlated with the immunostaining data ($p = 0.160$, Kruskal-Wallis; data not shown).

3.3.1.4 *Correlation between Caspase-3 Immunohistochemical analysis and Clinicopathological Factors*

As shown in Table 3.2 χ^2 tests showed that there was no correlation with age, sex or stage and the pattern of expression and immunostaining of Caspase-3. However, a punctate pattern of staining correlated with a complete response to treatment versus partial/no response (p value = 0.011). In addition this type of staining was associated with a very high probability that the patient was alive at the end of the study (p < 0.0001). Furthermore, a low TUNEL positivity was associated with a complete response versus no response (p=0.117). This pattern of staining also correlated with a high probability that the patient was alive at the end of the study (p=0.01).

3.3.1.5 *Survival Analysis.*

Fig 3.13 shows the log rank statistic and survival curves for Caspase-3 pattern of staining, immunostaining, gene expression and TUNEL positivity. Patients with tumour cells expressing diffuse cytosolic immunostaining for Caspase-3 had a poor prognosis when compared with those expressing a punctate staining (p> 0.0004 Log-Rank). Furthermore a low percentage of cells with positive immunostaining shows a borderline association with poor survival (p>0.09). Measurement of gene expression by a quantitative RT-PCR ELISA method does not show a significant association with survival probability, (p>0.17) although a trend is clearly present in that a low Caspase-3 gene expression is associated with a poor prognosis. In addition, patients with a high TUNEL positivity had a low survival probability (p> 0.02).

Other statistical analyses indicated that patients presenting with a stage III or IV disease tended to have a poor survival probability (p=0.018 (χ^2) and p=0069 (Kruskal-Wallis); data not shown). Furthermore, if the patient was >66 years of age at diagnosis, their survival probability also tended to be quite poor (p=0.009 Kruskal-Wallis; data not shown).

3.3.1.6 *Immunohistochemical investigation of the p17 fragment of Caspase-3 in lymph node and B cell DLCL*

The result of the p17 fragment of Caspase-3 immunostaining for lymph node tissue is shown in Fig. 3.11. A select number of cells within the germinal centre are positive

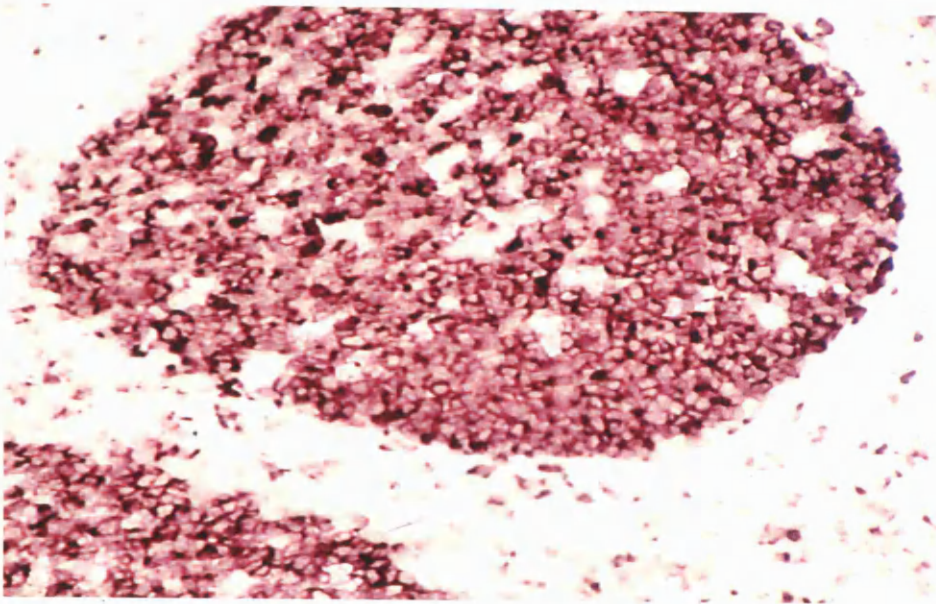
and they appear to have a punctate staining. In addition, many of the cells have a shrinking appearance, and would appear to be dying. The occasional cell within a tinged body macrophage is staining.

Similar to the proCaspase-3 staining, a marked difference in the pattern of expression was observed in the lymph nodes of DLCL patients. A punctate pattern, again similar to that seen with the punctate pattern with proCaspase-3 immunostaining, was observed in some lymphoma cells. With these cases the whole cell could often be seen with a crescent-shaped staining. Another punctate pattern of staining was observed with a more scattered profile. In these cases the cells were difficult to distinguish, and appeared to be dying. This was the pattern of expression most similar to that observed in the germinal centre of reactive lymph nodes. Finally, an extremely punctate pattern within a whole cell was also noted in some cases. Here the cells were not shrinking and a detailed staining within the cell could be seen.

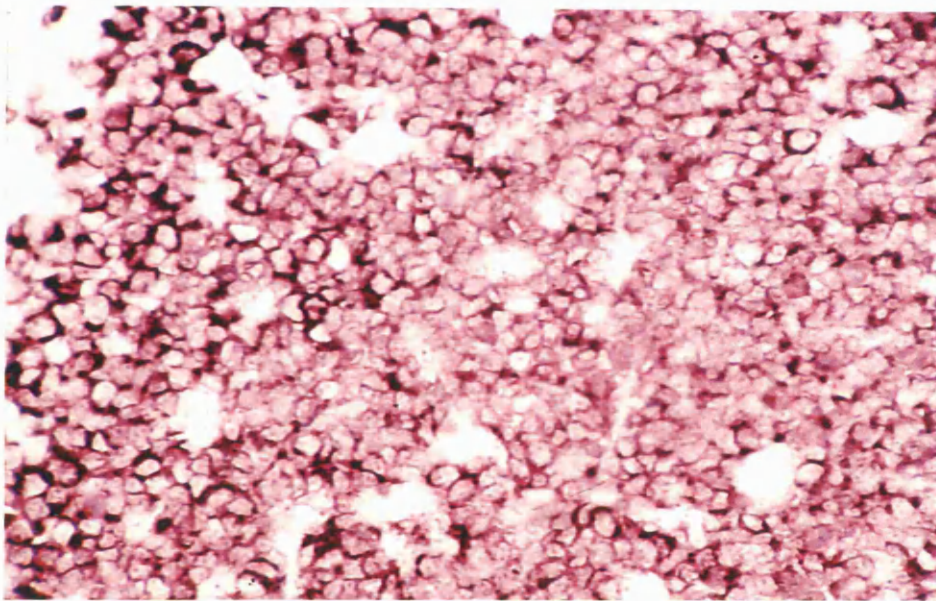
	% immunostaining ^a	RT-PCR ELISA ^b	TUNEL Positivity ^c	Immunohistochemical Localisation ^d
low	17	22	22	
high	37	20	32	
cytosolic				27
punctate				25

Table 3.1 Caspase-3 percentage immunostaining and mRNA expression, apoptotic rate and Caspase-3 immunohistochemical localisation of patients with B cell DLCL.

<50% of cells immunopositive for Caspase-3 represents a low % immunostaining^a. <1 represents a low quantitative RT-PCR Caspase-3 ratio^b. < 5 positive nuclei represents a low TUNEL positivity^c. Caspase-3 was graded as diffuse cytosolic or punctate cytosolic if >50% of tumour cells showed one of these patterns of immunohistochemical localisation^d. All scoring methods were measured in four random fields using a x40 objective. See text for more details.

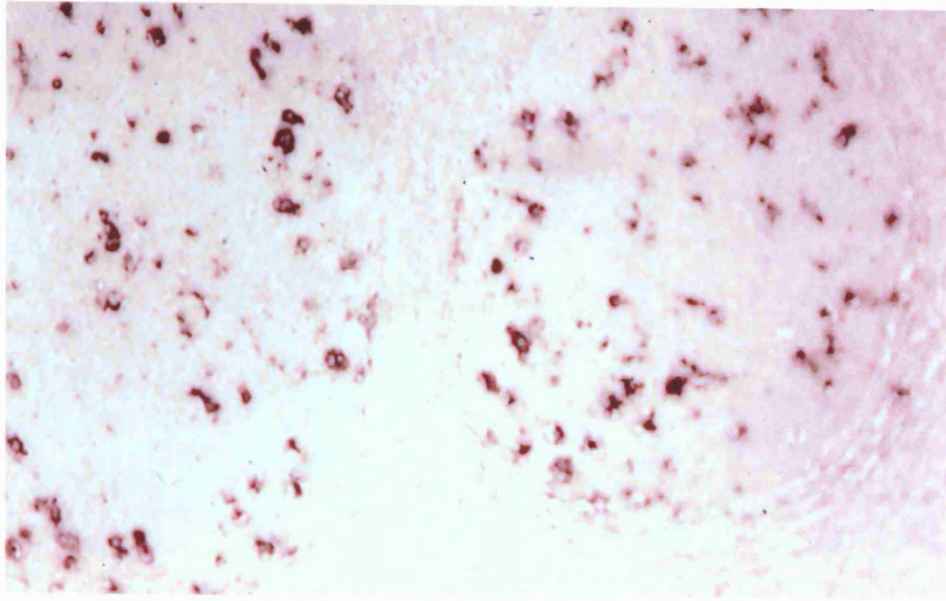


A

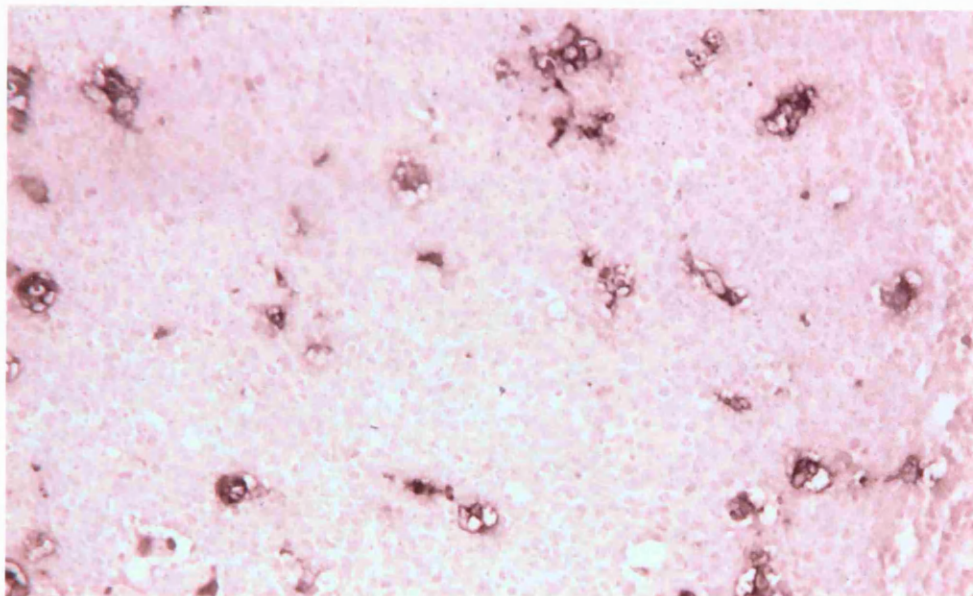


B

Fig. 3.4 Photomicrographs showing immunohistochemical staining of Caspase-3 in reactive tonsil tissue. The low power photomicrograph (A) illustrates the immunopositivity of the enzyme with most cells within the germinal centre positive and little positivity in the interfollicular region. The high power photomicrograph (B) illustrates the diffuse cytosolic pattern of staining.



A



B

Fig. 3.5 Photomicrograph showing TUNEL staining in reactive tonsil tissue. The low power photomicrograph (A) illustrates the TUNEL positivity within the germinal centre. The high power photomicrograph (B) shows that most staining was due to tingible body macrophages

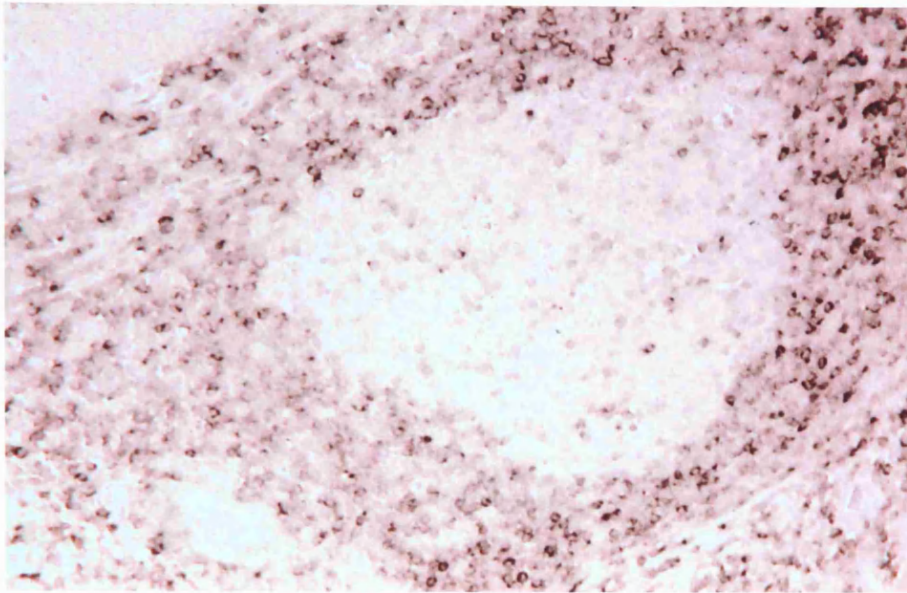


Fig. 3.6 Photomicrograph showing immunohistochemical staining of Bcl-2 in reactive tonsil tissue. The immunopositivity is almost directly converse with that of Caspase-3 in that most of the interfollicular region is positive with very little staining within the germinal centre.

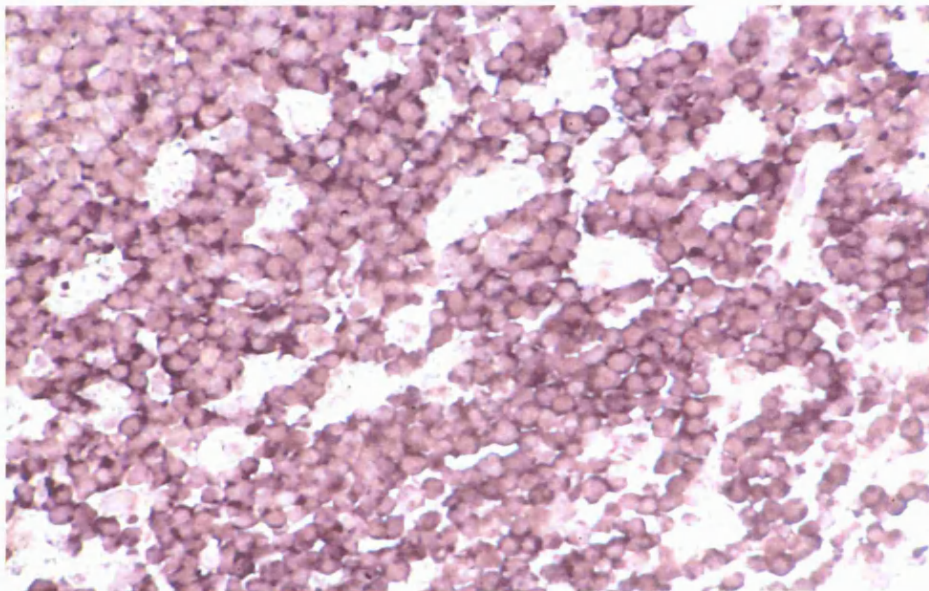
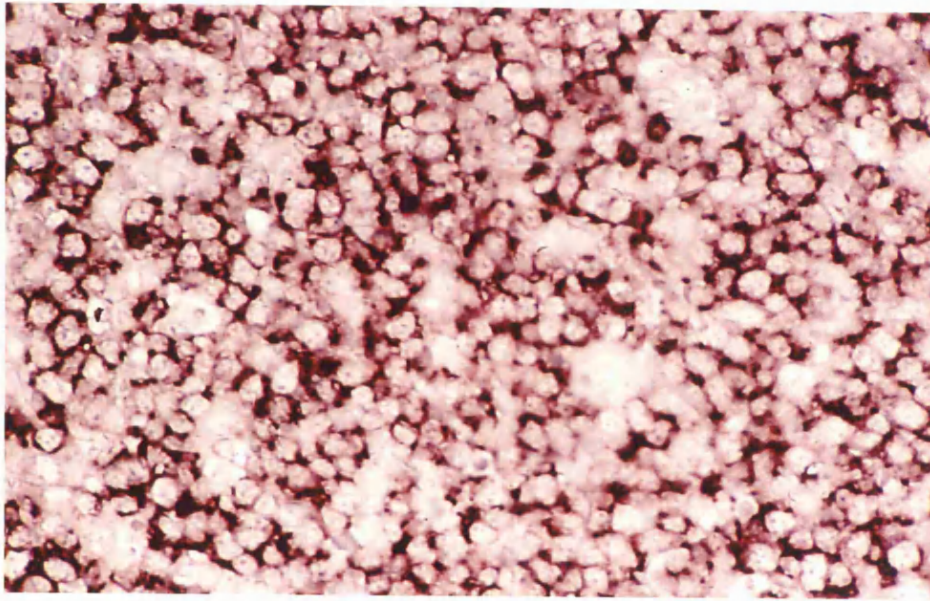
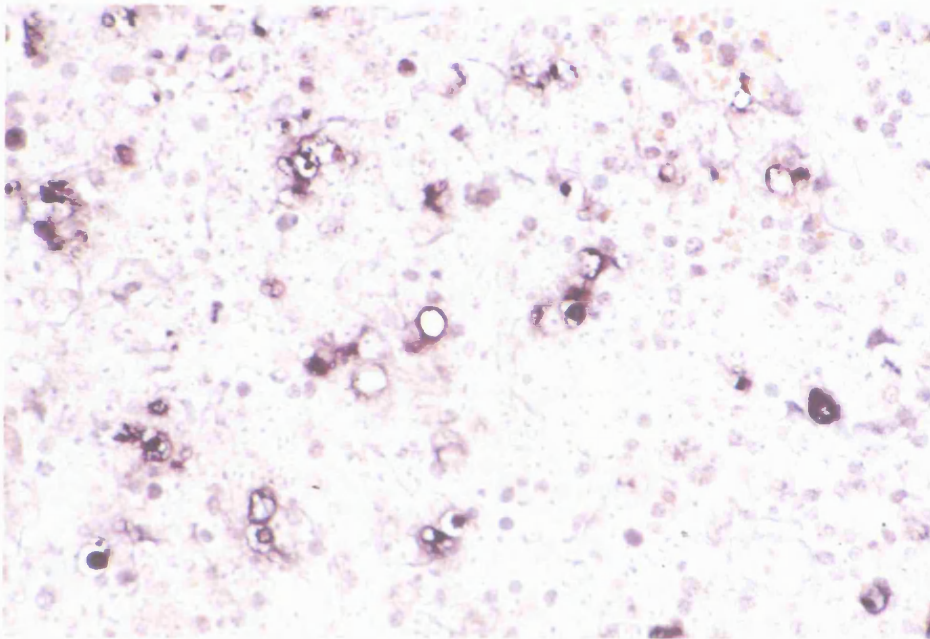


Fig. 3.7 Photomicrograph showing immunohistochemical staining of Caspase-3 in DLCL case. The vast majority of the staining has a diffuse cytoplasmic pattern.

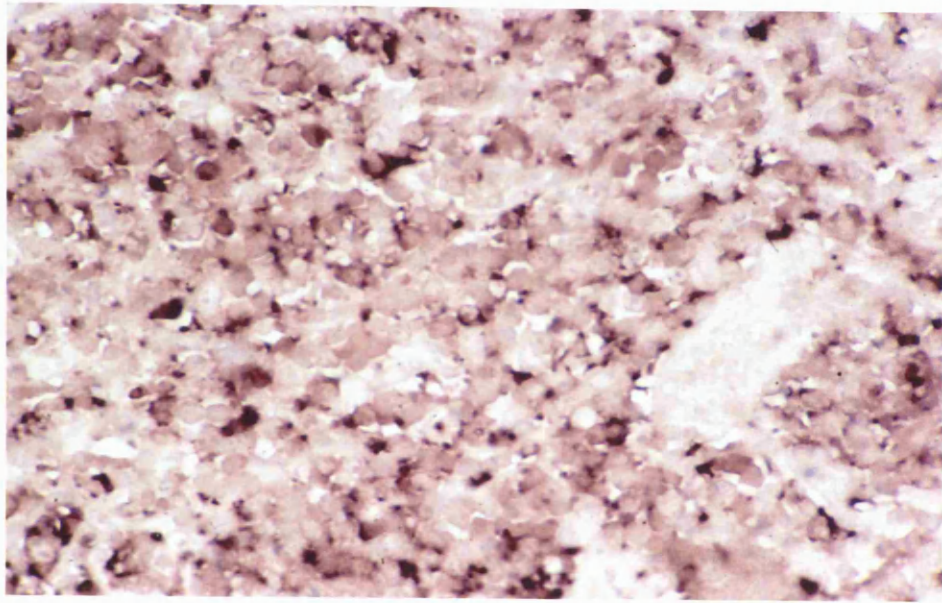


A

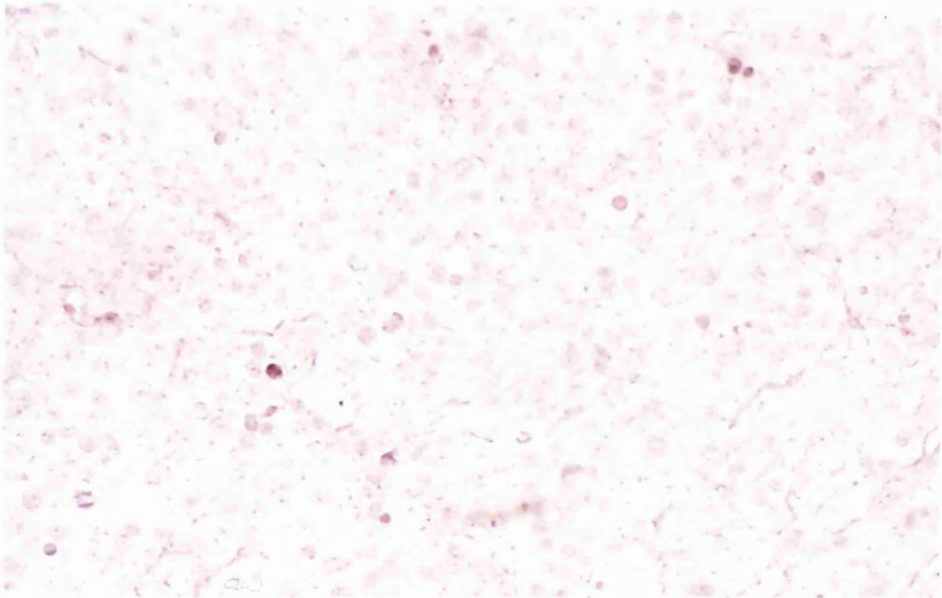


B

Fig. 3.8 Photomicrograph showing immunohistochemical staining of Caspase-3 (A) and DNA fragmentation by TUNEL staining (B) in DLCL case 06. The majority of cells immunopositive for Caspase-3 show a diffuse cytosolic pattern of staining (A). This type of staining was associated with a high TUNEL staining (B).

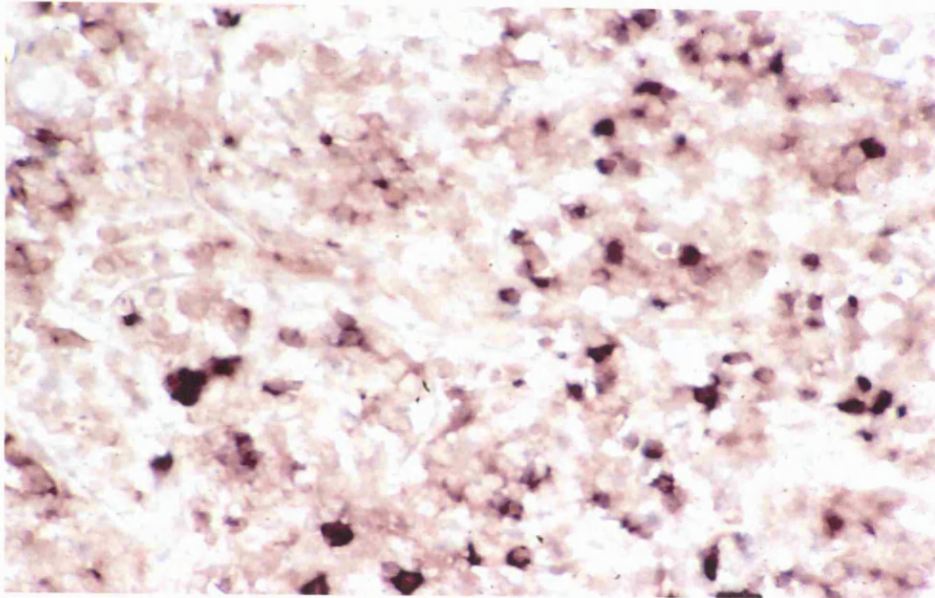


A

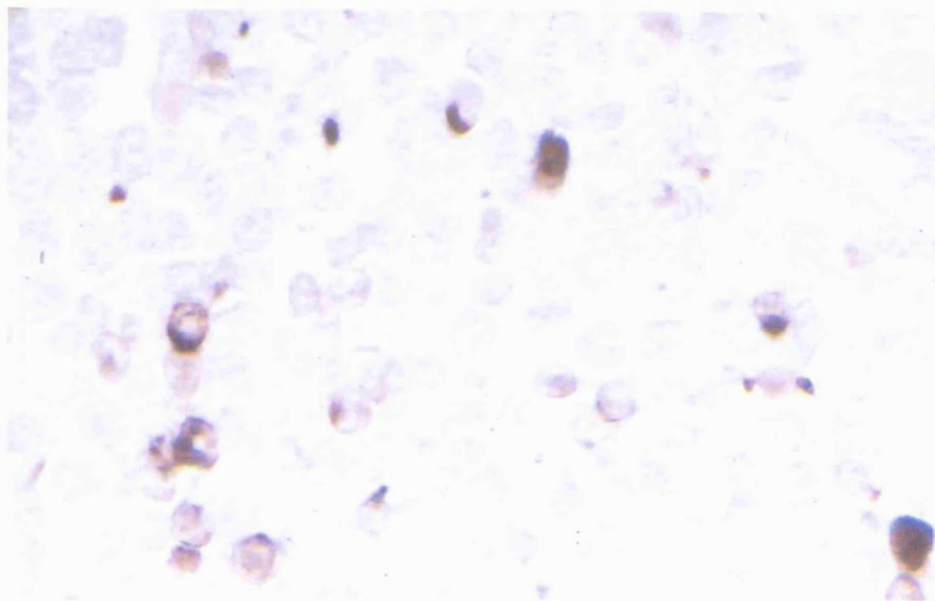


B

Fig. 3.9 Photomicrograph showing immunohistochemical staining of Caspase-3 (A) and DNA fragmentation by TUNEL staining (B) in DLCL case 25. The majority of cells immunopositive for Caspase-3 show a punctate pattern of staining (A). This type of staining was associated with a low TUNEL staining (B).

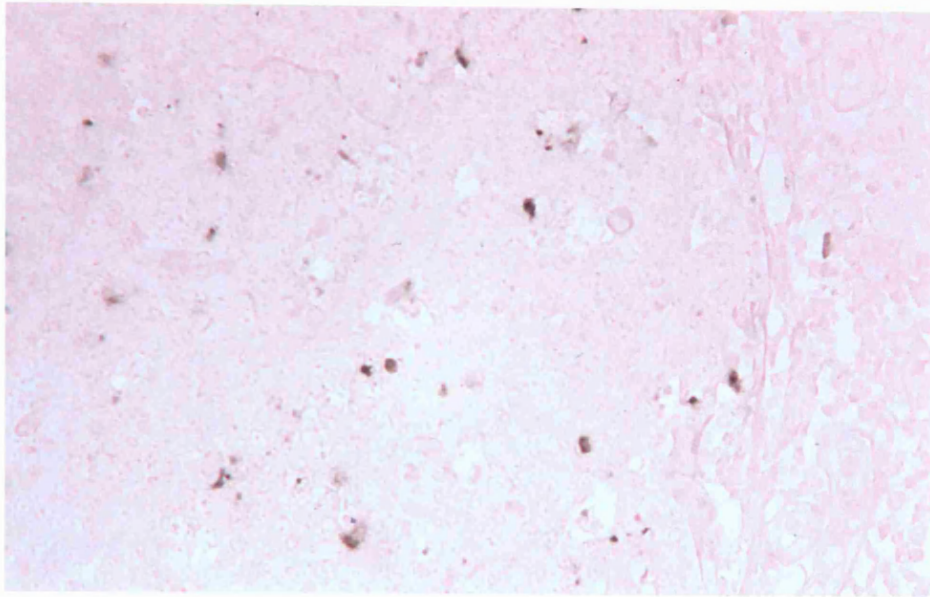


A

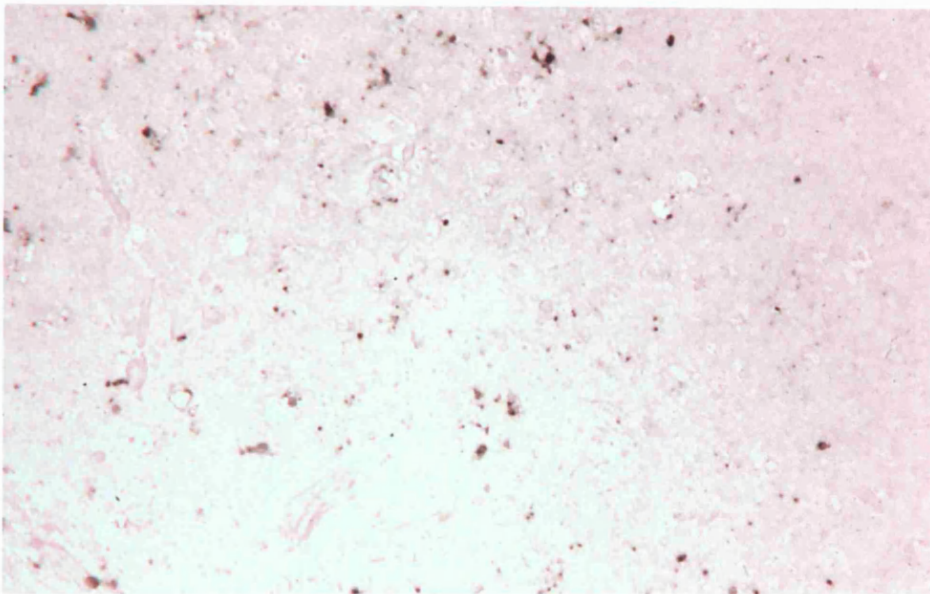


B

Fig. 3.10 Photomicrographs showing punctate immunohistochemical staining of Caspase-3 in DLCL cases. The lower power photograph (A) shows the majority of cells that are immunopositive display a punctate pattern of staining. The higher power photomicrograph (B) also shows a punctate pattern of staining.

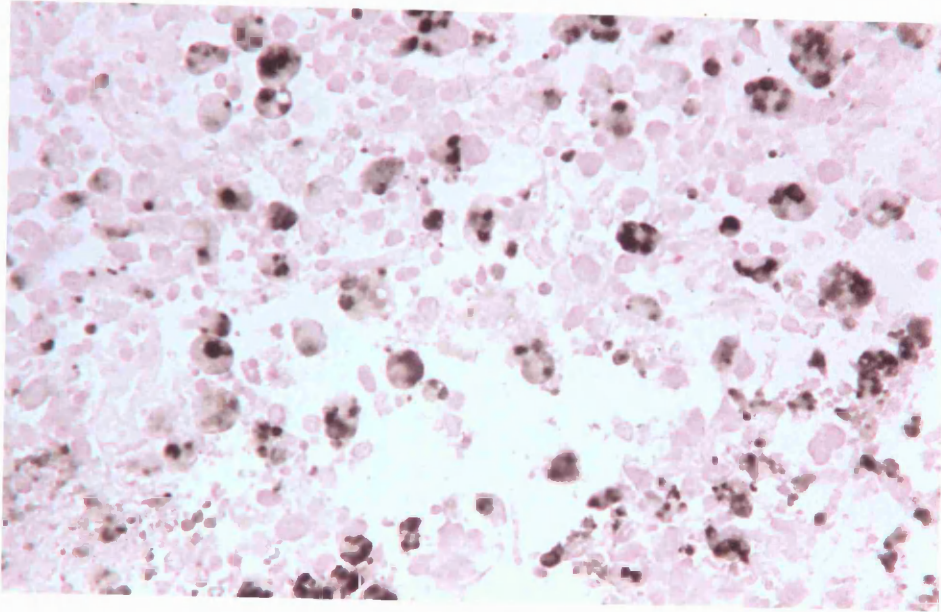


A

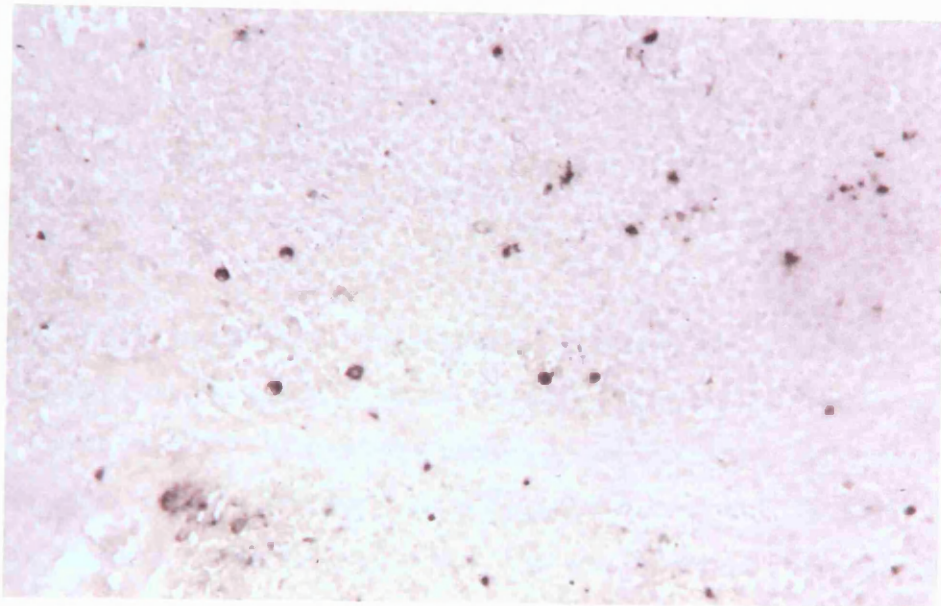


B

Fig. 3.11 Photomicrograph showing immunohistochemical staining of the active p17 fragment of Caspase-3 in reactive tonsil tissue (A) and DCLC cases (B, C, D). Photomicrograph A shows the majority of immunopositivity in the germinal centre. Many of the cells staining appear to be dying and the occasional tingible body macrophage is positive. Photomicrographs B, C and D illustrate the variety of patterns displayed in DLCL cases.



C



D

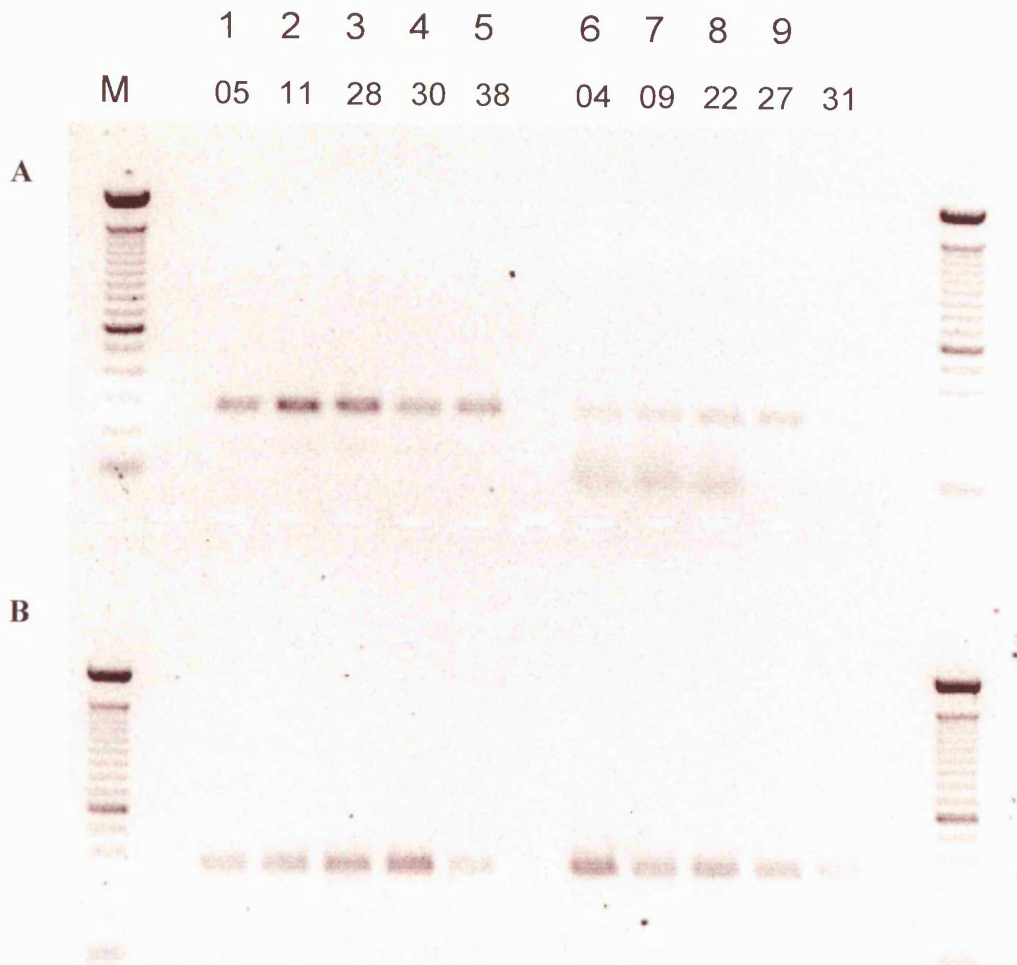


Fig. 3.12 RT-PCR amplification of Caspase-3 and GAPDH gene products. mRNA was extracted from DLCL cases (numbered) using the Dynabead™ extraction method. RT-PCR products were quantified using a DNA-based ELISA system, and the ratio of Caspase-3-amplified cDNA relative to GAPDH expression was calculated for each case. The median value of the Caspase-3 ratios was found to be 1, and the data were subsequently divided into ≥ 1 and < 1 . **A**, Caspase-3 RT-PCR products in cases where the ratio values were ≥ 1 (Lanes 1-5) and < 1 (Lanes 6-10); **B**, GAPDH RT-PCR products for the same cases. PCR products were run on a 1.5% agarose gel and visualised by exposure to UV light on a transilluminator.

	Immunohistochemical punctate localisation	High percentage of Immunostaining	mRNA ^a	Low TUNEL
Age (yr) ^b <66 vs ≥66	0.510	0.357	0.789	0.983
Sex	0.113	0.505	0.555	0.216
Stage I and II ^c	0.23	0.838	0.744	0.599
Complete Response ^d	0.011	0.572	0.235	0.117
Alive status	<0.001	0.623	0.13	0.01

Table 3.2 Correlation between clinicopathological factors and immunohistochemical localisation, percentage of immunostaining and quantitative RT-PCR analysis for *Caspase-3* and TUNEL positivity

mRNA was successfully extracted from 42 out of the 54 sections; the test variable here represents high levels of *Caspase-3* mRNA ^a. The median age of the cohort was 66 years ^b. Stage information was only available in 48 cases. Analysis of Stage I and II vs III and IV ^c. No treatment was given to 8 patients and response information was only available in 48 patients, analysis was made of no response and partial response vs complete response ^d. All *P* values represent chi-squared analyses of clinicopathological factors versus test variable.

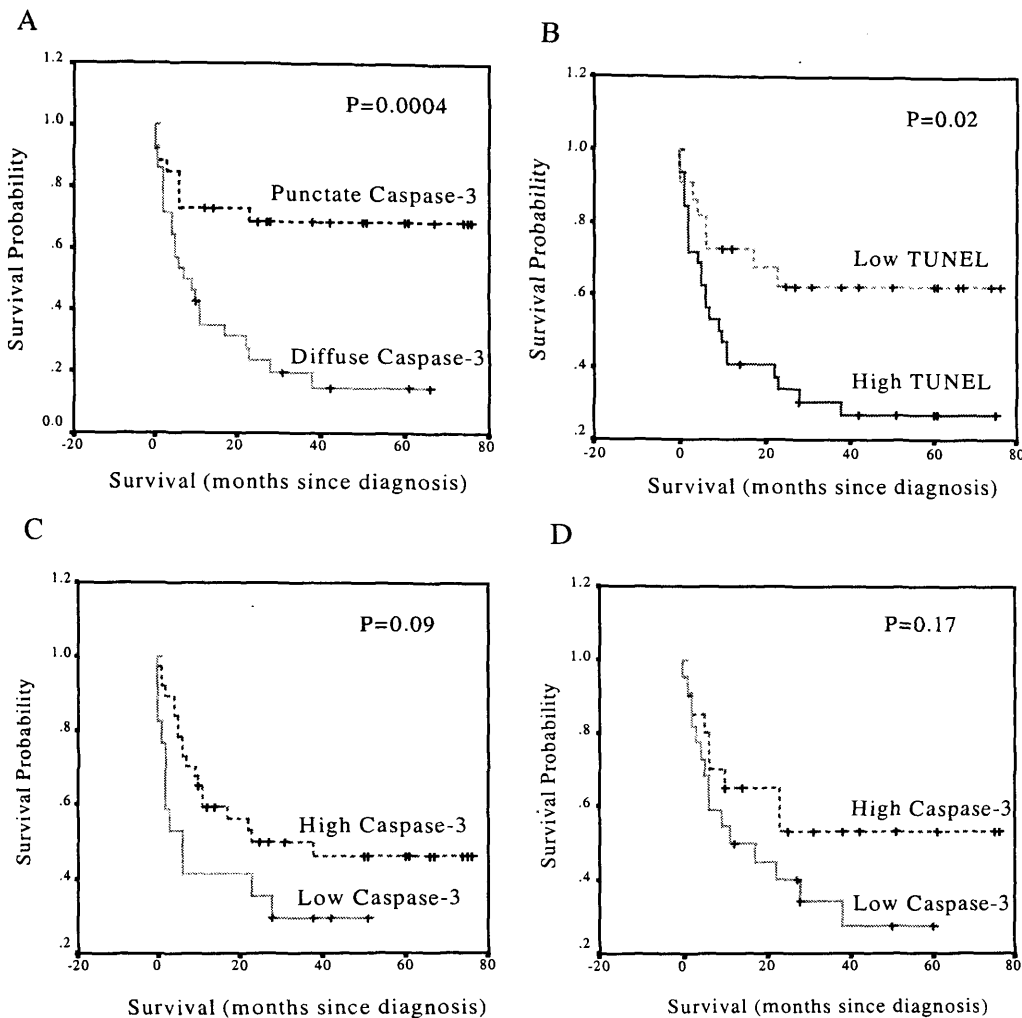


Fig. 3.13 Cumulative survival curves of patients with B cell DLCL, according to Caspase-3 immunohistochemical localisation, apoptotic rate, Caspase-3 percentage immunostaining and mRNA expression. The Kaplan-Meier survival curves show the probability of survival in terms of punctate/diffuse Caspase-3 staining (A), TUNEL staining (B), Caspase-3 immunostaining (>50%/<50%)(C) and quantitative RT-PCR Caspase-3 ratios (<1/≥1) (D). The *P* values were obtained using the log-rank test.

3.3.2 Western Blotting of frozen Lymphoma tissue

Fig. 3.14 illustrates that the levels of protein extracted from the frozen lymphoma tissue could be compared between different samples as the p85 subunit of P13K appears to have the same intensity in all cases. However, the polyclonal antibody seems to bind to a number of other bands also, albeit with the same intensity.

The Western blots of DLCL cases probed with both Caspase-3 and -2 seem to show a range of variation of expression (Figs. 3.15 and 3.16). For example, case 04 shows a high expression of proCaspase-3, however case 12 shows a reduced intensity for the protein. With respect to Caspase-2, even greater variation of expression was found. Most importantly, this antibody detects the short Caspase-2_S form of the enzyme (Ich-1_S) as well as the long form. Levels of the short form seemed to be higher in DLCL cases. The levels of the long form of the enzyme also seemed to be highly variable, with cases 04, 08, 09 and 12 producing very little.

The DLCL cases probed in a Western blot with anti-FLIP also produced a large degree of variation (Fig. 3.17). It was difficult to be certain, but the 55kDa and 53 kDa forms of the protein appear to be detected, although with varying degrees of intensity. Case 08 does not seem to produce much of either protein. There was, however, much variation in the intensity of the shorter form of the protein FLIP_S at 33kDa. Cases 08 and 09, in particular did not seem to produce much of the protein. In contrast, the DLCL cases probed with anti-Caspase-8 produced little or no variation (Fig. 3.18), but did detect both forms of the enzyme at 55 and 53 kDa.

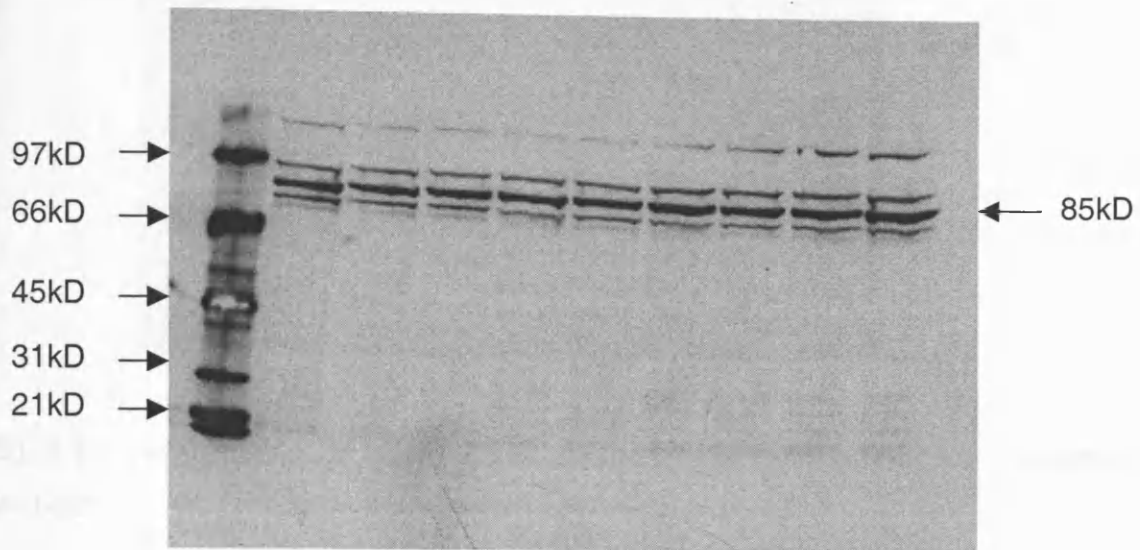


Fig. 3.14 Western blot of frozen DLCL tissue probed with anti-p85 subunit of P13K. Protein was extracted from frozen DLCL tissue and measured using the Bradford assay as described. An equivalent amount was loaded onto a 4-12% NuPAGE™ MES gel and electrophoresis and protein transfer onto a nitrocellulose membrane carried out as according to manufacturers instructions. The membrane was then probed with a polyclonal antibody directed against the p85 subunit of P13K and detected using ECL chemiluminescence and exposure to photographic film.

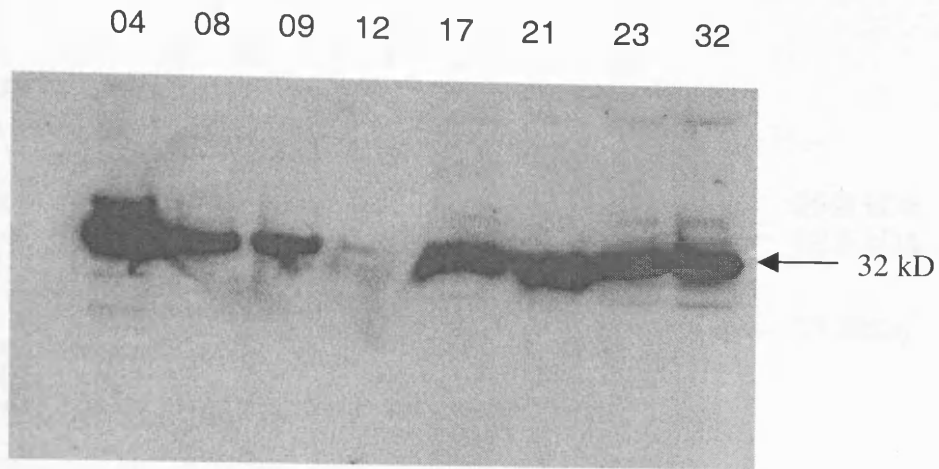


Fig. 3.15 Western blot of frozen DLCL tissue probed with anti-active Caspase-3 antibody

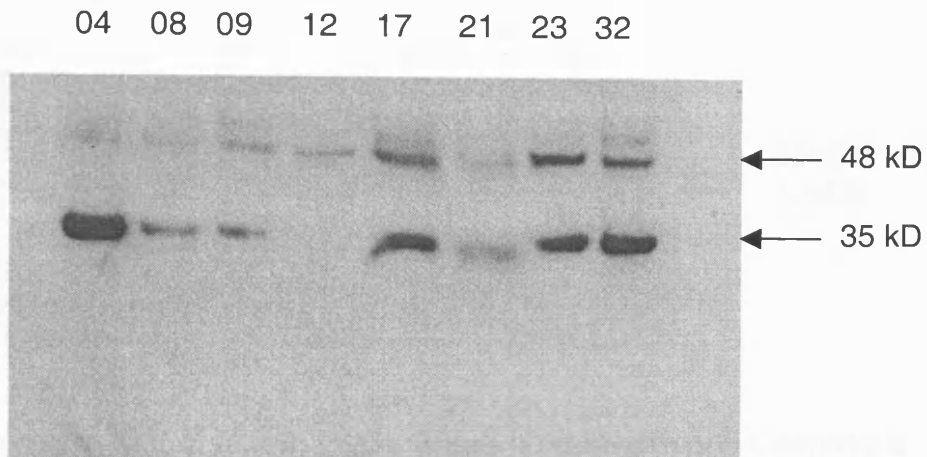


Fig. 3.16 Western blot of frozen DLCL tissue probed with anti-Caspase-2 antibody

Figs. 3.15 and 3.16 Western blots of frozen DLCL tissue probed with anti-Caspase-3 (Fig. 3.15) and anti-Caspase-2 (Fig. 3.16). Protein was extracted from frozen DLCL tissue and measured using the Bradford assay as described. An equivalent amount was loaded onto a 4-12% NuPAGE™ MES gel and electrophoresis and protein transfer onto a nitrocellulose membrane carried out as according to manufacturers instructions. The membrane was then probed with the appropriate antibody and detected using ECL chemiluminescence and exposure to photographic film.

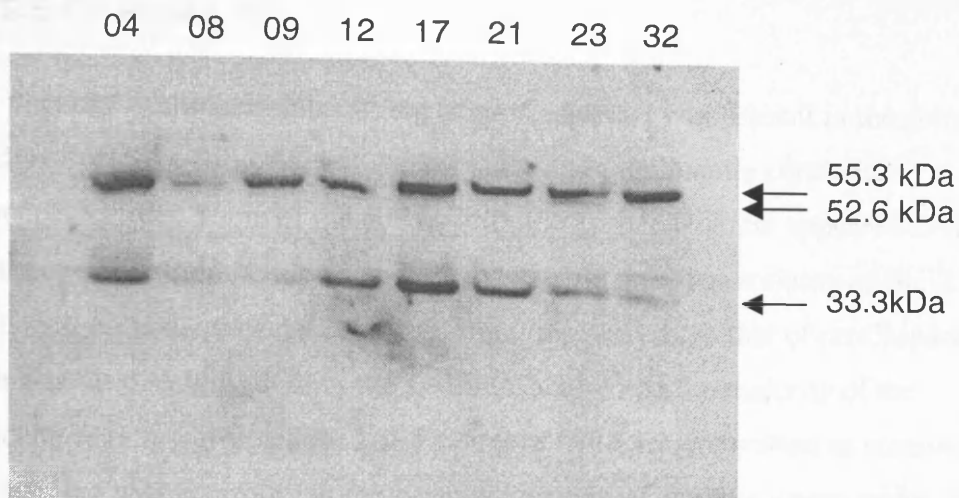


Fig. 3.17 Western blot of frozen DLCL tissue probed with anti-FLIP antibody

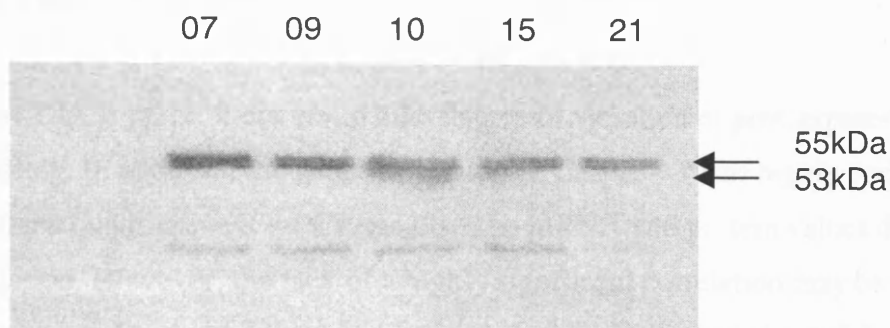


Fig. 3.18 Western blot of frozen DLCL tissue probed with anti-Caspase-8 antibody

Figs. 3.17 and 3.18 Western blots of frozen DLCL tissue probed with anti-FLIP (Fig. 3.17) and anti-Caspase-8 (Fig. 3.18). Protein was extracted from frozen DLCL tissue and measured using the Bradford assay as described. An equivalent amount was loaded onto a 4-12% NuPAGE™ MES gel and electrophoresis and protein transfer onto a nitrocellulose membrane carried out as according to manufacturers instructions. The membrane was then probed with the appropriate antibody and detected using ECL chemiluminescence and exposure to photographic film.

ANALYSIS OF RESULTS

The majority of the immunostaining of proCaspase-3 was present in the germinal centre cells of reactive follicles, with lesser staining in the mantle zone and interfollicular regions. Some of the cells within the germinal centre appeared to stain more intensely, although there was no way to evaluate this. The staining of Bcl-2 in a reactive lymph node displayed a converse immunopositivity to that of proCaspase-3, in that there was little staining within the germinal centre and the majority of the interfollicular region was positive. The amount of DNA fragmentation as measured by TUNEL staining was very high in the germinal centres of reactive lymph nodes, with both tinged body macrophages and apoptotic bodies staining positively. Furthermore, our results also indicate that in the germinal centre TUNEL-positive cells are not proCaspase-3 immunopositive.

With the DLCL cases, there was a high degree of variation of proCaspase-3 immunostaining. In addition, the gene expression of *Caspase-3* was highly variable according to the quantitative RT-PCR results. The mRNA and protein values did show a weak association. However, the lack of a highly significant correlation may be due to a number of reasons. Firstly, the immunohistochemical analysis carried out did not accurately evaluate the intensity of Caspase-3 protein expression, just the percentage of tumour cells with positive immunostaining. Also, the quantitative RT-PCR assay indiscriminately quantifies Caspase-3 gene expression levels within a tissue section. This can contain a mixture of reactive lymphoid cells, some of which express Caspase-3, along with tumour cells. With the DLCL specimens, the immunostaining data almost reached significance in that the greater the percentage of tumour cells expressing Caspase-3, the better the prognosis for the patient. A weak trend was also observed with the quantitative RT-PCR data in that low Caspase-3 mRNA expression was associated with a poor prognosis, although this was not statistically significant.

Nevertheless, there were cases of large cell lymphomas which had little or no staining for proCaspase-3 yet survived significantly greater than the median length of time. It is possible that these tumour cells used different caspases to effect programmed

cell death. The two cases of DLCL with no Caspase-3 tumour staining whatsoever also had no DNA fragmentation as detected by the TUNEL assay.

Large B cell Lymphoma cases with intense, punctate cytosolic proCaspase-3 staining tended to have a better prognosis than patients with diffuse cytosolic staining and these results were highly significant. The immunohistochemical localisation of the enzyme was more important than the immunopositivity with respect to survival and again emphasises the concept of redundancy within the apoptotic program. Furthermore, diffuse cytosolic staining is associated with a high degree of TUNEL staining. Many of the tumour cases exhibited an apoptotic pattern very similar to that seen in reactive lymph nodes; that is a diffuse localisation of proCaspase-3 and a high degree of DNA fragmentation. Patients exhibiting this pattern of expression tended to have a poor prognosis.

The vast majority of the immunostaining of the active p17 fragment of Caspase-3 was also in the germinal centres of reactive follicles, with little positivity elsewhere. The staining resembled the TUNEL staining, however, only the cells within the tingebale body macrophages were positive. Many other cells not being phagocytosed also appeared to be in the process of dying. Due to the extensively scattered, punctate nature of the staining with this antibody, no scoring was carried out with the DLCL cases. However, a variety of punctate patterns of expression were seen in the lymphomas.

Western blotting of selected DLL cases with the p85 subunit of P13K confirmed that the levels of expression of the various proteins could be compared between different samples. Variations in the levels of protein were found for Caspase-2, -3 and FLIP. No variation was found in the levels of Caspase-8. Interestingly, even though the antibody used to detect Caspase-3 in the Western blot could detect the active p17 subunit, no such fragment was detected despite the immunohistochemical results. This implies that only variations in the proforms of the enzymes could be detected using this procedure.

Chapter 4

INVESTIGATING THE *IN SITU* LOCALISATION OF
CASPASE-3 AND ITS P17 AND P12 FRAGMENTS
USING GREEN FLUORESCENT FUSION
PROTEINS

4.1 INTRODUCTION

Earlier reports with differential centrifugation and immuno-electron microscopy had indicated that Caspase-3 had both a cytosolic and a mitochondrial subcellular localisation within cells (Mancini *et al.* 1998; Samali *et al.* 1998). Furthermore, the ratio of this localisation seemed to indicate the propensity of the cell to undergo apoptosis and, perhaps, the ability of Bcl-2 family members to influence this apoptotic death (Mancini, Nicholson *et al.* 1998).

Reports by this author had showed that in B-cell DLCL both a punctate and a cytosolic expression was evident with immunohistochemical analysis (Donoghue *et al.* 1999). It was postulated that the punctate expression may represent a higher mitochondrial pool of Caspase-3. Immunohistochemical analysis of lymphoma cases with an anti-Caspase-3 p17 fragment also indicated an almost exclusive punctate pattern of staining, indicating the localisation of the active fragment of Caspase-3 at the mitochondria. Another report showed by differential centrifugation that the active p17 fragment of Caspase-3 was localised in both the mitochondria and the nucleus, as well as the cytosol (Zhivotovsky *et al.* 1999).

The aim of this section of the study was to fuse full-length Caspase-3 and its active p17 and p12 fragments to Enhanced Green Fluorescent Protein (EGFP) in order to determine the *in situ* localisation of the enzyme and its active fragments. This would allow the temporal tracking of Caspase-3 and its fragments after transient transfection in an appropriate cell line. This tracking could also, theoretically, be investigated after initiating cell death via receptor-mediated or damage-induced apoptosis.

4.2 MATERIALS AND METHODS

4.2.1 Cloning of full-length Caspase-3 and its p17 and p12 fragments into pEGFP-C1 vector

4.2.1.1 The pEGFP-C1 Plasmid

pEGFP-C1 is a mammalian expression vector that contains a multiple cloning site (MCS) at the C-terminus. The vector encodes for a red-shifted variant of wild type green fluorescent protein (GFP) when transfected into mammalian cells and excited at 488 nm. The MCS at the C-terminus allow for the expression of GFP fusion proteins. The use of GFP in this capacity provides a “fluorescent tag” on the protein, which allows for *in situ* localisation of the fusion protein and permits kinetic studies of protein localisation and trafficking.

Sequences flanking the enhanced GFP (EGFP) have been converted to a Kozak consensus translation initiation site to further increase the translation efficiency in eukaryotic cells. The MCS in PEGFP-C1 is between the EGFP coding sequences and the SV40 polyadenylation (poly A) site. Most importantly, any genes cloned into the MCS have to be in the same reading frame as EGFP with no intervening stop codons if they are to be expressed as fusion proteins. The SV40 poly A signals downstream of EGFP direct proper processing of the 3' end of the EGFP mRNA. The vector backbone also contains an SV40 origin of replication and when transfected into mammalian cells expressing the SV40 T antigen the copy number of the plasmid is greatly increased. A neomycin resistance cassette allows stably transfected eukaryotic cells to be selected using G418. A bacterial promoter upstream of this cassette expresses kanamycin resistance in *E. coli*. The vector backbone also provides a pUC origin of replication for propagation in *E. coli* and a f1 origin for single-stranded production.

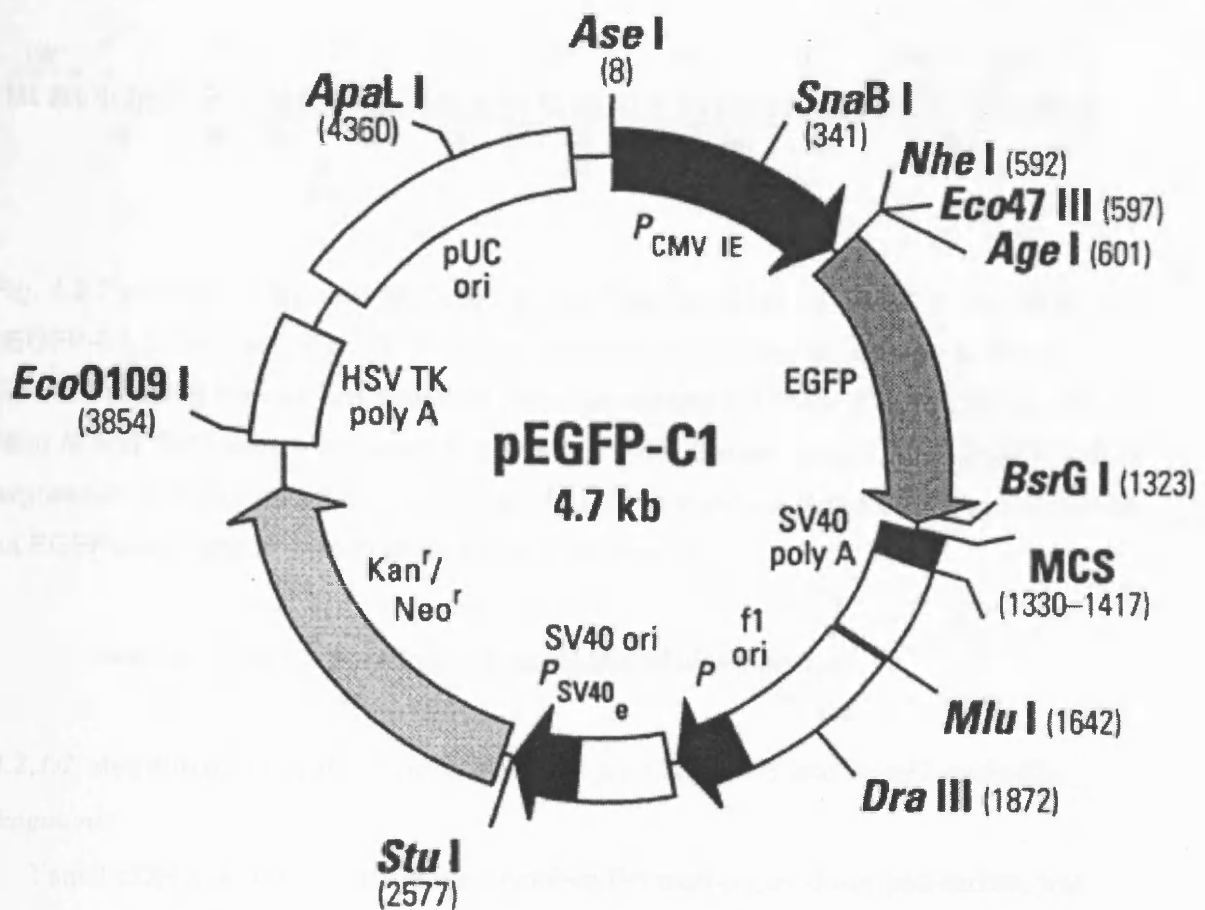


Fig. 4.1 Restriction map of pEGFP-C1 vector. pEGFP-C1 encodes a variant of wild-type GFP which has been optimised for brighter fluorescence and higher expression in mammalian cells (Excitation maximum=488nm; emission maximum=507nm). The coding sequence of the EGFP gene contains more than 190 silent base changes which correspond to human codon-usage preferences. Sequences flanking EGFP have been converted to a Kozak consensus translation initiation site to further increase the translation efficiency in eukaryotic cells. SV40 polyadenylation signals downstream of the EGFP give direct proper processing of the 3' ends of the GFP mRNA. The vector also contains an SV40 origin for replication in mammalian cells expressing the SV40 T antigen. A neomycin resistance cassette (neo^r), consisting of the SV40 early/promoter, the neomycin/kanamycin resistance gene of Tn5, and the polyadenylation signals from the Herpes simplex thymidine kinase gene, allows stably transfected eukaryotic cells to be selected using G418.

(Source: <http://www.clontech.com/techinfo/vectors>)

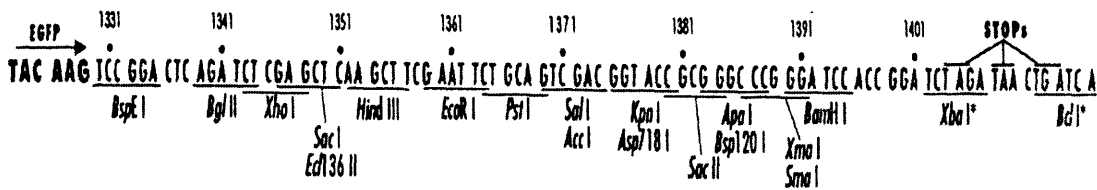


Fig. 4.2 Restriction Map and Multiple Cloning Site (MCS) of pEGFP-C1. The MCS in pEGFP-C1 is between the EGFP coding sequences and the SV40 poly A. Three different reading frames are available, thus explaining the three STOP codons. The *Hind III* and *Sal I* sites were used to clone in frame. Genes cloned into the MCS will be expressed as fusions to the C-terminus of EGFP if they are in the same reading frame as EGFP and there are no intervening STOP codons.

(Source: <http://www.clontech.com/techinfo/vectors>)

4.2.1.2 Amplification of the coding sequence for Caspase-3 and its p17 and p12 fragments

Tonsil cDNA, extracted using the Dynabead™ method, as described earlier, was used as template for the PCR reactions to clone the coding sequences for full-length Caspase-3, and the coding sequences for its p12 and p17 fragments into pEGFP-C1 in the correct reading frame for the expression of a fusion protein. As before, PCR reaction mixtures to amplify full-length Caspase-3 and its fragments were carried out in 50µl containing 1 x PCR buffer [45mM Tris, pH8.8; 11mM (NH₄)SO₄; 4.5mM MgCl₂; 200µM dNTPs; 110µg/ml BSA (Advanced Protein Products Ltd., Brierly Hill, UK) 6.7mM β-mercaptoethanol; 4.4µM EDTA, pH8.0], 1U of *Taq* polymerase and 10 pmoles of each primer. To amplify the full length Caspase-3 reactions were subjected to 5 cycles consisting of 95°C for 45s, 54°C for 1 min. and 72°C for 1 min.; and then 28 cycles of 95°C for 30s, 60°C for 45s and 72°C for 45s. To amplify the p17 fragment, reactions were subjected to 5 cycles consisting of 95°C for 30s, 55°C for 45s and 72°C for 45s; and then 28 cycles of 95°C for 30s, 62°C for 30s and 72°C for 30s. To amplify the p12 fragment, reactions were subjected to 5 cycles consisting of 95°C for 30s, 54°C for 30s and 72°C for 30s; and then 28 cycles of 95°C for 30s, 60°C for 30s and 72°C for 30s.

30s. In addition, all the PCR reactions were subjected to denaturation at 98°C for 5 min. and 72°C for 1 min. (hot start) before the first cycle.

The sequences of the primers used were:

Caspase-3 (F) 5' GCT CAA GCT TCG GAG AAC ACT GAA AAC 3'
(R) 5' ACC GTC GAC CCA ACC ATT TCT TTA GTG 3'

p17 fragment (F) 5' GCT CAA GCT TCG TCT GGA ATA TCC CTG 3'
(R) 5' ACC GTC GAC TTA GTC TGT CTC AAT GCC ACA 3'

p12 fragment (F) 5' GCT CAA GCT TCG AGT GGT GTT GAT GAT 3'
(R) 5' ACC GTC GAC CCA ACC ATT TCT TTA GTG 3'

The *Hind III* restriction site in the forward primer (F) and the *Sal I* restriction site in the reverse primer (R) are underlined. These restriction sites were engineered into the primers such that the amplicon would be inserted into the vector in the correct reading frame for expression of a fusion protein. The predicted sizes of the amplicons were 863, 465 and 341 bp for full-length Caspase-3, the p17 fragment and the p12 fragment, respectively. See Figs. 4.3 - 4.6 for more details about the cloning strategy.

4.2.1.3 Purification and Restriction of the coding sequence for full-length Caspase-3 and the p17 and p12 fragments

The Nucleon™ easiClene kit was used to excise the correctly sized PCR amplicons from the TAE gels. The procedure was followed as according to the manufacturers instructions. As described before, (see 2.2.1.2) the appropriate band was excised from an ethidium bromide-stained agarose gel with a razor band and chopped into small cubes and transferred into a 1.5ml centrifuge tube. After dissolution with stock NaI solution in a water bath, 5µl of easiClene™ silica solution was added to the mix containing the DNA. After a series of washing the pellet containing the purified DNA was resuspended in 5µl of TE and incubated at 55°C for 2 min. The tube was then centrifuged again for about 30 seconds and the supernatant containing the eluted DNA carefully removed and

placed in a new eppendorf. Several purifications were carried out and the solutions pooled. See 2.2.1.2 for exact details of procedure.

The restriction reaction for the excised DNA was carried out in 20 μ l, as described earlier (see 2.2.1.2). A small volume of the restricted, excised DNA was run on a 2% TAE electrophoretic gel beside a known quantity of 100 bp ladder DNA in order to estimate the concentration of DNA recovered. The PEGFP-C1 vector was restricted in 50 μ l. 4 μ g of the vector were used in the reaction with 10U of both *Hind III* and *Sal I*. Double restriction reactions of both the vector and the excised DNA were carried out at 37°C for 2 hours. As a restriction control, vector DNA that was only digested with *Hind III* was used. 4 μ g of the vector was restricted with *Hind III* only in a volume of 50 μ l.

4.2.1.4 Ligation/Transformation

As described before (see 2.2.1.3) ligation reactions were carried out in 20 μ l. The concentrations of the excised, restricted full-length Caspase-3 and p17 and p12 fragments were estimated at 10ng/ μ l, 8ng/ μ l and 5ng/ μ l respectively (see Fig.4.6). The *Hind III* and *Sal I* double digest of the pEGFP-C1 vector was assumed to be 100% efficient, and hence the concentration of restricted vector was estimated to be 0.5 μ g/ μ l. Two ligation reactions containing the restricted vectors and inserts were carried out at ratios of 1:3 and 1:10 vector:insert. 1.5 U of T4 DNA ligase was used and the reactions were incubated overnight at 16°C. A number of other ligation controls were also carried out; a reaction containing the double digest of the vector without the insert was ligated; a reaction containing vector restricted with *Hind III* with and without insert was also ligated. As before, all ligations were carried out in 20 μ l overnight at 16°C.

As outlined earlier, the vectors were transformed into DH5 α TM *E.coli* cells as according to the suppliers instructions (Life Technologies). This procedure has been described earlier (see 2.2.1.3). Briefly, 50 μ l of cells were transformed with 3 μ l of the DNA ligation reaction. The mix was incubated on ice for 45 minutes and the cells then heat-shocked. Afterwards, 0.95ml of SOC medium was added and the mixture shaken for up to 2 hours at 37°C. After expression, 100 μ l of a diluted (1:10 with SOC medium) and an undiluted reaction were spread onto LB plates containing 30 μ g/ml kanamycin.

5µl (0.5µg) of control pUC19 was also transformed into DH5α™ *E. coli* cells and the efficiency calculated using LB plates containing 50µg/ml ampicillin. All transformation colonies were counted and the efficiencies calculated.

START

```

181 cctgcacct gcctcttccc ccattctcat taataaaggt atccatggagaacactgaaa
241 ctcagtgga ttcaaaatcc attaaaaatt tggaaaccaa gatcatacat ggaagcgaat
301 caatggactc tggaatatcc ctgacaaca gttataaaat ggattatcct gagatgggtt
361 tatgtataat aattaataat aagaattttc ataaaagcac tggaatgaca tctcggctctg
421 gtacagatgt cgatgcagca aacctcaggg aaacattcag aaacttgaaa tatgaagtca
481 ggaataaaaa tgatcttaca cgtgaagaaa ttgtggaatt gatgcgtgat gtttctaaag
541 aagatcacag caaaaggagc agttttgttt gtgtgcttct gagccatggt gaagaaggaa
601 taatttttgg aacaaatgga cctgttgacc tgaaaaaaat aacaaacttt ttcagagggg
661 atcgtttaga aagtctaact ggaaaacca aacttttcat tattcaggcc tgccgtggta
721 cagaactgga ctgtggcatt gagacagaca gtggtgttga tgalgacatg gcgtgtcata
781 aaataccagt ggatgccgac ttcttgtatg catactccac agcacctgggtt attattctt
841 ggcgaaattc aaaggatggc tcttggttca tccagtcgct ttgtgccatg ctgaaacagt
901 atgccgacaa gcttgaattt atgcacattc ttaccoggt taaccgaaag gtggcaacag
961 aatttgagtc cttttccttt gacgctactt tcatgcaaa gaaacagatt ccatgtattg
1021 tttcatgct cacaaaagaa ctctatTTTT atcactaaag aaatgggttg ttggtggttt

```

STOP

- full -length Caspase-3
- p17 fragment of Caspase-3
- p12 fragment of Caspase-3

Fig. 4.3 Nucleotide sequence for Caspase-3. The coding region starts at 225bp and ends at 1058bp. The coding sequences used for primer hybridisation are colour-coded. Primers for full-length Caspase-3 range from 228-1070bp; primers for p17 fragment range from 308-749bp; primers for p12 fragment range from 750-1070bp. The START and STOP codons are indicated.

EGFP



TAC AAG TCC GGA CTC AGA TCT CGA GCT CAA GCT TCG AAT TCT GCA GTC GAC GGT ACC GCG GGC CCG GGA TCC ACC GGA TCT AGA

Hind III

Sal I

5' TCC GAG AAC ACT GAA AAC TCA ----- CAC AGA AAT GGT TGG TTG 3'
3' AGG CTC TTG TGA CTT TTG AGT ----- GTG TCT TTA CCA ACC AAC 5'

Primers for cloning of full length Caspase-3:

Forward 5' GCT CAA GCT TCG GAG AAC ACT GAA AAC 3'

Reverse 5' ACC GTC GAC CCA ACC ATT TCT GTG 3'

Fig. 4.4 Cloning strategy for the insertion of the coding sequence for full-length *Caspase-3* DNA into the pEGFP-C1 MCS in the correct reading frame. The sequences surrounding *Caspase-3* at the START and STOP sites are indicated. The forward primer for amplification of the DNA has a *Hind III* site incorporated into it at the 5' end. Likewise the reverse primer has a *Sal I* site incorporated into it.

EGFP
→

TAC AAG TCC GGA CTC AGA TCT CGA GCT CAA GCT TCG AAT TCT GCA GTC GAC GGT ACC GCG GGC CCG GGA TCC ACC GGA TCT AGA
Hind III *Sal I*

5' GAC TCT GGA ATA TCC CTG GAC AAC ----- CTG GAC TGT GGC ATT GAG ACA GAC 3'
3' CTG AGA CCT TAT AGG GAC CTG TTG ----- GAC CTG ACA CCG TAA CTC TGT CTG 3'

Primers for cloning of p17 fragment:

Forward 5' GCT CAA GCT TCG TCT GGA ATA TCC CTG 3'

Reverse 5' ACC GTC GAC TCG GTC TGT CTC AAT GCC ACA 3'

Fig. 4.5 Cloning strategy for the insertion of the coding sequence for p17 fragment of *Caspase-3* DNA into the pEGFP-C1 MCS in the correct reading frame. The sequences surrounding the p17 fragment are indicated. The forward primer for amplification of the DNA has a *Hind III* site incorporated into it at the 5' end. Likewise the reverse primer has a *Sal I* site incorporated into it. The reverse primer also has a STOP codon incorporated into it to ensure only the p17 fragment is cloned.

EGFP



TAC AAG TCC GGA CTC AGA TCT CGA GCT CAA GCT TCG AAT TCT GCA GTC GAC GGT ACC GCG GGC CCG GGA TCC ACC GGA TCT AGA
Hind III *Sal I*

5' AGT GGT GTT GAT GAT GAC ----- CAC AGA AAT GGT TGG TTG 3'
3' TCA CCA CAA CTA CTA CTG GTG TCT TTA CCA ACC AAC

Primers for cloning of p12 fragment

Forward 5' GCT CAA GCT TCG AGT GGT GTT GAT GAT 3'

Reverse 5' ACC GTC GAC CCA ACC ATT TCT GTG 3'

Fig. 4.6 Cloning strategy for the insertion of the coding sequence of p12 fragment of *Caspase-3* DNA into the pEGFP-C1 MCS in the correct reading frame. The sequences surrounding the p12 fragment are indicated. The forward primer for amplification of the DNA has a *Hind III* site incorporated into it at the 5' end. Likewise the reverse primer has a *Sal I* site incorporated into it.

4.2.1.5 Screening of Clones

As before, over twenty colonies from each plate containing a vector:insert ratio were picked and grown overnight in 5ml LB containing 30 μ g/ml kanamycin. Plasmid DNA from these cultures was then isolated using the WizardTM miniprep DNA purification system as outlined earlier. Putative clones were identified using restriction analysis with both *Hind III* and *Sal I*, or with just *Hind III*, as described earlier (see 2.2.1.4).

In addition, a PCR mini-prep was carried out on putative positive clones as described before (see 2.2.1.4). Clones from a vector:insert plate were resuspended in 0.5ml of UP H₂O and boiled for 5 minutes. After spinning in a microcentrifuge at 10,000 g for 2 min. 5 μ l of the supernatant was used as a template for a PCR reaction. All PCR reaction mixtures were carried out in 50 μ l containing 45mM Tris, pH 8.8; 11mM (NH₄)₂SO₄; 4.4mM MgCl₂; 200 μ M dNTPs; 110 μ g/ml of BSA; 6.7 mM β -mercaptoethanol; 4.4 μ M EDTA, pH 8.0 and 10pmoles of each primers. The primers used initially for screening were the same as those used for cloning. Most importantly, 2.5U of *Taq* polymerase were used in each amplification. All reactions were subjected to 5 cycles consisting of 95 $^{\circ}$ C for 1 min., 55 $^{\circ}$ C for 1 min. and 72 $^{\circ}$ C for 1 min.; and then 30 cycles of 95 $^{\circ}$ C for 45s, 62 $^{\circ}$ C for 45s and 72 $^{\circ}$ C for 45s. In addition, all the PCR reactions were subjected to denaturation at 95 $^{\circ}$ C for 5 min. and 72 $^{\circ}$ C for 1min. (hot-start) before the first cycle and a final extension of 72 $^{\circ}$ C for 10mi. Sterile UP H₂O was used as a negative control template for the reaction.

Once a positive clone was identified large scale maxi-prep plasmid purification was carried out as according to the manufacturers instructions (Qiagen). This procedure has been outlined earlier (see 2.2.1.4) and is based on a modified procedure of the alkaline lysis method. As before, DNA was quantified by O.D. at 260nm. Calculation of the A₂₆₀/A₂₈₀ was used to estimate the purity of the DNA.

A further confirmation of the correct insertion size of the clones was carried out using primers flanking the MCS of pEGFP-C1. The sequences of the primers used were:

pEGFP-C1 (forward) 5'-ACTACCTGAGCACCCAGTCC-3'

pEGFP-C1 (reverse) 5'-TTGCATTCATTTTATGTTTCAG-3'

See Fig. 4.7 for details of primer sites. The amplified product of a vector without any insert should be 206 bp. Therefore a clone containing full-length Caspase-3 would be 1068 bp; a clone containing the p17 fragment as an insert would be 671 bp and a clone containing a p12 fragment would be 547 bp.

4.2.2 Expression of putative pEGFP-C1 fusion constructs

4.2.2.1 Cell Lines

The MRC5 SV1 TG1 and MCF-7 cultures were obtained from the European Collection of Animal Cell Cultures (ECACC; Porton Down, UK). Each cell line was passaged every 48-72 hours, assuming they had reached confluence. The MRC5 cell line was maintained in medium described earlier (see 2.2.2.3). The MCF-7 cell line was maintained in MEM without phenol red, 10% FCS and 2mM glutamine. The MCF-7 cell line was passaged in a manner similar to that described for MRC5. Briefly, approximately 1×10^6 cells were seeded per 25cm² flask every passage. Spent media was removed by aspiration and the cells rinsed with 5 ml HBSS. The HBSS was removed before addition of 1ml trypsin-EDTA to each flask and incubation for several minutes at 37°C, until the cells could be dislodged by knocking the side of the flask. They were then resuspended in 10ml of media and pelleted by spinning in a centrifuge at 1000 rpm for 5 min. The supernatant was then removed by aspiration and the pellet resuspended by pipetting up and down in fresh media. Usually the cells were split between two 25cm² flasks with media to a total volume of 10ml per flask and replaced in the incubator at 37°C in a humidified atmosphere of 5% CO₂.

START

```
601 ccggtcgcca ccatggtgag caagggcgag gagctgttca ccggggtggt gcccatcctg
661 gtcgagctgg acggcgacgt aaacggccac aagttcagcg tgtccggcga gggcgagggc
721 gatgccacct acggcaagct gaccctgaag ttcatctgca ccaccggcaa gctgcccctg
781 ccctggccca ccctcgtgac caccctgacc tacggcgtgc agtgcttcag ccgctacccc
841 gaccacatga agcagcacga cttcttcaag tccgccatgc ccgaaggcta cgtccaggag
901 cgcacatct tcttcaagga cgacggcaac tacaagacct gcgccgaggt gaagtctgag
961 ggcgacacct tgggtgaaccg catcgagctg aagggcatcg acttcaagga ggacggcaac
1021 atctgggggc acaagctgga gtacaactac aacagccaca acgtctatat catggccgac
1081 aagcagaaga acggcatcaa ggtgaacttc aagatccgcc acaacatcga ggacggcagc
1141 gtgcagctcg ccgaccacta ccagcagaac acccccatcg gcgacggccc cgtgctgctg
1201 cccgacaacc actacctgag caccagtcc gccctgagca aagaccccaa cgagaagcgc
1261 gatcacatgg tcttctgctgga gttcgtgacc gccgccggga tcaactctcg catggacgag
1321 ctgtacaagt ccggactcag atctcgagct caagcttcga attctgcagt cgacgggtacc
1381 gcgggcccgg gatccaaccg atctagataa ctgatcataa tcagccatac cacatttgta
1441 gaggttttac ttgctttaa aaacctcca cacctcccc tgaacctgaa acataaaatg
1501 aatgcaattg ttgttgtaa cttgtttatt gcagcttata atggttacia
ataaagcaat
```

-  Multiple Cloning Site (MCS) of pEGFP-C1
-  Primers to screen for clones within the MCS (1301-1507bp)

Fig. 4.7 Nucleotide sequence of pEGFP-C1. The coding region starts at 613bp and ends at 1410bp. The multiple cloning site (MCS) ranges from 1330-1410. The primers to screen for clones within the MCS range from 1301-1507bp. The START and STOP codons are indicated.

4.2.2.2 *Transfection of MRC5 and MCF-7*

Transient transfection of MRC5 was carried out as described earlier (see 2.2.2.4). Transient transfection of MCF-7 cells was similar with slight differences. The cells were seeded in an incubator in growth medium at 37°C until they were 50-80% confluent. Two solutions were then prepared; in solution (A) 3µg plasmid DNA was added to 100µl of Opti-Mem™ I Reduced Serum Medium; in solution (B) 10µl of Lipofectamine reagent was added to 100µl of Opti-Mem™ I Reduced Serum Medium. The two solutions were then combined, mixed gently, and incubated at room temperature for 30 min. to allow the DNA-liposome complexes to form. While the complexes formed, the cells were rinsed once with 2ml of Opti-Mem™ I Reduced Serum Medium. For each transfection, 0.8ml of Opti-Mem™ I Reduced Serum Medium was added to the tube containing the complexes. The solution was mixed gently and overlaid onto the rinsed cells. The cells were incubated with the complexes for 4 hours at 37°C in a CO₂ incubator. Following incubation, 1 ml of growth medium containing twice the normal concentration of serum was added without removing the transfection mixture. The cells were maintained in this medium for up to 24 hours.

4.2.2.3 *Confocal Laser Scanning Microscopy*

Cells were grown in 6-plate wells on borosilicate coverslips with a thickness number of 0. When ready to analyse after transient transfection, the cells were washed twice at 37°C with HBSS. If the staining of the mitochondria was required see below. For fixation, 2 ml of paraformaldehyde in PBS at 4°C was added to the wells and the plates incubated at 4°C for 20 min. The cells were then washed twice in PBS and mounted in 1,4-diazobicyclo[2,2,2]octane (Dabco). An orange stick or tweezer was used to prise the coverslips containing the cells onto glass slides. The slides were then covered in a chamber and a confocal laser scanning microscope (CLSM) used to investigate the fluorescence. CLSM was carried out using a Zeiss epifluorescence microscope. Data acquisition was controlled with a Nimbus 386 microcomputer and COMOS software.

4.2.2.4 Staining for Mitochondria using MitoTracker™

MitoTracker™ (Molecular Probes, Eugene, OR, USA) probes are dyes that accumulate in the mitochondria and are well retained during cell fixation. The cell-permeant probes contain a thiol-reactive chloromethyl moiety that reacts with accessible thiol groups on peptides and proteins in the mitochondria to form an aldehyde-fixable conjugate. In these experiments the MitoTracker CMXRos, which requires oxidation to fluoresce, was used to stain for mitochondria. This dye is excited at 579nm and emission occurs at 598nm.

The preparation of the probe and staining of adherent cells was carried out as according to the manufacturer's instructions. The reagent is supplied in separate vials containing 50µg of lyophilised product. This was dissolved in high-quality anhydrous dimethylsulfoxide (DMSO) to a final concentration of 1mM. For staining of live cells a working concentration in growth medium of 25nM was used. Briefly, when the cells reached the desired confluence, the growth medium was removed and the cells washed in HBSS. Pre-warmed (37°C) probe –containing medium was then added and the cells were incubated for 30 min. under normal growth conditions. The solution containing the dye was then replaced with pre-warmed growth medium and fixed as according to above.

4.2.2.5 Western Blotting of Transfected Cells

Protein was extracted from transfected cells using the lysis buffer [2M NH_2CONH_2 ; 50mM Tris-HCl; 17mM NaCl; 2.7mM EDTA; 0.1mM phenylmethanesulphonylfluoride (PMSF) and 1ml/L Brij 35 adjusted to a pH of 7.6 with NaOH] described earlier (see 3.2.2.1). After the cells were transfected for the appropriate time the growth medium was replaced and the cells washed in 1ml HBSS. This solution was then removed and the cells incubated on ice for 1 hour in 0.5ml of lysis buffer. The solution containing the lysed cells was then put through a 25 x g needle using a 2ml syringe. This was also carried out on ice. This was repeated vigorously until no more cell debris could be seen. The mixture was then spun at 6500 rpm at 4°C for 10 min. The supernatant (90µl) was then removed. Care was taken not to disturb the pellet. The amount of extracted protein was then measured using the Bradford assay. Western

blotting was then carried out using the NuPage™ procedure described earlier (see 3.2.2). An anti-active-Caspase-3 polyclonal antibody, which detects the 32kDa proform of the enzyme and the cleaved p21 and p17 fragments, was used to detect the expression of GFP-Caspase-3 and GFP-p17 fusion proteins. An anti-GFP polyclonal antibody (Clontech, which recognises the expression of the 27kDa protein, was also used to detect the expression of the fusion proteins, as well as the expression of GFP. Anti-Caspase-7 (a gift from Dr. G. Poirer, Laval University, Quebec, Canada) and anti-Caspase-9 (a gift from Dr. X M Sun, University of Leicester, UK) polyclonal antibodies were used to detect the expression of the proform and the active fragments of these enzymes.

4.3 RESULTS

4.3.1 Cloning of full-length Caspase-3 and its p17 and p12 fragments into pEGFPC1 vector

Fig. 4.8 illustrates the individual PCR reactions for the amplification of the coding sequences of full-length Caspase-3 and its p17 and p12 fragments. The PCR reactions appeared to be successful in that the amplified products were of the correct approximate sizes. Furthermore, there seemed to be little or no mispriming as other non-specific products were not easily visible. Only the PCR reaction for the p12 fragment seemed to contain an inappropriately sized band of approximately 700 bp.

The efficiencies of the excise reactions are unknown, however Fig. 4.9 indicates that samples of the excised DNA solution of the full-length Caspase-3 and the p12 fragment, did not appear to contain any other contaminating bands when run on an agarose gel. A similar result was obtained with the p17 fragment (data not shown). From these gels the solutions containing the excised, restricted DNA for full-length Caspase-3, p17 fragment and p12 fragment were estimated to be approximately 10ng/ μ l, 8ng/ μ l and 5ng/ μ l, respectively. With regard to the transformation efficiencies, Table 4.1 indicates that the full-length Caspase-3 ligation reactions appeared to be significantly less efficient than the other reactions. In addition, in general the 1:10 ligation reactions tended to have a higher transformation efficiency. Furthermore, as described before, the transformation efficiency with the positive control pUC19 plasmid was sub-optimal.

Fig. 4.10 illustrates the nature of results obtained when a plate of colonies ligated with insert was screened. In this case putative pEGFP-C1-Caspase-3 clones were being screened. UP H₂O (colony 1) was used as a negative control and did not produce any band or smearing. In contrast, in the upper half of the gel, colonies 8, 9 and especially 13 appear to produce a band of the correct size of 863 bp when amplified using colony mini-prep PCR. Likewise, in the lower half of the gel, colonies 22, 24, 25, 28 and 29 again produce an appropriately sized band.

Fig. 4.8 PCR amplification of Caspase-3 and its p12 and p17 fragments. mRNA was extracted from frozen tonsil tissue and cDNA synthesised with controls for genomic DNA using the Dynabead™ method as described earlier. All PCR reactions were carried out in 50µl containing 1 x PCR buffer, 1U of Taq polymerase and 10 pmoles of each primer. See text for details of denaturation, annealing and extension temperatures used for the amplification of the full-length Caspase-3 (A), the p12 fragment (B) and the p17 fragment (C). A “hot-start” reaction was used for all PCR reactions. The predicted sizes of the amplicons were 863, 465 and 341 bp for full-length Caspase-3, p17 fragment and p12 fragment respectively. 20µl of each reaction were run on a 1.5% agarose gel at 100V for 1.5 hours and then stained with ethidium bromide (0.5µg/ml). The gel was then visualised by exposure to UV light on a transilluminator.

Fig. 4.9 Estimation of excised and restricted full-length Caspase-3 (A) and its p12 fragment (B). The PCR product was excised using Nucleon™ easiClene kit and then restricted with 10U of *Sal I* and 10U of *Hind III*. 5µl from a 20µl reaction were run on a 1.5% agarose gel at 100V for 2 hours and then stained with ethidium bromide (0.5µg/ml). The gel was then visualised by exposure to UV light on a transilluminator. 20 µl of a solution containing consecutive 100 bp DNA was used as a marker. The 900 bp DNA was estimated to contain approx. 70ng and the 400 bp DNA was estimated to contain 50ng; therefore it was estimated that the full-length Caspase-3 amplicon contained 50ng and the p12 fragment amplicon contained 25ng. Consequently, the solution containing the restricted full-length Caspase-3 was taken to be 10ng/µl and the solution containing the restricted p12 fragment was taken to be 5ng/µl. A similar procedure was carried out for p17 fragment; the restricted solution was taken to be 8ng/µl.

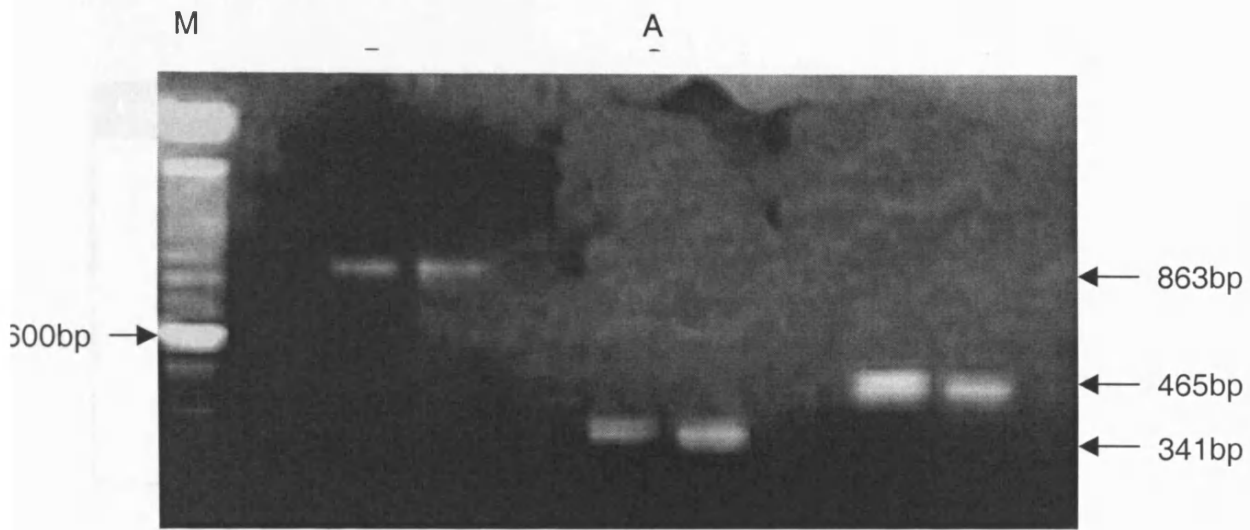


Fig. 4.8 PCR amplification of the coding sequence for Caspase-3 and its p12 and p17 fragments

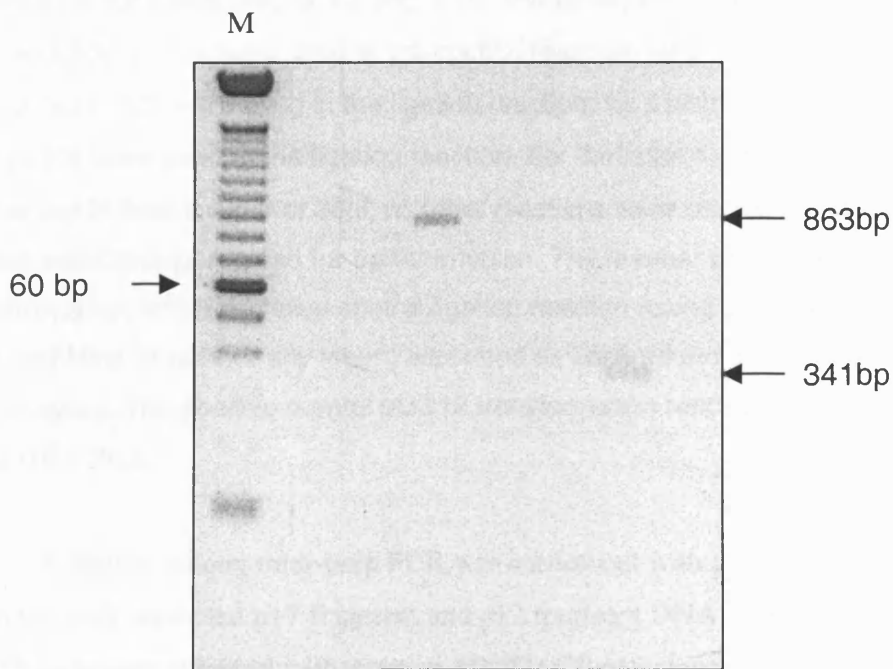


Fig. 4.9 Estimation of excised and restricted DNA sequence full-length Caspase-3 and its p12 fragment

Ligation Regime; vector:insert		Transformation Efficiency
Caspase-3	1:3	$2.4 \times 10^2 \pm 37.9$
	1:10	$2.9 \times 10^2 \pm 45.5$
p17 fragment	1:3	$1.3 \times 10^3 \pm 22.7$
	1:10	$4.4 \times 10^3 \pm 25.7$
p12 fragment	1:3	$3.5 \times 10^3 \pm 65.2$
	1:10	$4.4 \times 10^3 \pm 21.6$

Table 4.1 Transformation efficiencies for each cloning regime used in the ligation reactions for the insertion of the coding sequence of full-length Caspase-3 and its p17 and p12 fragments into pEGFP-C1. All reactions were subsequently transformed into DH5 α TM *E. coli* bacterial cells. Results are expressed as Average \pm S.E.M. 0.5 microlitre aliquots of a 1:25 dilution of the restricted vector (final concentration 20ng/ μ l) were used for ligation and the corresponding volume of the excised, restricted amplicon to give a vector:insert ratio of 1:3 and 1:10. Therefore, for full-length Caspase-3, 3 μ l (1:3) and 10 μ l (1:10) were used in the ligation reaction; for p17 fragment, 3.75 μ l (1:3) and 12.5 μ l (1:10) were used in the ligation reaction; for p12 fragment, 6 μ l (1:3) and 20 μ l (1:10) were used in the ligation reaction. For the latter the ligation reaction was carried out in final volume of 30 μ l; all other reactions were carried out in 20 μ l. 5 μ l of all ligation reactions were used for transformation. The number of colonies generated from transformation with a negative control ligation reaction (using a vector restricted with Sal I and Hind III without any insert) was used as background and subtracted from the colony count. The positive control pUC19 transformation reaction gave an efficiency of $8.7 \times 10^5 \pm 26.9$

A similar colony mini-prep PCR was carried out with plates containing ligation reactions with restricted p17 fragment and p12 fragment DNA as insert. Appropriately sized bands were obtained with putative pEGFP-C1-p17 clones, however no positive bands were obtained with the screening for putative pEGFP-C1-p12 clones (data not shown). Maxi-prep purifications were then carried out on a limited number of putative pEGFP-C1-Caspase-3 and pEGFP-C1-p17 clones.

Fig. 4.10 Screening for putative pEGFP-C1-Caspase-3 clones using colony mini-prep PCR. Clones from a vector:insert plate, using restricted, full-length Caspase-3 cDNA as the insert, were resuspended in 0.5ml of UP H₂O and boiled for 5 min. After spinning in a microcentrifuge at 10,000 g for 2 min. 5µl of the supernatant was used as a template for a PCR reaction. See Methods for details of PCR reaction. Sterile UP H₂O was used as a negative control. 20µl of each reaction were run on a 1.5% agarose gel at 100V for 1.5 hours and then stained with ethidium bromide (0.5µg/ml). The gel was then visualised by exposure to UV light on a transilluminator. Colonies 8, 9, 13, 22, 24, 25, 28 and 29 appear to have amplified a band of the correct of 863 bp for a clone. The negative control UP H₂O has not amplified any band

Fig. 4.11 Double *Hind III* / *Sal I* restriction analysis of putative pEGFP-C1-Caspase-3 and pEGFP-C1-p17 clones. The DNA from putative clones was purified using the maxi-prep™ Qiagen procedure as described in the Methods. 500 ng of plasmid DNA was double restricted with 2U of *Hind III* / *Sal I* as described before. 20µl of each reaction were run on a 1.5% agarose gel at 100V for 2 hours and then stained with ethidium bromide (0.5µg/ml). The gel was then visualised by exposure to UV light on a transilluminator. Restricted DNA from the putative pEGFP-C1-Caspase-3 and pEGFP-C1-p17 clones released fragments of approx. 863 bp and 463 bp respectively.

C1 = Unrestricted and restricted pEGFP-C1
C1-C3 = Unrestricted and restricted pEGFP-C1-Caspase-3
C1-p17 = Unrestricted and restricted pEGFP-C1-p17

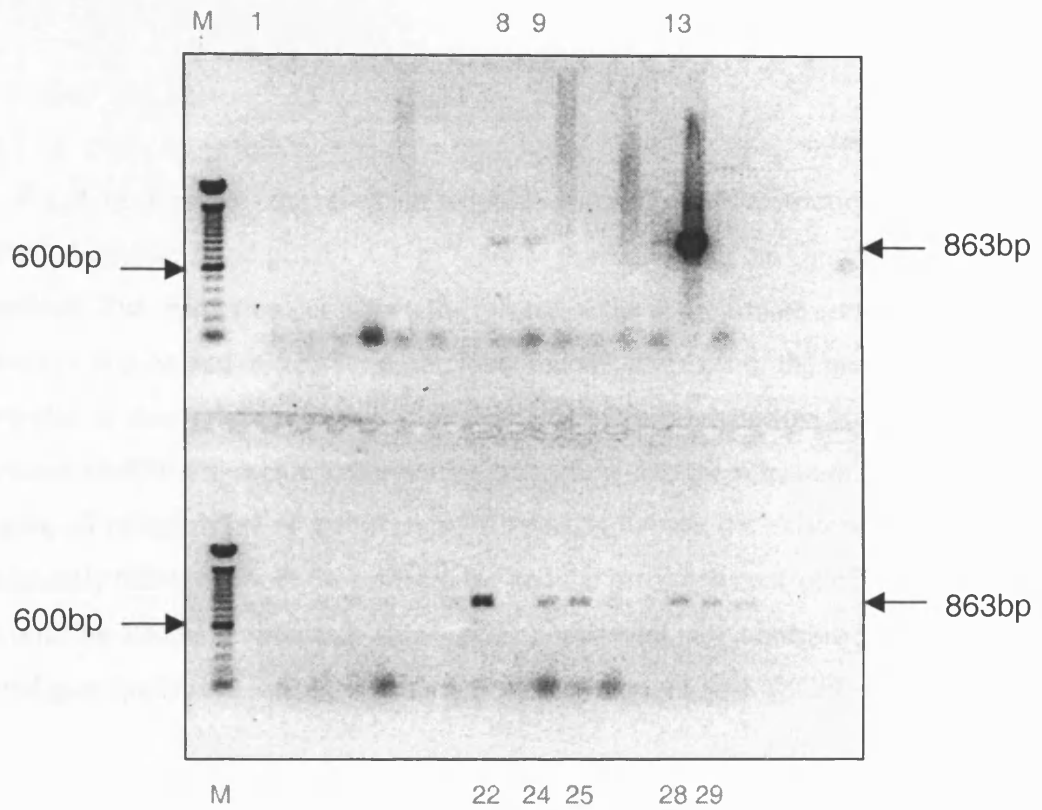


Fig. 4.10 Screening for putative pEGFP-C1-Caspase-3 clones using colony mini-prep PCR

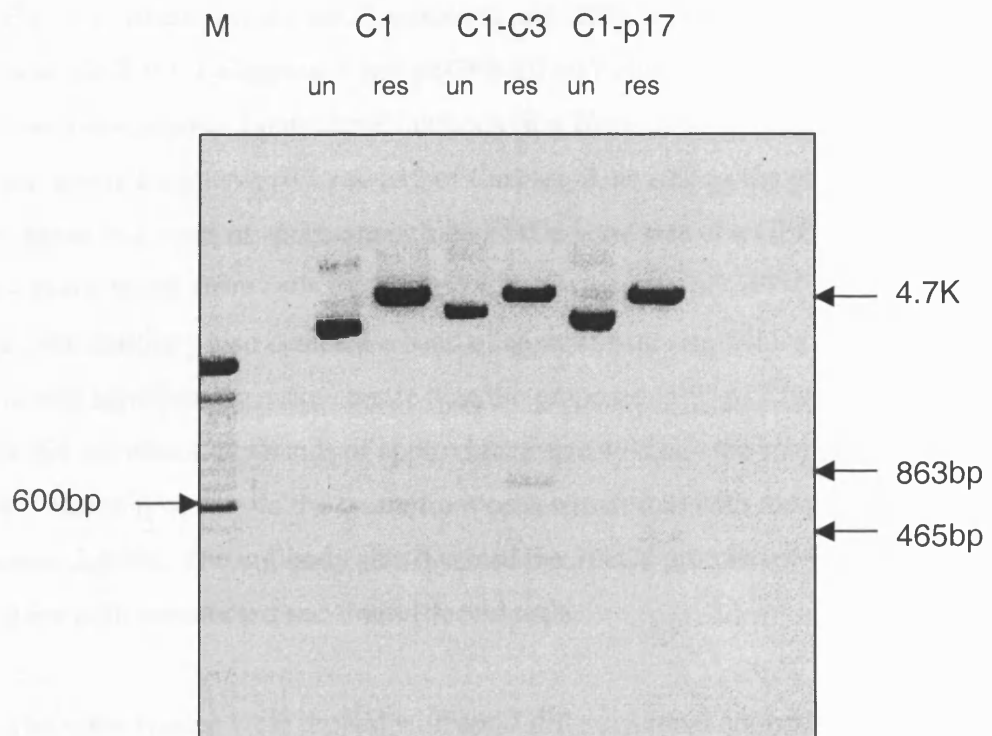


Fig. 4.11 Double *Hind III* / *Sal I* restriction analysis of putative pEGFP-C1-Caspase-3 and pEGFP-C1-p17 clones

Fig. 4.11 illustrates the results of a double *Hind III* / *Sal I* restriction of putative pEGFP-C1-Caspase-3 and pEGFP-C1-p17 clones purified using the Qiagen™ maxi-prep method. The restriction confirmed the release of the approximate correct size fragments of 863 bp and 465 bp for each clone. Indeed, the sizes of the unrestricted putative clones also indicates that they are the correct approximate size in relation to the unrestricted pEGFP-C1 vector. After double restriction, and the release of appropriate fragments, all plasmids are of a uniform 4.7Kb size. However, the existence of a band approximately 600 bp in both the unrestricted and the restricted control pEGFP-C1 vector must be also be considered. This band is not present in the unrestricted or restricted putative clones, indicating that it is common only to the pEGFP-C1 vector.

4.3.2 Expression of putative pEGFP-C1 fusion constructs

4.3.2.1 Western Blotting of Lysates from Cells Transfected with putative Clones

Fig. 4.12 illustrates the results obtained after MRC5 cells were transfected with the putative pEGFP-C1-Caspase-3 and pEGFP-C1-p17 clones and their lysates probed with anti-active-Caspase-3 polyclonal antibody in a Western blot. The antibody, which detects the active fragments p17 and p12 of Caspase-3, as well as the proform of the enzyme, binds to a band of approximate size 44kDa – the size of a GFP-p17 fusion protein – in the lysate from cells transfected with the putative pEGFP-C1-p17 clone. However, the antibody also detected a band of approximate size 54kDa in this lysate and this band was significantly more intense than the proposed GFP-p17 fusion protein. This antibody did not detect any bands of approximate size 49kDa – the size of a GFP-Caspase-3 fusion protein – in the lysate from cells transfected with the putative pEGFP-C1-Caspase-3 clone. The antibody also detected the 32kDa proform of Caspase-3 in lysates from both transfected and untransfected cells.

The same lysates were probed with anti-GFP polyclonal antibody in a Western blot (Fig. 4.13). The antibody detected the GFP at 27kDa in the lysate from cells transfected with pEGFP-C1. Surprisingly, the antibody also detected a similar-sized band, and no higher bands, in the lysate from cells transfected with the putative pEGFP-

C1-Caspase-3 and -p17 clones. The band detected in the lysate from cells transfected with the putative pEGFP-C1-p17 clone was less intense than the other bands. As expected, lysates from the untransfected cells did not express any GFP protein.

The putative clones were then re-screened using primers flanking the MCS of pEGFP-C1. Fig. 4.14 illustrates that no band of approximate size 1068 bp – the predicted size of a clone containing the amplified cDNA of Caspase-3 using these primers – was detected when the DNA from the putative pEGFP-C1-Caspase-3 clone was amplified. Indeed the only band detected in this PCR reaction was the same size as that from the PCR reaction using the DNA from the control pEGFP-C1 vector as a template. Furthermore, the PCR reaction with the DNA from the putative pEGFP-C1-p17 clone produced two bands – one the correct approximate size of 671 bp for a clone and another the same size of 206 bp as that of the DNA from the control pEGFP-C1 vector. High molecular-sized bands were also seen in all PCR reactions.

A re-screening of the putative clones using a double *Hind III* / *Sal I* restriction confirmed the results of the PCR reactions with the primers flanking the MCS of pEGFP-C1 (Fig. 4.15). Unrestricted DNA from the putative pEGFP-C1-Caspase-3 clone was the same size as that of the pEGFP-C1 vector confirming the putative clone had lost the cDNA encoding for Caspase-3. These restriction reactions were run on a low percentage agarose gel and this enabled the mixed clone from the pEGFP-C1-p17 DNA to be visualised. In the lane containing unrestricted DNA from this mixed clone two bands can readily be seen; one band the same size as the unrestricted DNA from the pEGFP-C1 vector and one band a higher size. Double restriction of this mixed clone with *Hind III* / *Sal I* releases a fragment of the correct size for a pEGFP-C1-p17 clone, although the intensity of the band is weak.

This larger band was excised from the gel using a razor and re-purified using the Nucleon™ easiClene kit as described earlier (see 2.2.1.1). This DNA was then transformed into DH5™ *E.coli* cells and a Qiagen™ maxi-prep carried out as described earlier (see 2.2.1.3 and 2.2.1.4) to produce DNA from a pure, unmixed clone (data not shown).

Fig. 4.16 illustrates the results obtained after MCF-7 cells were transfected with the pure pEGFP-C1-p17 clone and the lysates probed with anti-active Caspase-3 polyclonal antibody in a Western blot. After 4 hours no bands were detected by the antibody; however after 8 hours two bands of approximately 44kDa and 54kDa are detected. As described above, 44kDa is the predicted size of a GFP-p17 fusion protein. As with the MRC5 Western blot probed with same antibody a higher band of unknown origin was detected. Again, the higher unidentified band was more intense, although the difference was slight. After 18 hours both bands are more intense. No proform Caspase-3 was detected in any cell lysate, unlike the MRC5 western blot probed with the same antibody.

The same MCF-7 lysates were probed with an anti-GFP polyclonal antibody in a Western blot. As Fig. 4.17 shows, the antibody only detected the GFP protein at 27kDa in the lysate from cells transfected with pEGFP-C1 after 18 hours. No bands of a higher size were detected in any other lysates.

These same MCF-7 lysates were probed with polyclonal anti-Caspase-7 and -9 in a Western blot to determine if any apoptotic cell death had occurred. As Fig. 4.19 illustrates, only the 35kDa proform of Caspase-7 was detected in any of the lysates from transfected cells. Similarly, only the 46kDa proform of the Caspase-9 enzyme was detected in the lysates from the transfected cells (Fig. 4.18).

4.3.2.2 Confocal Laser Scanning Microscopy of Transfected Cells

MRC5 cells transfected with pEGFP-C1 after 24 hours displayed a green diffuse fluorescence in the cytoplasm of the appropriate cells according to the confocal microscopic images analysed (Fig. 4.20). In addition, the grey image (Fig. 4.20a) and its coloured version in Fig. 4.20b illustrate the specificity of the MitoTracker™ dye for the mitochondria in MRC5 cells. A punctate pattern of staining with the mitochondria was observed with the organelles aligned along the membrane. Fig. 4.20e confirms the cytoplasmic localisation of GFP with the nuclei omitting the signal very evident.

Fig. 4.12 Western blot of MRC5 cells transfected with pEGFP-C1 and putative clones and probed with anti-Caspase-3 polyclonal antibody. MRC5 cells were transfected in a 6 well plate using Lipofectamine and 2 μ g of vector DNA as described. After 24 hours the cells were lysed and the amount of protein extracted measured using the Bradford assay. 9 μ g of extracted protein from each well was run on a NuPage™ MES 4-12% polyacrylamide gel and transferred onto a nitrocellulose membrane as described before. The membrane was then probed with an anti-Caspase-3 polyclonal antibody that detects the 32kDa proform of the enzyme and the active p21 and p17 fragments. Binding of the antibody was then detected using the ECL chemiluminescence system.

Con	Untransfected Cells
C1	Transfected with pEGFP-C1
C1-C3	Transfected with putative pEGFP-C1-Caspase-3
C1-p17	Transfected with putative pEGFP-C1-p17

Fig. 4.13 Western blot of MRC5 cells transfected with pEGFP-C1 and putative clones and probed with anti-GFP polyclonal antibody. MRC5 cells were transfected in a 6 well plate using Lipofectamine and 2 μ g of vector DNA as described. After 24 hours the cells were lysed and the amount of protein extracted measured using the Bradford assay. 9 μ g of extracted protein from each well was run on a NuPage™ MES 4-12% polyacrylamide gel and transferred onto a nitrocellulose membrane as described before. The membrane was then probed with an anti-GFP polyclonal antibody that detects the 27kDa protein. Binding of the antibody was then detected using the ECL chemiluminescence system.

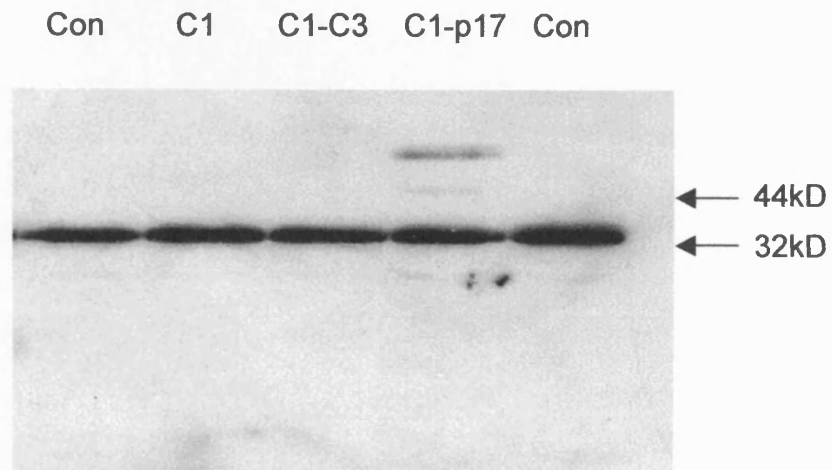


Fig. 4.12 Western blot of MRC5 cells transfected with pEGFP-C1 and putative clones and probed with anti-Caspase-3 polyclonal antibody

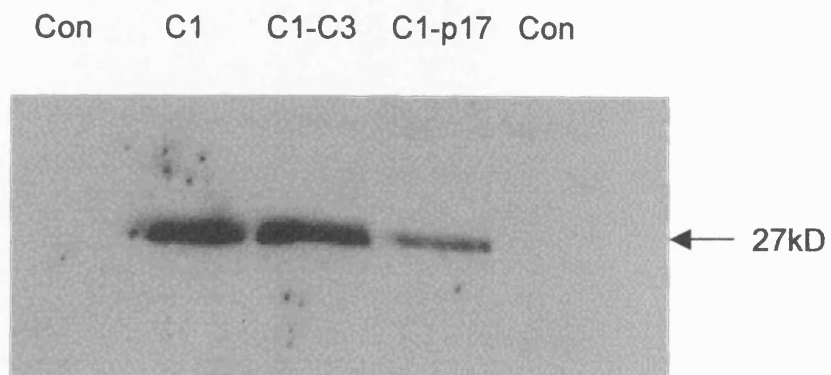


Fig. 4.13 Western blot of MRC5 cells transfected with pEGFP-C1 and putative clones and probed with anti-GFP polyclonal antibody

Fig. 4.14 Screening of putative clones using primers flanking the MCS of pEGFP-C1. Plasmid DNA from pEGFP-C1 (C), putative pEGFP-C1-Caspase-3 clone (A), and putative pEGFP-C1-p17 clone (B) was used as templates for a PCR reaction with primers flanking the MCS of pEGFP-C1. UP H₂O was also used as a template as a negative control (W). Details of PCR reaction and denaturation, annealing and extension temperatures are described in the Methods. C1, A1 and B1 contain twice the units of *Taq* polymerase. The predicted products for the putative pEGFP-C1-Caspase-3 and pEGFP-C1-p17 clones were 1068 bp and 671 bp respectively. The predicted product for the control pEGFP-C1 vector was 206 bp. 20µl of each reaction were run on a 1.5% agarose gel at 100V for 2 hours and then stained with ethidium bromide (0.5µg/ml). The gel was then visualised by exposure to UV light on a transilluminator. The only PCR reaction to contain any band above the control vector amplicon was the putative pEGFP-C1-p17 amplification.

Fig. 4.15 Screening of putative clones using double *Hind III* / *Sal I* restriction. 500 ng of maxi-prep plasmid pEGFP-C1 (C), and putative pEGFP-C1-Caspase-3 (A), and pEGFP-C1-p17 (B) DNA were double restricted with *Hind III* and *Sal I* to investigate the release of appropriately sized fragments. pEGFP-C1-Caspase-3 and pEGFP-C1-p17 clones should release fragments of 863 and 465 bp respectively after *Hind III* / *Sal I* restriction. 20µl of each reaction were run on a 0.5% agarose gel at 100V for 2 hours and then stained with ethidium bromide (0.5µg/ml). The gel was then visualised by exposure to UV light on a transilluminator. Only the restricted putative pEGFP-C1-p17 clone released an appropriately sized fragment. Furthermore, unrestricted putative pEGFP-C1-p17 DNA indicated a mixed clone.

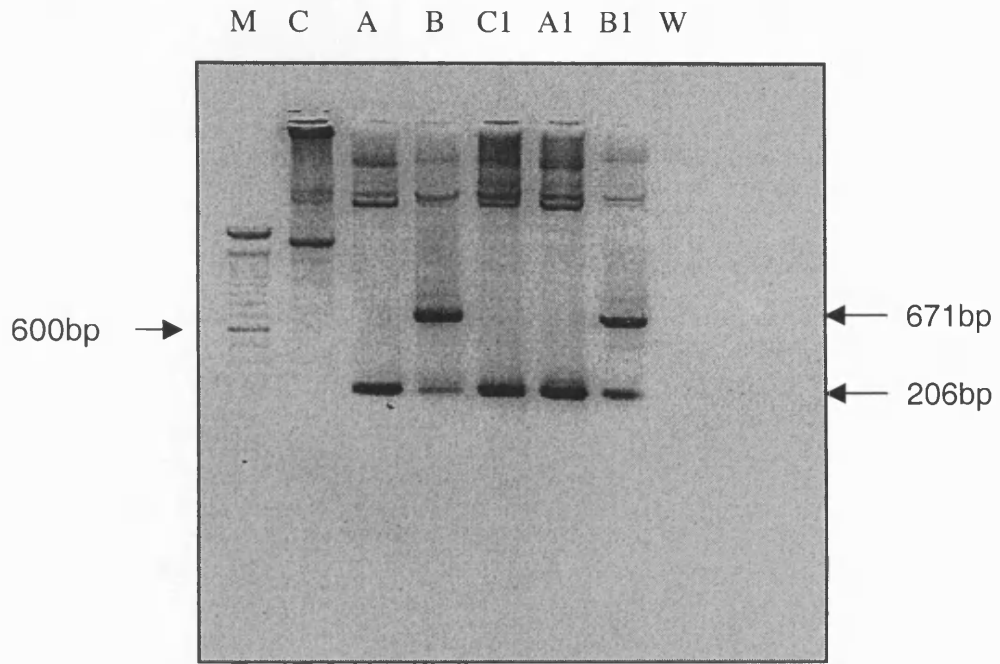


Fig. 4.14 Screening of putative clones using primers flanking the MCS of pEGFP-C1

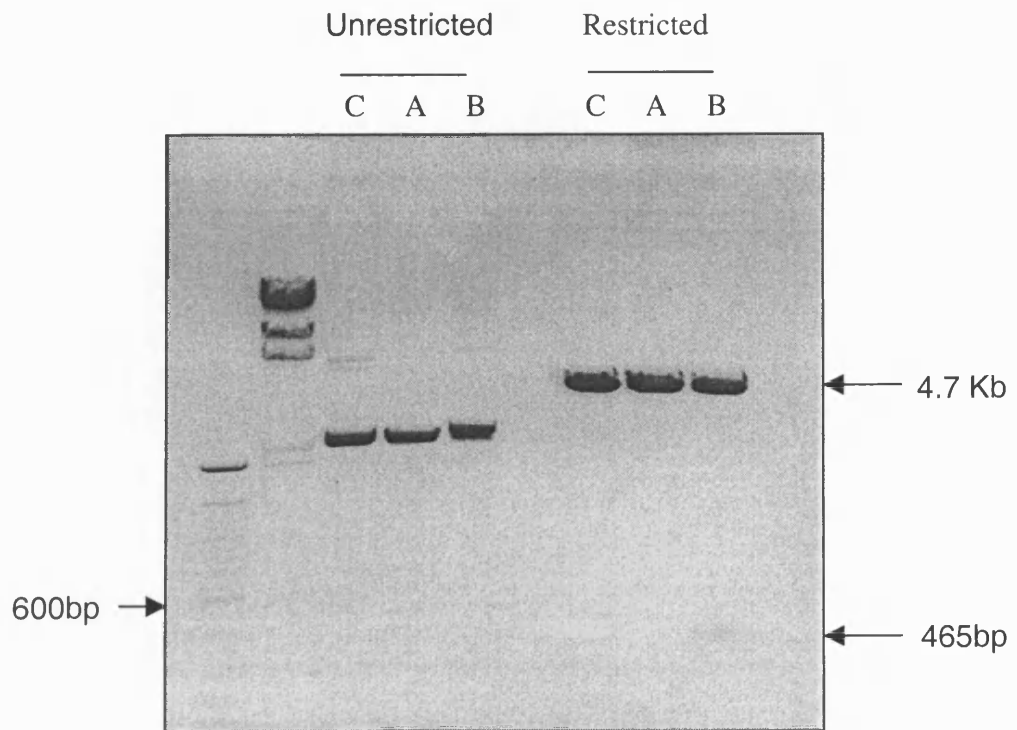


Fig. 4.15 Screening of putative clones using double *Hind III* / *Sal I* restriction

Fig. 4.16 Western blot of MCF-7 cells transfected with pEGFP-C1 and pEGFP-C1-p17 and probed with anti-active-Caspase-3 polyclonal antibody. MCF-7 cells were transfected in a 6 plate well using 10 μ l of Lipofectamine and 3 μ g of pEGFP-C1 (C1) and 3 μ g of pEGFP-C1-p17 (C1-p17) as described. After 4 hours (A), 8 hours (B) and 18 hours (C), the cells were lysed and the amount of protein extracted measured using the Bradford assay. 10 μ g of extracted protein from each well was run on a NuPage™ MES 4-12% polyacrylamide gel and transferred onto a nitrocellulose membrane as described before. The membrane was then probed with an anti-active Caspase-3 polyclonal antibody that recognise the p17 fragment. Binding of the antibody was detected using the ECL chemiluminescence system. The antibody detected a band of the correct approximate size 44kDa for a GFP-p17 fusion protein. An unidentified band of approximately 55kDa was also detected.

Fig. 4.17 Western blot of MCF-7 cells transfected with pEGFP-C1 and pEGFP-C1-p17 and probed with anti-GFP polyclonal antibody. The same procedure as above was carried out. The membrane was then probed with an anti-GFP polyclonal antibody that detects a 27kDa protein. The antibody detected a band of the correct approximate size for a GFP protein in the lysate of cells transfected with pEGFP-C1 after 18 hours.

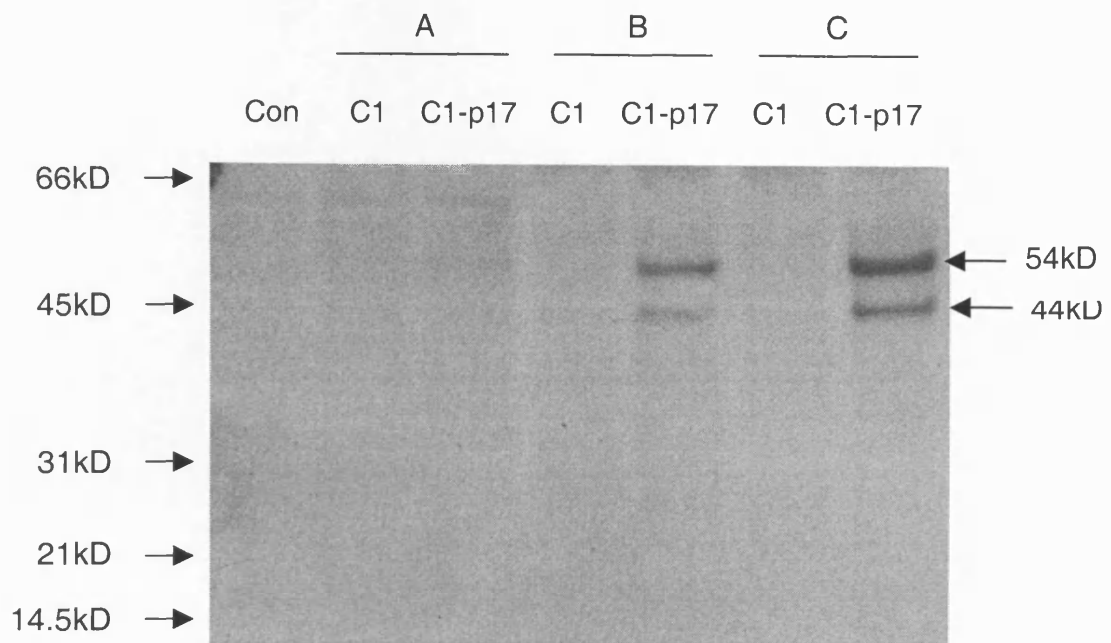


Fig. 4.16 Western blot of MCF-7 cells transfected with pEGFP-C1 and pEGFP-C1-p17 and probed with anti-active Caspase-3 polyclonal antibody

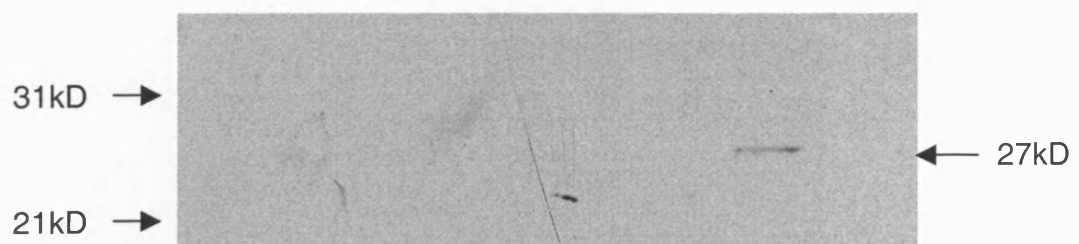


Fig. 4.17 Western blot of MCF-7 cells transfected with pEGFP-C1 and pEGFP-C1-p17 and probed with anti-GFP polyclonal antibody

Fig. 4.18 Western blot of MCF-7 cells transfected with pEGFP-C1 and pEGFP-C1-p17 and probed with anti-Caspase-9 polyclonal antibody. The same procedure as above was carried out. The membrane was then probed with an anti-Caspase-9 polyclonal antibody that recognises the 46kDa proform of the enzyme and its active fragments. The antibody only detected a band of the correct approximate size for the proform of the enzyme in all lysates including untransfected (Con) cells.

Fig. 4.19 Western blot of MCF-7 cells transfected with pEGFP-C1 and pEGFP-C1-p17 and probed with anti-Caspase-7 polyclonal antibody. The same procedure as above was carried out. The membrane was then probed with an anti-Caspase-7 polyclonal antibody that recognises the 35kDa proform of the enzyme and its active fragments. The antibody only detected a band of the correct approximate size for the proform of enzyme in all lysates including untransfected (Con) cells.

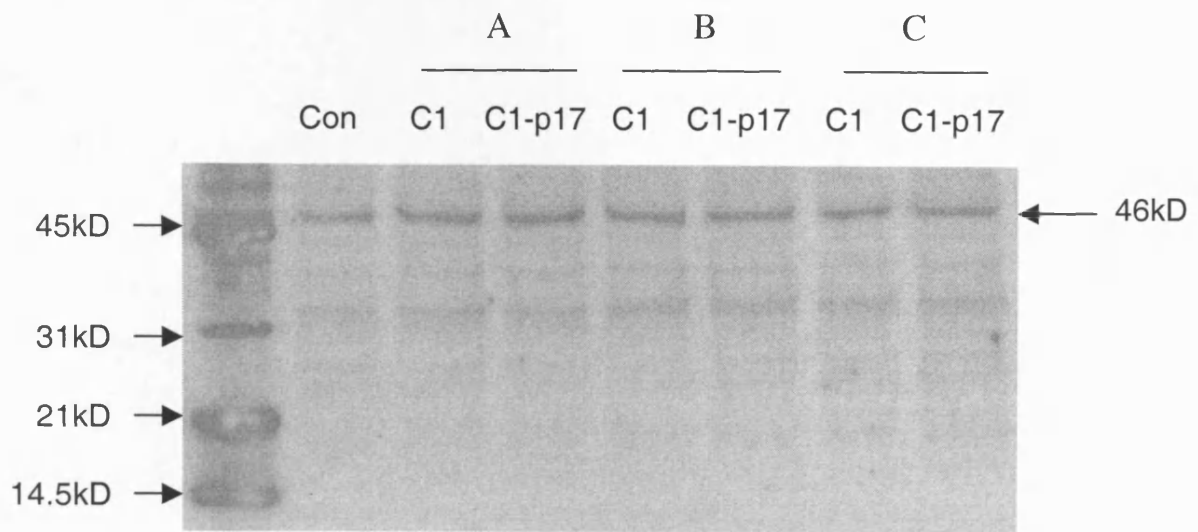


Fig. 4.18 Western blot of MCF-7 cells transfected with pEGFP-C1 and pEGFP-C1-p17 and probed with anti-Caspase-9

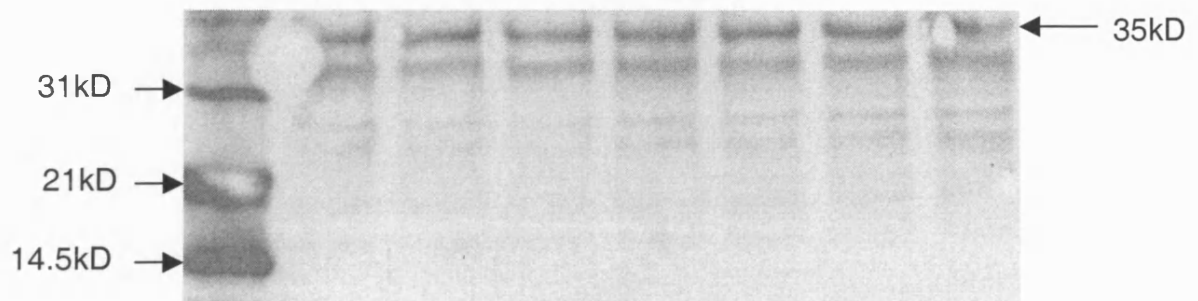


Fig. 4.19 Western blot of MCF-7 cell transfected with pEGP-C1 and pEGFP-C1-p17 and probed with anti-Caspase-9

Fig. 4.20 Confocal Microscopic images of MRC5 cells transfected with pEGFP-C1 after 24 hours.

MRC5 cells were grown on coverslips and transfected as described in Methods. After 24 hours they were fixed in paraformaldehyde in PBS at 4°C, washed and mounted in Dabco. When required, the cells were stained with MitoTracker™ dye as described in Methods.

Fig. 4.20a x 17 objective; Black and white photomicrograph of cells expressing GFP and stained with MitoTracker™ dye

Fig. 4.20b and c x 17 objective; as a in colour

Fig. 4.20d x 40 objective; Colour photomicrograph of cells expressing GFP and stained with MitoTracker™ dye.

Fig. 4.20e x 40 objective; Colour photomicrograph of cells expressing GFP

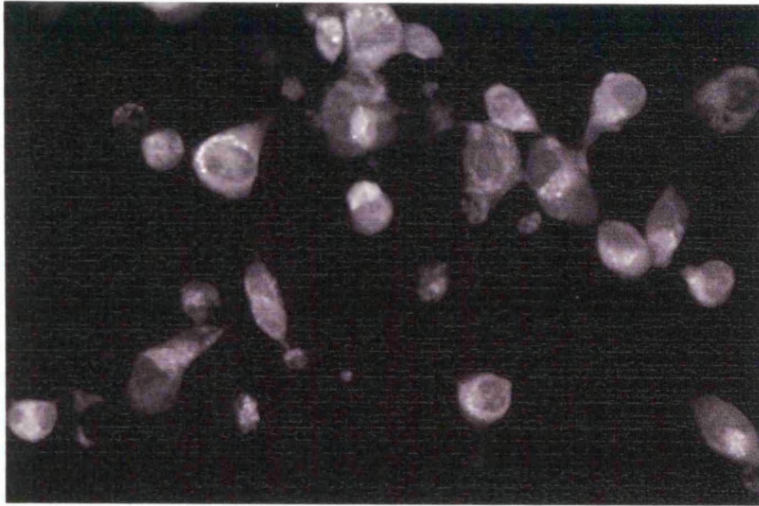


Fig. 4.20a

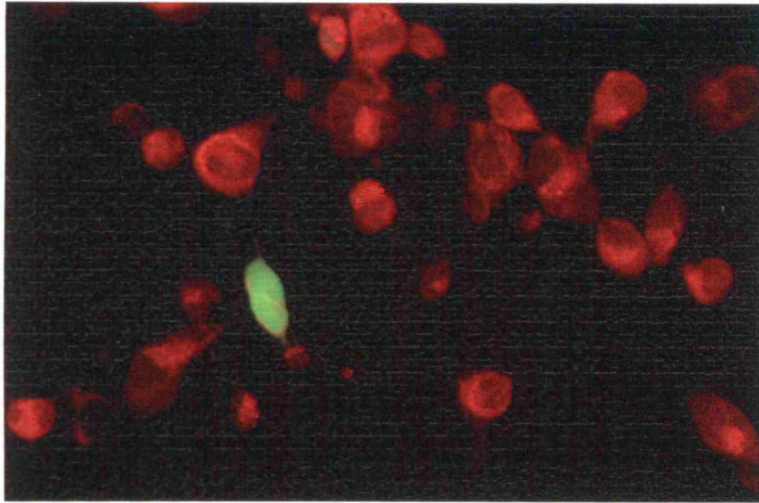


Fig. 4.20b

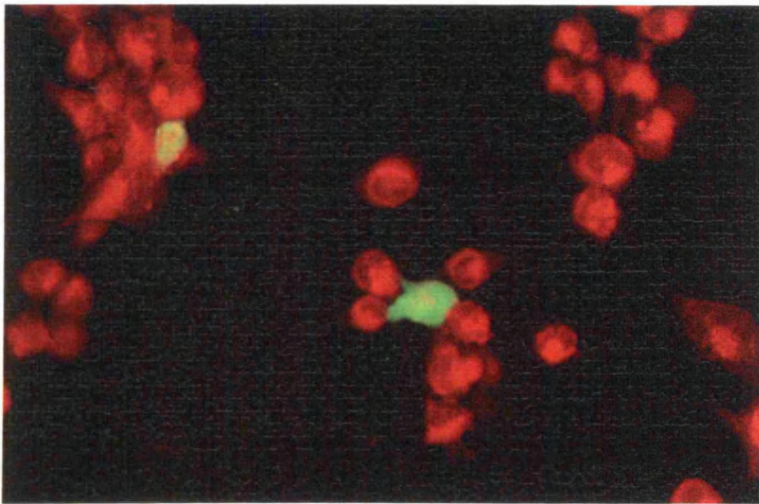


Fig. 4.20c

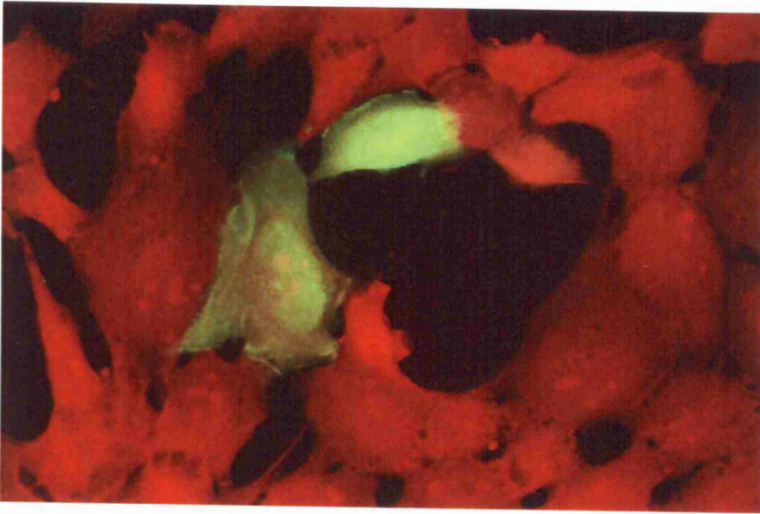


Fig. 4.20d

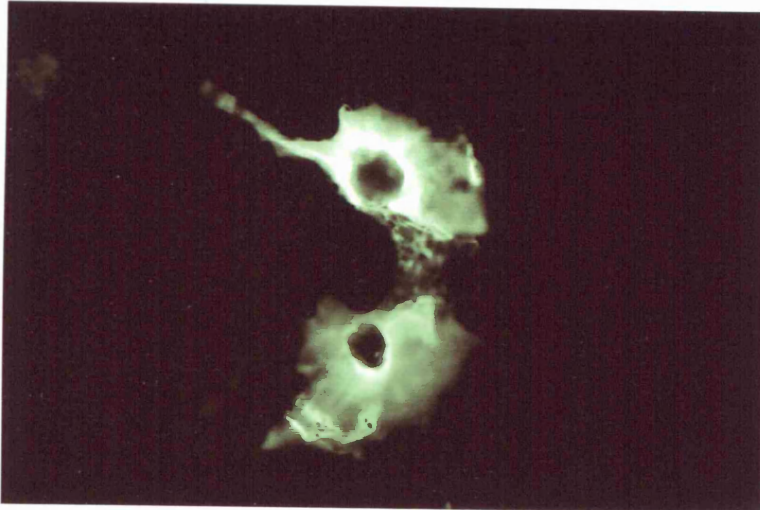


Fig. 4.20e

Fig. 4.21 Confocal Microscopic images of MCF-7 cells transfected with pEGFP-C1 and pEGFP-C1-p17.

MCF-7 cells were grown on coverslips and transfected with pEGFP-C1 and pEGFP-C1-p17 after 4, 8 and 18 hours as described in Methods. They were then fixed in paraformaldehyde in PBS at 4°C, washed and mounted in Dabco. When required, the cells were stained with MitoTracker™ dye as described in Methods.

Fig. 4.21a x 17 objective; Black and white photomicrograph MCF-7 cells stained with MitoTracker™ dye only

Fig. 4.21b x 17 objective; Colour photomicrograph of MCF-7 cells stained with MitoTracker™ dye only

Fig. 4.21c x 40 objective; Colour photomicrograph of MCF-7 cells expressing GFP and stained with MitoTracker™ dye

Fig. 4.21d x 63 magnification; Black and white photomicrograph of MCF-7 cells expressing GFP

Fig. 4.21e and f x 63 objective; Colour photomicrograph of MCF-7 cells expressing GFP

Fig. 4.21g and h x 40 objective; Colour photomicrograph of MCF-7 cells expressing GFP-p17 fusion protein after 8 hours transfection

Fig. 4.21i and j x 63 objective; Colour photomicrograph of MCF-7 cells expressing GFP-p17 fusion protein after 18 hours transfection

Fig. 4.21k x 40 objective; Colour photomicrograph of MCF-7 cells expressing GFP-p17 fusion protein after 18 hours transfection

Fig. 4.21l x 40 objective; Colour photomicrograph of MCF-7 cells expressing GFP-p17 fusion protein after 18 hours transfection and stained with MitoTracker™ dye

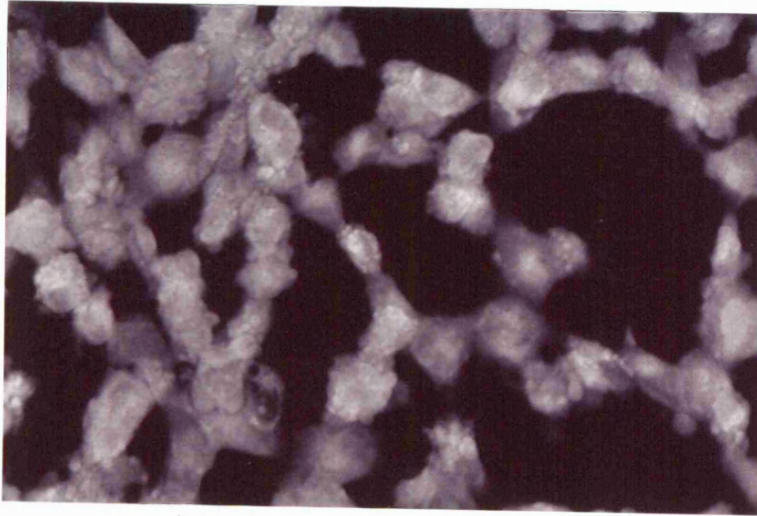


Fig. 4.21a

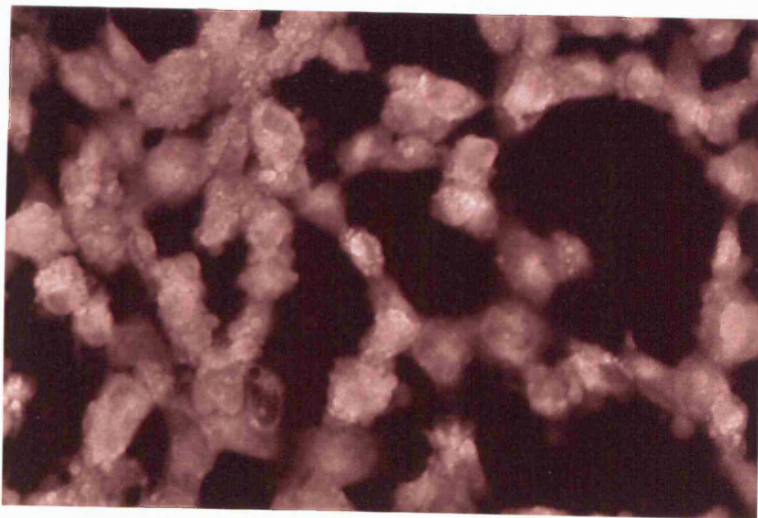


Fig. 4.21b

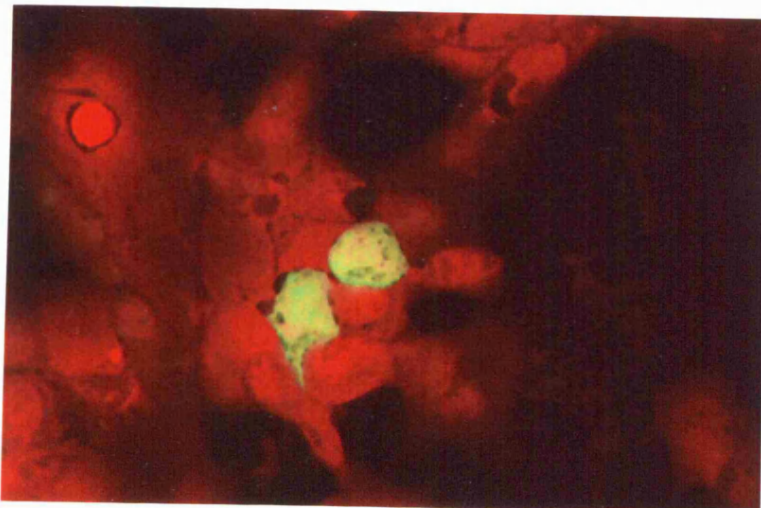


Fig. 4.21c



Fig. 4.21d

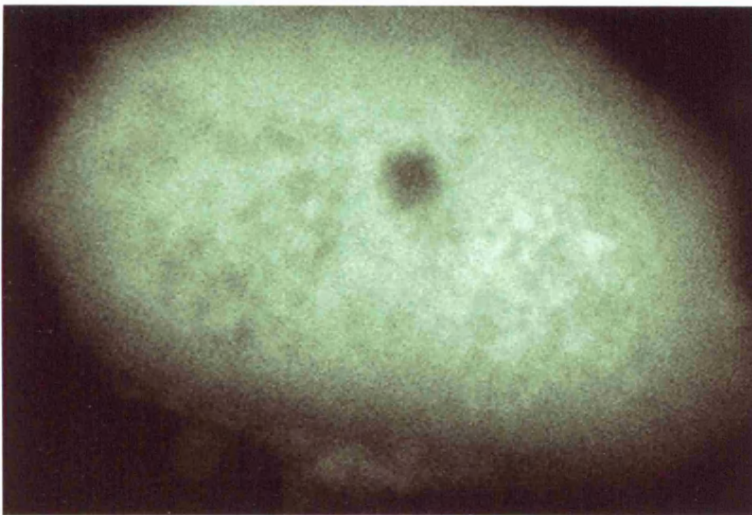


Fig. 4.21e

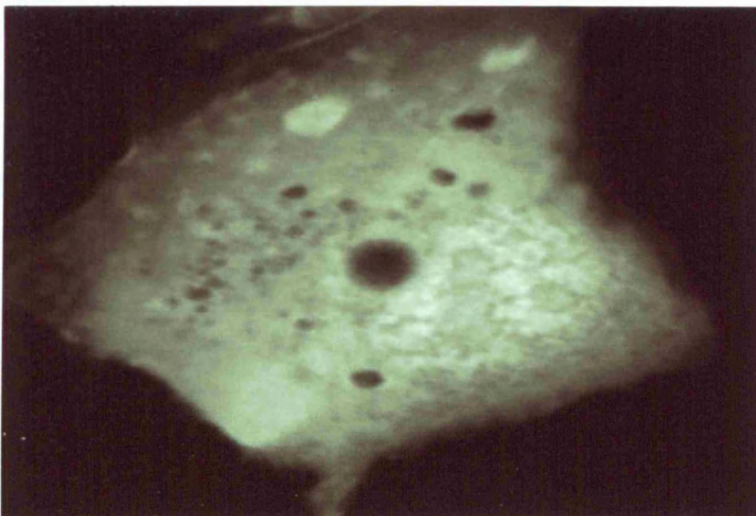
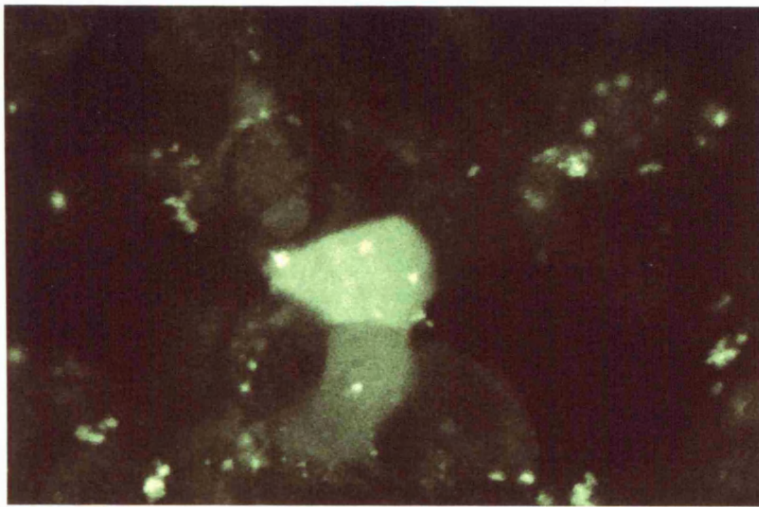
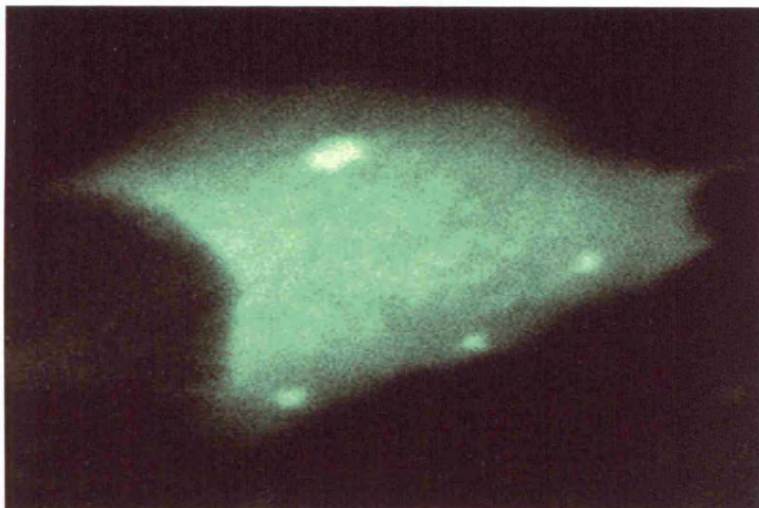


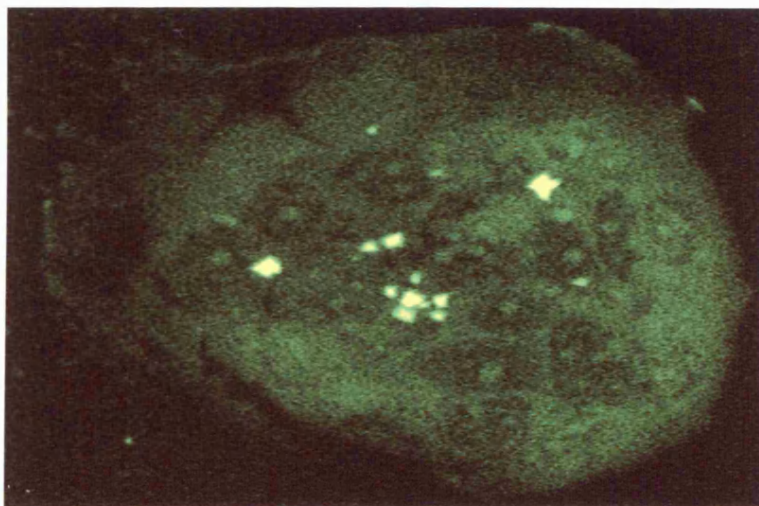
Fig. 4.21f



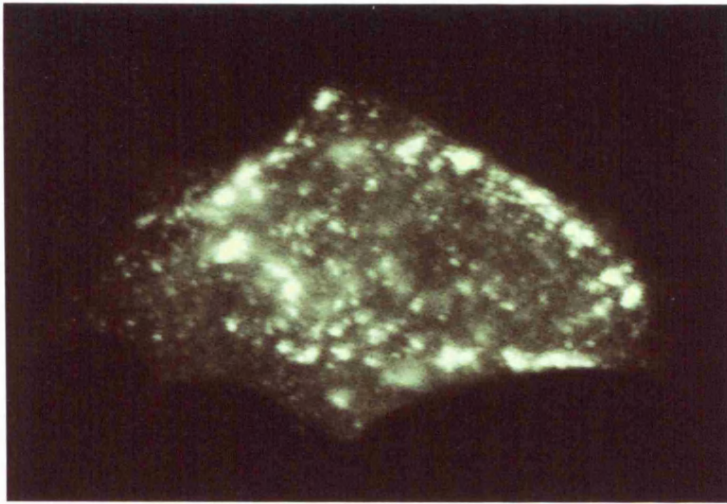
4.21g



4.21h



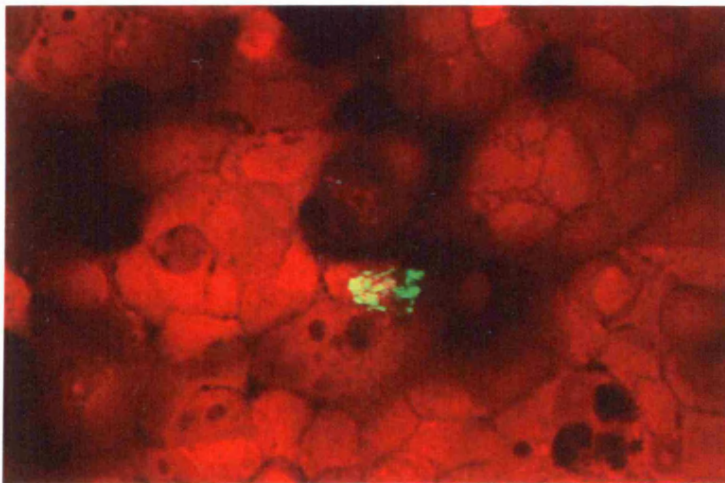
4.21i



4.21j



4.21k



4.21l

Similar to the Western blot results, no green fluorescence was observed in MCF-7 cells after 4 hours of transient transfection. After 8 hours the GFP was evidently being expressed (Fig. 4.21c, e, f) and, as with the MRC5 cells, this fluorescence was diffuse and cytosolic. Similar to the MRC5 cells, no nuclear fluorescence was observed in these MCF-7 cells either. Furthermore, specific organelles and subcellular structures, such as vacuoles, were more easily observed with MCF-7 cells transfected with pEGFP-C1. The MitoTracker™ dye also specifically stains the mitochondria in the MCF-7 cells (Fig. 4.21a and b), although the red signal appears to have more background. As with the MRC5 cells the majority of the mitochondria are aligned with the membranes of the cells, although the punctate nature of the pattern of staining is not as pronounced.

After 8 hours the majority of MCF-7 cells transfected with pEGFP-C1-p17 displayed a striking punctate pattern of green fluorescence. At least two distinct types of punctate staining was observed in these cells after 8 hours; one type of staining with a limited punctate pattern against a diffuse green background (Figs. 4.21g and h); and another type of staining with a multiple punctate pattern against little or no background of green fluorescence (Figs. 4.21h and i). After 18 hours many of the MCF-7 cells transfected with pEGFP-C1-p17 appeared to be either swollen (Figs. 4.21h and i) or disintegrated with membrane breakdown (Figs. 4.21j and k). Indeed, in Fig. 4.21i the organelles or structures the GFP-p17 protein has localised to also appear swollen.

It should be noted that although the transfection efficiency appears poor in both the MRC5 and the MCF-7 cells, this was not necessarily the case. Treatment of cells with the MitoTracker™ dye tended to disrupt many of the cells and make them less adherent. Therefore, cells transfected with pEGFP-C1 only tended to have efficiencies of approx. 15-30%; of course, the efficiencies of cells transfected with pEGFP-C1-p17 were more difficult to ascertain as once the protein was being expressed many of the cells appeared to be dying.

ANALYSIS OF RESULTS

Given the limitations imposed on primer design for the amplification of full-length Caspase-3 and the p12 and p17 fragments, the respective PCR reactions were surprisingly efficient and specific. A deliberate effort was made to restrict the extension times of the PCR reactions in order to reduce the possibility of introducing errors in the amplification step by *Taq* polymerase. Earlier efforts to amplify the sequences using *Pfu* polymerase, an enzyme with a much higher fidelity than *Taq* polymerase, failed to produce enough amplicon to clone into the pEGFP-C1 vector.

The transformation efficiencies for the cloning reactions were, in general, low in comparison to the pUC19 control vector. However, even the transformation efficiency for this plasmid was low, indicating a sub-optimal transformation procedure. Undoubtedly this would have effected the cloning efficiencies, however it probably does not account entirely for the poor transformation efficiencies. Prior to ligation, the efficiency of the T4 DNA ligase was investigated and found to be effective. Furthermore, the efficiency of the double *Hind III* / *Sal I* restriction was also investigated with the control vector and found to be effective. However, it was difficult to assess the efficiency of the double *Hind III* / *Sal I* restriction to act on an excised, fragment of DNA, and this may have been sub-optimal. The lack of presence of any putative clone for pEGFP-C1-p12 is surprising, especially as the p12 insert was the smallest, and therefore any clones should, theoretically have been more stable.

Initial Western data using MRC5 transfected lysates with the clone containing the full-length Caspase-3 cDNA indicated that there was no expression of a GFP protein fused to full-length Caspase-3. This was confirmed with a PCR reaction using primers flanking either side of the MCS of the pEGFP-C1 vector, and with a repeated restriction screening of the clone. Therefore, at sometime the cDNA for the full-length Caspase-3 was released. Another putative clone initially containing Caspase-3 cDNA was found to be the same size as the wild-type vector after re-screening. Indeed, single restrictions of the plasmid DNA of putative pEGFP-C1-Caspase-3 with *Hind III* alone also released an appropriately sized fragment, indicating an incorrect insertion of the DNA and a probable erroneous reading frame. Single restriction of the DNA from the putative pEGFP-C1-p17 clone with *Hind III* alone did not release a fragment (data not shown).

Again, this may have been a result of a sub-optimal restriction of the excised full-length Caspase-3 amplicon.

In contrast, initial transfection studies in MRC5 fibroblast cells with the clone containing the p17 fragment of Caspase-3 indicated a GFP fusion protein was being expressed. However, although Western blotting with anti-active Caspase-3 did indicate the existence of a band of the correct size for a p17-GFP fusion protein of approximately 44kDa, it also indicated the existence of a band approximately 55kDa. Furthermore, initial Western blotting results using an anti-GFP polyclonal antibody did not indicate the existence of any proteins higher than 27kDa – the size of GFP. Indeed, the lysate from cells transfected with the putative pEGFP-C1 –p17 clone appeared to express a GFP protein alone, similar to lysates from cells transfected with the pEGFP-C1 vector alone. Analysis with the primers flanking the MCS of pEGFP-C1 did indicate a band of the correct size for the pEGFP-C1-p17 clone, however, it also indicated a band of the correct size for a vector containing no cDNA. Therefore, it appeared that a mixed clone had been isolated. This was confirmed using restriction analysis on a low percentage agarose gel. The presence of a double band was confirmed for the putative pEGFP-C1-p17 clone.

Western blotting results using MCF-7 transfected lysates again confirm both a 44kDa protein and a 54-56kDa protein with probed with anti-active Caspase-3 antibody. Both bands were detected relatively early after 8 hours. The larger unidentified band actually appears stronger after 8 hours, however the band proposed to represent the GFP-p17 fusion protein appears as strong as the unidentified band after 18 hours. Western blotting results using an anti-GFP polyclonal antibody with the same MCF-7 transfected lysates only detected the 27kDa protein after 18 hours in the cells transfected with pEGFP-C1 only. This indicates that not enough GFP protein was being expressed in these cells until after 18 hours of expression. It also indicates that the anti-GFP polyclonal antibody was not capable of detecting the GFP-p17 fusion protein. Western blot results with the anti-active Caspase-3 polyclonal antibody, which detects the p17 fragment, confirmed the expression of this GFP-p17 fusion protein.

Early confocal microscopic studies with MRC5 confirmed the specificity of the MitoTracker™ dye for the mitochondria in the fibroblast cell line. A punctate pattern of

staining was observed with the mitochondria usually aligned along the membranes. The MRC5 cells transfected with pEGFP-C1 displayed a diffuse green fluorescent signal. Although confocal microscopic studies with MCF-7 cells gave a similar pattern of staining as the MRC5 cells, there was some non-specific staining as the adenocarcinoma cell line displayed a red diffuse signal throughout. The reason for the higher background in these cells is unknown; indeed the concentration of dye used was the lowest suggested by the manufacturers. Interestingly, more details of the cellular structure could also be observed with the MCF-7 cells transfected with pEGFP-C1. Even though these cells displayed a diffuse green fluorescent signal similar to MRC5 cells, the specific structures of organelles within the MCF-7 cells could be determined more readily than those within the MRC5 cells. This indicated that, for this particular cell type, there may be slight differential staining of the green fluorescent protein.

Both confocal microscopic and Western blotting studies from cells transfected with the pEGFP-C1 vector indicated the expression of GFP after 8 hours. After this time confocal microscopic studies with MCF-7 cells transfected with pEGFP-C1-p17 displayed a striking fluorescent pattern. The majority of cells displayed a punctate pattern of green fluorescence. This punctate pattern of staining was too scattered to indicate a nuclear pattern of staining, especially as the structure of the cells appeared intact in these images. Given the other available data with respect to the localisation of the active p17 fragment of the Caspase-3 enzyme it seems likely that this punctate pattern of staining of the GFP-p17 fragment represents mitochondrial staining.

After 18 hours the majority of MCF-7 cells transfected with pEGFP-C1-p17 were either swollen or fragmented. The exact nature of death was difficult to assess, however many of the cells displayed a “necrotic-like” appearance of death with cell membranes ruptured and little or no evidence of shrinking or membrane budding. After 8 hours the presence of many vacuoles was also noted in these cells. This phenomenon has been observed before and is described as ‘autophagic necrosis’. Furthermore, Western blotting of lysates of cells transfected with pEGFP-C1-p17 using anti-Caspase-7 and -9 antibodies did not indicate any cleavage of the proform of the enzymes, again suggesting the involvement of a necrotic form of cell death.

However, care must be taken in assuming that the cells transfected with pEGFP-C1-p17 were not dying due to apoptotic cell death. The transfection efficiency for the MCF-7 cells was not high, as assessed by confocal microscopy, and the copy number of the fusion protein would not be particularly high due to the lack of a SV40 T antigen in the host cell line. Therefore, there simply may not have been enough apoptotic dying cells to be detected by an anti-Caspase-7 or -9 antibody in a Western blot. In addition, a phenomenon known as “secondary necrosis”, may account for the morphological appearance of the cells. This occurs when neighbouring cells required by apoptotic cells for phagocytosis are absent; consequently the cells appear to die by a process similar to necrosis.

Chapter 5

DISCUSSION

DISCUSSION

Ironically, considering the importance of apoptosis in biological processes, the methods used to detect and quantify it are not ideal (Alison 1999). Differences between apoptotic cells *in vivo* and *in vitro* also contribute to a greater confusion. Some of the methods used to detect apoptosis involve the detection of DNA strand breaks using the addition of enzyme-mediated addition of labelled nucleotides. The most popular of these methods, *in situ* end-labelling (TUNEL), adds a terminal deoxynucleotidyl transferase (Tdt) to free 3'-hydroxyl ends of DNA strand breaks, and enables labelled dUTP to be incorporated and detected. This method is believed to be more specific for apoptosis, although it can still label necrotic cells (Grasl-Kraupp *et al.* 1995). Another method of detecting apoptotic cells uses the cleavage of appropriate substrates, such as the revealing of a new epitope of cytokeratin 18 after proteolytic cleavage at aspartate 396 in epithelial cells (Leers *et al.* 1999). However, these methods do not give much information with respect to the activation of specific caspases and the type of pathways being utilised, and as the experiments with the caspase knockout mice illustrate (see section 1.13), the activation of caspases is highly cell- and signal-specific.

The greater complexity of the apoptotic cell death machinery in mammalian systems is also indicated by the presence of multiple homologues of the *C. elegans* death genes *ced-3* and *ced-9*. Although 11 human caspases are known to exist, only a subset of these enzymes is detectably proteolytically activated by various distinct death stimuli in different cell types. Caspase-3 is the most frequently activated member of this family of enzymes in different cell types, and given the apparent ubiquitous activation of this enzyme it may be possible to determine the efficacy of chemotherapy by measuring the levels of either, or both, the inactive and the active form of this enzyme. Furthermore, the likelihood of success with a certain anti-tumour agent may be predicted by quantitatively measuring the levels of inactive and active Caspase-3.

However, at least two recent studies indicate that measuring the active form of this enzyme might not necessarily be indicative of chemotherapeutic efficacy. Firstly, one group (Adjei *et al.* 1996) provided evidence for the induction of apoptosis in a human hepatocellular carcinoma (HCC) cell line by a topoisomerase I poison

camptothecin (CPT) without the apparent activation of either Caspase 1 or Caspase-3. Apoptosis was assessed using classical morphological observation and the detection of internucleosomal DNA cleavage. Furthermore, etoposide, a topoisomerase II poison, failed to induce apoptosis in these cells.

Many of the reports of caspase-3 activation occur in leukemic and lymphoid cell lines. Concomitantly, many cells of the lymphoid system stained intensely for Caspase-3 in the first immunohistochemical study (Krajewska *et al.* 1997). Furthermore, as already described, another group (Chen *et al.* 1996) observed Caspase-3 activation in an ovarian carcinoma cell line. Again, many of the cells of the ovary stain in a moderate to strong manner with the anti-Caspase-3 antibody. However, hepatocytes also stain intensely in the study by Krajewska and as mentioned earlier Adjei *et al.* (1996) showed that HCC cells do not activate Caspase-3. In this report the authors also confirmed the presence of the Caspase-3 transcript by RT-PCR. Therefore, it would appear in this case that even though the Caspase-3 enzyme was present, the particular apoptotic signalling pathway induced did not involve its activation.

Nevertheless, the situations where Caspase-3 is not activated in apoptotic cell death appear to be exceptional and developing tools which can distinguish between the inactive and the active form of the enzyme should give vital clues to the efficiency of chemotherapy in various cell types. Furthermore, developing monoclonal antibodies against the inactive and active forms of other caspase family members, such as Caspase-1, -2 and -8 would also provide information with respect to the role played by these enzymes in tumorigenesis.

The peptide ELISA developed to measure the immunogenic response (see section 2.2.4.1) was not necessarily an indication of the specificity of the immune response for antibodies reactive to either the newly created N-terminus of the p12 fragment or the p17 fragment of Caspase-3. This depends on the three-dimensional structure of the peptide in solution with the newly created N-terminus of the p12 or p17 fragment. Some effort was also spent on developing an ELISA using lysate from an apoptotic HL60 cell line to measure the polyclonal response (data not shown), however this was unsuccessful. Little effort was invested into developing this protein

ELISA to measure the polyclonal response. This was because it was not planned to use an ELISA system to measure the activation of specific caspases in the future.

The antigenic reactivity of a protein is not the same in the native and denatured forms of the molecule. It is thus important to specify whether the epitopes being studied pertain to native protein or not. This problem has become particularly relevant in recent years because of the popularity of solid - phase immunoassays. When proteins are adsorbed to a layer of plastic in such assays, they tend to undergo some physical distortion or denaturation, and it is questionable whether the epitopes corresponding to the native states are preserved. Furthermore, developing such an ELISA; that is, producing a cell lysate without the use of detergents, which would interfere with both the binding of the lysate to the plate, and the subsequent binding of antibodies, can be an extremely difficult task. Therefore, neither a peptide ELISA or a protein ELISA as an ideal test to measure the specificity of the immune response in relation to an antibody recognising the p12 fragment of Caspase-3.

The patterns of immunostaining illustrated by the majority of the anti-peptide antibodies (see Fig. 2.17A), whereby the germinal centre and epithelial cells stain intensively, was initially reported by Krajewska *et al* (1997). Unfortunately, initial Western blot results with these antibodies indicated that they may also detect other proteins, as a range of bands were detected (data not shown). Krajewska *et al* (1997) also admitted that, although their polyclonal antibodies recognised both the pro-form and the active form (p17 fragment) of Caspase-3 on a Western blot, they could not detect the active form from human tissue samples, but from an *in vitro* enzymatic cleavage of caspase-3 by Granzyme B. Therefore, they could not be certain which form the antibody recognised on a paraffin-embedded tissue slide. Nevertheless this pattern of staining was also confirmed with the commercial antibody used in this study against proCaspase-3, that, by our analysis, only recognised the proform of the enzyme.

The supernatant from one 'pre-monoclonal' antibody did, however, appear to produce a pattern of staining on a tonsil tissue highly specific for apoptotic cells within the germinal centre (see Fig. 2.17). Unfortunately, there was not enough sample to test this supernatant on a Western blot. Furthermore, this 'pre-monoclonal' was not

stabilised after dilution to produce a stable monoclonal antibody. However, the pattern of expression obtained after immunohistochemistry with a commercial anti-p17 polyclonal antibody within the germinal centre was highly similar to that of this supernatant, indicating that it may have been an apoptotic marker of some kind. However, it cannot be discounted that the reactive antibodies produced in this well may have recognised a cleaved fragment of a substrate with similar conformation to the N-terminus of the p12 fragment.

One group (Kikuchi and Imajoh-Ohmi 1995) raised polyclonal antibodies that detected proteolysed protein kinase C β (PKC β) using a synthetic peptide corresponding to the newly created N-terminus. The group found that to obtain a cleavage - site directed antibody, length of the peptides used for immunogens is important. With shorter peptides, antibodies raised did not react though they bound to the peptide used for immunisation. In fact, such antibodies did not bind a longer peptide of the same amino terminus. When longer peptides were used for immunisation, antibodies produced recognised both proteolysed and unproteolysed PKC. These antibodies were at least in part a mixture of two types of antibodies; cleavage - site - directed antibodies that bound to the amino terminus of the proteolysed fragment only and antibodies reacting to both the proteolysed and native PKC β . Although their analysis did not indicate so, it is also likely that their antibodies also contained a species that reacted only with the unproteolysed form. From this study it would appear that the peptide for the p12 fragment (of 10 amino acids) may have been too long as the antibodies generated appeared to recognise both the proteolysed and inactive form. However, the amino acid sequence which gave this group the ideal antibody, which reacted only with the cleaved form, was 11 amino acids long.

The specificity of the immune response may have to do with the structural limitations of the peptide in solution. In general, antibodies induced by a protein cross - react only weakly with peptide fragments derived from it, which testifies to the limited structural resemblance between the peptides and the protein. There is growing evidence that peptides in solution have distinct conformational preferences. Many investigators believe that the majority of protein epitopes are discontinuous and that

short linear peptides possess a low antigenic cross - reactivity with proteins because they mimic, in a conformationally imperfect way, only part of the epitope structure.

Mhashilkar *et al* (1995) never indicated why the C κ domain fused at the C-terminus of ScFvs should produce more stable proteins. Considering the quantity of antibodies with differing affinities the B-cell can produce, it is plausible that a constant area of every immunoglobulin contains sequences which are not targeted for rapid proteolysis. Amino acid sequences which contain domains that are targeted for rapid proteolysis are generally referred to as “PEST” sequences (proline, glutamic acid, serine and threonine). Proteins which need to circulate in any system generally do not contain such sequences, and this allows them to avoid rapid degradation.

The immunopositivity of proCaspase-3 staining in reactive lymph node (see section 3.3.1) is similar to that reported earlier (Krajewska *et al.* 1997; Krajewski *et al.* 1997). That is, a homogenous diffuse cytosolic immunostaining was present in the germinal centre cells of reactive follicles, with lesser staining in the mantle zone and interfollicular regions. With respect to the immunohistochemical localisation of the enzyme, early reports indicated a cytosolic and occasional nuclear staining, but no punctate staining (Krajewska *et al.* 1997). A more recent report (Mancini *et al.* 1998) however proposed that the precursor form of Caspase-3 has both a mitochondrial and a cytosolic distribution. A punctate staining associated with mitochondrial localisation of proCaspase-3 was described in this report. Furthermore, the immature form of the enzyme has been detected in the cytosol and the mitochondria of various tissues using protein fractionation (Samali *et al.* 1998). Therefore, the punctate staining described in this report may be associated with the mitochondrial localisation of proCaspase-3.

The variation on protein expression of Caspase-3 in DLCL again appears to confirm earlier reports (Krajewski *et al.* 1997). However, the better patient prognosis associated with the greater the percentage of tumour cells expressing proCaspase-3 has not been observed in DLCL before (see section 3.3.1.5). Overexpression of caspase-1 and -3 has in the past been associated with an increased sensitivity to therapy and a recent report indicated that those childhood neuroblastomas that can spontaneously regress also had high levels of Caspase-1 and Caspase-3 (Nakagawara *et al.* 1997).

Other researchers have implicated low levels of Caspase-3 in resistance to chemotherapy and radiotherapy-induced apoptosis in cell lines (Eichholtz-Wirth *et al.* 1997).

There was a lack of any staining for either the proform of Caspase-3 or the p17 fragment of Caspase-3 in two cases. These cases also lacked any DNA fragmentation as detected by the TUNEL assay. This would appear to confirm the earlier report of Caspase-3 being essential for the nuclear changes associated with apoptosis in mouse embryonic stem cells and fibroblasts (Woo *et al.* 1998).

The exact localisation of the active and inactive enzyme in a cell, and its importance with respect to the apoptotic process, is still uncertain as indicated above. Many of the early substrates discovered for Caspase-3 were associated with the nucleus and hence it was initially assumed that this protease translocated into the nucleus at some stage during the apoptotic process. This view was also reinforced by some researchers describing occasional nuclear staining (Krajewski *et al.* 1997; Nakagawara *et al.* 1997). For example, the translocation of Caspase-1 and -3 to the nucleus has been associated with neuroblastomas susceptible to regression (Nakagawara *et al.* 1997). Recent evidence, however, indicates that Caspase-3 is capable of activating a cytosolic protein that translocates into the nucleus and degrades chromatin DNA during apoptosis (Liu *et al.* 1997; Enari *et al.* 1998). One report also suggested that this nuclear staining co-localised with TUNEL staining and apoptotic cells (Nakagawara *et al.* 1997). The issue is controversial as an earlier report suggested most cells positive for Caspase-3 were not TUNEL positive (Krajewska *et al.* 1997). Certainly our results also indicate that in the germinal centre TUNEL-positive cells are not Caspase-3 immunopositive.

The pattern of expression of exhibited in reactive lymph nodes – a diffuse cytosolic staining for proCaspase-3 associated with a high degree of TUNEL staining – indicated a poor prognosis when observed in DLCL cases There are a number of reasons why this may occur. It has been suggested that the separate forms of proCaspase-3 - cytosolic and mitochondrial - indicated the existence of distinct activation pathways (Mancini *et al.* 1998). The diffuse cytosolic staining exhibited in the germinal centres of secondary follicles may indicate a sensitisation to a particular

form of receptor-mediated cell death. Whereas tumour cells expressing a punctate immunohistochemical localisation may be sensitised to a different form of cell death - such as chemotherapy or radiotherapy.

Were this the case, the role of the B cell receptor (BCR) and BCR-mediated apoptosis would be critical. The exact nature of BCR-mediated apoptosis is unknown and is believed to involve a new type of pathway. A very recent study (Bouchon *et al.* 2000) indicates a critical role for the mitochondria in BCR-mediated apoptosis. It is not mediated via known death receptors, nor does it involve initial activation of Caspase-8. Instead, it appears to be initiated by the caspase-independent induction of mitochondrial PT resulting in release of cytochrome c and subsequent activation of Caspase-9. Another group indicated that BCR-mediated apoptosis involves a calcineurin-mediated step, with the sequential activation of Caspase-2, -3 and -9. In this situation Caspase-9 was believed to function in amplifying the cell death signal (Chen *et al.* 1999). Conversely, one group found that in the WEHI-321 B lymphoma cell line Caspase-7 was activated, but not Caspase-2 or -3 (Bras *et al.* 1999). Finally, another group showed in the same cell line that calpain specifically triggers the processing of Caspase-7. Without question, the mechanisms involved are complex and seem to involve direct interaction with the mitochondria, however the role of Caspase-3 in this process is still obscured.

In addition, the higher apoptotic rate detected by DNA fragmentation in the DLCL cases probably indicates a higher proliferative rate. Gisbertz *et al.* (1997) recently reported a correlation between high proliferation and high apoptotic rates in DLCL. This correlation was not seen in low grade lymphomas. Other reporters have also shown a correlation between apoptotic and proliferative indices in malignant NHLs (Leoncini *et al.* 1993).

Early descriptions of the death programme divided it into three phases. The 'initiation' phase, during which a cell can receive a variety of signals that may result in the activation of the death programme. The 'commitment' phase, the point after which death signals become irreversible. The 'demolition' phase, during which the cell becomes dismantled and processed for phagocytosis. Recently, a new phase - the

'amplification' phase has been proposed. In this phase, post commitment to die, multiple caspases are recruited to co-operate in the destruction of the cell.

As one would expect, both the commitment and amplification phases involve, at some stage, the mitochondria. Numerous pro-apoptotic stimuli provoke changes in the permeability of the mitochondrial outer membrane that permits escape of certain proteins – such as AIF and cytochrome c – that are normally confined to the mitochondrial intermembrane space. Indeed, changes in mitochondrial outer membrane are probably also responsible for the release of proCaspases –2, -3 and –9 from the mitochondrial intermembrane space (Samali *et al.* 1999; Susin *et al.* 1999). The exact role of these caspases localised in the mitochondria is still unclear. Indeed, how these proteins escape is also the subject of much debate.

AIF appears to exert its effects in a caspase-independent manner by translocating to the nucleus and triggering the chromatin change (Susin *et al.* 1999) and digestion into high molecular weight fragments that is commonly observed during apoptosis. Of course, cytochrome c exerts its effects by regulating the activities of Apaf-1, a molecule that promotes Caspase-9 activation via a proximity-induced mechanism (Saleh *et al.* 1999). The caspase activation events driven by Caspase-9 appear to be the simultaneous activation of Caspases –3 and –7. Caspase-3 then promotes the activation of Caspases-2 and –6, followed by the activation of Caspases-2 and –6, followed by the activation of Caspases-8 and –10 (Slee *et al.* 1999). In the absence of Caspase-3, Caspase-7 and –9 are still activated but activation of other caspases downstream of this point is arrested. Removal of Caspase-6 blocked the activation of Caspase-8 and –10 in this situation, suggesting that these activation events are driven by Caspase-6 (Slee *et al.* 1999). Therefore, caspases that act as apical (initiator) caspases in receptor-mediated death appear to participate in an amplification role in other contexts.

In addition, the general system of grouping caspases into either upstream/initiator enzymes or downstream/effector enzymes, based primarily on their prodomain size, would appear to be flawed. With respect to receptor-mediated cell death it may be useful, but as a method of analysing chemical/damage-induced apoptotic cell death it not appropriate. The instances of the activation of supposed

upstream caspases by supposed downstream caspases have been further supported by the caspase knockout experiments. Thymocytes from Apaf-1 and Caspase-9 *-/-* mice treated with dexamethasone do not process Caspase-8 or Caspase-2 (Kuida *et al.* 1998; Yoshida *et al.* 1998).

It is important again to point out that not all of the caspases that are activated during the apoptotic process may be necessary for the cell to die. However, they are probably likely to be required for a dying cell to adopt the typical apoptotic phenotype. All cell types examined from Caspase-3 *-/-* mice fail to display some typical hallmarks of apoptosis, such as DNA fragmentation and chromatin condensation, after treatment with various death insults (Kuida *et al.* 1996). The human MCF-7 breast carcinoma cell line does not have a functional Caspase-3 protein due to a genomic mutation, introducing a premature stop codon in the mRNA (Janicke *et al.* 1998). Many inducers of apoptosis are known to kill MCF-7 cells without many of the characteristic morphological changes and in the complete absence of DNA strand breakage (Oberhammer *et al.* 1993). However, re-introduction of the Caspase-3 cDNA restores the phenomena of membrane blebbing and DNA fragmentation in MCF-7 cells undergoing apoptosis (Janicke *et al.* 1998).

All these results indicate that in multiple cell types, Caspase-3 is required for some typical nuclear and other morphological changes associated with the completion of apoptosis and the formation of apoptotic bodies. And, as outlined earlier, when all caspase activity is blocked using a broad spectrum inhibitor, cells that progress beyond the mitochondrial commitment point normally exhibit features of necrosis rather than apoptosis (Xiang *et al.* 1996).

Most importantly, one group has shown that the mitochondrial pool of proCaspase-3 in Jurkat T cells is present in a complex with the chaperone proteins Hsp 60 and Hsp 10 (Samali *et al.* 1999). Treatment with staurosporine led to the activation of mitochondrial proCaspase-3 and its disassociation from the heat-shock proteins (Hsps) which were released from the mitochondrial intermembrane space along with cytochrome c. This occurred prior to a loss of mitochondrial transmembrane potential ($\Delta\Psi_M$). Once Caspase-3 is activated, downstream death substrates are cleaved,

irrespective of the releases of cytochrome c from mitochondria. However, Caspase-3 probably also re-amplifies the death cascade through its interaction with the mitochondria. Active Caspase-3 cleaves Bcl-2, converting it from an anti-apoptotic protein to a pro-apoptotic protein. Active Caspase-3 is also believed to bring about the release of cytochrome c and interact with the constituents of the PT pore (Marzo *et al.* 1998). Therefore, Caspase-3 acts as both an initiator of cytochrome c release, and hence a key protein in the 'commitment' phase, and as a key protein in the interaction with mitochondria to amplify the signal.

Overexpression of a GFP-p17 fusion protein in MCF-7 cells appeared to produce a scattered, punctate pattern of expression that probably indicated a localisation to mitochondria. It is likely that it is the p17 fragment of Caspase-3 that either brings about the release of cytochrome c, or interacts with the constituents of the PT pore to bring about $\Delta\psi_M$. Therefore, this localisation of a p17 fragment from an activated Caspase-3 may constitute the 'amplification' step. The immunohistochemical results for the DLCL cases (see section 3.3.1.6) are intriguing as there appears to be staining in whole cells with some specimens. This is in direct contrast to the results obtained within the germinal centre of a reactive node where only dying cells appear immunopositive.

In the MCF-7 cell line this interaction of the p17 fragment with the mitochondria would not, however, result in the appearance of apoptotic cell death. This is due to the lack of a functional Caspase-3 enzyme in this cell line, and the crucial nature of this enzyme in the morphological appearance of apoptosis has been described. This may explain the necrotic appearance of the MCF-7 cells transfected with the clone expressing a GFP-p17 fusion protein. This phenomenon may be rather similar to that of the overexpression of Bax in cells treated with z-VAD.fmk – a general caspase inhibitor (Xiang *et al.* 1996). These cells also display a necrotic appearance due to the inhibition of caspases, despite the release of cytochrome c. Indeed, the continued release of cytochrome c and concomitant $\Delta\psi_M$ is probably responsible for the necrotic appearance of the cells. Hence, in cells without a functional caspases, the 'amplification' step result in a necrotic appearance.

Interestingly, the anti-GFP polyclonal antibody recognised the GFP-C κ fusion protein, however the GFP-p17 protein was not recognised. This indicates that this antibody recognises the C-terminus of GFP, and that the p17 fragment has a conformation that interferes with the recognition of this terminus. This implies a complex conformation becoming unmasked after cleavage to a p17 fragment.

The identity of the higher protein recognised by the anti-active Caspase-3 antibody in cells transfected with pEGFP-C1-p17 is unknown. Given the degree of heterogeneity between the caspases and their active fragments, it may be possible that a catalytic heterodimer consisting of a p12 subunit from Caspase-7, and a p17 subunit from Caspase-3 may form. That is, the active fragments of the homologues may be interchangeable. Indeed, it has been shown that a recombinant Caspase-3 p17 subunit can form an active heterodimeric enzyme complex with recombinant Caspase-7 p12 subunit and vice versa (Fernandes-Alnemri *et al.* 1995). In addition, the same group illustrated that co-expression of Caspase-3 and Caspase-1 subunits does not induce apoptosis. This compatibility, therefore, may be restricted to group families. However, the pre-treatment of the lysates before Western blotting makes this somewhat unlikely.

Some important issues with respect to the subcellular localisation of the proforms and the active fragments of the enzyme remain. Primarily, how does a cell produce the same protein with different localisation within a cell; for example, proCaspase-3 exists in both the mitochondria and the cytoplasm. Indeed, many members of the Bcl-2 family also display a differential localisation within a cell. Elucidating the mechanism of how this phenomenon is regulated would have extremely important benefits, as it appears that this differential localisation is cell-type specific. Furthermore, how is the localisation of the activated fragments regulated? Presumably, after cleavage a signal or leader peptide is revealed that directs the cell to its destination. And, of course, very little is known about the mechanism of regulating the levels of these enzymes.

Indeed, extremely little is known about how the levels of both caspase and Bcl-2 family members are transcriptionally regulated. It is becoming increasingly obvious that malignant cells may become resistant to apoptosis, but they do not lose the

capacity to undergo apoptosis. Therefore, they reset the threshold. This threshold involves the regulation of the levels and the intracellular localisation of members of the caspase and the Bcl-2 family. Elucidating the mechanisms behind tumorigenesis and effective chemotherapy in diseases such as high grade NHL is surely dependent on determining the factors responsible for these thresholds.

Nevertheless, in this study it has been shown that the levels and localisation of proCaspase-3 are relevant to the treatment of patients with B-cell DLCL (Donoghue *et al.* 1999). The surprising poor prognosis observed in patients presenting with a high apoptotic rate as measured by TUNEL only further confirms the complexity of apoptosis. Indeed, this complexity is confirmed with the results observed with the GFP-p17 fragment, and hints that there is even much more diversity to Caspase-3 than previously thought. It also emphasises the need for more specific markers for the activation of specific caspases, in order to try to determine what type of cell death is occurring. Undoubtedly, the development of such tools would produce major benefits in the understanding of the pathogenesis of a range of diseases, and would result in more successful treatments of these diseases.

REFERENCES

- Adjei, P.N., Kaufmann, S.H., Leung, W.Y., Mao, F. and Gores, G.J. Selective induction of apoptosis in Hep 3B cells by topoisomerase I inhibitors: evidence for a protease-dependent pathway that does not activate cysteine protease P32. *Journal of Clinical Investigation* 98(11): 2588-96, 1996.
- Ahmad, M., Srinivasula, S. M., Hegde, R., Mukattash, R., Fernandes-Alnemri, T. and Alnemri, E. S. Identification and characterization of murine caspase-14, a new member of the caspase family. *Cancer Research* 58(22): 5201-5, 1998.
- Alison, M. R. Identifying and quantifying apoptosis: a growth industry in the face of death [editorial]. *J Pathol* 188(2): 117-8, 1999.
- Alnemri, E. S., Fernandes, T. F., Haldar, S., Croce, C. M. and Litwack, G. Involvement of BCL-2 in glucocorticoid-induced apoptosis of human pre-B- leukemias. *Cancer Research* 52(2): 491-5, 1992.
- Alnemri, E. S., Fernandes-Alnemri, T. and Litwack, G. Cloning and expression of four novel isoforms of human interleukin-1 beta converting enzyme with different apoptotic activities. *Journal of Biological Chemistry* 270(9): 4312-7, 1995.
- Alnemri, E. S., Livingston, D. J., Nicholson, D. W., Salvesen, G., Thornberry, N. A., Wong, W. W. and Yuan, J. Human ICE/CED-3 protease nomenclature [letter]. *Cell* 87(2): 171, 1996.
- Ambrosini, G., Adida, C. and Altieri, D. C. A novel anti-apoptosis gene, survivin, expressed in cancer and lymphoma. *Nature Medicine* 3(8): 917-21, 1997.
- Ashkenazi, A. and Dixit, V. M. Death receptors: signaling and modulation. *Science* 281(5381): 1305-8, 1998.
- Basu, A. and Haldar, S. Microtubule-damaging drugs triggered bcl2 phosphorylation-requirement of phosphorylation on both serine-70 and serine-87 residues of bcl2 protein. *International Journal of Oncology* 13(4): 659-64, 1998.
- Beerli, R.R., Wels, W. and Hynes, N.E. Inhibition of signaling from Type I receptor tyrosine kinases via intracellular expression of single-chain antibodies. *Breast Cancer Research and Treatment* 38(1): 7-11, 1996

Benson, R. S. P., Dive, C. and Watson, A. J. M. Comparative effects of Bcl-2 overexpression and ZVAD.FMK treatment on dexamethasone and VP-16-induced apoptosis in CEM cells. *Cell. Death and Differentiation*. 5: 432-439, 1998.

Bergeron, L., Perez, G. I., Macdonald, G., Shi, L., Sun, Y., Jurisicova, A., Varmuza, S., Latham, K. E., Flaws, J. A., Salter, J. C., Hara, H., Moskowitz, M. A., Li, E., Greenberg, A., Tilly, J. L. and Yuan, J. Defects in regulation of apoptosis in caspase-2-deficient mice. *Genes and Development* 12(9): 1304-14, 1998.

Berridge, M. J., Bootman, M. D. and Lipp, P. Calcium--a life and death signal [news]. *Nature* 395(6703): 645-8, 1998.

Bertin, J., Nir, W. J., Fischer, C. M., Tayber, O. V., Errada, P. R., Grant, J. R., Keilty, J. J., Gosselin, M. L., Robison, K. E., Wong, G. H., Glucksmann, M. A. and DiStefano, P. S. Human CARD4 protein is a novel CED-4/Apaf-1 cell death family member that activates NF-kappaB. *Journal of Biological Chemistry* 274(19): 12955-8, 1999.

Bettinardi, A., Brugnoli, D., Quiros-Roldan, E., Malagoli, A., La Grutta, S., Correr, A. and Notarangelo, L. D. Missense mutations in the Fas gene resulting in autoimmune lymphoproliferative syndrome: a molecular and immunological analysis. *Blood* 89(3): 902-9, 1997.

Bird, C. H., Sutton, V. R., Sun, J., Hirst, C. E., Novak, A., Kumar, S., Trapani, J. A. and Bird, P. I. Selective regulation of apoptosis: the cytotoxic lymphocyte serpin proteinase inhibitor 9 protects against granzyme B-mediated apoptosis without perturbing the Fas cell death pathway. *Molecular and Cellular Biology* 18(11): 6387-98, 1998.

Boise, L. H., Gonzalez-Garcia, M., Postema, C. E., Ding, L., Lindsten, T., Turka, L. A., Mao, X., Nunez, G. and Thompson, C. B. bcl-x, a bcl-2-related gene that functions as a dominant regulator of apoptotic cell death. *Cell* 74(4): 597-608, 1993.

Boise, L. H. and Thompson, C. B. Hierarchical control of lymphocyte survival. *Science* 274(5284): 67-8, 1996.

Borner, C., Martinou, I., Mattmann, C., Imler, M., Schaefer, E., Martinou, J. C. and Tschopp, J. The protein bcl-2 alpha does not require membrane attachment, but two conserved domains to suppress apoptosis. *Journal of Cell Biology* 126(4): 1059-68, 1994.

Borner, C. and Monney, L. Apoptosis without caspases: an inefficient molecular guillotine? *Cell Death and Differentiation* 6(6): 497-507, 1999.

Borner, C., Monney, L., Olivier, R., Rosse, T., Hacki, J. and Conus, S. Life and death in a medieval atmosphere. *Cell Death and Differentiation* 6(2): 201-6, 1999.

Bortner, C. D., Oldenburg, N. B. E. and Cidlowski, J. A. The role of DNA fragmentation in apoptosis. *Trends in Cell Biology* 5: 21-26, 1995.

Bouchon, A., Krammer, P. H. and Walczak, H. Critical role for mitochondria in B cell receptor-mediated apoptosis. *Eur J Immunol* 30(1): 69-77, 2000.

Brancolini, C., Lazarevic, D., Rodriguez, J. and Schneider, C. Dismantling cell-cell contacts during apoptosis is coupled to a caspase-dependent proteolytic cleavage of beta-catenin. *Journal of Cell Biology* 139(3): 759-71, 1997.

Bras, A., Ruiz-Vela, A., Gonzalez de Buitrago, G. and Martinez, A. C. Caspase activation by BCR cross-linking in immature B cells: differential effects on growth arrest and apoptosis. *Faseb J* 13(8): 931-44, 1999.

Brunet, C. L., Gunby, R. H., Benson, R. S., Hickman, J. A., Watson, A. J. and Brady, G. Commitment to cell death measured by loss of clonogenicity is separable from the appearance of apoptotic markers. *Cell Death and Differentiation* 5(1): 107-15, 1998.

Brustugun, O. T., Fladmark, K. E., Doskeland, S. O., Orrenius, S. and Zhivotovsky, B. Apoptosis induced by microinjection of cytochrome c is caspase-dependent and is inhibited by Bcl-2 [published erratum appears in *Cell Death Differ* 1999 Mar;6(3):301]. *Cell Death and Differentiation* 5(8): 660-8, 1998.

Campbell, C., Sawka, C., Franssen, E. and Berinstein, N. L. Delivery of full dose CHOP chemotherapy to elderly patients with aggressive non-Hodgkin's lymphoma without G-CSF support. *Leukaemia and Lymphoma* 35(1-2): 119-27, 1999.

Cardone, M. H., Roy, N., Stennicke, H. R., Salvesen, G. S., Franke, T. F., Stanbridge, E., Frisch, S. and Reed, J. C. Regulation of cell death protease caspase-9 by phosphorylation. *Science* 282(5392): 1318-21, 1998.

Cecconi, F. Apaf1 and the apoptotic machinery [In Process Citation]. *Cell Death and Differentiation* 6(11): 1087-98, 1999.

Cecconi, F., Alvarez-Bolado, G., Meyer, B. I., Roth, K. A. and Gruss, P. Apaf1 (CED-4 homolog) regulates programmed cell death in mammalian development. *Cell* 94(6): 727-37, 1998.

Chandler, J. M., Cohen, G. M. and MacFarlane, M. Different subcellular distribution of caspase-3 and caspase-7 following Fas-induced apoptosis in mouse liver. *Journal of Biological Chemistry* 273(18): 10815-8, 1998.

Chen, Z., Naito, M., Mashima, T. and Tsuruo, T. Activation of actin-cleavable interleukin 1beta-converting enzyme (ICE) family protease CPP-32 during chemotherapeutic agent-induced apoptosis in ovarian carcinoma cells. *Cancer Research* 56(22): 5224-9, 1996.

Chen, W., Wang, H. G., Srinivasula, S. M., Alnemri, E. S. and Cooper, N. R. B cell apoptosis triggered by antigen receptor ligation proceeds via a novel caspase-dependent pathway. *J Immunol* 163(5): 2483-91, 1999.

Cheng, E. H., Kirsch, D. G., Clem, R. J., Ravi, R., Kastan, M. B., Bedi, A., Ueno, K. and Hardwick, J. M. Conversion of Bcl-2 to a Bax-like death effector by caspases. *Science* 278(5345): 1966-8, 1997.

Chhanabhai, M., Krajewski, S., Krajewska, M., Wang, H. G., Reed, J. C. and Gascoyne, R. D. Immunohistochemical analysis of interleukin-1beta-converting enzyme/Ced-3 family protease, CPP32/Yama/Caspase-3, in Hodgkin's disease. *Blood* 90(6): 2451-5, 1997.

Chi, S., Kitanaka, C., Noguchi, K., Mochizuki, T., Nagashima, Y., Shirouzu, M., Fujita, H., Yoshida, M., Chen, W., Asai, A., Himeno, M., Yokoyama, S. and Kuchino, Y. Oncogenic Ras triggers cell suicide through the activation of a caspase-independent cell death program in human cancer cells. *Oncogene* 18(13): 2281-90, 1999.

Chinnaiyan, A. M., O'Rourke, K., Lane, B. R. and Dixit, V. M. Interaction of CED-4 with CED-3 and CED-9: a molecular framework for cell death [see comments]. *Science* 275(5303): 1122-6, 1997.

Chinnaiyan, A. M., O'Rourke, K., Tewari, M. and Dixit, V. M. FADD, a novel death domain-containing protein, interacts with the death domain of Fas and initiates apoptosis. *Cell* 81(4): 505-12, 1995.

Chinnaiyan, A. M., O'Rourke, K., Yu, G. L., Lyons, R. H., Garg, M., Duan, D. R., Xing, L., Gentz, R., Ni, J. and Dixit, V. M. Signal transduction by DR3, a death domain-containing receptor related to TNFR-1 and CD95. *Science* 274(5289): 990-2, 1996.

Chinnaiyan, A. M., Tepper, C. G., Seldin, M. F., O'Rourke, K., Kischkel, F. C., Hellbardt, S., Krammer, P. H., Peter, M. E. and Dixit, V. M. FADD/MORT1 is a common mediator of CD95 (Fas/APO-1) and tumor necrosis factor receptor-induced apoptosis. *Journal of Biological Chemistry* 271(9): 4961-5, 1996.

Clarke, P. G. H. Developmental cell death: morphological diversity and multiple mechanisms. *Anat. Embryol.* 181: 195-213, 1990.

Clem, R. J., Cheng, E. H., Karp, C. L., Kirsch, D. G., Ueno, K., Takahashi, A., Kastan, M. B., Griffin, D. E., Earnshaw, W. C., Veluona, M. A. and Hardwick, J. M. Modulation of cell death by Bcl-XL through caspase interaction. *Proceedings of the National Academy of Sciences of the United States of America* 95(2): 554-9, 1998.

Clem, R. J., Fechheimer, M. and Miller, L. K. Prevention of apoptosis by a baculovirus gene during infection of insect cells. *Science* 254(5036): 1388-90, 1991.

Cole, S. P., Bhardwaj, G., Gerlach, J. H., Mackie, J. E., Grant, C. E., Almquist, K. C., Stewart, A. J., Kurz, E. U., Duncan, A. M. and Deeley, R. G. Overexpression of a transporter gene in a multidrug-resistant human lung cancer cell line [see comments]. *Science* 258(5088): 1650-4, 1992.

Cohen, G. M. Caspases: the executioners of apoptosis. *Biochemical Journal* 326(Pt 1): 1-16, 1997.

Colussi, P. A., Harvey, N. L. and Kumar, S. Prodomain-dependent nuclear localization of the caspase-2 (Nedd2) precursor. A novel function for a caspase prodomain. *Journal of Biological Chemistry* 273(38): 24535-42, 1998.

Crook, N. E., Clem, R. J. and Miller, L. K. An apoptosis-inhibiting baculovirus gene with a zinc finger-like motif. *Journal of Virology* 67(4): 2168-74, 1993.

Crouch, D. H., Fincham, V. J. and Frame, M. C. Targeted proteolysis of the focal adhesion kinase pp125 FAK during c- MYC-induced apoptosis is suppressed by integrin signalling. *Oncogene* 12(12): 2689-96, 1996.

Cryns, V. L., Bergeron, L., Zhu, H., Li, H. and Yuan, J. Specific cleavage of alpha-fodrin during Fas- and tumor necrosis factor-induced apoptosis is mediated by an interleukin-1beta-converting enzyme/Ced-3 protease distinct from the poly(ADP-ribose) polymerase protease. *Journal of Biological Chemistry* 271(49): 31277-82, 1996.

Datta, R., Banach, D., Kojima, H., Talanian, R. V., Alnemri, E. S., Wong, W. W. and Kufe, D. W. Activation of the CPP32 protease in apoptosis induced by 1-beta-D-arabinofuranosylcytosine and other DNA-damaging agents. *Blood* 88(6): 1936-43, 1996.

Davidson, W. F., Giese, T. and Fredrickson, T. N. Spontaneous development of plasmacytoid tumors in mice with defective Fas-Fas ligand interactions. *Journal of Experimental Medicine* 187(11): 1825-38, 1998.

de Jong, D., Prins, F. A., Mason, D. Y., Reed, J. C., van Ommen, G. B. and Kluin, P. M. Subcellular localization of the bcl-2 protein in malignant and normal lymphoid cells. *Cancer Research* 54(1): 256-60, 1994.

De Maria, R., Lenti, L., Malisan, F., d'Agostino, F., Tomassini, B., Zeuner, A., Rippo, M. R. and Testi, R. Requirement for GD3 ganglioside in CD95- and ceramide-induced apoptosis [published erratum appears in Science 1998 Apr 17;280(5362):363]. *Science* 277(5332): 1652-5, 1997.

Deas, O., Dumont, C., MacFarlane, M., Rouleau, M., Hebib, C., Harper, F., Hirsch, F., Charpentier, B., Cohen, G. M. and Senik, A. Caspase-independent cell death induced by anti-CD2 or staurosporine in activated human peripheral T lymphocytes. *Journal of Immunology* 161(7): 3375-83, 1998.

Deshane, J., Grim, J., Loechel, S., Siegal, G. P., Alvarez, R. D. and Curiel, D. T. Intracellular antibody against erbB-2 mediates targeted tumor cell eradication by apoptosis. *Cancer Gene Therapy* 3(2): 89-98, 1996.

Deveraux, Q. L., Takahashi, R., Salvesen, G. S. and Reed, J. C. X-linked IAP is a direct inhibitor of cell-death proteases. *Nature* 388(6639): 300-4, 1997.

Dianzani, U., Bragardo, M., DiFranco, D., Alliaudi, C., Scagni, P., Buonfiglio, D., Redoglia, V., Bonissoni, S., Correr, A., Dianzani, I. and Ramenghi, U. Deficiency of the Fas apoptosis pathway without Fas gene mutations in pediatric patients with autoimmunity/lymphoproliferation. *Blood* 89(8): 2871-9, 1997.

Dierlamm, J., Baens, M., Wlodarska, I., Stefanova-Ouzounova, M., Hernandez, J. M., Hossfeld, D. K., De Wolf-Peeters, C., Hagemeijer, A., Van den Berghe, H. and Marynen, P. The apoptosis inhibitor gene API2 and a novel 18q gene, MLT, are recurrently rearranged in the t(11;18)(q21;q21)p6 associated with mucosa-associated lymphoid tissue lymphomas [see comments]. *Blood* 93(11): 3601-9, 1999.

Djerbi, M., Screpanti, V., Catrina, A. I., Bogen, B., Biberfeld, P. and Grandien, A. The inhibitor of death receptor signaling, FLICE-inhibitory protein defines a new class of tumor progression factors [see comments]. *Journal of Experimental Medicine* 190(7): 1025-32, 1999.

Dole, M. G., Jasty, R., Cooper, M. J., Thompson, C. B., Nunez, G. and Castle, V. P. Bcl-xL is expressed in neuroblastoma cells and modulates chemotherapy- induced apoptosis. *Cancer Research* 55(12): 2576-82, 1995.

Donoghue, S., Baden, H. S., Lauder, I., Sobolewski, S. and Pringle, J. H. Immunohistochemical localization of caspase-3 correlates with clinical outcome in B-cell diffuse large-cell lymphoma. *Cancer Research* 59(20): 5386-91, 1999.

Drappa, J., Vaishnav, A. K., Sullivan, K. E., Chu, J. L. and Elkon, K. B. Fas gene mutations in the Canale-Smith syndrome, an inherited lymphoproliferative disorder associated with autoimmunity [see comments]. *New England Journal of Medicine* 335(22): 1643-9, 1996.

Eichholtz-Wirth, H., Stoetzer, O. and Marx, K. Reduced expression of the ICE-related protease CPP32 is associated with radiation-induced cisplatin resistance in HeLa cells. *British Journal of Cancer* 76(10): 1322-7, 1997.

Ellis, H. M., Yuan, J. Y. and Horvitz, H. R. Mechanisms and functions of cell death. *Annual Review of Cell Biology* 7: 663-698, 1991.

Enari, M., Sakahira, H., Yokoyama, H., Okawa, K., Iwamatsu, A. and Nagata, S. A caspase-activated DNase that degrades DNA during apoptosis, and its inhibitor ICAD [see comments] [published erratum appears in Nature 1998 May 28;393(6683):396]. *Nature* 391(6662): 43-50, 1998.

Erhardt, P., Tomaselli, K. J. and Cooper, G. M. Identification of the MDM2 oncoprotein as a substrate for CPP32-like apoptotic proteases. *Journal of Biological Chemistry* 272(24): 15049-52, 1997.

Faucheu, C., Blanchet, A. M., Collard-Dutilleul, V., Lalanne, J. L. and Diu-Hercend, A. Identification of a cysteine protease closely related to interleukin-1 beta-converting enzyme. *European Journal of Biochemistry* 236(1): 207-13, 1996.

Fernandes-Alnemri, T., Armstrong, R. C., Krebs, J., Srinivasula, S. M., Wang, L., Bullrich, F., Fritz, L. C., Trapani, J. A., Tomaselli, K. J., Litwack, G. and Alnemri, E. S.

In vitro activation of CPP32 and Mch3 by Mch4, a novel human apoptotic cysteine protease containing two FADD-like domains. *Proceedings of the National Academy of Sciences of the United States of America* 93(15): 7464-9, 1996.

Fernandes-Alnemri, T., Takahashi, A., Armstrong, R., Krebs, J., Fritz, L., Tomaselli, K. J., Wang, L., Yu, Z., Croce, C. M., Salveson, G. and et al. Mch3, a novel human apoptotic cysteine protease highly related to CPP32. *Cancer Res* 55(24): 6045-52, 1995.

French, L. E. and Tschopp, J. The TRAIL to selective tumor death [news; comment]. *Nature Medicine* 5(2): 146-7, 1999.

Friesen, C., Fulda, S. and Debatin, K. M. Deficient activation of the CD95 (APO-1/Fas) system in drug-resistant cells. *Leukemia* 11(11): 1833-41, 1997.

Fuchs, E. J., McKenna, K. A. and Bedi, A. p53-dependent DNA damage-induced apoptosis requires Fas/APO-1-independent activation of CPP32beta. *Cancer Research* 57(13): 2550-4, 1997.

Gabriele, L., Phung, J., Fukumoto, J., Segal, D., Wang, I. M., Giannakakou, P., Giese, N. A., Ozato, K. and Morse, H. C., 3rd Regulation of apoptosis in myeloid cells by interferon consensus sequence-binding protein. *J Exp Med* 190(3): 411-22, 1999.

Galle, P. R., Hofmann, W. J., Walczak, H., Schaller, H., Otto, G., Stremmel, W., Krammer, P. H. and Runkel, L. Involvement of the CD95 (APO-1/Fas) receptor and ligand in liver damage. *Journal of Experimental Medicine* 182(5): 1223-30, 1995.

Garcia-Calvo, M., Peterson, E. P., Rasper, D. M., Vaillancourt, J. P., Zamboni, R., Nicholson, D. W. and Thornberry, N. A. Purification and catalytic properties of human caspase family members. *Cell Death and Differentiation* 6(4): 362-9, 1999.

Giatromanolaki, A., Stathopoulos, G. P., Tsiobanou, E., Papadimitriou, C., Georgoulas, V., Gatter, K. C., Harris, A. L. and Koukourakis, M. I. Combined role of tumor angiogenesis, bcl-2, and p53 expression in the prognosis of patients with colorectal carcinoma. *Cancer* 86(8): 1421-30, 1999.

Gisbertz, I., Schouten, H., Bot, F. and Arends, J. Proliferation and apoptosis in primary gastric B-cell non-Hodgkin's lymphoma. *Histopathology* 30(2): 152-159, 1997.

Glaser, T., Wagenknecht, B., Groscurth, P., Krammer, P. H. and Weller, M. Death ligand/receptor-independent caspase activation mediates drug-induced cytotoxic cell death in human malignant glioma cells. *Oncogene* 18(36): 5044-53, 1999.

Grandgirard, D., Studer, E., Monney, L., Belser, T., Fellay, I., Borner, C. and Michel, M. R. Alphaviruses induce apoptosis in Bcl-2-overexpressing cells: evidence for a caspase-mediated, proteolytic inactivation of Bcl-2. *Embo Journal* 17(5): 1268-78, 1998.

Grasl-Kraupp, B., Ruttkay-Nedecky, B., Koudelka, H., Bukowska, K., Bursch, W. and Schulte-Hermann, R. In situ detection of fragmented DNA (TUNEL assay) fails to discriminate among apoptosis, necrosis, and autolytic cell death: a cautionary note. *Hepatology* 21(5): 1465-8, 1995.

Gronbaek, K., Straten, P. T., Ralfkiaer, E., Ahrenkiel, V., Andersen, M. K., Hansen, N. E., Zeuthen, J., Hou-Jensen, K. and Guldborg, P. Somatic Fas mutations in non-Hodgkin's lymphoma: association with extranodal disease and autoimmunity. *Blood* 92(9): 3018-24, 1998.

Gutierrez, M. I., Cherney, B., Hussain, A., Mostowski, H., Tosato, G., Magrath, I. and Bhatia, K. Bax is frequently compromised in Burkitt's Lymphomas with irreversible resistance to Fas-induced apoptosis. *Cancer Research* 59: 696-703, 1999.

Hahne, M., Renno, T., Schroeter, M., Irmeler, M., French, L., Bornard, T., MacDonald, H. R. and Tschopp, J. Activated B cells express functional Fas ligand. *European Journal of Immunology* 26(3): 721-4, 1996.

Hakem, R., Hakem, A., Duncan, G. S., Henderson, J. T., Woo, M., Soengas, M. S., Elia, A., de la Pompa, J. L., Kagi, D., Khoo, W., Potter, J., Yoshida, R., Kaufman, S. A., Lowe, S. W., Penninger, J. M. and Mak, T. W. Differential requirement for caspase 9 in apoptotic pathways in vivo. *Cell* 94(3): 339-52, 1998.

Haldar, S., Jena, N. and Croce, C. M. Inactivation of Bcl-2 by phosphorylation. *Proceedings of the National Academy of Science U S A* 92(10): 4507-11, 1995.

Hannun, Y. A. Apoptosis and the dilemma of cancer chemotherapy. *Blood* 89(6): 1845-53, 1997.

Hara, H., Fink, K., Endres, M., Friedlander, R. M., Gagliardini, V., Yuan, J. and Moskowitz, M. A. Attenuation of transient focal cerebral ischemic injury in transgenic mice expressing a mutant ICE inhibitory protein. *Journal of Cerebral Blood Flow and Metabolism* 17(4): 370-5, 1997.

Harada, J. and Sugimoto, M. Inhibitors of interleukin-1 beta-converting enzyme-family proteases (caspases) prevent apoptosis without affecting decreased cellular ability to

reduce 3-(4,5-dimethylthiazol-2-yl)-2, 5-diphenyltetrazolium bromide in cerebellar granule neurons. *Brain Research* 793(1-2): 231-43, 1998.

Harris, N. L., Jaffe, E. S., Stein, H., Banks, P. M., Chan, J. K., Cleary, M. L., Delsol, G., De Wolf-Peeters, C., Falini, B. and Gatter, K. C. A revised European-American classification of lymphoid neoplasms: a proposal from the International Lymphoma Study Group [see comments]. *Blood* 84(5): 1361-92, 1994.

Havell, E. A., Fiers, W. and North, R. J. The antitumor function of tumor necrosis factor (TNF), I. Therapeutic action of TNF against an established murine sarcoma is indirect, immunologically dependent, and limited by severe toxicity. *Journal Experimental Medicine* 167(3): 1067-85, 1988.

Hengartner, M. O. Apoptosis. CED-4 is a stranger no more [news; comment]. *Nature* 388(6644): 714-5, 1997.

Hengartner, M. O. and Horvitz, H. R. C. elegans cell survival gene ced-9 encodes a functional homolog of the mammalian proto-oncogene bcl-2. *Cell* 76(4): 665-76, 1994.

Holmgren, S. P., Huang, D. C., Adams, J. M. and Cory, S. Survival activity of Bcl-2 homologs Bcl-w and A1 only partially correlates with their ability to bind pro-apoptotic family members. *Cell Death and Differentiation* 6(6): 525-32, 1999.

Hoogenboom, H. R., Griffiths, A. D., Johnson, K. S., Chiswell, D. J., Hudson, P. and Winter, G. Multi-subunit proteins on the surface of filamentous phage: methodologies for displaying antibody (Fab) heavy and light chains. *Nucleic Acids Research* 19(15): 4133-7, 1991.

Hopp, T. P. Protein surface analysis. Methods for identifying antigenic determinants and other interaction sites. *J Immunological Methods* 88(1): 1-18, 1986.

Hopp, T. P. and Woods, K. R. Prediction of protein antigenic determinants from amino acid sequences. *Proceedings of the National Academy of Sciences U S A* 78(6): 3824-8, 1981.

Howard, A. D., Kostura, M. J., Thornberry, N., Ding, G. J., Limjuco, G., Weidner, J., Salley, J. P., Hogquist, K. A., Chaplin, D. D., Mumford, R. A. and et al. IL-1-converting enzyme requires aspartic acid residues for processing of the IL-1 beta precursor at two distinct sites and does not cleave 31- kDa IL-1 alpha. *Journal of Immunology* 147(9): 2964-9, 1991.

Hsu, S. Y., Kaipia, A., McGee, E., Lomeli, M. and Hsueh, A. J. Bok is a pro-apoptotic Bcl-2 protein with restricted expression in reproductive tissues and heterodimerizes with selective anti-apoptotic Bcl-2 family members. *Proceedings of the National Academy of Science U S A* 94(23): 12401-6, 1997.

Hsu, Y. T., Wolter, K. G. and Youle, R. J. Cytosol-to-membrane redistribution of Bax and Bcl-X(L) during apoptosis. *Proceedings National Academy of Sciences U S A* 94(8): 3668-72, 1997.

Hu, Y., Benedict, M. A., Wu, D., Inohara, N. and Nunez, G. Bcl-XL interacts with Apaf-1 and inhibits Apaf-1-dependent caspase-9 activation. *Proceedings of the National Academy of Sciences of the United States of America* 95(8): 4386-91, 1998.

Huang, D. C., O'Reilly, L. A., Strasser, A. and Cory, S. The anti-apoptosis function of Bcl-2 can be genetically separated from its inhibitory effect on cell cycle entry. *Embo J* 16(15): 4628-38, 1997.

Huang, P., Robertson, L. E., Wright, S. and Plunkett, W. High molecular weight DNA fragmentation: a critical event in nucleoside analogue-induced apoptosis in leukemia cells. *Clinical Cancer Research* 1(9): 1005-13, 1995.

Hughes, F. M., Jr., Evans-Storms, R. B. and Cidlowski, J. A. Evidence that non-caspase proteases are required for chromatin degradation during apoptosis. *Cell Death and Differentiation* 5(12): 1017-27, 1998.

Hyland, J., Lasota, J., Jasinski, M., Petersen, R. O., Nordling, S. and Miettinen, M. Molecular pathological analysis of testicular diffuse large cell lymphomas. *Human Pathology* 29(11): 1231-9, 1998.

Imai, Y., Kimura, T., Murakami, A., Yajima, N., Sakamaki, K. and Yonehara, S. The CED-4-homologous protein FLASH is involved in Fas-mediated activation of caspase-8 during apoptosis [see comments] [published erratum appears in Nature 1999 Jul 1;400(6739):89]. *Nature* 398(6730): 777-85, 1999.

Institute, N. C. Sponsored study of the classification of non-Hodgkin's lymphoma. *Cancer* 49: 2112-2135, 1982.

Irmeler, M., Thome, M., Hahne, M., Schneider, P., Hofmann, K., Steiner, V., Bodmer, J. L., Schroter, M., Burns, K., Mattmann, C., Rimoldi, D., French, L. E. and Tschopp, J.

Inhibition of death receptor signals by cellular FLIP [see comments]. *Nature* 388(6638): 190-5, 1997.

Janicke, R. U., Sprengart, M. L., Wati, M. R. and Porter, A. G. Caspase-3 is required for DNA fragmentation and morphological changes associated with apoptosis. *Journal of Biological Chemistry* 273(16): 9357-60, 1998.

Janicke, R. U., Walker, P. A., Lin, X. Y. and Porter, A. G. Specific cleavage of the retinoblastoma protein by an ICE-like protease in apoptosis. *Embo Journal* 15(24): 6969-78, 1996.

Kaufmann, S. H., Brunet, G., Talbot, B., Lamarr, D., Dumas, C., Shaper, J. H. and Poirier, G. Association of poly(ADP-ribose) polymerase with the nuclear matrix: the role of intermolecular disulfide bond formation, RNA retention, and cell type. *Experimental Cell Research* 192(2): 524-35, 1991.

Kayalar, C., Ord, T., Testa, M. P., Zhong, L. T. and Bredesen, D. E. Cleavage of actin by interleukin 1 beta-converting enzyme to reverse DNase I inhibition. *Proceedings of the National Academy of Sciences of the United States of America* 93(5): 2234-8, 1996.

Kelekar, A. and Thompson, C. B. Bcl-2-family proteins: the role of the BH3 domain in apoptosis. *Trends in Cell Biology* 8(8): 324-30, 1998.

Kerr, J. F. Shrinkage necrosis: a distinct mode of cellular death. *Journal of Pathology* 105(1): 13-20, 1971.

Kerr, J. F. R., Wyllie, A. H. and Currie, A. R. Apoptosis: a basic biological phenomenon with wide-ranging implications in tissue kinetics. *British Journal of Cancer* 26: 239-257, 1972.

Kikuchi, H. and Imajoh-Ohmi, S. Antibodies specific for proteolyzed forms of protein kinase C alpha. *Biochim Biophys Acta* 1269(3): 253-9, 1995.

Kischkel, F. C., Hellbardt, S., Behrmann, I., Germer, M., Pawlita, M., Krammer, P. H. and Peter, M. E. Cytotoxicity-dependent APO-1 (Fas/CD95)-associated proteins form a death-inducing signaling complex (DISC) with the receptor. *Embo Journal* 14(22): 5579-88, 1995.

Kitanaka, C. and Kuchino, Y. Caspase-independent programmed cell death with necrotic morphology. *Cell Death and Differentiation* 6(6): 508-15, 1999.

Kluck, R. M., Bossy-Wetzell, E., Green, D. R. and Newmeyer, D. D. The release of cytochrome c from mitochondria: a primary site for Bcl-2 regulation of apoptosis [see comments]. *Science* 275(5303): 1132-6, 1997.

Kondo, S., Tanaka, Y., Kondo, Y., Ishizaka, Y., Hitomi, M., Haqqi, T., Liu, J., Barnett, G. H., Alnemri, E. S. and Barna, B. P. Retroviral transfer of CPP32beta gene into malignant gliomas in vitro and in vivo. *Cancer Research* 58(5): 962-7, 1998.

Kothakota, S., Azuma, T., Reinhard, C., Klippel, A., Tang, J., Chu, K., McGarry, T. J., Kirschner, M. W., Kohts, K., Kwiatkowski, D. J. and Williams, L. T. Caspase-3-generated fragment of gelsolin: effector of morphological change in apoptosis. *Science* 278(5336): 294-8, 1997.

Krajewska, M., Wang, H. G., Krajewski, S., Zapata, J. M., Shabaik, A., Gascoyne, R. and Reed, J. C. Immunohistochemical analysis of in vivo patterns of expression of CPP32 (Caspase-3), a cell death protease. *Cancer Research* 57(8): 1605-13, 1997.

Krajewski, S., Blomqvist, C., Franssila, K., Krajewska, M., Wasenius, V. M., Niskanen, E., Nordling, S. and Reed, J. C. Reduced expression of proapoptotic gene BAX is associated with poor response rates to combination chemotherapy and shorter survival in women with metastatic breast adenocarcinoma. *Cancer Research* 55(19): 4471-8, 1995.

Krajewski, S., Gascoyne, R. D., Zapata, J. M., Krajewska, M., Kitada, S., Chhanabhai, M., Horsman, D., Berean, K., Piro, L. D., Fugier-Vivier, I., Liu, Y. J., Wang, H. G. and Reed, J. C. Immunolocalization of the ICE/Ced-3-family protease, CPP32 (Caspase-3), in non-Hodgkin's lymphomas, chronic lymphocytic leukemias, and reactive lymph nodes. *Blood* 89(10): 3817-25, 1997.

Krajewski, S., Tanaka, S., Takayama, S., Schibler, M. J., Fenton, W. and Reed, J. C. Investigation of the subcellular distribution of the bcl-2 oncoprotein: residence in the nuclear envelope, endoplasmic reticulum, and outer mitochondrial membranes. *Cancer Research* 53(19): 4701-14, 1993.

Krammer, P. H., Galle, P. R., Moller, P. and Debatin, K. M. CD95(APO-1/Fas)-mediated apoptosis in normal and malignant liver, colon, and hematopoietic cells. *Adv Cancer Research* 75: 251-73, 1998.

Kroemer, G. The mitochondrion as an integrator/coordinator of cell death pathways. *Cell Death and Differentiation* 5(6): 547, 1998.

Kuida, K., Haydar, T. F., Kuan, C. Y., Gu, Y., Taya, C., Karasuyama, H., Su, M. S., Rakic, P. and Flavell, R. A. Reduced apoptosis and cytochrome c-mediated caspase activation in mice lacking caspase 9. *Cell* 94(3): 325-37, 1998.

Kuida, K., Lippke, J. A., Ku, G., Harding, M. W., Livingston, D. J., Su, M. S. and Flavell, R. A. Altered cytokine export and apoptosis in mice deficient in interleukin-1 beta converting enzyme. *Science* 267(5206): 2000-3, 1995.

Kuida, K., Zheng, T. S., Na, S., Kuan, C., Yang, D., Karasuyama, H., Rakic, P. and Flavell, R. A. Decreased apoptosis in the brain and premature lethality in CPP32-deficient mice. *Nature* 384(6607): 368-72, 1996.

Kumar, S., Kinoshita, M. and Noda, M. Characterization of a mammalian cell death gene Nedd2. *Leukemia* 11 Supplement 3: 385-6, 1997.

Kumar, S., Kinoshita, M., Noda, M., Copeland, N. G. and Jenkins, N. A. Induction of apoptosis by the mouse Nedd2 gene, which encodes a protein similar to the product of the *Caenorhabditis elegans* cell death gene ced-3 and the mammalian IL-1 beta-converting enzyme. *Genes and Development* 8(14): 1613-26, 1994.

Kyte, J. and Doolittle, R. F. A simple method for displaying the hydropathic character of a protein. *Journal of Molecular Biology* 157(1): 105-32, 1982.

LaCasse, E. C., Baird, S., Korneluk, R. G. and MacKenzie, A. E. The inhibitors of apoptosis (IAPs) and their emerging role in cancer. *Oncogene* 17(25): 3247-59, 1998.

Landowski, T. H., Qu, N., Buyuksal, I., Painter, J. S. and Dalton, W. S. Mutations in the Fas antigen in patients with multiple myeloma. *Blood* 90(11): 4266-70, 1997.

Lee, S. T., Hoeflich, K. P., Wasfy, G. W., Woodgett, J. R., Leber, B., Andrews, D. W., Hedley, D. W. and Penn, L. Z. Bcl-2 targeted to the endoplasmic reticulum can inhibit apoptosis induced by Myc but not etoposide in Rat-1 fibroblasts. *Oncogene* 18(23): 3520-8, 1999.

Leers, M. P., Kolgen, W., Bjorklund, V., Bergman, T., Tribbick, G., Persson, B., Bjorklund, P., Ramaekers, F. C., Bjorklund, B., Nap, M., Jornvall, H. and Schutte, B. Immunocytochemical detection and mapping of a cytokeratin 18 neo-epitope exposed during early apoptosis [In Process Citation]. *J Pathol* 187(5): 567-72, 1999.

Leoncini, L., Delvecchio, M., Megha, T., Barbini, P., Galieni, P., Pileri, S., Sabbatini, E., Gherlinozini, F., Tosi, P. and Kraft, R. Correlations between apoptotic and proliferative

indexes in malignant Non-Hodgkins Lymphomas. *American Journal of Pathology* 142(3): 755-763, 1993.

Levkau, B., Koyama, H., Raines, E. W., Clurman, B. E., Herren, B., Orth, K., Roberts, J. M. and Ross, R. Cleavage of p21Cip1/Waf1 and p27Kip1 mediates apoptosis in endothelial cells through activation of Cdk2: role of a caspase cascade. *1(4): 553-63, 1998.*

Li, F., Ambrosini, G., Chu, E. Y., Plescia, J., Tognin, S., Marchisio, P. C. and Altieri, D. C. Control of apoptosis and mitotic spindle checkpoint by survivin. *Nature* 396(6711): 580-4, 1998.

Li, H., Zhu, H., Xu, C. J. and Yuan, J. Cleavage of BID by caspase 8 mediates the mitochondrial damage in the Fas pathway of apoptosis. *Cell* 94(4): 491-501, 1998.

Li, P., Allen, H., Banerjee, S., Franklin, S., Herzog, L., Johnston, C., McDowell, J., Paskind, M., Rodman, L., Salfeld, J., Townes, E., Tracey, D., Wardwell, S., Wei, F.-Y., Wong, W. and Seshadri, T. Mice deficient in IL-1 β -converting enzyme are deficient in production of mature IL-1 β and resistant to endotoxic shock. *Cell* 80: 401-411, 1995.

Li, P., Nijhawan, D., Budihardjo, I., Srinivasula, S. M., Ahmad, M., Alnemri, E. S. and Wang, X. Cytochrome c and dATP-dependent formation of Apaf-1/caspase-9 complex initiates an apoptotic protease cascade. *Cell* 91(4): 479-89, 1997.

Liu, X., Zou, H., Slaughter, C. and Wang, X. DFF, a heterodimeric protein that functions downstream of caspase-3 to trigger DNA fragmentation during apoptosis. *Cell* 89(2): 175-84, 1997.

Linette, G. P., Li, Y., Roth, K. and Korsmeyer, S. J. Cross talk between cell death and cell cycle progression: BCL-2 regulates NFAT-mediated activation. *Proceedings of the National Academy of Sciences U S A* 93(18): 9545-52, 1996.

Loddick, S. A., MacKenzie, A. and Rothwell, N. J. An ICE inhibitor, z-VAD-DCB attenuates ischaemic brain damage in the rat. *Neuroreport* 7(9): 1465-8, 1996.

Lukes, R. J. and Collins, R. D. New approaches to the classification of the lymphomata. *British Journal of Cancer* 31: 1-26, 1975.

Luo, X., Budihardjo, I., Zou, H., Slaughter, C. and Wang, X. Bid, a Bcl2 interacting protein, mediates cytochrome c release from mitochondria in response to activation of cell surface death receptors. *Cell* 94(4): 481-90, 1998.

- Mancini, M., Nicholson, D. W., Roy, S., Thornberry, N. A., Peterson, E. P., Casciola-Rosen, L. A. and Rosen, A. The caspase-3 precursor has a cytosolic and mitochondrial distribution: implications for apoptotic signaling. *Journal of Cell Biology* 140(6): 1485-95, 1998.
- Mandruzzato, S., Brasseur, F., Andry, G., Boon, T. and van der Bruggen, P. A CASP-8 mutation recognized by cytolytic T lymphocytes on a human head and neck carcinoma. *Journal of Experimental Medicine* 186(5): 785-93, 1997.
- Mao, P. L., Jiang, Y., Wee, B. Y. and Porter, A. G. Activation of caspase-1 in the nucleus requires nuclear translocation of pro-caspase-1 mediated by its prodomain. *Journal of Biological Chemistry* 273(37): 23621-4, 1998.
- Mapara, M. Y., Bargou, R., Zugck, C., Dohner, H., Ustaoglu, F., Jonker, R. R., Krammer, P. H. and Dorken, B. APO-1 mediated apoptosis or proliferation in human chronic B lymphocytic leukemia: correlation with bcl-2 oncogene expression. *European Journal of Immunology* 23(3): 702-8, 1993.
- Mariani, S. M., Matiba, B., Armandola, E. A. and Krammer, P. H. Interleukin 1 beta-converting enzyme related proteases/caspases are involved in TRAIL-induced apoptosis of myeloma and leukemia cells. *Journal of Cell Biology* 137(1): 221-9, 1997.
- Marsters, S. A., Pitti, R. M., Donahue, C. J., Ruppert, S., Bauer, K. D. and Ashkenazi, A. Activation of apoptosis by Apo-2 ligand is independent of FADD but blocked by CrmA. *Current Biology* 6(6): 750-2, 1996.
- Marsters, S. A., Sheridan, J. P., Pitti, R. M., Huang, A., Skubatch, M., Baldwin, D., Yuan, J., Gurney, A., Goddard, A. D., Godowski, P. and Ashkenazi, A. A novel receptor for Apo2L/TRAIL contains a truncated death domain. *Current Biology* 7(12): 1003-6, 1997.
- Martinou, I., Desagher, S., Eskes, R., Antonsson, B., Andre, E., Fakan, S. and Martinou, J. C. The release of cytochrome c from mitochondria during apoptosis of NGF- deprived sympathetic neurons is a reversible event. *Journal of Cell Biology* 144(5): 883-9, 1999.
- Marzo, I., Brenner, C. and Kroemer, G. The central role of the mitochondrial megachannel in apoptosis: evidence obtained with intact cells, isolated mitochondria, and purified protein complexes. *Biomedicine and Pharmacotherapy* 52(6): 248-51, 1998.

- Marzo, I., Brenner, C., Zamzami, N., Jurgensmeier, J. M., Susin, S. A., Vieira, H. L., Prevost, M. C., Xie, Z., Matsuyama, S., Reed, J. C. and Kroemer, G. Bax and adenine nucleotide translocator cooperate in the mitochondrial control of apoptosis. *Science* 281(5385): 2027-31, 1998.
- Marzo, I., Susin, S. A., Petit, P. X., Ravagnan, L., Brenner, C., Larochette, N., Zamzami, N. and Kroemer, G. Caspases disrupt mitochondrial membrane barrier function. *Febs Letters* 427(2): 198-202, 1998.
- McCarthy, N. J., Whyte, M. K., Gilbert, C. S. and Evan, G. I. Inhibition of Ced-3/ICE-related proteases does not prevent cell death induced by oncogenes, DNA damage, or the Bcl-2 homologue Bak. *Journal of Cell Biology* 136(1): 215-27, 1997.
- Medema, J. P., Hahne, M., Walczak, H. and Laurenzi, V. D. The First European Workshop on Cell Death: (Death on the Rocks) held at Gran Sasso, Italy, 21 - 25 October 1998. Rocking cell death. *Cell Death and Differentiation* 6(3): 297-300, 1999.
- Mhashilkar, A. M., Bagley, J., Yi Chen, S., Szilvay, A. M., Helland, D. G. and Marasco, W. A. Inhibition of HIV Tat-mediated LTR transactivation and HIV-1 infection by anti-Tat single-chain intrabodies. *14: 1542-1551, 1995.*
- Miller, T. M., Moulder, K. L., Knudson, C. M., Creedon, D. J., Deshmukh, M., Korsmeyer, S. J. and Johnson, E. M., Jr. Bax deletion further orders the cell death pathway in cerebellar granule cells and suggests a caspase-independent pathway to cell death. *Journal of Cell Biology* 139(1): 205-17, 1997.
- Miller, T. P., Dahlberg, S., Cassady, J. R., Adelstein, D. J., Spier, C. M., Grogan, T. M., LeBlanc, M., Carlin, S., Chase, E. and Fisher, R. I. Chemotherapy alone compared with chemotherapy plus radiotherapy for localized intermediate- and high-grade non-Hodgkin's lymphoma [see comments]. *New England Journal of Medicine* 339(1): 21-6, 1998.
- Miura, M., Zhu, H., Rotello, R., Hartwig, E. A. and Yuan, J. Induction of apoptosis in fibroblasts by IL-1 beta-converting enzyme, a mammalian homolog of the *C. elegans* cell death gene *ced-3*. *Cell* 75(4): 653-60, 1993.
- Monni, O., Franssila, K., Joensuu, H. and Knuutila, S. BCL2 overexpression in diffuse large B-cell lymphoma. *Leukaemia and Lymphoma* 34(1-2): 45-52, 1999.

Muchmore, S. W., Sattler, M., Liang, H., Meadows, R. P., Harlan, J. E., Yoon, H. S., Nettesheim, D., Chang, B. S., Thompson, C. B., Wong, S. L., Ng, S. L. and Fesik, S. W. X-ray and NMR structure of human Bcl-xL, an inhibitor of programmed cell death. *Nature* 381(6580): 335-41, 1996.

Muller, M., Strand, S., Hug, H., Heinemann, E. M., Walczak, H., Hofmann, W. J., Stremmel, W., Krammer, P. H. and Galle, P. R. Drug-induced apoptosis in hepatoma cells is mediated by the CD95 (APO- 1/Fas) receptor/ligand system and involves activation of wild-type p53. *Journal of Clinical Investigation* 99(3): 403-13, 1997.

Muzio, M. Signalling by proteolysis: death receptors induce apoptosis. *International Journal of Clinical Laboratory Research* 28(3): 141-7, 1998.

Muzio, M., Stockwell, B. R., Stennicke, H. R., Salvesen, G. S. and Dixit, V. M. An induced proximity model for caspase-8 activation. *Journal of Biological Chemistry* 273(5): 2926-30, 1998.

Nagata, S. Fas and Fas ligand: a death factor and its receptor. *Advances in Immunology* 57: 129-44, 1994.

Nagata, S. Apoptosis mediated by the Fas system. *Progress in Molecular Subcellular Biology* 16: 87-103, 1996.

Nagata, S. and Golstein, P. The Fas death factor. *Science* 267(5203): 1449-56, 1995.

Nagata, S. and Suda, T. Fas and Fas ligand: lpr and gld mutations. *Immunology Today* 16(1): 39-43, 1995.

Nakagawara, A., Nakamura, Y., Ikeda, H., Hiwasa, T., Kuida, K., Su, M. S., Zhao, H., Cnaan, A. and Sakiyama, S. High levels of expression and nuclear localization of interleukin-1 beta converting enzyme (ICE) and CPP32 in favorable human neuroblastomas. *Cancer Research* 57(20): 4578-84, 1997.

Naumovski, L. and Cleary, M. L. The p53-binding protein 53BP2 also interacts with Bcl2 and impedes cell cycle progression at G2/M. *Molecular Cell Biology* 16(7): 3884-92, 1996.

Nguyen, M., Millar, D. G., Yong, V. W., Korsmeyer, S. J. and Shore, G. C. Targeting of Bcl-2 to the mitochondrial outer membrane by a COOH- terminal signal anchor sequence. *Journal of Biology and Chemistry* 268(34): 25265-8, 1993.

Nicholson, D. W. Caspase structure, proteolytic substrates, and function during apoptotic cell death [In Process Citation]. *Cell Death and Differentiation* 6(11): 1028-42, 1999.

Nicholson, D. W., Ali, A., Thornberry, N. A., Vaillancourt, J. P., Ding, C. K., Gallant, M., Gareau, Y., Griffin, P. R., Labelle, M., Lazebnik, Y. A. and et al. Identification and inhibition of the ICE/CED-3 protease necessary for mammalian apoptosis [see comments]. *Nature* 376(6535): 37-43, 1995.

Oberhammer, F., Wilson, J. W., Dive, C., Morris, I. D., Hickman, J. A., Wakeling, A. E., Walker, P. R. and Sikorska, M. Apoptotic death in epithelial cells: cleavage of DNA to 300 and/or 50 kb fragments prior to or in the absence of internucleosomal fragmentation. *Embo J* 12(9): 3679-84, 1993.

Offen, D., Beart, P. M., Cheung, N. S., Pascoe, C. J., Hochman, A., Gorodin, S., Melamed, E., Bernard, R. and Bernard, O. Transgenic mice expressing human Bcl-2 in their neurons are resistant to 6-hydroxydopamine and 1-methyl-4-phenyl-1,2,3,6-tetrahydropyridine neurotoxicity. *Proceedings of the National Academy of Sciences U S A* 95(10): 5789-94, 1998.

Oltvai, Z. N., Milliman, C. L. and Korsmeyer, S. J. Bcl-2 heterodimerizes in vivo with a conserved homolog, Bax, that accelerates programmed cell death. *Cell* 74(4): 609-19, 1993.

Pan, G., Ni, J., Wei, Y. F., Yu, G., Gentz, R. and Dixit, V. M. An antagonist decoy receptor and a death domain-containing receptor for TRAIL [see comments]. *Science* 277(5327): 815-8, 1997.

Pan, G., O'Rourke, K. and Dixit, V. M. Caspase-9, Bcl-XL, and Apaf-1 form a ternary complex. *Journal of Biological Chemistry* 273(10): 5841-5, 1998.

Parker, J. M., Guo, D. and Hodges, R. S. New hydrophilicity scale derived from high-performance liquid chromatography peptide retention data: correlation of predicted surface residues with antigenicity and X-ray-derived accessible sites. *Biochemistry* 25(19): 5425-32, 1986.

Plumas, J., Jacob, M. C., Chaperot, L., Molens, J. P., Sotto, J. J. and Bensa, J. C. Tumor B cells from non-Hodgkin's lymphoma are resistant to CD95 (Fas/Apo-1)-mediated apoptosis. *Blood* 91(8): 2875-85, 1998.

- Polyak, K., Li, Y., Zhu, H., Lengauer, C., Willson, J. K., Markowitz, S. D., Trush, M. A., Kinzler, K. W. and Vogelstein, B. Somatic mutations of the mitochondrial genome in human colorectal tumours. *Nature Genetics* 20(3): 291-3, 1998.
- Quignon, F., De Bels, F., Koken, M., Feunteun, J., Ameisen, J. C. and de The, H. PML induces a novel caspase-independent death process [see comments]. *Nature Genetics* 20(3): 259-65, 1998.
- Rao, L., Perez, D. and White, E. Lamin proteolysis facilitates nuclear events during apoptosis. *Journal of Cell Biology* 135(6 Pt 1): 1441-55, 1996.
- Rao, P. H., Houldsworth, J., Dyomina, K., Parsa, N. Z., Cigudosa, J. C., Louie, D. C., Popplewell, L., Offit, K., Jhanwar, S. C. and Chaganti, R. S. Chromosomal and gene amplification in diffuse large B-cell lymphoma. *Blood* 92(1): 234-40, 1998.
- Rappaport, H., Winter, W. J. and Hicks, E. B. Follicular lymphoma. *Cancer* 9: 792-821, 1956.
- Ray, C. A., Black, R. A., Kronheim, S. R., Greenstreet, T. A., Sleath, P. R., Salvesen, G. S. and Pickup, D. J. Viral inhibition of inflammation: cowpox virus encodes an inhibitor of the interleukin-1 beta converting enzyme. *Cell* 69(4): 597-604, 1992.
- Reed, J. C. Bcl-2 and the regulation of programmed cell death. *Journal of Cell Biology* 124(1-2): 1-6, 1994.
- Reed, J. C., Jurgensmeier, J. M. and Matsuyama, S. Bcl-2 family proteins and mitochondria. *Biochimica Et Biophysica Acta* 1366(1-2): 127-37, 1998.
- Rieux-Laucat, F., Le Deist, F., Hivroz, C., Roberts, I. A., Debatin, K. M., Fischer, A. and de Villartay, J. P. Mutations in Fas associated with human lymphoproliferative syndrome and autoimmunity. *Science* 268(5215): 1347-9, 1995.
- Rodriguez, I., Matsuura, K., Ody, C., Nagata, S. and Vassalli, P. Systemic injection of a tripeptide inhibits the intracellular activation of CPP32-like proteases in vivo and fully protects mice against Fas-mediated fulminant liver destruction and death. *Journal of Experimental Medicine* 184(5): 2067-72, 1996.
- Rosse, T., Olivier, R., Monney, L., Rager, M., Conus, S., Fellay, I., Jansen, B. and Borner, C. Bcl-2 prolongs cell survival after Bax-induced release of cytochrome c [see comments]. *Nature* 391(6666): 496-9, 1998.

Rothe, M., Pan, M. G., Henzel, W. J., Ayres, T. M. and Goeddel, D. V. The TNFR2-TRAF signaling complex contains two novel proteins related to baculoviral inhibitor of apoptosis proteins. *Cell* 83(7): 1243-52, 1995.

Rotonda, J., Nicholson, D. W., Fazil, K. M., Gallant, M., Gareau, Y., Labelle, M., Peterson, E. P., Rasper, D. M., Ruel, R., Vaillancourt, J. P., Thornberry, N. A. and Becker, J. W. The three-dimensional structure of apopain/CPP32, a key mediator of apoptosis. *Nature Structural Biology* 3(7): 619-25, 1996.

Roy, N., Deveraux, Q. L., Takahashi, R., Salvesen, G. S. and Reed, J. C. The c-IAP-1 and c-IAP-2 proteins are direct inhibitors of specific caspases. *Embo Journal* 16(23): 6914-25, 1997.

Rudel, T., Zenke, F. T., Chuang, T. H. and Bokoch, G. M. p21-activated kinase (PAK) is required for Fas-induced JNK activation in Jurkat cells. *Journal of Immunology* 160(1): 7-11, 1998.

Salar, A., Fernandez de Sevilla, A., Romagosa, V., Domingo-Claros, A., Gonzalez-Barca, E., Pera, J., Climent, J. and Granena, A. Diffuse large B-cell lymphoma: is morphologic subdivision useful in clinical management? *European Journal of Haematology* 60(3): 202-8, 1998.

Saleh, A., Srinivasula, S. M., Acharya, S., Fishel, R. and Alnemri, E. S. Cytochrome c and dATP-mediated oligomerisation of Apaf-1 is a prerequisite for proCaspase9 activation. *J.Biol. Chem.* 274: 17941-17945, 1999.

Samali, A., Cai, J., Zhivotovsky, B., Jones, D. P. and Orrenius, S. Presence of a pre-apoptotic complex of pro-caspase-3, Hsp60 and Hsp10 in the mitochondrial fraction of jurkat cells. *Embo J* 18(8): 2040-8, 1999.

Samali, A., Zhivotovsky, B., Jones, D. P. and Orrenius, S. Detection of pro-caspase-3 in cytosol and mitochondria of various tissues. *Febs Letters* 431(2): 167-9, 1998.

Sarris, A. and Ford, R. Recent advances in the molecular pathogenesis of lymphomas [see comments]. *Current Opinion in Oncology* 11(5): 351-63, 1999.

Schendel, S. L., Montal, M. and Reed, J. C. Bcl-2 family proteins as ion-channels. *Cell Death and Differentiation* 5(5): 372-80, 1998.

- Schotte, P., Declercq, W., Van Huffel, S., Vandenaabeele, P. and Beyaert, R. Non-specific effects of methyl ketone peptide inhibitors of caspases. *FEBS Letters* 442(1): 117-21, 1999.
- Schwartz, S., Jr., Yamamoto, H., Navarro, M., Maestro, M., Reventos, J. and Perucho, M. Frameshift mutations at mononucleotide repeats in caspase-5 and other target genes in endometrial and gastrointestinal cancer of the microsatellite mutator phenotype. *Cancer Research* 59(12): 2995-3002, 1999.
- Shaham, S. and Horvitz, H. R. An alternatively spliced *C. elegans* ced-4 RNA encodes a novel cell death inhibitor. *Cell* 86(2): 201-8, 1996.
- Shibata, Y., Takiguchi, H., Tamura, K., Yamanaka, K., Tezuka, M. and Abiko, Y. Stimulation of interleukin-1beta-converting enzyme activity during growth inhibition by CPT-11 in the human myeloid leukemia cell line K562. *Biochemical and Molecular Medicine* 57(1): 25-30, 1996.
- Shustik, C., Dalton, W. and Gros, P. P-glycoprotein-mediated multidrug resistance in tumor cells: biochemistry, clinical relevance and modulation. *Mol Aspects Med* 16(1): 1-78, 1995.
- Singer, II, Scott, S., Chin, J., Bayne, E. K., Limjuco, G., Weidner, J., Miller, D. K., Chapman, K. and Kostura, M. J. The interleukin-1 beta-converting enzyme (ICE) is localized on the external cell surface membranes and in the cytoplasmic ground substance of human monocytes by immuno-electron microscopy. *Journal of Experimental Medicine* 182(5): 1447-59, 1995.
- Slee, E. A., Adrain, C. and Martin, S. J. Serial killers: ordering caspase activation events in apoptosis. *Cell Death and Differentiation* 6(11): 1067-74, 1999.
- Smith, C. A., Farrah, T. and Goodwin, R. G. The TNF receptor superfamily of cellular and viral proteins: activation, costimulation, and death. *Cell* 76(6): 959-62, 1994.
- Snell, V., Clodi, K., Zhao, S., Goodwin, R., Thomas, E. K., Morris, S. W., Kadin, M. E., Cabanillas, F., Andreeff, M. and Younes, A. Activity of TNF-related apoptosis-inducing ligand (TRAIL) in haematological malignancies. *British Journal of Haematology* 99(3): 618-24, 1997.

Soengas, M. S., Alarcon, R. M., Yoshida, H., Giaccia, A. J., Hakem, R., Mak, T. W. and Lowe, S. W. Apaf-1 and caspase-9 in p53-dependent apoptosis and tumor inhibition. *Science* 284(5411): 156-9, 1999.

Song, Q., Kuang, Y., Dixit, V. M. and Vincenz, C. Boo, a novel negative regulator of cell death, interacts with Apaf-1. *Embo Journal* 18(1): 167-78, 1999.

Squier, M. K. and Cohen, J. J. Calpain, an upstream regulator of thymocyte apoptosis. *Journal of Immunology* 158(8): 3690-7, 1997.

Squier, M. K., Miller, A. C., Malkinson, A. M. and Cohen, J. J. Calpain activation in apoptosis. *Journal of Cell Physiology* 159(2): 229-37, 1994.

Srinivasula, S. M., Ahmad, M., Guo, Y., Zhan, Y., Lazebnik, Y., Fernandes-Alnemri, T. and Alnemri, E. S. Identification of an endogenous dominant-negative short isoform of caspase-9 that can regulate apoptosis. *Cancer Research* 59(5): 999-1002, 1999.

St. Clair, E. G., Anderson, S. J. and Oltvai, Z. N. Bcl-2 counters apoptosis by Bax heterodimerization-dependent and -independent mechanisms in the T-cell lineage. *Journal of Biological Chemistry* 272(46): 29347-55, 1997.

Stroh, C. and Schulze-Osthoff, K. Death by a thousand cuts: an ever increasing list of caspase substrates [editorial]. *Cell Death and Differentiation* 5(12): 997-1000, 1998.

Sumantran, V. N., Ealovega, M. W., Nunez, G., Clarke, M. F. and Wicha, M. S. Overexpression of Bcl-XS sensitizes MCF-7 cells to chemotherapy-induced apoptosis. *Cancer Research* 55(12): 2507-10, 1995.

Sun, X. M., MacFarlane, M., Zhuang, J., Wolf, B. B., Green, D. R. and Cohen, G. M. Distinct caspase cascades are initiated in receptor-mediated and chemical-induced apoptosis. *Journal of Biological Chemistry* 274(8): 5053-60, 1999.

Susin, S. A., Lorenzo, H. K., Zamzami, N., Marzo, I., Brenner, C., Larochette, N., Prevost, M. C., Alzari, P. M. and Kroemer, G. Mitochondrial release of caspase-2 and -9 during the apoptotic process. *Journal of Experimental Medicine* 189(2): 381-94, 1999.

Susin, S. A., Lorenzo, H. K., Zamzami, N., Marzo, I., Snow, B. E., Brothers, G. M., Mangion, J., Jacotot, E., Costantini, P., Loeffler, M., Larochette, N., Goodlett, D. R., Aebersold, R., Siderovski, D. P., Penninger, J. M. and Kroemer, G. Molecular characterization of mitochondrial apoptosis-inducing factor [see comments]. *Nature* 397(6718): 441-6, 1999.

Susin, S. A., Zamzami, N., Castedo, M., Daugas, E., Wang, H. G., Geley, S., Fassy, F., Reed, J. C. and Kroemer, G. The central executioner of apoptosis: multiple connections between protease activation and mitochondria in Fas/APO-1/CD95- and ceramide-induced apoptosis. *Journal of Experimental Medicine* 186(1): 25-37, 1997.

Susin, S. A., Zamzami, N., Castedo, M., Hirsch, T., Marchetti, P., Macho, A., Daugas, E., Geuskens, M. and Kroemer, G. Bcl-2 inhibits the mitochondrial release of an apoptogenic protease. *Journal of Experimental Medicine* 184(4): 1331-41, 1996.

Takayama, S., Sato, T., Krajewski, S., Kochel, K., Irie, S., Millan, J. A. and Reed, J. C. Cloning and functional analysis of BAG-1: a novel Bcl-2-binding protein with anti-cell death activity. *Cell* 80(2): 279-84, 1995.

Tamm, I., Wang, Y., Sausville, E., Scudiero, D. A., Vigna, N., Oltersdorf, T. and Reed, J. C. IAP-family protein survivin inhibits caspase activity and apoptosis induced by Fas (CD95), Bax, caspases, and anticancer drugs. *Cancer Research* 58(23): 5315-20, 1998.

Tepper, C. G. and Seldin, M. F. Modulation of caspase-8 and FLICE-inhibitory protein expression as a potential mechanism of Epstein-Barr virus tumorigenesis in Burkitt's lymphoma. *Blood* 94(5): 1727-37, 1999.

Tew, K. D. Glutathione-associated enzymes in anticancer drug resistance. *Cancer Research* 54(16): 4313-20, 1994.

Thomas, A. L., Price, C., Martin, S. G., Carmichael, J. and Murray, J. C. Identification of two novel mRNA splice variants of bax [letter]. *Cell Death and Differentiation* 6(2): 97-8, 1999.

Thompson, C. B. Apoptosis in the pathogenesis and treatment of disease. *Science* 267(5203): 1456-62, 1995.

Thornberry, N. A. The caspase family of cysteine proteases. *British Medical Bulletin* 53(3): 478-90, 1997.

Thornberry, N. A., Bull, H. G., Calaycay, J. R., Chapman, K. T., Howard, A. D., Kostura, M. J., Miller, D. K., Molineaux, S. M., Weidner, J. R., Aunins, J. and et al. A novel heterodimeric cysteine protease is required for interleukin-1 beta processing in monocytes. *Nature* 356(6372): 768-74, 1992.

Thornberry, N. A. and Lazebnik, Y. Caspases: enemies within. *Science* 281(5381): 1312-6, 1998.

- Thornberry, N. A., Peterson, E. P., Zhao, J. J., Howard, A. D., Griffin, P. R. and Chapman, K. T. Inactivation of interleukin-1 beta converting enzyme by peptide (acyloxy)methyl ketones. *Biochemistry* 33(13): 3934-40, 1994.
- Thornberry, N. A., Rano, T. A., Peterson, E. P., Rasper, D. M., Timkey, T., Garcia-Calvo, M., Houtzager, V. M., Nordstrom, P. A., Roy, S., Vaillancourt, J. P., Chapman, K. T. and Nicholson, D. W. A combinatorial approach defines specificities of members of the caspase family and granzyme B. Functional relationships established for key mediators of apoptosis. *Journal of Biological Chemistry* 272(29): 17907-11, 1997.
- Torgler, C. N., de Tiani, M., Raven, T., Aubry, J. P., Brown, R. and Meldrum, E. Expression of bak in *S. pombe* results in a lethality mediated through interaction with the calnexin homologue Cnx1. *Cell Death and Differentiation* 4: 263-271, 1997.
- Tschopp, J., Irmeler, M. and Thome, M. Inhibition of fas death signals by FLIPs. *Current Opinion in Immunology* 10(5): 552-8, 1998.
- Tsujimoto, Y. and Croce, C. M. Recent progress on the human bcl-2 gene involved in follicular lymphoma: characterization of the protein products. *Current Topics in Microbiology and Immunology* 141: 337-40, 1988.
- Tsujimoto, Y., Jaffe, E., Cossman, J., Gorham, J., Nowell, P. C. and Croce, C. M. Clustering of breakpoints on chromosome 11 in human B-cell neoplasms with the t(11;14) chromosome translocation. *Nature* 315(6017): 340-3, 1985.
- Tu, Y., Renner, S., Feng-hao, X., Fleishman, A., Taylor, J., Weisz, J., Vescio, R., Rettig, M., Berenson, J., Krajewski, S., Reed, J. C. and Liechtenstein, A. Bcl-x expression in multiple myeloma: possible indicator of chemoresistance. *Cancer Research* 58: 256-262, 1998.
- Tuscano, J. M., Druey, K. M., Riva, A., Pena, J., Thompson, C. B. and Kehrl, J. H. Bcl-x rather than Bcl-2 mediates CD40-dependent centrocyte survival in the germinal center. *Blood* 88(4): 1359-64, 1996.
- Uren, A. G., Beilharz, T., O'Connell, M. J., Bugg, S. J., van Driel, R., Vaux, D. L. and Lithgow, T. Role for yeast inhibitor of apoptosis (IAP)-like proteins in cell division. *Proceedings of the National Academy of Sciences U S A* 96(18): 10170-5, 1999.

Vander Heiden, M. G., Chandel, N. S., Williamson, E. K., Schumacher, P. T. and Thompson, C. B. Bcl-xL regulates the membrane potential and volume homeostasis of mitochondria. *Cell* 91: 627-637, 1997.

Varfolomeev, E. E., Schuchmann, M., Luria, V., Chiannilkulchai, N., Beckmann, J. S., Mett, I. L., Rebrikov, D., Brodianski, V. M., Kemper, O. C., Kollet, O., Lapidot, T., Soffer, D., Sobe, T., Avraham, K. B., Goncharov, T., Holtmann, H., Lonai, P. and Wallach, D. Targeted disruption of the mouse Caspase 8 gene ablates cell death induction by the TNF receptors, Fas/Apo1, and DR3 and is lethal prenatally. *Immunity* 9(2): 267-76, 1998.

Vercammen, D., Beyaert, R., Denecker, G., Goossens, V., Van Loo, G., Declercq, W., Grooten, J., Fiers, W. and Vandenabeele, P. Inhibition of caspases increases the sensitivity of L929 cells to necrosis mediated by tumor necrosis factor. *Journal of Experimental Medicine* 187(9): 1477-85, 1998.

Walker, N. P., Talanian, R. V., Brady, K. D., Dang, L. C., Bump, N. J., Ferez, C. R., Franklin, S., Ghayur, T., Hackett, M. C., Hammill, L. D. and et al. Crystal structure of the cysteine protease interleukin-1 beta- converting enzyme: a (p20/p10)₂ homodimer. *Cell* 78(2): 343-52, 1994.

Wang, H. G., Rapp, U. R. and Reed, J. C. Bcl-2 targets the protein kinase Raf-1 to mitochondria [see comments]. *Cell* 87(4): 629-38, 1996.

Wang, J., Zheng, L., Lobito, A., Chan, F. K., Dale, J., Sneller, M., Yao, X., Puck, J. M., Straus, S. E. and Lenardo, M. J. Inherited human Caspase 10 mutations underlie defective lymphocyte and dendritic cell apoptosis in autoimmune lymphoproliferative syndrome type II. *Cell* 98(1): 47-58, 1999.

Wang, K., Yin, X. M., Chao, D. T., Milliman, C. L. and Korsmeyer, S. J. BID: a novel BH3 domain-only death agonist. *Genes and Development* 10(22): 2859-69, 1996.

White, K., Tahaoglu, E. and Steller, H. Cell killing by the Drosophila gene reaper. *Science* 271(5250): 805-7, 1996.

Wiley, S. R., Schooley, K., Smolak, P. J., Din, W. S., Huang, C. P., Nicholl, J. K., Sutherland, G. R., Smith, T. D., Rauch, C., Smith, C. A. and et al. Identification and characterization of a new member of the TNF family that induces apoptosis. *Immunity* 3(6): 673-82, 1995.

Willis, T. G., Jadayel, D. M., Du, M. Q., Peng, H., Perry, A. R., Abdul-Rauf, M., Price, H., Karran, L., Majekodunmi, O., Wlodarska, I., Pan, L., Crook, T., Hamoudi, R., Isaacson, P. G. and Dyer, M. J. Bcl10 is involved in t(1;14)(p22;q32) of MALT B cell lymphoma and mutated in multiple tumor types [see comments]. *Cell* 96(1): 35-45, 1999.

Wilson, K. P., Black, J. A., Thomson, J. A., Kim, E. E., Griffith, J. P., Navia, M. A., Murcko, M. A., Chambers, S. P., Aldape, R. A., Raybuck, S. A. and et al. Structure and mechanism of interleukin-1 beta converting enzyme [see comments]. *Nature* 370(6487): 270-5, 1994.

Winter, G and Milstein, C. Man-made antibodies. *Nature* 349(6307): 293-9, 1991

Woo, M., Hakem, R., Soengas, M. S., Duncan, G. S., Shahinian, A., Kagi, D., Hakem, A., McCurrach, M., Khoo, W., Kaufman, S. A., Senaldi, G., Howard, T., Lowe, S. W. and Mak, T. W. Essential contribution of caspase 3/ CPP32 to apoptosis and its associated nuclear changes. *Genes and Development* 12(6): 806-19, 1998.

Woodle, E. S., Smith, D. M., Bluestone, J. A., Kirkman, W. M., 3rd, Green, D. R. and Skowronski, E. W. Anti-human class I MHC antibodies induce apoptosis by a pathway that is distinct from the Fas antigen-mediated pathway. *Journal of Immunology* 158(5): 2156-64, 1997.

Xerri, L., Devilard, E., Ayello, C., Brousset, P., Reed, J. C., Emile, J. F., Hassoun, J., Parmentier, S. and Birg, F. Cysteine protease CPP32, but not Ich1-L, is expressed in germinal center B cells and their neoplastic counterparts. *Human Pathology* 28(8): 912-21, 1997

Xerri, L., Devilard, E., Hassoun, J., Haddad, P. and Birg, F. Malignant and reactive cells from human lymphomas frequently express Fas ligand but display a different sensitivity to Fas-mediated apoptosis. *Leukemia* 11(11): 1868-1877, 1997.

Xiang, J., Chao, D. T. and Korsmeyer, S. J. BAX-induced cell death may not require interleukin 1 beta-converting enzyme-like proteases. *Proceedings of the National Academy of Sciences of the United States of America* 93(25): 14559-63, 1996.

Xie, X., Clausen, O. P., De Angelis, P. and Boysen, M. The prognostic value of spontaneous apoptosis, Bax, Bcl-2, and p53 in oral squamous cell carcinoma of the tongue. *Cancer* 86(6): 913-20, 1999.

Yang, X., Chang, H. Y. and Baltimore, D. Essential role of CED-4 oligomerization in CED-3 activation and apoptosis [see comments]. *Science* 281(5381): 1355-7, 1998.

Yeh, W. C., Pompa, J. L., McCurrach, M. E., Shu, H. B., Elia, A. J., Shahinian, A., Ng, M., Wakeham, A., Khoo, W., Mitchell, K., El-Deiry, W. S., Lowe, S. W., Goeddel, D. V. and Mak, T. W. FADD: essential for embryo development and signaling from some, but not all, inducers of apoptosis. *Science* 279(5358): 1954-8, 1998.

Yoshida, A., Takauji, R., Inuzuka, M., Ueda, T. and Nakamura, T. Role of serine and ICE-like proteases in induction of apoptosis by etoposide in human leukemia HL-60 cells. *Leukemia* 10(5): 821-4, 1996.

Yoshida, H., Kong, Y. Y., Yoshida, R., Elia, A. J., Hakem, A., Hakem, R., Penninger, J. M. and Mak, T. W. Apaf1 is required for mitochondrial pathways of apoptosis and brain development. *Cell* 94(6): 739-50, 1998.

Yuan, J., Shaham, S., Ledoux, S., Ellis, H. M. and Horvitz, H. R. The *C. elegans* cell death gene *ced-3* encodes a protein similar to mammalian interleukin-1 β -converting enzyme. *Cell* 75: 641-652, 1993.

Zamzami, N., Marchetti, P., Castedo, M., Decaudin, D., Macho, A., Hirsch, T., Susin, S. A., Petit, P. X., Mignotte, B. and Kroemer, G. Sequential reduction of mitochondrial transmembrane potential and generation of reactive oxygen species in early programmed cell death. *Journal of Experimental Medicine* 182(2): 367-77, 1995.

Zeuner, A., Eramo, A., Peschle, C. and Maria, R. D. Caspase activation without death [In Process Citation]. *Cell Death and Differentiation* 6(11): 1075-80, 1999.

Zheng, T. S., Hunot, S., Kuida, K. and Flavell, R. A. Caspase knockouts: matters of life and death. *Cell Death and Differentiation* 6(11): 1043-53, 1999.

Zhivotovsky, B., Samali, A., Gahm, A. and Orrenius, S. Caspases: their intracellular localization and translocation during apoptosis. *Cell Death and Differentiation* 6(7): 644-51, 1999.

Zhou, Q., Krebs, J. F., Snipas, S. J., Price, A., Alnemri, E. S., Tomaselli, K. J. and Salvesen, G. S. Interaction of the baculovirus anti-apoptotic protein p35 with caspases. Specificity, kinetics, and characterization of the caspase/p35 complex. *Biochemistry* 37(30): 10757-65, 1998.

Zinzani, P. L., Storti, S., Zaccaria, A., Moretti, L., Magagnoli, M., Pavone, E., Gentilini, P., Guardigni, L., Gobbi, M., Fattori, P. P., Falini, B., Lauta, V. M., Bendandi, M., Gherlinzoni, F., De Renzo, A., Zaja, F., Mazza, P., Volpe, E., Bocchia, M., Aitini, E., Tabanelli, M., Leone, G. and Tura, S. Elderly aggressive-histology non-Hodgkin's lymphoma: first-line VNCOP-B regimen experience on 350 patients. *Blood* 94(1): 33-8, 1999.

Zou, H., Henzel, W. J., Liu, X., Lutschg, A. and Wang, X. Apaf-1, a human protein homologous to *C. elegans* CED-4, participates in cytochrome c-dependent activation of caspase-3 [see comments]. *Cell* 90(3): 405-13, 1997.

APPENDIX A

Immunisation of Mice and Monoclonal Antibody Production

Balb/c mice of 6-10 weeks old were used for all immunization procedures. All animals were prebled by tail bleed. 10-25µg of the antigen + Titermax Research adjuvant were injected subcutaneously at the base of the tail. The mice were then left for at least 3 weeks. They were then boosted intraperitoneally with 10µg of the relevant antigen in 200µl of PBS. After 7 days the mice were tail bled and the serum tested for response to the antigen. Once a high response was established, the mice were re-boosted intraperitoneally with 10µg of the relevant antigen in 200µl of PBS. 3-4 days after this final boost, the mice were culled, a blood sample taken, and the peritoneal and spleen cells removed and used for fusion with NSO mouse myeloma cells.

2-3 days before the fusion, the mouse myeloma cells were set up and maintained in log phase. On the day of fusion, the waterbath was set at 41°C and 10ml of the washing medium and polyethylene glycol (PEG) were warmed. The spleen was removed and teased apart using sterile forceps. The cells were then pushed through a 106µ sterile mesh with a syringe plunger handle. The cells were washed through with washing medium and centrifuged at 1300 rpm for 10 min. The cells were then resuspended in 20 ml washing medium. After counting, 50 µl of cells were added to 450µl 0.1M Tris Ammonium Chloride, mixed and left for 1 min. 20µl of the cell mix were then counted. Approximately 100-200 x 10⁶ cells should be present.

The NSO myeloma cells were resuspended in medium and counted as before (20µl of the cell mix were then added to 20µl trypan blue). They were then centrifuged at 1300 rpm for 10 min. and resuspended in washing medium. The spleen and myeloma cells were then mixed in a ratio of 4:1 in a 50 ml tube and spun at 1300 rpm for 10 min. The pellet was drained completely, loosened by tapping and placed in an insulated beaker of water at 41°C. 800µl of PEG were added over 1 min. with constant stirring with a

pipette. The mixture was then stirred for another minute. The following volumes of warm washing medium was then added over continuous stirring at 41°C:

1ml over 1 min.

2ml over 1 min.

6ml over 2 min.

The cells were then spun at 1300 rpm for 10 min. and resuspended in a final suspension medium to give 2×10^6 spleen cells per well including the peritoneal macrophage feeder population. The cells were then plated out in 24 well plates and placed in an incubator at 37°C. Within 2-3 days, the wells were fed by removing 1ml of medium and replaced with fresh suspension medium. The wells were fed 3 times weekly thereafter.

Approximately 2 weeks after, when the cells covered greater than 40% of the bottom of each well, 1ml of supernatant from each well was harvested and tested for specific antibody production. 1ml of medium containing 15% FCS and HA was added to each well. Those wells that were found to contain antibody-producing cells were split into two.